GREEN SYNTHESIS, CHARACTERISATION AND BIOLOGICAL EVALUATION OF SOME ANTI CANCEROUS NANOPARTICLES FROM HERBS

Thesis Submitted to
GOA UNIVERSITY

for the award of the degree of

DOCTOR OF PHILOSOPHY

in

PHARMACY

By

RAJASHREE RAMACHANDRA JIRAGE

Under the guidance of

Prof. Dr. Arun B. JOSHI

GOA COLLEGE OF PHARMACY
PANAJI – GOA

GOA UNIVERSITY
TALEIGAO PLATEAU, GOA

May 2020

DECLARATION

I, **Ms. Rajashree Ramachandra Jirage**, do hereby declare that this dissertation entitled "**GREEN SYNTHESIS, CHARACTERISATION AND BIOLOGICAL EVALUATION OF SOME ANTI CANCEROUS NANOPARTICLES FROM HERBS**" is a bonafide record of research work done by me under the supervision and guidance of **Prof. Dr. Arun B. Joshi,** Goa College of Pharmacy, Goa University.

I also declare that the same has not been previously formed the basis for the award of any degree, diploma or certificate or similar title of this or any other University. I have duly acknowledged all the sources used by me in the preparation of this thesis.

Rajashree Ramchandra Jirage
Research Scholar,
Goa College of Pharmacy,
18th June Road, Panaji
Goa- 403 001, INDIA

GOA UNIVERSITY

CERTIFICATE

This is to certify that the Ph.D. thesis entitled "**GREEN SYNTHESIS, CHARACTERISATION AND BIOLOGICAL EVALUATION OF SOME ANTI CANCEROUS NANOPARTICLES FROM HERBS**", is a bonafide record of the original work done by **Ms. RAJASHREE RAMACHANDRA JIRAGE,** under my guidance and supervision and the same has not been previously formed the basis for the award of any degree, diploma or certificate or similar title of this or any other University.

ABJoshi 09/05/2020

Dr. Arun B. Joshi
Professor & Head
Department of Pharmacognosy
Goa College of Pharmacy
Panaji-Goa

GOA UNIVERSITY

GOVERNMENT OF GOA
GOA COLLEGE OF PHARMACY
PANAJI - GOA

CERTIFICATE

This is to certify that the thesis entitled **"GREEN SYNTHESIS, CHARACTERISATION AND BIOLOGICAL EVALUATION OF SOME ANTI CANCEROUS NANOPARTICLES FROM HERBS"** submitted by **Ms. RAJASHREE RAMACHANDRA JIRAGE,** Goa College of Pharmacy, Goa University, Panaji - Goa for the award of the degree of Doctor of Philosophy in **Pharmacy** is a record of bonafide research work carried out at this institute.

Date: 05/05/2020
Panaji

Dr. Gopal Krishna Rao
Principal
Goa College of Pharmacy
Panaji-Goa

Email: gcpprincipal@yahoo.com Phone No.0832-2226883/2226882
Goa College of Pharmacy, 18th June Rd, Panaji, Goa. 403001

ACKNOWLEDGEMENT

I begin with praises and thanks to God, Almighty, for his showers of blessings during my research work to complete the research successfully.

I would like to express my deep and sincere gratitude to my research guide, ***Dr Arun B. Joshi,*** Professor and Head, Department of Pharmacognosy, Goa College of Pharmacy, for giving me the opportunity to accomplish my research work and providing invaluable guidance throughout this research. His dynamism, vision, sincerity, motivation and immense patience has deeply inspired me. It was a great privilege and honour to work and study under his guidance.

My special heartfelt gratitude to ***Late Shri. Manohar Parrikar***, ex-Chief Minister, Goa, for believing and encouraging me to complete the research work. Without him, this project wouldn't have seen the light of the day.

My profound gratitude to ***Dr. Gopal Krishna Rao***, Principal, Goa College of Pharmacy, for his unstinting support and motivation. His invaluable inputs as the DRC member helped to plan my research work. He has always believed in me and inspired me to give my best at everything I do. I profusely thank him for providing the facilities in the campus for my research activities.

My earnest thanks and indebtedness to ***Dr. Anant Bhandarkar***, Assistant Professor, Department of Pharmacognosy, Goa College of Pharmacy, for his remarkable unselfish and magnanimous support at every phase of the research work with his able guidance, encouragement and endurance to ensure the completion of my research work.

Immeasurable appreciation and gratitude extended to ***Dr. Umesh V. Banakar***, Professor and President of Banakar Consulting Services, USA, for being my greatest inspiration, motivation, a guide, mentor and philosopher who has supported me navigate through and complete my research work. His valuable inputs at all stages of my research work, encouragement, insightful comments and advice has helped me complete the research work. His unconditional commitment helped me achieve my dream. I feel blessed.

My deep gratitude to my DRC expert, ***Dr. B. Madhava Reddy*** for his guidance and invaluable suggestions during my research. I remain indebted to him for his patience and willingness to attend the DRC meetings and contribute immensely.

My gratitude to ***Dr. Anand Mahajan***, Associate Professor, Department of Pharmaceutical Analysis, Goa College of Pharmacy, for his invaluable inputs and guidance.

I would like to express my heartfelt sincere gratitude to ***Mr. Prasad Tamba***, for his constant motivation and standing by me at all times. He stood by me against all odds to help me accomplish my goal. I remain grateful to him.

I extend my heartfelt gratitude to ***Dr. Sanjay Pai P.N***., Professor and Head, Department of Pharmaceutical Chemistry, Goa College of Pharmacy, the silent figure who was instrumental in motivating and standing by me to keep the positivity throughout this journey and also allowing me to use the facilities in the department for my research work.

Sincere thanks to ***Shri. S. S. Sardessai*** for being a great source of inspiration and encouragement in my life.

My sincere thanks to ***Dr. Shanker Kalkotla***, Hyderabad who set the ball rolling for my research work by giving an insight on nanoparticles and being a great support at every phase of my research work.

Words are few to express my deepest gratitude to ***Akshata,*** for being my greatest support system in all my endeavours during the project. She has been through the thick and thin of my life during this research work. Her selfless commitment and sincerity are incredible.

My special gratitude goes to ***Dr. Chandrashekar N.S.*** and ***Dr. Bhupinder Singh Bhoop*** for their constant motivation and consistent interest in my endeavour.

My sincere thanks to Dr. Dinesh Nayak and Dr. Gopal Krishna Bhatt for providing the plant material. I extend my gratitude to Punjab University, Deshpande Labs Pvt. Ltd, SAIF Centre, Kochi for providing their analytical services.

I am extremely thankful to my dear friend, ***Mrs. Sachi Kudchadkar***, Assistant Professor, Department of Pharmaceutical Analysis, Goa College of Pharmacy, for being a great support and always being there at all times.

I express my sincere gratitude and appreciation to ***Dr. Srinivas Mutalik*** and ***Dr. Sridhar Pai,*** Manipal College of Pharmaceutical Sciences (MCOPS), for being a valuable support throughout this journey.

My heartfelt thanks to ***Mrs. Saba Jamadar,*** Assistant Professor, Department of Pharmaceutics, Goa College of Pharmacy for being a great help whenever required.

My sincere thanks to ***Dr. Prashant Bhide***, Professor and Head, Department of Pharmaceutics, Goa College of Pharmacy, for allowing me to use the facilities of the department for the research work. I would also like to thank ***Mrs. Yogita Sardessai***, Associate Professor, Department of Microbiology and ***Dr. M. P. Joshi***, Professor, Department of Pharmacology, Goa College of Pharmacy for permitting to use the facilities in the departments.

My sincere gratitude to all my colleagues, specially ***Dr. Shailendra Gurav, Dr. Mythili Krishna J., Ms. Liesl Fernandes Mendonca, Dr. Raghuvir Pissurlenkar and Ms. Nutan Naik***, who facilitated me through this journey.

My special thanks to ***Mr. Kalidas Phadte, Mrs. Varsha Rasaikar, Mrs. Shanti Naik*** and all the laboratory staff for their cooperation and help provided during the research.

My heartfelt gratitude to ***Mrs. Arlette Baretto*** for the administrative help provided during the research work. My deep gratitude to ***Mrs. Kanchan Kalangutkar*** and ***Mr. Sandesh Gomes*** for being a great support at all times. My sincere appreciations to ***Mr. Vinay Naik*** for computational help which was a real time saver.

I am grateful to my friend ***Mr. Rajesh Parab***, for being a great moral support and an inspiration having voyaged together in our profession.

My sincere thanks to ***Dr. V Gopakumar***, Librarian, Goa University for being a great help and providing me with necessary inputs.

My heartfelt thanks to ***Divyata, Reeshwa*** and ***Rucheera*** for their help at all times. I would like to thank ***Shraddha, Steffi, Niddhi, Ankita, Krupa, Prerna, Krati, Preetesh*** and ***Suman*** for their invaluable support.

My deepest heartfelt gratitude to my husband, ***Subodh,*** for being my pillar. I thank him for his unselfish support, understanding, patience and sacrifice. My sincere thanks to my dearest kids, ***Manjiri, Manasi*** and ***Mehul*** for always being a wonderful support and dynamos to move ahead ! My earnest thanks to my brother ***Kedar*** and sister-in-law, ***Archana***, for being the pillars of support. Their constant support, motivation and patience have helped me to complete my project.

I feel a deep sense of gratitude for my ***parents*** and ***father in law***, for their infallible love and support and for being my strength and encouragement. My special gratitude to ***Suneeta Di (Mrs. Banakar)*** for her constant encouragement and motivation. I would like to thank ***Shirodkar Kaka, Bhau***, ***Maya*** and ***Gaurang*** for their consistent interest and motivation. My sincere gratitude to ***Supriya*** and ***Rajesh*** for their valuable inputs and support at all times.

My deep gratitude for the whole hearted cooperation extended by the authorities of Government of Goa for granting me approval and extending support towards the completion of my Ph.D. Sincere thanks to the authorities at Goa University for their continued cooperation.

My thanks and appreciation to all the well-wishers for their support that is often taken for granted, however, needs to be recognized.

THANK YOU…

TABLE OF CONTENTS

LIST OF ABBREVIATIONS	
RG-A	Sample- Extract of *A. polystachya*
BcL2	B-cell lymphoma 2
STAT3	Signal transducer and activator of transcription 3
b Actin	human gene and protein
G_0	Cellular state outside of the replicative cell cycle
G_2M	Mitosis Phase
G_1	Cell cycle that takes place in eukaryotic cell division
DMEM	Dulbecco's Modified Eagle Medium
EtOAc	Ethyl Acetate
h	Hours
gm	grams
mg	milligram
ml	millilitre
L	litre
nm	nanometre
µl	microliters
µg	microgram
min	minimum
max	maximum
Conc.	concentration
ΔCt	Number of amplification cycles required to reach a fixed signal threshold.
ΔCTC	Coincidence Time Correction for qRT-PCR analysis
ΔΔCt	ΔCT test sample – ΔCT calibrator sample
IC_{50}	Half maximal inhibitory action
DMSO	Dimethyl Sulfoxide
ft	feet
HSC-2, HSC-3 cell lines	Oral cancer cell lines

LIST OF ABBREVIATIONS	
TUNEL assay	Method to detect apoptotic DNA fragmentation
DNA	Deoxyribonucleic acid
$AgNO_3$	Silver Nitrate
HeLa cells	Human cell lines
MIC	Minimum Inhibitory Concentration
ELISA	Enzyme-linked Immunosorbent Assay
Jurkat cells	Human T lymphocyte cells
SAED	Selected Area Electronic Diffraction
Hep-2 cells	Human Epithelial Type-2 cells
HepG2 cells	Human Liver Carcinoma Cells
AKT	Serine/threonine-specific protein kinase
ERK	Extracellular-Signal-Regulated kinase
JNK	c-Jun N-terminal kinase
T47D cells	Human Breast Cancer Cell Lines
DEPT	Distortion less enhancement by polarization transfer
HSQC	Heteronuclear single quantum coherence spectroscopy
HMBC	Heteronuclear Multiple Bond Correlation
$^{1}H–^{1}H$ COSY	Correlation Spectroscopy
NOESY	Nuclear Overhauser Effect Spectroscopy
HAADF	High-angle annular dark-field imaging
STEM	Scanning Transmission Electron Microscopy
PLGA	Poly (lactic-co-glycolic acid)
PLA	Polylactic acid
HMQC	Heteronuclear Multiple Quantum Coherence
HMBC	Heteronuclear Multiple Bond Correlation
L-929 cells	Adriamycin-resistant cell
PARP cleavage	Poly (ADP-ribose) polymerase (PARP-1) is a nuclear enzyme that catalyses the transfer of ADP-ribose polymers onto itself and other nuclear proteins in response to DNA strand breaks

LIST OF ABBREVIATIONS	
HSC-2, HSC-3 cell lines	Oral cancer cell lines
DNA	Deoxyribonucleic acid
TUNEL assay	Method to detect apoptotic DNA fragmentation
$AgNO_3$	Silver Nitrate
HeLa cells	Human cell lines
MIC	Minimum Inhibitory Concentration
ELISA	Enzyme-linked Immunosorbent Assay
Jurkat cells	Human T lymphocyte cells
SAED	Selected Area Electronic Diffraction
Hep-2 cells	Human Epithelial Type-2 cells
HepG2 cells	Human Liver Carcinoma Cells
AKT	Serine/threonine-specific protein kinase
ERK	Extracellular-Signal-Regulated kinase
JNK	c-Jun N-terminal kinase
T47D cells	Human Breast Cancer Cell Lines
DEPT	Distortion less enhancement by polarization transfer
HSQC	Heteronuclear single quantum coherence spectroscopy
HMBC	Heteronuclear Multiple Bond Correlation
$^1H–^1H$ COSY	Correlation Spectroscopy
NOESY	Nuclear Overhauser Effect Spectroscopy
HAADF	High-angle annular dark-field imaging
STEM	Scanning Transmission Electron Microscopy
PLGA	Poly (lactic-co-glycolic acid)
PLA	Polylactic acid
HMQC	Heteronuclear Multiple Quantum Coherence
HMBC	Heteronuclear Multiple Bond Correlation
L-929 cells	Adriamycin-resistant cell
ALP	Alkaline phosphatase enzyme
CPT	Camptothecins

LIST OF ABBREVIATIONS	
CPT	Camptothecins
ALP	Alkaline phosphatase
ALAT	Alanine Transaminase
GOT	Glutamic Oxaloacetate Transaminase
ASAT	Aspartate aminotransferase
LDH	Lactate Dehydrogenase
TEAC Assay	Trolox Equivalent Antioxidant Capacity
spp	species
NK cells	Natural Killer cells

LIST OF FIGURES

LIST OF TABLES

ABSTRACT

"Intuition is a very powerful thing, more powerful than intellect."

ABSTRACT

Herbal therapy in India, often serves as the first line of treatment for various ailments as well as supplemental treatment in treating different types of carcinoma. Treatment of cancer, despite significant health care advances as of date, continues to be a major health care challenge globally affecting 15% of the population. Over the past century and beyond, herbal sources have provided many therapeutically active compounds, drug substances, that have been successfully launched as pharmaceutical products in the treatment of various diseases. Leads as anticancer agents discovered from plants are no exceptions. At present, it is estimated that over 60% of currently used anti-cancer agents have been derived from natural sources that include herbs.

Nanotechnology within the domain of modern material science has played a significant role in improving therapeutics, witnessed in the healthcare literature, and has been recognized as an emerging field in nanobiomedicine. Some noteworthy benefits presented by nanobiomedicine include, facilitating drug delivery, enhancing the bioefficacy and therapeutic efficacy of the drug, among others. Development and the use of green synthesis of metal nanoparticles has attracted the attention of many researchers. Such metal nanoparticles when conjugated with biologically active compounds provide a viable and potential therapeutically active drug delivery platform or a carrier system for the active compound either individual or in combination of active compounds, e.g., herbal extract, for administration in the human body.

It was learnt from the review of literature that the various parts of the plant of *Aphanamixis polystachya* exhibit anti-cancer activity. However, the root of this plant has not been explored. Hence, there is a need for evaluation of the role of the components of the roots to explore the possibility for anti-cancer activity.

This research investigation was designed to prepare the methanolic extract of the root bark of *A. polystachya*. The extract was subjected to preliminary phytochemical investigation which confirmed the presence of phytoconstituents viz., alkaloids, carbohydrates, triterpenoids, steroids, tannins and phenolic compounds. The methanolic extract of the root bark of *A. polystachya* was fractionated with petroleum ether (60:80, defatting) and chloroform to yield petroleum ether extract and chloroform extract. The chloroform extract was subjected to column chromatography and eluted by gradient technique using various solvents from non-polar (petroleum ether) to polar (methanol) solvents. Flash chromatography was utilised for the purification of the compounds. The components isolated were viz., Rohituka 7 (RG-APE1), Rohituka 3 (RG-APE2), Amoorinin-3-O-α-L-rhamnopyranosyl–(1→6)–β-D-glucopyranoside (RG-APE3) and 8-methyl-7,2′4,′-tri-O-methylflavonone-5-O-α-L-rhamnopyranosyl(1→4)-β-D-glucopyranosyl-1→6)-β-D-glucopyranoside (RG-APE4).

The cytotoxic activity of the methanolic extract of the root bark of *A. polystachya* was carried out using SRB assay. The methanolic extract exhibited growth inhibition (GI50) of <10µg in MCF-7 cell lines and >80 µg in MDA-MB231 cell lines thus confirming its anticancer activity against MCF-7 cell lines over MDA-MB231 cell lines.

Subsequently, silver nanoparticles of the methanolic extract of the root bark of *A. polystachya* (AgNPs) were synthesized and characterised using various current techniques.

Specific effects of AgNPs of *A. polystachya* on cell cycle and apoptosis in human breast cancer cells (MCF-7) by employing flow cytometry using Doxorubicin (Adriamycin) as the standard were investigated. The cell cycle and apoptosis analysis of AgNPs of *A. polystachya* (40 µg/ml) were found to be 13.62 as compared to the untreated AgNPs (18.43) and Doxorubicin (1.5) respectively. Additionally, these results revealed that the AgNPs caused a significant arrest of cells at G_2M phase which were found to be higher than those for the standard, Doxorubicin. This outcome potentially suggested that the AgNPs from the methanolic extract of the root bark of *A. polystachya* may be acting by some cell cycle specific mechanism inducing mitotic arrest and apoptosis in breast cancer cells.

Caspases, which are aspartic acid specific cysteine proteases, often referred to as executioners of apoptosis, are used as effective markers for assessment of cytotoxic activity of a potential drug substance(s). The ability of the AgNPs of the methanolic extract of the root bark of *A. polystachya* to induce apoptosis were measured. The results revealed that treatment with AgNPs of the methanolic extract of the root bark of *A. polystachya* produced a significant increase of 41.2% in levels of Caspase 7, when compared to the untreated control samples indicative of execution of apoptosis. In case of Caspase 9, there was a 57.6% increase in Caspase levels when compared with untreated

samples confirming initiation of apoptosis. Overall, in general, the AgNPs exhibited better cytotoxic activity than the methanolic extract of the root bark of the plant.

Apoptosis is an active type of cell suicide regulated by a gene network, in which the BcL-2 family proteins play a major role in apoptosis control. The AgNPs of the methanolic extract of the root bark of *A. polystachya*, produced a significant decrease in BcL-2 expression (approximately 5.7-fold change) when compared to that of the untreated control. The decrease in BcL-2, in general and potentially nonspecific, may be attributed as a possible mechanism of apoptosis contributed by *A. polystachya* AgNPs.

Signal transducer and activator of transcription 3 (STAT3) is persistently activated in a wide variety of cancer. The treatment with AgNPs produced a considerable decrease in STAT3 suggesting a mechanism contributing to Go/G1 phase arrest.

Based on the preliminary findings from the apoptotic studies, silver nanosuspension (AgNS) were formulated with the objective to explore their cytotoxic potential via measurements of scavenging activities, among others. In determining the scavenging activities on the methanolic extract of the root bark of *A. polystachya* and the formulated AgNS, it was observed that the nanosuspension of *A. polystachya* exhibited significant IC_{50} value of 8.36 µg/ml compared to that of 300.24 µg/ml for the extract.

AgNS was further evaluated for cytotoxic activity by Sulforhodamine B Cytotoxic Assay on MCF-7 and MDA-MB 231 cell lines. The results revealed enhanced potential cytotoxic activity on MCF-7 cell lines (IC_{50} 0.58 µM) compared to MDA-MB231 cell

lines (IC_{50} 1000 µM). Thus, the formulated nanosuspension reconfirmed better cytotoxic activity than the methanolic extract and the AgNPs from the root bark of *A. polystachya*.

Overall, this investigation has successfully determined the *in vitro* cytotoxic activity of the AgNS, of the methanolic extract of the root bark of *A. polystachya* by targeting the cancerous breast cells. This investigation provides the necessary rationale and possible preliminary proof of the cytotoxic potential of AgNS prepared from the methanolic extract of *A. polystachya*.

Based on the findings of this investigation, the viability of methanolic extract based AgNS of *A. polystachya* as a potential product for treatment of breast cancer can be pursued. This preliminary investigation will provide the necessary impetus for researchers in this discipline to generate the required additional data to take this project further in the future.

INTRODUCTION

"Ambition is the path to success. Persistence is the vehicle you arrive in"

1.0 INTRODUCTION

1.1 HISTORY AND BACKGROUND

Many synthetic and chemotherapeutic agents have been developed in the treatment of cancer, which have been proven to show various side effects. To overcome these flaws, more convenient herbal drugs have been developed as they are known for lesser toxic side effects. Plants have been well known for the treatment of cancer and it is seen that over 60% of currently used anti-cancer agents come from natural sources. Many of the plants, traditionally have reported to possess anticancer activity.

Drugs discovered from plants, marine organisms and micro-organisms have led to the development of anticancer agents. The majority of the population depends on herbal medicine for their primary health care needs. Cancer is a major health problem globally, affecting 15% of the world's population. Regardless of all advances in medical sciences, it is anticipated that by 2030, the occurrence of malignant growth levels will increment to 15 million cases causing deaths.

Hence, natural products are a significant source of new drugs, medication leads and new chemical elements. The drug discovery from plants, marine living beings and micro-organisms have brought about the development of anticancer agents[1].

1.2 CANCER

The term 'Cancer' was first coined by Hippocrates. Cancer is an abnormal growth of cells in the body leading to death. It is a condition where the cells grow in an uncontrolled manner by forming lumps or masses of tissues that are called tumours. The cancerous cells also destroy the healthy normal cells and surrounding tissues. Cancer cells differ from normal cells as they grow out of control and are invasive[2]. An imbalance in the body leads to the formation of cancer cells. This imbalance can be treated by destroying the cancer cells[3].

There are more than 100 types of cancer, where each is classified based on the symptoms and the cells it affects. The different types of cancer are classified as carcinoma, leukemia, myeloma and central nerve system cancer[4].

1.3 CELL CYCLE

Accelerated growth and disrupted apoptotic mechanism are the characteristic features of cancer cells. The prerequisite for a cell to replicate comprise of reproduction of DNA, adequate production of cellular organelles, membranes, soluble proteins, etc., empowering the daughter cells to survive, partition the DNA and cytoplasm equally to form two daughter cells. The process can be achieved only when the molecular steps are consecutive and suitably oriented. Failure in controlling cell cycle leads to tremendous loss. The basic life plan undergoes apoptosis in the presence of eukaryotes.

Cell proliferation is a controlled process containing multiple check points responsible for the regulation of abnormal cell cycle progression. Transitions between GI, S and G2/M are biochemically regulated by the actions of cyclins, cyclin-dependent kinases (CDKs) and CDK inhibitors (CDKIs), in turn be modulated by intracellular signals transduced from extracellular growth[5]. GI to S phase transition through the restriction point (R) or by the entry of S phase, regulated by mitogenic reagents, intact cytoskeletal network and cell adhesion[6]. It is also observed that cellular systems often arrest at a G2-check point avoiding cell division capable of synthesizing daughter cell with damaged or abnormally synthesized DNA[7]. The protein p53 involved in the growth of cell, induces cell cycle regulators, $p21^{Waf1\ CKI}$ [8]. In turn, $p21^{Waf1\ CKI}$ inhibits CDC2-cyclin B complex, leading to the arrest of G2.

1.4 APOPTOSIS IN HUMAN CANCER CELL LINES

Apoptosis is a strictly controlled pathway responsible for the removal of redundant, aged and damaged cells[9]. It plays an important role in the development and maintenance of tissue homeostasis, also representing effective mechanism in the elimination of harmful cells[10]. Morphological milestones of this process include loss of cell volume, hyperactivity of the plasma membrane and condensation of peripheral heterochromatin[11]. It is followed by cleavage of the nucleus and cytoplasm into multiple membrane enclosed bodies comparing chromatin pigment[12,13]. Apoptosis is either

created by extrinsic pathway (death receptors) utilizing Caspase 8 and 10. It has been reported that Caspase 2, 3, 6, 7 and 9 can cleave poly (ADP ribose) polymerase (PARP).

BcL-2 family proteins are one of the identified regulators of apoptosis. A BcL-2 family of homologous proteins indicates critical checkpoint within the apoptotic pathways causing damage to the cellular constituents[14]. At least 15 BcL-2 family members in the mammalian cells have been identified. They function either as proapoptotic (Bax, Bak, Bad) or antiapoptotic (BcL-2, BcL-x_L) regulators. The ratio of antiapoptotic and proapoptotic proteins give an idea, how a cell responds to apoptosis or survival signals[14].

The other pathway includes an intrinsic pathway (mitochondrial path) involving Caspase 9[15]. Detection of the mechanism involved in the development of cancer is a great importance for developing neoplastic treatment. Induction of apoptosis holds a key role as a marker of the cytotoxic antitumor agent. Some natural compounds from plant origin induce apoptotic pathways, which are blocked in cancer[16].

1.5 HERBAL COMPOUNDS WITH ANTICANCER ACTIVITY

1.5.1 Phenolic compounds

- **Curcumin** (diferuloylmethane) is a phenolic compound obtained from the rhizomes of curcuma spp. Preclinical studies of curcumin have revealed inhibitory effects on carcinogenic procedures in colorectal pancreatic, gastric and prostate cancers. Curcumin acts as a chemosensitizer resulting in increased activity of other anticancer factors in treating multidrug resistant cancers. Phase II clinical trial studies revealed that curcumin at a dose of 8000 µg/day is non-toxic[17-19].
- **Ginger** contains phenolic compounds and its rhizome is widely used in traditional medicine. The phenolic compounds present in this plant are responsible for cytotoxic activity through apoptosis[20].
- **Resveratrol** is a phytoalexin present in grapes. It was proved that resveratrol causes apoptosis in HL60 and T470 cells (breast carcinoma cells). The apoptosis was induced through CD95 signalling-dependent apoptosis in HL60 and T470 cells[21].

1.5.2 Flavonoids

- **Genistein** is a phytosterol belonging to the class of flavonoid**.** The induction of apoptosis in human promyelocytic HL-60 leukemic cells is confirmed by flow

cytometric analysis[17]. It causes inhibition of tyrosine kinase, angiogenesis and arrests cell cycle in G2/M phase.

- **Biocalein** is a 5,6,7-trihydroxy flavone obtained from the roots of *S. baicalensis*. It induces apoptosis in cell lines human hepato-cellular carcinoma (HCC) acting through inhibition of Topoisomerase II[2].
- **Quercetin** is 3,3', 4', 5,7-pentahydroxy flavonone. It induces apoptosis by increasing the number of cells in sub-G1 phase. It increases proteolytic cultivation of caspase 3,7 and 9[20].

1.5.3 Alkaloids

- **7-hydroxystaurosporine** (UCN-01) is a natural alkaloid, which enhances the cytotoxicity and apoptosis of cis-diamine dichloroplatinum II in ovarian cancer cells. UCN-01 along with 5-fluouracil exhibited synergistic effect on apoptosis production[20].
- **Lectins** *Visum album* (VAL), a phyto preparation has been used in adjuvant cancer therapy for many years. It stimulates the immune system by increasing the activity and number of NK cells and neutrophils. Cytotoxic lectin, obtained from Korean mistletoe (*viscum album*) exhibited cytotoxic and apoptosis effect on tumour cells[20].

1.5.4 Terpenoids

- **Xanthorrhizol** a sesquiterpenoid complex obtained from the rhizome of *Curcuma xanthorrhizza*. It induces apoptosis via the intrinsic pathway involving release of cytochrome C, followed by a modulation of Caspase 3 and 9 activities and regulates the inactivation of PARP-1 protein. Thus, indicating it to be a potential antiproliferative agent for breast cancer cells[22].

1.6 TYPES OF HERBAL MEDICINES

The herbal medicines can be categorized into

(i) Immunomodulation herbs

(ii) Chemopreventive or Adaptogenic herbs

A. Immunomodulation Herbs – This class of medicines include *Ganoderm lucidum, Sophora flovescens, Scutellaria baicalensis* and *Isatis tinctorial.*

- ***G. lucidum*** is a medical fungus. *In vitro* and *in vivo* studies indicate anti-tumour activity, causing macrophages, T cell production of cytokines (TNF), interleukins and interferons[23].
- ***S. flovescens*** increases leukocytes and enhances immune response [24].
- ***S. baicalensis*** possesses anti-tumour and stimulating effects on the immune system, causing inhibition of platelet aggregation, thus inducing apoptosis[2].

B. Chemopreventive or Adaptogenic Herbs – Synthetic or natural complexes are employed to interfere or prevent carcinogenesis development. Induction of apoptosis is the main objective of Chemopreventive plants[25,26].

- **Saffron** is the stigmas obtained from the plant *Crocus sativus* belonging to the family Indiaceae. *In vivo* studies indicated that it is capable of inhibiting tumorigenesis through various mechanisms, including RNA, DNA synthesis inhibition, inhibitory effect on free radical chain reaction and inhibition of Topoisomerase II[27].
- **Curcumin** inhibits cycloeskinase-2 production in epithelial colon cells. It blocks NF-KB signalling pathway by controlling 1KB enzyme phosphorylation, thus inducing apoptosis in cancer cells[28,29].

1.7 ANTICANCER AGENTS APPROVED BY FDA

The anti-cancer agents in clinical use derived from plants are divided into four groups viz. vinca alkaloids, taxanes, podophyllotoxin and camptothecins.

- **Vinca Alkaloids:** Vinblastine and Vincristine are the important alkaloids obtained from the leaves of *Catharanthus roseus*. Clinically, they are in use since 1960.These alkaloids inhibit microtubule assembly via tubulin interaction and disruption, leading to the termination of cell division[30].

  Vinblastine is used to treat breast cancer, Hodgkin's lymphoma and Kaposis sarcoma.

Vincristine is used in treating severe lymphoblastic leukemia, non-Hodgkin's Leukemia and William's tumour[31].

- **Taxanes:** Experimental studies and various clinical trials have indicated that taxanes are the first choice of drugs for treating breast, ovary, lung and other metastatic cancers.

  Paclitaxel (Taxol) and **Docetaxel** (Taxotene) are obtained from the Pacific Yew bark *Taxas brevifolia* belonging to the family Taxaceae[29]. In 1992, this drug was approved by FDA to treat breast, neck, prostate, head and gastric cancer. Abraxane® (2205), a nanoparticle Paclitaxel was approved by FDA to treat metastatic breast cancer[32].

- **Podophyllotoxins:** The isomer of podophyllotoxin, epipodophyllotoxin is obtained from the roots of *Podophyllum hexandrum* belonging to the family Berberidaceae. The two semi-synthetic analogs of epipodophyllotoxin, Etopside and Teniposide act by inhibiting Topoisomerase II. Etopside is approved by FDA for the treatment of chorio carcinoma, lung, ovarian and testicular cancers. However, Teniposide is approved for the treatment of central nervous system tumours, lymphoma and bladder cancer[31,33].

1.8 BREAST CANCER

The most common malignant disease among women is breast cancer. About one third of the women develop metastasis and die due to breast cancer. Incidence rates are found to be higher in the urban areas[34]. Breast cancer spreads into other areas of the body, or when cells of the breast cancer pass through the blood vessels and/or lymph vessels to other parts of the body[35]. It is observed that the breast cancer cases are more prevalent in women after the age of 40 years. It is not well-known what causes breast cancer. But, epidemiology of the disease shows that hormonal factors play an important role. Early and late menopause, administration of contraceptive pills, obesity, pregnancy have shown to cause imbalance of the hormone, oestradiol which leads to mitosis of the breast epithelial cells, thus leading to a high risk of breast cancer[36].

1.8.1 Anatomy of Breast

The breast consists of different tissues, ranging from very fatty to very hard adipose tissues. The adipose tissue is found to be stretched form collarbone, under arm and around the ribcage. Adipose tissue, known for storing and releasing energy, contains nerve cells and blood vessels. There is a network of lobes (12-20 sections) within the adipose tissue. Each lobe consists of small, tube-like structures called lobules, which contain milk glands. Narrow ducts attach the glands, lobules and lobes, bringing milk from the lobes to the nipples. The nipple is in the middle of the isola, which is the darker portion.[37] Within the breast, there is a lymph- and vascular network. The vascular system

is made up of blood vessels, and the lymphatic system is made up of lymph channels. These two systems function together to transport blood and fluid to and from the tissue of the breast to the rest of the body. Lymph nodes are clusters of bean-shaped cells found in the lymph system. They are immune cells, which serve as filters. They are the most likely to spread breast cancer in the first place[38].

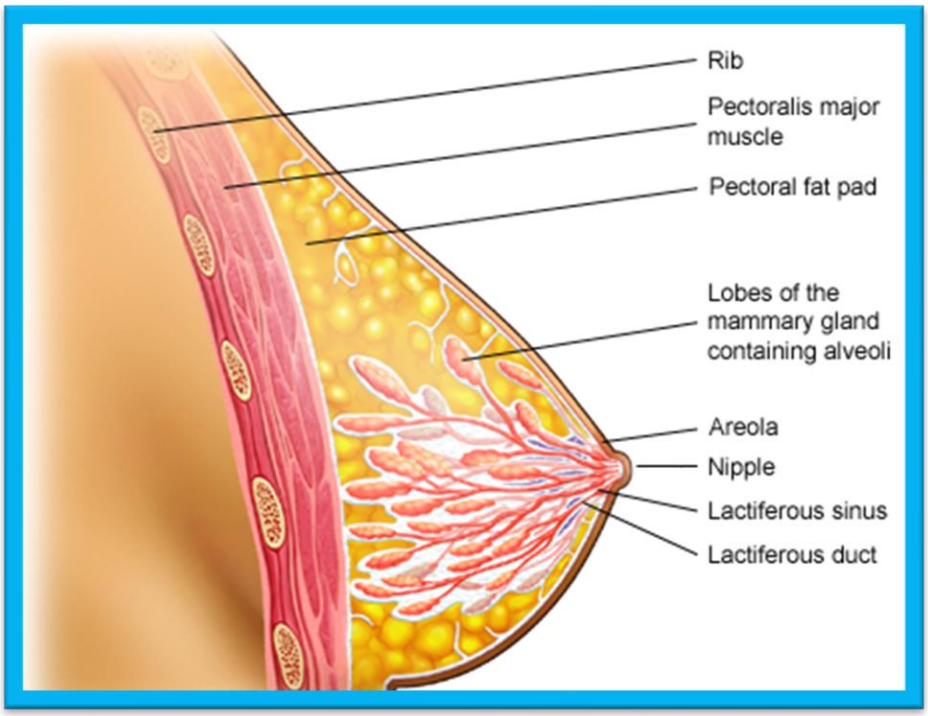

Fig 1: Structure of Breast

1.9 NANOTECHNOLOGY

Nanotechnology was first conceptualized by the Nobel Laureate Richard Feynman in 1960 in his article titled, “There is Plenty of Room at the Bottom”, where he discussed the idea of nanoparticles. Nanotechnology, with its ever-expanding horizons, has always been rightly awaited as the 21st-century wonder technology. It is defined as "intentionally designing, characterizing and producing materials, structures and systems by controlling their size and form within the range of 1 to 100 nm nanoscales”[39].

Physical characteristics of nanomaterials for the treatment of diseases at the molecular level plays an important role in the field of Nanomedicine. Nanotechnology is one of the imminent emerging areas of research in the modern field of material science. Novel applications of nanoparticles and nanomaterials are emerging rapidly in various research areas like pharmacy and medicine with an emphasis in drug delivery, controlled release systems, etc[40]., Nanotechnology being a promising field in the therapeutic and pharmaceutical sectors assumes a significant role in enhancing the quality of life. The applications of Nanotechnology in the medical sector are many, including diagnosis and therapeutic. Therapeutic use is viewed as the principle application of nanotechnology in the health sector. Nanotechnology has been found to affect therapeutics by facilitating drug delivery, enhancing the efficacy of the drug, improving its circulation and stability and reducing its toxic side effects[41].

1.10 NANOPARTICLES

Nanoparticles are particles admeasuring in the size range of 1-100 nm with a surrounding interfacial layer. Nanoparticles have a unique advantage of size, shape and high specific surface area which offers enhanced stability, protection and bioavailability. Because of their unique physicochemical characteristics, including anti-cancer, anti-diabetic, anti-bacterial properties and magnetic properties, they are gaining interest of the researchers for novel methods of synthesis.

Further, due to the varied advantages, nanoparticles can be formulated to customize for targeted drug delivery to the tissues, helping in dose reduction and enhanced therapeutic outcome. The majority of the active compounds being demonstrated to treat certain ailments or reduce pain are categorized as organic compounds. It is seen that these active organic compounds exhibit insolubility in aqueous media, poor bioavailability, instability and toxicity. Hence, nanoparticles open new avenues to improve the drug delivery and reduce toxic effects[42].

1.11 GREEN NANOTECHNOLOGY AND APPLICATIONS

Nanotechnology has been shown to influence medical advancement by promoting the delivery of drugs, enhancing the drug's effectiveness, improving its absorption, safety and reducing harmful side effects. Most of the active organic compounds are shown to have insolubility in aqueous media, low bioavailability, instability and toxicity[39].

The term 'Green Nanotechnology' refers to the use of technology to enhance sustainability and eco-friendly environment. The parts of the plants are used to synthesize nanoparticles from metal salts. Metals like Ag, Au, Fe, Pt, Pd, and Cu are commonly used to synthesize nanoparticles. The biologically active compounds derived from microorganisms (both living and dead), herbal extracts, animal extracts etc., have been found to be biologically compatible as they possess reducing capability. These are used to produce metal nanoparticles with effective therapeutic potential. Till now, anti-cancer, anti-microbial, anti-anaemic, anti-arthritic, anti-diabetic, antioxidant properties of green nanoparticles have been established[43,44]. The green synthesis is preferred as it is environmentally friendly, safe and cost effective.

Development of metal nanoparticles by the green synthesis process has gained the attraction of many researchers. Metals in their bulk form, significantly differ from their properties in nanoscale dimension. When conjugated with biologically active compounds, metals and their nanoparticles exhibit the active potential of the compound in the human body[45].

The synergistic impacts of the nanoparticle and conjugated mixes are additionally observed. The extracts selected for green synthesis have been known to possess medicinal values. Synthesizing the herbal extracts into nanoparticle conjugation makes them more effective.

Nanotechnology focusses on the synthesis of nanoparticles by two common methods, namely, Chemical synthesis and Green synthesis. The importance of

nanotechnology in research field emphasis on the synthesis of nanoparticles with different chemical compositions, particle size, surface area and morphologies. The nanoparticles are synthesized using chemical methods that involve chemical reduction with different metals and chemicals. Chemical method of synthesis of nanoparticles involves the use of toxic solvents, high pressures and high temperatures. In Green synthesis, phytochemical extracts of different parts of the plant have been proven to provide a vast scope for new drug discoveries[45,46].

Many papers have reported the synthesis of nanoparticles using the extracts of the plants viz. *A. polystachya, Cochlospermium religiosum, Pisonia grandis. Amoora rohituka, Coriander sativum*, etc., and metals like silver, gold and iron. The characterization of the synthesized nanoparticles using various sophisticated techniques like UV-Vis, FTIR, XRD, SEM and PSA plays a major role in assessing the physical and chemical stability of the nanoparticles[39,40].

Particle size is of central significance for pharmacological activity and stability of the nanoparticles while structuring and designing the targeted drug delivery systems. Smaller the particle size, the greater is the ability of the nanoparticles to target the cells and tissues. Bigger particle size may cause body retention and poor clearance. Along these lines, one needs to understand the size of the nanoparticles that will exhibit the required pharmacological action[41,42].

1.12 SILVER AS AN ANTIMICROBIAL

Silver has been known for its antimicrobial properties by the ancient Greeks and Romans who used silver particles to fight infections. But its use had decreased due to the arrival of new antibiotics. In recent years, multi drug resistance to antibiotics has led to new interest in the use of silver as an anti-microbial agent. Silver is proven to be an anti-microbial in various applications. Silver ions and silver-based compounds have shown high biocidal effects on microorganisms. Silver used in the synthesis of nanoparticles has shown to be an alternative to the development of bactericides[47,48]. Physical and chemical properties of the AgNPs synthesized from herbs have been shown to interact in different inexplicable ways with the biological system[42].

Although numerous toxicological studies have been conducted and articles published on nanoparticles, it is still difficult to draw any definite conclusions about their toxicity. A number of experiments has been carried out without a thorough characterization and description of the nanoparticles and solvents used under different experimental conditions. So far it is not clear to which degree the obtained silver ions show toxicity[39]. Although the toxicity of silver ions (chemically synthesized) is understood, determination of the dose at which AgNPs cause toxic effect in a biological cell is a major criterion. AgNPs must be synthesized by biological methods using specific plant extracts to minimize toxicity.

Several reports have demonstrated that antimicrobial activities of silver nanoparticles are dependent on the size, shape, and stabilizing agents of nanoparticles.

The antibacterial activities increased with size reduction of silver nanoparticles[48,49]. Aggregation of nanoparticles causes reduction in antibacterial activities of silver nanoparticles. Hence, combining nanoparticles with stabilizers prevents aggregation and retains silver nanoparticles' antibacterial activities.

The plant chosen for the study is *Aphanamixis polystachya* (Wall) Parker [Syn *Amoora rohituka* (Roxb.) Wight & Arn.] known in Sanskrit as Lohita. It is commonly known as Amoora, belonging to the family Meliaceae. The stem barks of *A. polystachya* are known to be traditionally used in the treatment of tumors, cancer, skin and spleen disorders, leprosy, diabetes, ophthalmology, intestinal worms, jaundice and rheumatism[50,51].

The extensive literature survey revealed the presence of limonoids, tannins, flavonoids, glycosides, and alkaloids from the stem barks, leaves and fruits of the plant *A. polystachya*. Pharmacological activities like cytotoxicity, anthelmintic, hepatoprotective, antimicrobial, and antirheumatic have been reported[50,52,53]. Triterpenoids, Flavonoids, Limonoids have proven to possess anti-cancer activity[54-56].

The present investigation was undertaken to synthesize nanoparticles, characterization, phytochemical investigation, formulation of silver nanosuspensions and cytotoxic studies of the methanolic extract of the root barks of *A. polystachya* to justify its claim in the treatment of cancer. The study substantiates the new light on the medicinal value of this plant, leading to new panoramas for the development of medicine.

PLANT PROFILE

"The mind is not a vessel to be filled but a fire to be kindled."

2.0 PLANT PROFILE

Fig 2: *A. polystachya* Plant

Fig 3: Fruits of *A. polystachya*

Fig 4: Bark of *A. polystachya*

Fig 5: Leaves of *A. polystachya*

Fig 6: Roots of *A. polystachya*

2.1 PLANT DESCRIPTION[57-59]

A. polystachya (Wall) Parker [Syn *Aglaia polystachya* Wall., *Amoora rohituka* (Roxb.) Wight & Arn.], commonly known Amoora, belonging to the family Meliaceae. In Sanskrit it is known as Rohituka. It is a large, beautiful tree that holds green leaves throughout the year, with an umbrella shaped or thick, spreading crown. It has a straight cylindrical ball up to 15 m in height and 1.5-1.8 m in girth distributed in the sub-Himalayan regions. In North India, the bark of the plant, *Tecoma undulata is* used for *Rohituka.* The Ayurvedic formulary of India says that *A. polystachya* can be used as a substitute for *T. undulata***.**

2.2 SCIENTIFIC CLASSIFICATION [59,60]

Kingdom	Plantae
Phylum	Magnoliophyta
Class	Magnoliospida
Order	Sapindales
Family	Meliaceae
Genus	Aphanamixis
Species	*Aphanamixis polystachya*

2.3 VERNACULAR NAMES [57,59,60]

- Common name Pithraj Tree
- Hindi Harin-hara
- Marathi Rakhtharohida
- Bengali Tiktaraj
- Sanskrit Rohitaka, Lakshmi, Saptavha,
- Kannada Mukhyamuttage
- Malayalam: Cemmaram
- Tamil Malampuluvan, Semmaram
- Telegu Sevamanu

2.4 DISTRIBUTION OF THE PLANT[57,60-62]

A. polystachya is native to temperate Asia, tropical China, Indian subcontinent-Peninsula, North east India, Bhutan, Sri Lanka, Myanmar, Thailand, Malaysia, Indonesia, Papua, New Guinea and Philippines. In India, it is found distributed in the Sub-Himalayan tract from the Rapti river eastwards, Sikkim up to 6000 ft., Assam, Burma, Chota Nagpur, Konkan, W. Ghats and adjoining hill ranges from the Poona district southwards to Tinnevelly up to 3500 ft.

2.5 STUDY OF *A. POLYSTACHYA*

2.5.1 Characteristics of Meliaceae Family [57,61,62]

The Meliaceae family is a flowering plant consisting of shrubs and trees of the order spindles. They are characterised by alternate, usually pinnate leaves without stipules. Being mostly bisexual and bearing flowers in panicles, cymes, spikes, or clusters. Most of the species are evergreen, but few are deciduous present in both, dry or winter seasons. The family includes 53 genera and 600 known species, with a pantropical distribution.

2.5.2 Morphological Study [57,63,64]

Leaves

An evergreen tree 9-18 m. high, bearing large imparipinnate leaves, 30-75 cm long, spiral, clustered at twig ends, stipules absent; opposite leaflets (4-8 pairs); elliptic oblong, glabrous on both surfaces, very inequilateral, obtuse or acute at the base; oblong lanceolate, apex acuminate, base asymmetric and margin entire.

Flowers

Inflorescence axillary (sweetly aromatic), flowers on an unbranched axis, Male flowers in panicles of spikes or racemes. Female flowers in long spikes. Calyx lobes 5, Petals 3,

deeply imbricate in bud. Stamens usually 6, included. Ovary is hairy, ovoid, tomentous, 3 celled, cells 2-ovuled; stigma large, 3-grooved.

Fruits

Infructescence arranged on unbranched axis, fruit 20.0-40.0 mm long, yellow when young or pale red, not spiny, slightly fleshy, simple, dehiscent, capsule. Flowering month October –April.

Seeds

Oblong with scarlet aril and globous. Seeds are either winged and usually attached to a large woody columella or unwinged usually with a fleshy arillode or sarcotesta, rarely with a woody or corky sarcotesta.

Trunk and Barks

Trunk longitudinally fissured, bark up to 1 cm thick. The outer surface is blackish grey in colour, while the inner surface is dark brown. Bark is rough due to the presence of numerous small projections. The bulk of bark is composed of parenchyma cells containing starch and colouring matter.

Roots

Roots are woody brown in colour, covered with striated reddish brown scaborous bark.

Branches, Branchlets and Twigs

Branches pubescent, the first twigs yellow in colour, tomentous than glabrescent, terminal bulge densely covered with yellow hair.

Diagnostic Characters

Leaves are paripinnate and imparipinnate crowded at the apex of the branches. Leaflets opposite, base acute and asymmetrical, flowers polygamous, fruit a capsule and seeds scarlet aril.

2.5.3 Cultivation Aspects [57, 61,62,63]

A. polystachya can be propagated by seed. The seeds are collected from the branches or beneath the tree. Seed germination ranges from 80-90% in 20-22 days after sowing the seeds. The seeds lose their viability in 2-3 months. Fruits are collected essentially when ripe during Jan-June. The seeds are removed from the capsule and collected for sowing. The seeds are oily and perishable. Sowing of fresh ripe seeds in shady moist conditions give best results. Shade is required at the early stage and later the plant needs to be protected from excessive sunlight. Planting of 1-2-month-old seedling can also be taken up for propagation.

2.5.4 Chemical Constituents [57-59,63]

The chemical constituents present in *A. polystachya* can be categorised as terpenes, sterols, flavonoids, flavonoid glycosides, limonoids, alkaloids, glycosides and saponins.

- **Triterpenoids** Aphanamixin, Aphananin, Aphanamixinin, Rohitukine, Dregeanin, Rohituka 1-9, Polystachin, Prieurianin acetate, Prieurianin, Amoorinin, Dammer-(20:21)-ene-(24:25)-epoxy-3b-O-a-L-rhamnopyranosyl-(1→4)-b-xylopyranoside, Betulin-3b-O-b-D-xylopyranoside, Amoorinin-3-O-a-L-rhamnopyranosyl-(1→6)-b-D-glucopyranoside, Kihadalactone, Dihydroamoorinin, Dregeana, Aphanamolide A-B, Dregeana 1, Tr-B, Aphanamixoid A-B, Aphapolynin A-I, Aphanalide A-H, Polystanin A-D, Aphanamolide C.
- **Sesquiterpenoids** 6b,7b-Epoxyguai-4-en-3-one, 6b,7b-Epoxy-4b,5 dihydroxyguaiane
- **Diterpenoids** Aphanamixol
- **Flavonoids** 8-C-Methyl-quercetin-3-O-b-Dxylopyranoside, Dihydrorobinetin-7-b-D-glucopyranosyl-a-Lrhamnopyranoside, 8-Methyl-7,20,40-tri-O-methylflavanone 5-O-L-rhamnopyranosyl-(1→4)-b-D glucopyranosyl-(1→6)-b-D glucopyranoside, 8-C-Methyl-5,7,30,40-tetrahydroxyflavone 3-O-a-L-arabinopyranoside.

- **Sterols** Stigmasta-5, 24(28)-dien-3b-O-b-Dglucopyranosyl-O-a-L-rhamnopyranoside, Poriferasterol 3-O-a-L-rhamnopyranoside, b-Sitosterol, Stigmasterol, Ergosta-4,6,8(14),22-tetraen-3-one.
- **Alkaloids** Rohitukine, Ficine and Isoficine
- **Lignans** Polystachyol, Lyoniside and Nudiposide

Fruit shell contains triterpenes, aphanamixin. Bark contains tetra nortriterpene, aphanamixinin. Leaves contain diterpene, alcohol, aphanamixol and β-sitosterol. Limonoids, rohitukine, polystachin, alkaloids, glycosides and saponin are found in seeds. The roots have been reported to contain a chromone and three flavonoid glycosides.

2.5.5 Ethnobotanical Uses [57,59,61,65,66]

- The bark of *A. polystachya* is astringent, anthelmintic, used to treat tumours, cancer, cardiac, hepatic, skin and spleen diseases, leprosy, diabetes, intestinal worm, jaundice and rheumatism.
- Leaves are used by tribal healers of Western Ghats of India to ameliorate cancer.
- Stem bark is used in the treatment of breast cancer.
- Pounded bark is used as topical application in rheumatism.
- Seed oil is used to treat rheumatism.
- The decoction from the root bark is used to treat enlargement of glands, liver, spleen disorders and corpulence.
- Seeds have anthelmintic, laxative effect and are used to treat ulcers.
- Infusion of the plant mixed with honey is used to treat skin disorders.
- Various parts of the plant possess analgesic, antimicrobial, antioxidant, antitumour, CNS depressant, hepatoprotective and membrane stabilizing activities.

2.5.6 Scientifically Proved Pharmacological Activities of *A. polystachya* [50-54,67-69]

- Evaluation of the cytotoxic and anthelmintic activities of bark extracts of *A. polystachya* (Wall,) using the brine shrimp lethality test method and time of paralysis on earthworms respectively.
- Evaluation of the cytotoxicity effects of *Amoora rohituka* and *chittagonga* on pancreatic and breast cancer cells using the MTT assay method.
- Evaluation of the extract of *A. polystachya* (Wall.) Parker Leaves for their anticancer activity. The study was carried on T47D breast carcinoma cell lines and HeLa human cervical carcinoma cell lines to assess the *in vitro* anticancer activity. The *in vivo* anticancer activity was studied on EAC cell lines.
- Antibacterial activity and free radical scavenging potential of the leaves of *A. polystachya* (wall.) R.N. Parker using DPPH assay.
- Hepatoprotective activity on rats were investigated using the *A. rohituka* suspension.
- Evaluation of antineoplastic activity of Rohituka obtained from *A. polystachya* in Hela Cells and their correlation with clonogenicity and DNA Damage.
- Evaluation of hepatoprotective activity from the components isolated from the bark of *A. polystachya*.
- Evaluation of the *A. polystachya* bark by *in vitro* and *in vivo* antioxidant activity for the treatment of liver, spleen, arthritic and tumour disorders.

OBJECTIVE

"Research is to see what everybody else has seen, and to think what nobody else has thought."

3.0 OBJECTIVE

It is well known from the previous research that various parts of the plant of *A. polystachya* have exhibited anti-cancer activity. However, the root of this plant has not been explored. Hence, there is a need for evaluation of the role of the components of the roots to explore the possibility for anti-cancer activity.

The investigation had the following objectives:

- Prepare a stable methanolic extract from the root bark of *A. polystachya*.
- Isolation of the phytochemical constituents from the methanolic extract of the root bark of *A. polystachya.*
- Synthesis and characterisation of silver nanoparticles from the methanolic extract of the root bark of *A. polystachya.*
- To formulate the silver nanosuspension to target breast cancer.

In order to accomplish the aforementioned objectives, the following investigations were proposed:

1. Collection and authentification of the plant material. Extraction and phytochemical screening of the methanolic extract of the root bark of *A. polystachya.*
2. Isolation and characterisation of phytoconstituents from the methanolic extract of the root bark of *A. polystachya.*
3. *In-vitro* cytotoxic study of methanolic extract of the root bark of *A. polystachya* on MCF-7 and MDA-MB231 cell lines.
4. Green synthesis and characterisation of AgNPs from the methanolic extract of the root bark of *A. polystachya*
5. Cell cycle apoptosis, Elisa & Gene expression, analysis of AgNPs of *A. polystachya.*
6. Preparation and *in vitro* cytotoxic activity of AgNS of *A. polystachya*.
7. Free radical scavenging activity of methanolic extract, AgNPs and AgNS of *A. polystachya.*
8. Comprehensive analysis of resulting data to explore the potential of AgNS of *A. polystachya* in the treatment of breast cancer.

REVIEW OF LITERATURE

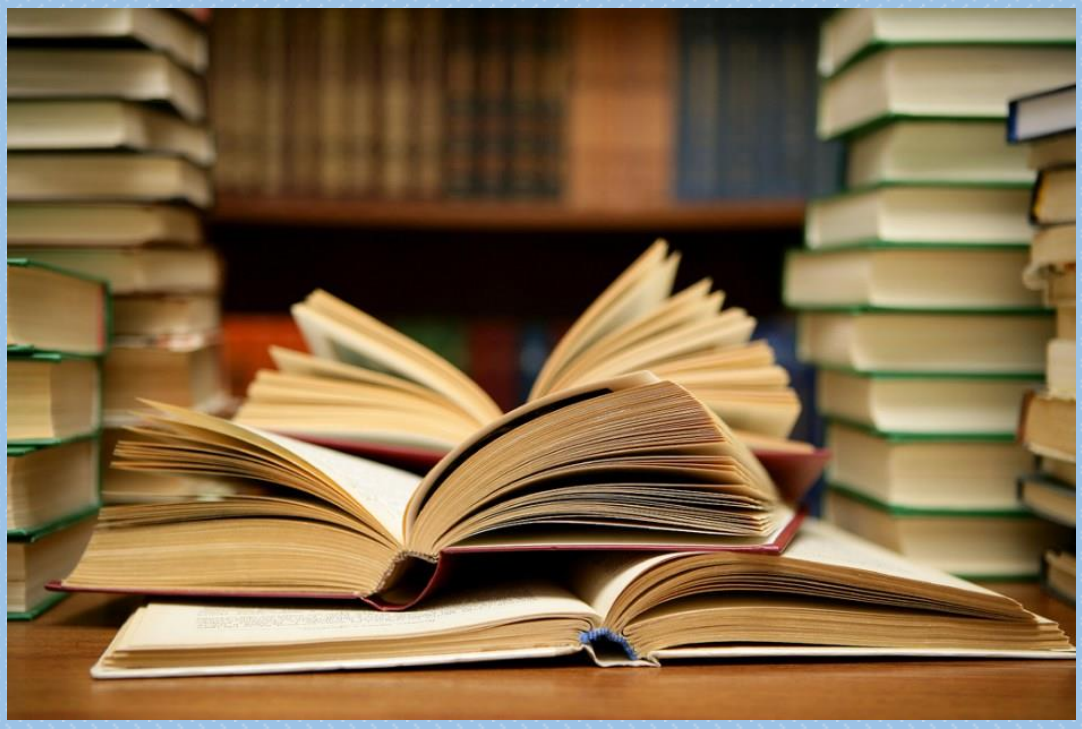

"Imagination is the highest form of Research."

4.0 REVIEW OF LITERATURE

1. Liza Meutia Sari *et al.,* (2019)[70] reported the ability of areca nut to induce apoptosis and studied evaluation and comparison of Caspase -3 activity at 24 and 48 h time intervals in oral cancer cell lines (HSC-2 and HSC-3). Flow cytometry was utilised for the quantification of the cells undergoing apoptosis and expressing the caspase-3 enzyme for 24 and 48 h. The results of flow cytometry on HSC-2 cells indicated that areca nut significantly induced late apoptosis activity after 24 and 48 h exposure. In case of HSC-3 cells, a significant increase ($P<0.01$) in the percentage of early apoptosis after 24 h and late apoptosis at 48 h was observed. It was reported that treatment with ethanolic extract of areca nut (IC_{50} 77 µg/ml) for 48 h inhibited the growth of MCF-7 cells as good as 13-84 %. Caspase-3 activity in both the cells increased on exposure to areca nut after 24 and 48 h. The study reflected that areca nut could be considered as a potential anticancer agent through its capability in inducing a caspase-dependent apoptosis.

2. Zhou C. *et al.,* (2018)[71] showed that knockdown of STAT3 in human oesophageal carcinoma cell lines (ECA-109) induced noticeable apoptotic morphological changes like cell shrinkage, apoptotic vacuoles, membrane blebbing time-dependently and were tested through various techniques like DNA ladder, TUNEL assay and Annexin V-PI staining. The induction of G1 phase cell cycle arrest of ECA-109 cells were shown by cell cycle phases determined by a flow cytometry study. Decreasing content of c-Myc and cyclin

D1 in protein levels were reported. Furthermore, they concluded that knockdown of STAT3 could induce the apoptosis and G1 cell cycle arrest in oesophageal carcinoma ECA109 cells and inhibited the migration ability of the cells.

3. Sharma G *et al.,* (2018)[41] reported ecofriendly method to synthesize AgNPs using the aqueous extract of *Coptidis rhizome*, where the silver ions were reduced to silver nanoparticles. The anti-microbial property of AgNPs were evaluated using turbidity measurements. Time and concentration for conversion of silver ions into AgNPs were optimized using UV-absorbance spectroscopy and Inductively coupled Plasma spectroscopy (ICP). The biosynthesized AgNPs depicted a peak at 420 nm in UV-Vis spectroscopy. The ICP analysis showed that the biosynthesis were achieved within 20 min. The microscopic images confirmed that the synthesized nanoparticles were of spherical shape and the average diameter was less than 30 nm. The XRD analysis revealed size and crystalline nature of the nanoparticles. Effective anti-bacterial activity was observed against *E. coli* and *S. aureus* from the biosynthesized AgNPs proving them as potent antibacterial agent.

4. Shanker K. *et al.,* (2017)[42] investigated the oral toxicity and *in vitro* anti-diabetic activity of the silver nanoparticles synthesized from the seed extract of *Psoralea corylifolia*. The herbal AgNPs were subjected to characterization techniques like XRD, EDX, TEM and DLS to determine the crystallinity, size, shape and elemental

composition. Inhibition of protein tyrosine phosphatase 1B (PTP1B) enhances insulin action in mice. PTP1B assay was performed to determine the PTP1 B inhibitory effect of the herbal AgNPs of the seed extract of *P. corylifolia*. The particle size of the AgNPs were in the range of 18-20 nm. LD_{50} studies conducted on albino mice did not show any mortality. The *in vitro* anti-diabetic activity of the synthesized AgNPs showed 37.16 % of inhibition of PTP 1B enzyme, while the chloroform extract showed an inhibition of 32.09 % and hexane extract showed partial inhibition of 26.08 %. The studies clearly revealed that the synthesized AgNPs were found to be non-toxic and safe, exhibiting potential *in vitro* anti-diabetic activity.

5. Banerjee P. *et al.*, (2017)[72] carried out the synthesis of AgNPs and also investigate its anticancer potential against breast cancer using the leaf extract of M*entha arvensis*. The metallic nanoparticles were characterised by UV-Vis, DLS, FTIR, XRD, EDXRD, AFM and TEM analysis. The results revealed the formation of spherical nanoparticles with a size range of 3-9 nm. Cell survival of nanoparticles (treated and untreated cells) were studied by MTT assay. The synthesized AgNPs exhibited significant cytotoxicity at the concentration of 6.25 µg/ml against MCF7 and MDA-MB-231 breast cancer cells which were comparable with chemically synthesized sodium borohydrate AgNPs.

6. Mohanta YK. *et al.,* (2017)[73] investigated the biosynthesis of AgNPs using aqueous leaf extract of *Erythrina suberosa (Roxb.)* to investigate the presence of phytoconstituents, antimicrobial, antioxidant and cytotoxic activity. The AgNPs were characterised by UV-Vis spectroscopy, DLS, ATR-FTIR and TEM analysis. The phytochemical screening of the leaf extract revealed the presence of flavonoids, tannins, phenolic compounds, glycoside and proteins. The AgNPs were evaluated by DPPH free radical scavenging potential using butylated hydroxytoluene (BHT) as the standard having IC_{50} value of 30.04 µg/ml. UV-Vis spectrum revealed absorption peak at 428 nm confirming the biosynthesis of AgNPs. FTIR spectral analysis indicated the presence of polyphenols due to the involvement of -C=C, N-O and OH groups confirming the formation of AgNPs. DLS studies revealed the particle size in the range of 12 -115 nm. TEM studies confirmed the size of the AgNPs in nanoscale. Antimicrobial activity of the AgNPs were reported against the bacterial strains namely, *S. aureus, B. subtilis, E. coli, P. aeruginosa, C. albicans, C. kruseii, C. viswanathii and T. mentagrophytes* using the agar-cup method and broth dilution method. The AgNPs showed maximum zone of inhibition (ZI) of 24 ± 0.8 mm for *P. aeruginosa* by agar-cup method and *S. aureus* showed growth of inhibition of 99.26 % using broth dilution method. AgNPs were studied for cytotoxic activity against A-431 osteosarcoma cell lines. The IC_{50} values for leaf extract, AgNPs and $AgNO_3$ were found to be 106.15 $\pm$ 2.6, 74.02 $\pm$ 2.4, 136.73 $\pm$ 2.02 µg/ml respectively. It was concluded that the AgNPs showed good anticancer and antimicrobial activity.

7. Patil SP. *et al.,* (2017)[74] carried out a diligent study on the green synthesis, antioxidant, antibacterial and cytotoxic effects of AgNPs using terpene rich extract of the leaves of *Lantana camara L.* The synthesized AgNPs were characterised by advanced techniques like UV–Vis spectroscopy, FTIR, XRD and SEM techniques. UV-Vis spectra revealed an absorption peak at 439 nm indicating reduction of Ag^+ ions to Ag^0 due to presence of terpenes present in *L. camara*. FTIR of synthesized AgNPs indicated the capping of compounds with functional groups on the surface of AgNPs using the leaf extract of *L. camara*. XRD studies showed the crystalline structure of the synthesized AgNPs. SEM revealed the spherical geometry with a mean size of 410-450nm without agglomeration. Zeta potential was found to be -15.2 mV, suggesting good stability of AgNPs. Further, synthesized AgNPs exhibited dose dependent antioxidant and good to moderate antibacterial activity against *S. aureus*, *E. coli* and *P. aeruginosa*. Brine shrimp cytotoxicity studies revealed LD_{50} value of 514.50 µg/ml.

8. Mitiku A. *et al.,* (2017)[75] explored the green synthesis, characterization, antibacterial and antioxidant activity of AgNPs using aqueous leaf extract of *Moringa stenopetala.* The AgNPs were characterised by UV-Vis spectroscopy, FTIR and XRD techniques. The average particles size was found to be 11.24 nm. The UV-Vis spectrum of the synthesized AgNPs showed a peak at 412 nm indicating the bioreduction of Ag^+. FTIR spectral analysis indicated the involvement of -C=O, -O-H and -N-H in the formation of AgNPs. XRD revealed the face centred cubic crystal structure of AgNPs with average particle size

of 11.44 nm. The synthesized AgNPs showed stronger antibacterial activity against *E. coli* than *S. aureus* and exhibited better antioxidant activity than the standard ascorbic acid.

9. Otunola G. *et al.,* (2017)[76] investigated the synthesis, characterisation, antibacterial and antioxidant activity from the aqueous extracts of *Allium sativum, Zingiber officinale* and *Capsicum frutescens*. Characterisation of AgNPs were performed using UV-Vis spectroscopy, FTIR, SEM, EDX, TEM and XRD methods. Antibacterial activity of the synthesized AgNPs were evaluated by agar dilution method using Mueller-Hinton agar medium. Antioxidant activity was evaluated by DPPH and ABTS radical scavenging assay. Strong resonance were observed at 375, 400 and 480 nm at 60, 25 and 60 min for the AgNPs of *A. sativum, Z. officinale* and *C. frutescens* respectively. It also revealed that the AgNPs formed rapidly within 60 min and remained stable even after 24 h. SEM analysis of AgNPs revealed crystalline nature of the nanoparticles. The EDX spectra revealed that the AgNPs reduced by the spices have the weight percentage of silver as 45.84 % (*A. sativum), 79.27 % (Z. officinale)* and 57.16 % *(C. frutescens).* TEM analysis exhibited uniform particle size distribution and spherical shape of the AgNPs with average size of 5.28 nm (*A. sativum),* 12.97 nm *(Z. officinale)* and 10.86 nm (*C. frutescens).* FTIR spectra showed the reduction and capping of silver ions into AgNPs. XRD showed that the intensity of peaks reflected high degree of crystalline nature of the AgNPs. The AgNPs showed strong antibacterial activity against all tested bacterial strains for both gram-

positive and gram-negative bacteria. However, *A. sativum* and *C. frutescens* AgNPs exhibited equipotent antibacterial property. DPPH and ABTS assays exhibited potent free radical antioxidant activity. The activity is attributed mainly due to the presence of polyphenolic compounds such as flavonoids, flavanols, proanthocyanidin and phenolics from the selected plants.

10. Jagetia GC. *et al.,* (2016)[67] reported the antineoplastic activity of chloroform extract of the stem bark of *A. polystachya* on HeLa cells using clonogenic and micronucleus assays. An optimum time of treatment of 6 h for the extract were carried out. HeLa cells were treated with different concentrations (0, 5, 10, 25, 50, 75 and 100 µg/ml) of the extract. 72 % cell death was observed at a dose of 100 µg/ml of the chloroform extract of the stem bark of *A. polystachya* in comparison with the control group. Micronucleus assay revealed the IC_{50} value of the extract to be 25 µg/ml. It was also observed that the chloroform extract of the stem bark of *A. polystachya* effectively killed HeLa cell lines by inducing DNA damage.

11. Geetanjali B. *et al.,* (2016)[53] investigated the free radical scavenging and antibacterial activity of the leaf extract of *A. polystachya*. The leaves were successively extracted with hexane, ethyl acetate, methanol, aqueous methanol and water to yield their respective extracts. DPPH free radical scavenging activity were performed using ascorbic acid as the standard drug at concentrations of 1, 10, 50 and 100 µg/ml. Methanolic extract

and aqueous methanolic extract showed maximum inhibition of 87.7 % at 100 µg/ml (due to the presence of polyphenolic compounds). The antibacterial activity of the plant extracts were reported against four pathogenic bacterial strains namely, *S. aureus*, *B. subtilis*, *E. coli*, *V. cholerae* using the broth dilution method and disc diffusion method. The aqueous methanolic leaf extract showed MIC of 4, 5 and 7 mg/ml against *S. aureus*, *B. subtilis*, and *E. coli* respectively in broth dilution method. However, MIC of methanolic extract was 6, 4, 5 and 6 mg/ml against *S. aureus*, *B. subtilis*, *E. coli* and *V. cholera* respectively. Methanolic extract exhibited potent anti-bacterial activity against *S. aureus* (12.22 ± 0.27 mm), *B. subtilis* (13.66 ± 0.33 mm), *E. coli* (10.66 ± 0.33 mm) and *V. cholerae* (12.33 ± 0.32 mm) by disc diffusion method at 500 µg/ml. The aqueous methanolic leaf extract (500 µg/ml) also exhibited significant activity against *S. aureus* (10.88 ± 0.26 mm), *B. subtilis* (12.22 ± 0.40 mm) and *V. cholerae* (12.66 ± 0.7 mm). Hence it was concluded that the leaf extracts of the selected plant exhibited potent free radical scavenging and antibacterial activity.

12. Ahmed S. *et al.,* (2016)[77] carried out a simple and rapid approach for the synthesis and characterisation of AgNPs using UV-Vis spectroscopy, FTIR, DLS, Photoluminescence, TEM techniques and antibacterial activity of the aqueous leaf extract of *Azadirachta indica*. The reaction time and stability of the synthesized nanoparticles were found to be successful. The synthesized AgNPs exhibited efficient antibacterial activities against *E. coli* and *S. aureus*. They concluded that the protocol developed was

rapid, energy efficient, cost effective, and environment friendly. The AgNPs consumed only 15 min for the conversion of silver ions into silver nanoparticles at room temperature without the use of hazardous chemicals.

13. Mona Orangi *et al.,* (2016)[78] investigated the cytotoxic effects of methanolic subfractions of *Scrophularia oxysepala* and the mechanism responsible for cell death in human breast carcinoma (MCF-7 cells) and mouse fibrosarcoma (WEHI-164 cells). Four subfractions (Fa, Fb, Fc, and Fd), yielded from size exclusion by Sephadex-LH20 column chromatography of 60 % and 80 % methanolic fraction were chosen. MTT assay showed that all the subfractions decreased cell viability significantly. The ELISA, TUNEL, and DNA fragmentation assay showed that the antiproliferative effects of all subfractions on cancer cells were correlated with apoptosis, with no noticeable effect on normal cells (L929). qRT-PCR data showed increased caspase-3 and decreased BcL-2 expression in cancer cells at IC_{50} concentrations (52.9 and 61.2 µg/ml) after 24 h. The methanol subfractions of *S. oxysepala* induced apoptosis (MCF-7, WEHI-164 cells), may be regarded as a source of natural anticancer agents.

14. Thilagavathi T. *et al.,* (2016)[79] interpreted the green synthesis of AgNPs from the ethanolic extract of *Limonia acidissima* by the bioreduction of silver nitrate using different concentrations of plant extract. Preliminary phytochemical screening was performed to identify the presence of various phytoconstituents like flavonoids, sterols,

polyphenols and terpenoids. The UV-Vis spectrum showed a peak at 450 nm indicating the formation of nanoparticles. SEM confirmed spherical shape of the nanoparticles. The ethanolic leaf extract exhibited significant antioxidant activity.

15. Mahendran G. *et al.,* (2016)[80] reported the green synthesis of AgNPs using fruit aqueous extract of *Nothapodytes nimmoniana*. The synthesized nanoparticles were characterised by UV-Vis spectroscopy, XRD and SEM techniques. Antioxidant, anticancer and antimicrobial activities of AgNPs were also evaluated. UV-Vis analysis revealed that the AgNPs exhibited a sharp peak at 416 nm indicating the formation of nanoparticles. XRD confirmed the peaks at 111, 200, 220 and 311 indicating the face centred cubic structure of the crystals. SEM confirmed the spherical shape of the AgNPs with average particle size ranging from 46-235 nm. DLS analysis confirmed the average particle size distribution profile and enveloping of the capping agent around the metallic particles. The zeta potential was -23.1 mV. The total phenolic content of the fruit extract (194.56 ± 3.15 mg) was found to be higher when compared to AgNPs. The maximum content of tannins and flavonoids of the fruit extract were found to be 48.20 ± 2.03 mg and 283.33 ± 7.18 mg respectively. Antioxidant activity by DPPH, ABTS, FRAP, metal chelating and phophomolybdenum activities along with antibacterial activity were performed against *B. subtilis, P. aeruginosa, K. Pneumoniae, S. aureus* and *E. coli.* Fruit extract exhibited potent radical scavenging activity when compared to AgNPs. The cytotoxicity determined by MTT assay revealed that the synthesized AgNPs inhibited

proliferation of HeLa cells with IC_{50} of 87.32 ± 1.43 µg/ml. The AgNPs exhibited enhanced antibacterial activity.

16. Upendra N. *et al.,* (2016)[81] reported the extraction of the flavonoids from the apple extract, synthesized them into AgNPs and ultimately loaded the nanoparticles into hydrogels. Dilute ammonia and magnesium ribbon test confirmed the presence of flavonoids. The synthesized AgNPs were characterised by UV-Vis spectroscopy, particle size, surface morphology and zeta potential. The pH, viscosity, spreadability, porosity, *in vivo* release, *ex vivo* permeation, antibacterial (*E. coli* and *S. aureus*) and antioxidant activity (DPPH assay) were evaluated for AgNPs loaded hydrogels. Good dispersion of AgNPs were observed in SEM images. Hydrogels displayed *in vitro* release of 98.01 ± 0.37 % upto 24 h. E*x-vivo* permeation of 98 ± 0.24 % up to 24 h was observed. Hydrogel effectively inhibited the growth of microorganisms suggesting significant antibacterial activity. Free radical inhibition was 75.16 ± 0.04 %, indicating high antioxidant activity.

17. Phull AR. *et al.,* (2016)[82] synthesized AgNPs from the methanolic extract of the rhizomes of *Bergenia ciliate* and studied their biological evaluation. The formation of metallic nanoparticles was confirmed using UV-Vis at 425 nm. FTIR and SEM studies revealed spherical nanoparticles having average particle size of 35 nm. The synthesized nanoparticles have shown higher total antioxidant activity of 60.48 ± 2.2 µg/ml in comparison with crude extract (38.8 ± 1.08 µg/ml). The nanoparticles have shown LD_{50}

of 33.92 µg/ml using brine shrimp lethality test. The metallic nanoparticles showed higher antibacterial activity against *Micrococcus luteus, Staphylococcus aureus, Bordetella bronchiseptica* and *Enterobactor aerogens* in comparison to the extract.

18. Nazish J. *et al.,* (2015)[46] gave an account of the nanosuspension approach for increasing the aqueous solubility and bioactivity of the seeds of three plant extracts (*Silybum marianum, Elettaria cardamomum* and *Coriandrum sativum*). They were formulated into nanoparticles by nanoprecipitation technique using polyvinyl alcohol (1.5 % w/v) as a stabiliser. SEM was used for characterisation. The anti-oxidant activity of formulated nanosuspension were assessed. Nanosuspensions of the three chosen plant extracts *S. marianum, E. cardamomum* and *C. sativum* exhibited particle size in the range of 446.1 ± 112.6, 456.63 ± 339.2 and 432.1 ± 172.8 nm, respectively. Most of the particles were found to be spherical and had smooth topology. Free radical scavenging potential against DPPH and superoxide free radical scavenging assays (IC_{50} 0.59 ± 0.01 and 0.81 ± 0.11 mg/ml) were observed in *C. sativum* nanosuspension. *S. marianum* nanosuspension exhibited DPPH radical scavenging activity (IC_{50} 0.34 ± 0.02 mg/ml). It was concluded that nanosuspension of herbal medicines potentiates the antioxidant activity.

19. Saminathan K. *et al.,* (2015)[83] published the synthesis and its antibacterial activity of AgNPs using leaf extracts of *Eclipta alba*. The synthesized metallic nanoparticles

exhibited an average particle size of 60 nm. The antibacterial activity revealed inhibitory effect against *S. aureus* (8 mm*), Pseudomonous spp.,* (6 mm*), P. vulgaris* (6 mm*),* and *S. typhi* (7 mm*).*

20. Mollick M. *et al.*, (2015)[84] testified an ecofriendly approach to synthesize AgNPs from the pulp extract of *Abelmoschus esculentus* and studied the cytotoxicity, apoptosis and antimicrobial activity. The phytochemicals present in *A. esculentus* pulp extract were used as a reducing and stabilizing agent for the synthesis of AgNPs. The AgNPs were characterized using various techniques like UV-Vis Spectroscopy, FTIR, XRD, TEM, SAED and DLS. A sharp peak at 403 nm confirmed the synthesis of AgNPs. FTIR studies justified the stabilization of AgNPs with phytochemicals. XRD studies revealed the formation of face centered cubic structure, while DLS measurements confirmed the average particle size of AgNPs ~ 21.29 nm. TEM studies revealed the spherical shape and uniform distribution of AgNPs without agglomeration. The crystalline nature was confirmed by SAED studies. The cytotoxicity of the synthesized AgNPs were determined by MTT assay in Jurkat cells at concentrations of 0, 1, 10, 25 and 50 µg/ml for 24 h. The IC_{50} value of AgNPs were found to be 16.15 µg/ml. Caspase-3 activity significantly increased ($p<0.05$) in comparison with untreated cells. Chromatin condensation and fragmentation were observed in the treated group at the concentration of 16.15 µg/ml. The studies revealed that AgNPs of the pulp extract of *A. esculentus* caused cell death due to apoptosis. Significant antibacterial activity against *B. subtilis* (33mm), *B. cereus* (28mm),

E. coli (19mm), *M. luteus* (40mm) and *P. aeruginosa* (26 mm) were reported at the concentration of 0.2 mg/ml.

21. Firdhouse J. *et al.,* (2013)[85] studied the biosynthesis of AgNPs using aqueous extract of *Alternanthera sessilis* and studied the cytotoxic activity by MTT assay against breast cancer cells (MCF-7 cell line). The results revealed that the cytotoxic effect of synthesized AgNPs by MTT assay against MCF-7 cell lines exhibited significant cytotoxic activity with IC_{50} value of 3.04 µg/ml. TEM analysis confirmed the spherical particles within the size range of 10-30 nm. It was concluded that 25 µg/ml of mediated AgNPs showed significant apoptotic activity when compared to the standard drug, cisplatin.

22. Krishnamurthy P. *et al.,* (2015)[86] reported the anti-cancer potential on the isolated molecules/fractions from the leaf extract of *Moringa oleifeira.* The n-hexane, chloroform, ethyl acetate and methanol extracts of *Moringa oleifeira* and fifteen fractions (F1-F15) of ethyl acetate extract were subjected for their *in vitro* and *in vivo* anti-cancer activity using Hep-2 cell lines and Dalton's lymphoma ascites model in mice. The F1 fraction showed significant cytotoxic effect in Hep-2 cell lines with IC_{50} value of 12.5 ± 0.5 µg/ml. *In vivo* studies revealed that, at a dose of 5 and 10 mg/kg, p.o indicated significant reduction in body weight and increased the mean survival time when compared to the control group. The results obtained were comparable to the standard drug, 5-flurouracil.

23. Bhatia D. *et al.,* (2015)[87] explored the apoptosis inducing potential of aqueous extract of aerial parts of O*riganum dayi* and *Ochradenus baccatus*. HepG2 cells were used in the study at varying concentrations of 0, 2 and 5 mg/ml for 24 and 48 h. V-fluorescein isothiocyanate binding assay and flow cytometry were used to measure the cell apoptosis. Semi quantitative rt-PCR was used to measure the expression levels of apoptosis related genes. Both the extracts have shown apoptotic effect for 48 h through modulation of mitochondrial pathway. The authors concluded that the selected desert plants help to develop promising remedy against carcinogens in humans.

24. Yin Sim Torr *et al.,* (2015)[88] recorded the molecular mechanisms involved in ethyl acetate extract of *Dillenia suffruticosa* (EADs) induced apoptosis and to identify the components present in the extract. EADs promoted oxidative stress in MCF-7 cells leading to cell death due to pre-treatment with antioxidants, α- tocopherol and ascorbic acid by inducing the cytotoxicity of the extract ($P<0.05$). DCFM-DA assay revealed that treatment with EADs attenuated the generation of intracellular reactive oxidative species (ROS). Apoptosis induced by EADs was not inhibited by the use of caspase-inhibitor Z-VAD-FMK indicating that the cell death is caspase independent. The use of JC-1 dye indicated that EADs caused disruption in the mitochondrial membrane. The related pathways involved in EADs induced apoptosis were determined by GeXP multiplex system and western blot analysis. The elevated Bax/BcL-2 ratio and the depolarisation of mitochondrial membrane potential indicated that EADs-induced apoptosis is

mitochondria-dependent. Oxidative stress related apoptosis by EADs was mediated by inhibition of AKT and ERK and activation of JNK. Column chromatography of EADs resulted in six compounds including 3-epimaslinic acid, Kaempferal, Kaempferide, protocatechuic acid, gallic acid and β-sitosterl-3-o-β-D glucopyranoside. Cytotoxicity of the isolated compounds were analysed by MTT assay. Gallic acid was proved to possess cytotoxic effect against MCF-7 cell lines with IC_{50} of 36 ± 1.7 µg/ml ($P<0.05$). Thus, EADs has the potential to develop as an anti-cancer agent against breast cancer.

25. Gaddala B. *et al.*, (2014)[43] recorded the synthesis of AgNPs using the leaf extract of *Abrus precatorius* and were characterised by various techniques like UV-Vis spectroscopy, FTIR, XRD, EDAX, SEM and AFM. The synthesized nanoparticles showed characteristic absorbance peaks between 320 - 400 nm. SEM images revealed agglomerated relatively spherical shaped particles. The XRD data revealed particle size range of 35 - 40 nm. Additionally, the biosynthesized nanoparticles of *A. precatorius* were tested for antibacterial activity against *P. aeruginosa, S. aureus, E. coli* and *B. thuringiensis* by disk diffusion method. The results showed maximum anti-bacterial activity against *P. aeruginosa* (24 mm) and minimum against *B. thuringiensis* (19 mm) when compared with the standard drug, ciprofloxacin. It was concluded that the green synthesis of AgNPs is very fast, easy, cost effective and eco-friendly without any side effects.

26. Hegde K. *et al.,* (2014)[52] demonstrated the *in vitro* and *in vivo* anticancer activity of methanolic extract of leaves of *A. polystachya* (MLAP). *In vitro* activity were studied against T47D breast carcinoma cell lines and HeLa human cervical carcinoma cell lines at a concentration of 1000 µg/ml, 500 µg/ml, 250 µg/ml, 125 µg/ml, 62.5 µg/ml and 31.25 µg/ml concentrations. *In vivo* activity against EAC bearing mice cell lines with doses of 200 mg/kg and 400 mg/kg body weight were used for the study. Radio protective activity of the extract was also studied on human breast carcinoma cell lines using UV radiation (15 W, 365 nm), with an exposure time of 15 min, with the cell lines placed at a distance of 3 cm from the radiation. MLAP exhibited significant *in vitro* anticancer activity against T47D (IC_{50} 115.84 µg/ml), and HeLa (IC_{50} 31.48 µg/ml) cell lines and *in vivo* anticancer activity in EAC bearing mice with a potential of radioprotection against UV radiation. The findings justified the traditional use of this plant in the treatment of cancer.

27. Valan *et al.,* (2014)[68] testified the hepatoprotective activity of the ethanolic extract of the bark of *A. polystachya*. Phytochemical findings revealed that the plant contained flavonoids as the major constituent. The R_f values, UV, ^{1}H-NMR,^{13}C-NMR and EIMS spectral studies disclosed that the compound isolated was 5,4'-Dihydroxy 6,8-dimethoxy 7-O-rhamnosyl flavone, named as Aphanamixine possessing hepatoprotective activity.

28. Shweta SS. *et al.,* (2014)[64] reported the extraction of the dried stem bark of *A. polystachya* using petroleum ether, chloroform and methanol as solvents for 48 h. The extracts obtained from these solvents were subjected to phytochemical investigation and HPLC analysis. The results indicated that HPLC was a suitable analytical method to determine β- sitosterol and stigmasterol from the petroleum ether fraction with a retention time of 6.12 and 11.05 min for standard drug and 6.16 and 11.03 min retention time for petroleum ether fraction of methanolic extract of *A. polystachya* using acetonitrile: water (90:10).

29. Vinmathi V. *et al.,* (2014)[89] established a cost-effective and eco-friendly technique for green synthesis of AgNPs using the aqueous leaf extract of *Crataeva nurvala.* Antibacterial and cytotoxic activities were also performed. The metallic nanoparticles were characterized using UV-Vis spectroscopy, SEM and FTIR. The peak at 444 nm confirmed the formation of AgNPs with particle size of 32-38 nm. The AgNPs showed promising antibacterial activity against *S. aureus, P. aeruginosa, E. coli and K. pneumonia.* IC_{50} value of 695.65 µg/ml was reported against MCF-7 human breast cancer cell lines.

30. Sriram T. *et al.,* (2014)[90] reported the green synthesis of AgNPs from the leaf extract of *Psidium guajava* and studied their antibacterial activity. The AgNPs were characterized by UV-Vis spectroscopy, SEM and FTIR techniques. A broad peak at 460 nm with

average particle size of 100-500 nm was observed. The IR value indicated the reduction of silver ions to silver nanoparticles. A strong inhibitory effect was observed against *E. coli* and *S. aureus.*

31. Vega J. *et al.,* (2014)[91] designed a sonochemical synthesis for AgNPs coated with chitosan. The chitosan was treated with sodium hydroxide to neutralise its charge and facilitate its binding and reduction of silver ions. The synthesized AgNPs were characterised by UV-Vis spectroscopy, AFM and DLS. UV-Vis and AFM showed that spherical nanoparticles of diameter 10 nm were obtained. DLS analysis exhibited a polydispersion index of 0.532 indicating several nanoparticle groups of different sizes. The DLS results showed that 98 ± 5 % of the nanoparticles have a diameter ≤ 20 nm and represent 87 ± 5 % of the total volume of particles in the solution. In conclusion, despite having large single dispersion, the evaluated method is simple and feasible in obtaining cost effective AgNPs in quick time.

32. Revathi S. *et al.,* (2014)[92] performed *in vitro* apoptosis studies by DNA fragmentation analysis and clonogenic assay on hydro-ethanolic extract of polyherbal formulation *Chathurmuka chooranam* in Hep G2 cell lines. Gene expression was carried out on tumour suppressor gene p53 by rT-PCR analysis. The results revealed that apoptosis was evident by fragmentation of DNA. The DNA fragmentation assay carried out in Hep G2 cells after treatment with 1000 µg and 500 µg of the hydro-ethanolic extract

of polyherbal formulation, exhibited a characteristic feature of apoptosis due to internucleosomal DNA fragmentation pattern. The fragmented DNA was prominent in Hep G2 cells treated with doxorubicin and hydro-ethanolic extract of polyherbal formulation when compared to the untreated control. It was suggested that the damage may be due to the inhibition of topoisomerase II, a key enzyme in DNA replication, leading to apoptosis.

33. Sung-Hwan Kim *et al.,* (2014)[93] investigated the induction of apoptotic cell death and oxidative stress in cultured cortical neurons in response to the exposure of AgNPs. Apoptosis induced by AgNPs were analyzed using terminal deoxynucleotidyl transferase dUTP nick-end labelling (TUNEL), DNA ladder assay and western blot analysis. AgNPs inhibited the viability of cerebral cortical neurons in a dose and time-dependent manner. DNA fragmentation in AgNPs-exposed cells suggested apoptosis. Western blot analysis demonstrated that cleaved caspase-3 protein expression increased significantly in a time-dependent manner. The findings suggested that AgNPs cause cytotoxicity and neuronal apoptosis through intracellular reactive oxygen species (ROS) production in cultural cortical neurons.

34. Abdel-Aziz M. *et al.,* (2013)[94] carried out the biosynthesis and characterisation of AgNPs from the leaf extract of C*henopodium murale* and evaluated their antibacterial and antioxidant activity. TEM studies revealed the particle size in the range of 30 - 50 nm.

Total Phenolic content of 74.9 ± 0.23 mg/ml and 80.83 ± 0.23 mg/ml were reported for the leaf extract and AgNPs respectively. 12.77 ± 0.07 mg/gm and 14.1 ± 0.12 mg/gm of total flavanoidal content were observed for the leaf extract and AgNPs respectively. DPPH activity revealed IC_{50} value of 13.27 ± 0.12 µg/ml for AgNPs. The synthesized AgNPs showed positive response against *S. aureus* for their antibacterial activity.

35. Ragasa CY. *et al.,* (2014)[95] reported the isolation and structure elucidation of α-copaene along with identification of squalene, polyprenol, β-sitosterol, lutein, and β-carotene from the dichloromethane extract of the leaves of *A. polystachya.* α-copaene was elucidated extensively by 1D and 2D NMR spectroscopy and confirmed by mass spectrometry. The remaining compounds were identified by comparing with the reported values from the literature.

36. Rajasekhar R. *et al.,* (2013)[40] communicated an eco-friendly method for the preparation of gold nanoparticles using aqueous extract of the seeds of *Senna siamea*. The gold nanoparticles were formed using chloroauric acid which was confirmed by UV-Vis spectroscopy at 543 nm. XRD studies revealed the crystalline structure of the nanoparticles, while FTIR analysis showed a prominent peak at 1639 cm^{-1} confirming the secondary structure of protein. Further, the gold nanoparticles were analysed for anti-bacterial activity against *S. aureus* (13 mm), *P. aeuroginosa* (15 mm), *B. subtilis* (18 mm),

E. coli (15 mm) and *K. pneumoniae* (21mm). The maximum anti-bacterial activity were observed against *K. pneumoniae,* followed by *B. subtilis.*

37. **Raihan Khan T. *et al.,*** (2013)[50] gave an account of the cytotoxicity using brine shrimp lethality test and anthelmintic activity with the determination of time of paralysis and death using adult earthworms (*Pheretima posthuma*) at four concentrations namely, 10, 20, 40 and 60 mg/ml of the methanolic bark extract of *A. polystachya.* The study revealed that the methanolic bark extract of *A. polystachya* exhibited mild cytotoxic activity (LC_{50} 26.01 ± 0.013µg/ml) in comparison to the standard vincristine sulphate (LC_{50} 0.8389 ± 0.325 µg/ml). The methanolic extract showed better anthelmintic activity when compared to the standard drug Albendazole (10mg/ml). At concentrations 10, 20, 40 and 60 mg/ml, the methanolic extract of *A. polystachya* exhibited mean paralysis time of 35.66 ± 0.72, 32.66 ± 0.47, 27.66 ± 0.72 and 25.66 ± 0.27 min whereas the standard drug Albendazole exhibited paralysis and death time of 56.20 ± 0.20 and 77.40 ± 0.24 min respectively.

38. Zhang Y. *et al.,* (2013)[56] reported the isolation of a new aphanomolide type limonoid and prieurianin-type of limonoids, Aphapolynin C-1 along with seventeen known compounds from the fruits of *A. polystachya*. The structures were confirmed on the basis of spectral data along with electronic circular dichroism (ECD) calculation, CD exciton chirality, and single X-ray crystallography. The inhibitory effects of the isolates were

tested on lipopolysaccharides (LPS) induced RAW264.7 murine macrophages. Their fungicidal, insecticidal and herbicidal activities were reported. Aphapolynin, Rohituka-15, Aphanomolide A and Aphapolynin A have shown promising fungicidal activity. Aphapolynin-1 and Aphanolide H have shown good insecticidal activity.

39. Lalitha P. *et al.,* (2013)[96] detailed the synthesis of AgNPs using aqueous extract of *Portulaca oleracea*. The AgNPs were synthesized by three different experimental conditions (sonication method, reaction at room temperature and reaction at 75°C) and were characterized by UV-Vis spectroscopy, XRD and SEM techniques. The AgNPs synthesized by sonication method showed a particle size of less than 60 nm with a spherical shape. XRD and FTIR studies confirmed the formation of nanoparticles. They concluded that sonication method was most efficient when compared to the other two experimental conditions.

40. Lalitha A. *et al.,* (2013)[97] reported the synthesis of AgNPs, antibacterial and antioxidant activity from the leaf extract of *Azhadirachta indica.* The synthesized nanoparticles showed a peak at 351 nm with a particle size of 21.07nm. The FTIR results suggested the presence of protein in the extract. The AgNPs showed inhibition against *S. typhi* and *K. pneumoniae*. The leaf extract of *A. indica* exhibited antioxidant activity at a dose of 250µg/ml and 100µg/ml for DPPH and hydrogen peroxide assay respectively.

41. Maliyakkal N. *et al.,* (2013)[98] investigated the cytotoxic and apoptotic effects of ethanolic and aqueous extracts of *Withania Somnifera* and *Tinospora Cardifolia.* Ethanolic extract of *W. Somnifera* at concentrations of 10, 20, 40, 60, 100 µg/ml and *T. Cardifolia* at concentrations of 12.5, 25, 50, 100 µg/ml were subjected to cytotoxic activity against MCF7 and MDA MB 231 cell lines. MTT assay revealed a dose-dependent cytotoxicity with increased sub-G_0 content confirming the induction of apoptosis. Further, studies indicated the arrest in the G2/M phase by the extracts. Aqueous extract of both the plants failed to show cytotoxic activity.

42. Sarkar A. *et al.,* (2013)[99] investigated the crude n-hexane, ethyl acetate and methanol extracts from the leaves of *A. polystachya* for their antimicrobial, antioxidant, cytotoxic and thrombolytic activities. Promising antibacterial effect of methanolic extract were reported against *S. aureus* (9-10 mm), *S. dysenteriae* (10 mm) and *C. albicans* (8.1 mm). The antioxidant activity revealed that methanolic extract have shown highest IC_{50} value of 12.54 µg/ml in DPPH assay, while 39.90 µg/ml were observed by the extract in nitric oxide scavenging assay. Brine Shrimp lethality assay have shown lethal concentration of 20.09, 36.33 and 60.12 µg/ml for n-Hexane, ethyl acetate and methanol extract respectively. A significant thrombolytic activity was observed in all the extracts.

43. Ansari Q. *et al.,* (2013)[100] investigated antioxidant activity of extracts from *Withania somnifera* for its free radical scavenging activity by adopting various *in vitro* methods. The extracts were investigated for the antioxidant activity using DPPH radical scavenging activity, reducing capacity, competition with DMSO, hydroxyl group reducing activity, estimation of total phenol and estimation of ascorbic acid. 83.07 % of scavenging activity was reported in polar flavonoid extract (1mg/ml) by DPPH assay. The measurement of total phenolics by folin - ciocalteau reagent indicated that 20 mg of powdered *W. somnifera* contain 0.115 mg of phenols equivalent of catechol.

44. Yuet YL. *et al.,* (2012)[101] reported the biosynthesis and characterisation of AgNPs using tea leaf extract from *Camellia Sinensis*. The synthesized AgNPs were characterised by UV-Vis spectroscopy, FTIR, TEM and XRD techniques. UV-Vis spectroscopy exhibited absorption peak at 436 nm confirming the synthesis of AgNPs. FTIR studies revealed the presence of proteins as capping agent for synthesized AgNPs. XRD analysis showed face centred cubic structured nanoparticles, while TEM images confirmed the average particle size as 4 nm. They concluded that these synthesized nanoparticles can have potential applications in the field of cosmetics, food and medicines.

45. Geethalakshmi R. *et al.,* (2012)[47] described the synthesis, characterization and antimicrobial properties of gold and silver nanoparticles using Kirby-Baeur method from the root extract of *Trianthema decandra* using chloroauric acid and silver nitrate. Field

Emission Scanning Electron Microscopy (FESEM) analysis of gold nanoparticles confirmed the shapes as spherical, cubical, triangular, circular and hexagonal with a particle size of 33-65 nm, while silver nanoparticles were of spherical form with a particle size of 36-74 nm. Energy dispersive X-ray and FTIR confirmed the presence of metallic silver and gold in the synthesized nanoparticles. The synthesized nanoparticles showed strong antibacterial activity against *S. aureus, S. faecalis, E. faecalis, E. coli, P. aeruginosa, P. vulgaris, B. subtilis, Y. enterocolitica* and *C. albicans*. The gold nanoparticles exhibited zone inhibition of 13.5–15.5 mm, while the silver nanoparticles exhibited zone inhibition of 15.5–20.5 mm. They concluded that the phytoconstituents present in *T. decandra* extract reduce the metallic silver and gold ions in the respective nanoparticles thus reducing the cost of production and input on the environment.

46. **Sasikala A.** ***et al.,*** (2012)[102] chronicled the synthesis and characterization of ecofriendly AgNPs from the leaf of *Cochlospermum religiosum* and studied its activity on bacterial pathogens. The synthesized AgNPs have shown UV-Vis absorbance at 260 nm and the spherical shape varied in the size ranging from 40-100 nm. They exhibited effective inhibitory activity against *Bacillus, E. coli, Pseudomonas, Staphylococcus and Klebsiella.* However, they were highly toxic to *E. coli* and *Staphylococcus* and moderately toxic to *Bacillus, Pseudomonas* and *Klebsiella.*

47. Firdhouse J. *et al.,* (2012)[103] reported synthesis of AgNPs using the ethanolic extract of the leaves of *Pisonia grandis*. The AgNPs were synthesized by three different experimental conditions (room temperature, temperature at 90°C and sonication) and characterized by UV-Vis spectroscopy, XRD and SEM. The AgNPs synthesized by sonication method showed a particle size of less than 150 nm with a spherical shape. XRD studies revealed a sharp peak at 32.3° confirming the formation of nanoparticles.

48. Vanmathi S. *et al.,* (2012)[104] investigated that exposure of *Fusarium oxysporum* to silver ion leading to the synthesis of AgNPs, which were examined using UV-Vis spectroscopy, SEM, XRD, TEM and FTIR techniques. UV-Vis spectrum confirmed the formation of AgNPs. SEM studies showed the formation of stable agglomerates of spherical nanoparticles in the size range of 20-50 nm. XRD pattern showed the crystalline plane of the cubic Ag. FTIR spectrum revealed the stability of the protein structure on binding with the silver ions or AgNPs. The authors confirmed the stability of the synthesized AgNPs for several months in the absence of light.

49. Shameli K. *et al.,* (2012)[105] testified the biosynthesis of AgNPs by using *Curcuma longa* tuber powder extracts. Characterizations of nanoparticles were done by using different methods, including UV-Vis spectroscopy, FTIR, XRD, TEM, SEM and EDXRD techniques. The UV-Vis spectrum exhibited an absorption peak at 415 nm confirming the formation of AgNPs. TEM showed that mean diameter of AgNPs were 6.30 ± 2.64 nm.

Powder XRD method revealed that the particles were crystalline in nature, with a face centred cubic structure. The results concluded that *C. longa* tuber powder extract can play an important role in the bioreduction and stabilization of silver ions to AgNPs.

50. Boucher D, *et al.,* (2012)[106] reported that during apoptosis, hundreds of proteins are cleaved by caspases, most of them by the executioner caspase-3. However, caspase-7, which shares the same substrate primary sequence preference as caspase-3, was better at cleaving poly (ADP ribose) polymerase 1 (PARP) and Hsp90 cochaperone p23, despite having lower intrinsic activity. They identified key lysine residues (K38KKK) within the N-terminal domain of caspase-7 as critical elements for the efficient proteolysis of these two substrates. Caspase-7's N-terminal domain binds PARP and improves its cleavage by a chimeric caspase-3 by ~30-fold. Cellular expression of caspase-7 lacking the critical lysine residues resulted in less-efficient PARP and p23 cleavage compared with cells expressing the wild-type peptidase. They uncovered a role for the N-terminal domain (NTD) and the N-terminal peptide of caspase-7 in promoting key substrate proteolysis.

51. Tamizhamudu E. *et al.,* (2011)[107] designed to synthesize silver and gold nanoparticles from the aqueous leaf extract of *Memecylon edule*. Characterization of silver and gold nanoparticles were done by UV-Vis spectroscopy, FTIR, SEM, TEM, and EDAX techniques. The SEM studies showed that the gold ions were reduced and resulted in particle size in the range of 20-50nm. The TEM studies revealed formation of particle

shapes as triangular, hexagonal and circular in the size range of 50-90nm. EDAX results confirmed the presence of triangular nanoparticles in the absorption peak of 2.30 keV. FTIR analysis confirmed the functional groups in the AgNPs and gold nanoparticles. They concluded that saponins from the aqueous leaf extract of *Memecylon edule* were responsible for the synthesis of the nanoparticles and have a great potential for medical and industrial applications.

52. Hussain J. *et al.,* (2011)[48] gave an account of the effect of aniline concentrations on the growth and size of silver nanocrystals using aniline and silver nitrate as reductant and oxidant, respectively. The synthesized AgNPs were characterized using UV-Vis spectroscopy, TEM and SAED. UV-Vis spectroscopy showed a sharp peak at 400 nm indicating the formation of nanoparticles, while TEM images revealed that AgNPs were roughly spherical and uniform in particle size (average particle size is 25 nm). Plasmon resonance proved the adsorption of aniline and interaction on Ag-nanocrystals through electrostatic interactions between lone pair of electrons ($-NH_2$) and positive surface of AgNPs.

53. Chan LL. *et al.,* (2011)[51] explored the anticancer potential of petroleum ether, dichloromethane and ethanol fractions of *Rohituka* and *Chittagonga*, against MCF-7 and HTB-126 (breast cancer cell lines), Panc-1, Mia-Paca2, and Capan1 (pancreatic cancer cell lines) and Hs68 (human foreskin fibroblast). Each fraction were analysed for

cytotoxicity using MTT assay and label-free photonic crystal biosensor assay. The results revealed that the extracts of C*hittagonga* (Petroleum Ether and Dichloromethane) and *Rohituka* (Petroleum Ether) induced cytotoxicity in MCF-7 cell lines, while the extracts of *Chittagonga* (Ethyl Acetate) and *Rohituka* (Methanol) did not induce cytotoxicity. Significant cytotoxic activity was observed on the extract of *Chittagonga* fractionated with CH_2Cl_2 on HTB126, Panc-1, Mia-Paca2, and Capan-1 cancer cells. It was observed that *Amoora* extracts were not cytotoxic to normal fibroblast Hs68 cells, but to the cancerous cells.

54. Veerasamy R. *et al.,* (2011)[108] reported the eco-friendly biosynthesis and characterization of AgNPs using *Garcinia mangosteen* leaf extract as reducing agent. AgNPs have been characterized using UV –Vis spectroscopy, FTIR and TEM techniques. These synthesized nanoparticles were spherical in shape with an average size of 35 nm and exhibited antimicrobial activity against drug resistant human pathogens.

55. Saklani S, *et al.,* (2011)[109] investigated the antioxidant activity of the crude extracts of *A. polystachya* bark by DPPH and FRAP assays. The IC_{50} values were found to be >25µg/ml with alcohol, 5.33µg/ml with aqueous methanol and >25µg/ml with petroleum ether. *A. polystachya* bark extracts exhibited maximum ferric reducing antioxidant power. Due to the potent free-radical scavenging ability, *A. polystachya* was suggested to be a potential medicine to treat free radical-mediated diseases.

56. Saumya SM. *et al.,* (2010)[110] investigated the free radical scavenging potential as well as total phenolic and flavonoid contents of aqueous extract of *ginseng* and *banaba*. They analysed the total antioxidant activity by TEAC assay, superoxide, hydroxyl, hydrogen peroxide and nitric oxide radical scavenging activities as well as total phenolic and flavonoid contents. The total phenolic contents were 66.83 ± 0.268 and 72.3 ± 0.293 mg/ml gallic acid equivalent per 100 mg plant extract for *ginseng* and *banaba* respectively. The IC_{50} value of *ginseng* were found to be equivalent to the standard, ascorbic acid. *Banaba* exhibited least potential in hydrogen peroxide and hydroxyl radical scavenging activity as compared to *ginseng.*

57. Alluri KV. *et al.,* (2009)[69] revealed *in-vitro* and *in-vivo* antioxidant potential of methanolic, aqueous methanolic and aqueous extract from the bark of *A. polystachya*. All the extracts have shown potent antioxidant activity in NBT, DPPH, ABTS and FRAP assays. A potent fraction (AP-110/82C) obtained from the bioactivity guided fractionation was further subjected for *in vivo* antioxidant studies at the dose of 50 and 10 mg/kg. A dose dependent reduction in hepatic malondialdehyde (320.6, 269.3 µm/mg protein) with improvement in hepatic glutathione (6.9 and 17.1 µg/mg protein) and catalase levels (668.9 and 777.0 µg/mg protein) were observed. The results indicated the potential preventive intervention of *A. polystachya* in free radial mediated diseases.

58. Lamkanfi *et al.,* (2008)[111] discovered new caspase-1 substrates which were found to be responsible for the proteolytic maturation of the cytokines IL-1β and IL-18 during infection and inflammation. Among 1022 identified proteins, 20 were cleaved with aspartate specific cysteine protease enzyme caspase-1 to identify the specific substrate. Caspase-7 was identified as the substrate for Caspase-1. This was confirmed with *in-vivo* activation of Caspase-7 with *salmonella* and lipopolysaccharide + ATP induced activation techniques. This provides substantial claim of Caspase-7 as substrate for Caspase-1.

59. Zhang H. *et al.,* (2007)[112] isolated seven rings, A, B- secolimonoids (1-7) from the ethanolic extract of the seeds of *A. polystachya*. Their structures were identified as rohituka-7, dregeana-1, rohituka-15, Tr-B, rohituka-3, rohituka-5 and rohituka-14 by spectral studies, including DEPT, HSQC, HMBC, $^{1}H–^{1}H$ COSY, and NOESY.

60. Houghton P. *et al.,* (2007)[113] discussed the major approach in searching for potential anticancer agents based on the selective cytotoxic effects on mammalian cancer cell lines and cell-based methods for cytotoxicity. The authors have described the SRB assay in detail as the method of preference and developed a novel approach based on the hypothesis that, some of the compounds act as prodrugs. Bioassays based on mammalian cells involving antioxidant and upregulation of some cellular self-defence mechanisms were in relation to prevention and treatment of cancer.

61. Morones J. *et al.,* (2005)[49] reported the effect of AgNPs in the size range of 1-100 nm on gram negative bacteria using HAADF and STEM techniques. The studies indicated that the bactericidal property is size dependent and the nanoparticles were found to be in the range of 1-10 nm. The AgNPs showed penetration inside the bacteria leading to the damage by interacting with DNA. The studies also revealed the release of silver ions from the nanoparticles possessing additional bactericidal effect.

62. Panyam J. *et al.,* (2004)[44] formulated biodegradable nanoparticles using polymers like PLGA and PLA. Emulsion-solvent evaporation technique were used for the synthesis of dexamethasone and flutamide nanoparticles, which were further subjected to characterisation by using DSC and XRD techniques. The results revealed that the solubility of the drug depends on molecular weight and composition of polymer. The drug exhibited enhanced solubility (67 mg/gm) in low molecular weight polymer than the high molecular one (32 mg/gm). In conclusion, the solid-state drug-polymer solubility affects the nanoparticle characteristics and can be used as an important preformulation parameter.

63. Chowdhury R. *et al.,* (2003)[65] studied the laxative effects of the stem barks of *Amoora rohituka* and their action on gastrointestinal transit in mice. The mice were fed with the suspensions of the extract and examined for laxation hourly for 5 h. The mice were sacrificed, intestine removed and the length measured. It was demonstrated that petroleum ether, dichloromethane and methanol extracts of the plant exhibited good

laxative potential at concentrations of 400, 250 and 400 mg/kg respectively. They concluded that the crude extracts of the plant have laxative property compared to Sennoside B (50 mg/kg).

64. Zhang HP. *et al.,* (2002)[114] explored a new limonoid Rohituka-15 and a known limonoid dregeana-1 from the seeds of *A. polystachya*. The structures were confirmed through spectral studies including ^{1}H-^{1}H COSY, HMQC and HMBC studies.

65. Chowdhury R. *et al.,* (2003)[115] reported the isolation of two sesquiterpenoids, 6β,7β-epoxyguai-4-en-3-one and 6β,7β-epoxy-4b,5-dihydroxyguaiane from the petroleum ether extract of the stem bark of *Amoora rohituka*. The structures were elucidated by spectral data and chemical corelation.

66. Rabi T. *et al.,* (2002)[116] investigated the cytotoxic activity of Amooranin and its derivatives from the stem bark of *Amoora rohituka.* Amooranin and its methyl ester exhibited greater cytotoxicity against MCF-7 and HeLa cells derived from tumour tissues with IC_{50} of 1.8–3.4 µg/ml when compared with Chang liver cells from normal tissue with IC_{50} of 6.2–6.4 µg/ml. Amooranin exhibited no activity on HEp-2 and L-929 cells. However, its monoacetate derivative showed no inhibitory activity at 1–10 µg/ml dose levels. *in vivo* evaluation of methyl ester derivative in the Ehrlich ascites tumour cells

were inactive at dose levels of 50 and 100 mg/kg/day, indicating tumour growth inhibition index (T/C values) of 106 % and 114 % respectively.

67. Kang Beom Kwon *et al.,* (2002)[117] investigated the cellular effects of H*erba houttuyniae* extract (HHE) and the signal pathways of HHE-induced apoptosis in HL-60 human promyelocytic leukemia cell line. The study suggested that HHE possibly causes mitochondrial damage leading to cytochrome C release into cytosol and activation of caspases resulting in PARP cleavage and execution of apoptotic cell death in HL-60 cells. The IC_{50} of HHE for cell viability was 0.5 mg/ml.

68. Agarwal S. *et al.,* (2001)[55] reported a new limonoid, Dihydroamoorinin, along with two known limonoids namely Aphanamixinin and Amooranin from the stem bark extract of *A. polystachya.* The structures were confirmed by spectral studies and chemical corelation.

69. Zhou G. (1998)[118] studied the effect of silver ions on *E. coli* for initial inhibitory concentration, complete inhibitory concentration, post agent effect for bacteriostatic susceptibility, minimum bactericidal concentration, maximum tolerant concentration, and log killing time for bactericidal activity of silver ions. Growth delay was reported at 9.45 µM concentration, while complete inhibition of bacterial growth were seen at 18.90 mM. After exposure for 48 h, inhibitory concentration of silver tolerance was found

to be 20 times of initial concentration. They concluded that the method adopted can be a reference for the quantitative analysis to assess the susceptibility of bacteria on silver ions.

70. Gole *et al.,* (1997)[54] studied the anti-hepatotoxic activity of a resuspended alcohol extract residue of *Amoora rohituka* in rats with hepatic injury induced by carbon tetrachloride. Carbon tetrachloride (1 ml/kg, i.p.) and extract of *A. rohituka* (50 mg/kg/day) were administered orally for 3 weeks, twice a week. Carbon tetrachloride was used to induce the elevation of ALP, CPT, ALAT, GOT, ASAT and LDH. Treatment of suspension of *A. rohituka* on rats exhibited a significant reduction in total plasma bilirubin and total plasma cholesterol concentration. Histological architecture of the liver produced by $CC1_4$ were protected by the administration of *A. rohituka* suspension confirming the hepatoprotective action.

71. Chatterjee A. *et al.,* (1967)[119] performed a chemical investigation by isolating aphanamixin from the petrol extract of the seeds of *A. polystachya*. The structural elucidation were carried out by spectral analysis (IR, ^{1}HNMR and Mass).

MATERIALS & METHODS

"In the field of observation, chance favours only the prepared mind."

5.0 MATERIALS AND METHODS

5.1 CHEMICALS USED IN THE EXPERIMENT

Table No. 1: List of Chemicals used in the experiment

Sr. No	Chemical	Supplier
1	Silver Nitrate	Sigma Aldrich
2	Methanol	Loba Chemie
3	Chloroform	Loba Chemie
4	Phosphate buffer	Loba Chemie
5	Sodium Lauryl Sulphate	Sigma Aldrich
6	DMSO	Loba Chemie
7	TCA	Merck
8	SRB	Sigma Aldrich
9	DPPH	Loba Chemie
10	Sodium Nitroprusside	Loba Chemie
11	Sulfanilamide	Loba Chemie
12	N-1-napthylethylenediamine dihydrochloride	Loba Chemie
13	PBS	Merck
14	Gelatin	Merck
15	Tween 20	Merck
16	o-Dianisidine dihydrochloride	Sigma Aldrich, USA
17	Total RNA isolation kit	Invitrogen-Product Code 10296010
18	DMEM Media	Sigma Aldrich
19	Trizol Agent	Sigma Aldrich
20	Ethanol	Merck
21	TRI Reagent	Sigma Aldrich
22	cDNA preparation kit	Thermoscientific, Product code-AB1453A
23	SYBR Green Master Mix	Applied Biosystem, Life technologies

5.2 INSTRUMENTS USED IN THE EXPERIMENT

Table No. 2: List of Instruments/Equipment Used

Sr. No.	INSTRUMENT NAME	Make & Model	USED FOR
1	Magnetic stirrer	Remi, 2-LMH	Mixing of nanoparticles
2	Centrifuge	Remi CM12	Separation of liquid and solid
3	Ultrasonicator	Biolinx	Breakdown of particles to smaller size
4	Brookfield Viscometer	Brookfield	Viscosity of nano formulation
5	UV-Visible Spectrophotometer	Labindia	Quantitative determination of nano formulation
6	FTIR	Shimadzu, IR Affinity 1S	Identification of functional groups
7	Particle Size Analyser	DLC	Determination of particle size
8	X-ray Diffraction (XRD)	BRUKER, D8 Advanced	Crystalline nature of nanoparticles
9	Scanning Electron Microscope (SEM)	Hitachi, S-3000N	Morphology of nanoparticles
10	Transmission Electron Microscope (TEM)	Hitachi, HT-7700	Surface morphology and size of nanoparticles
11	Energy Dispersive X-Ray Analysis	Hitachi, S-520	Elemental analysis of nanoparticles
12	Atomic Force Microscopy	Bruker	ultra-high resolution in particle size measurement
13	Flow Cytometer	BD FACS Cali bur	Detection of cycle and apoptosis
14	ELISA Reader	NeoBiolabs	Optical density
15	Multi-well Plate Reader	ELx800, BioTek Instruments Inc., Winooski, VT, USA	Absorbance
16	NMR	Bruker	Spectral characterisation

5.3 COLLECTION AND AUTHENTIFICATION OF PLANT MATERIAL

The root bark of *A. polystachya* was identified and obtained from Mangalore, Dakshina Karnataka, India. The plant part was identified by Dr. Gopal Krishna Bhatt, Poorna Prajnya College Udupi- Karnataka, India and Dr. Dinesh Nayak, Mangalore-Karnataka, India bearing number: GCP.Pharmacog.05/2013. The herbarium was deposited in Department of Pharmacognosy, Goa College of Pharmacy, Panaji-Goa.

5.4 PREPARATION OF PLANT EXTRACT

Roots along with the bark of *A. polystachya* were obtained, washed and dried in shade. The dried material was powdered (50 gm) and then exhaustively extracted by maceration with 500 ml of methanol for 3 days. After 3 days, the methanolic layer was decanted off. The process was repeated three times. Solvents from the total extract was distilled off using rotary vacuum evaporator (Roteva) and concentrated to a syrupy consistency and then evaporated to dryness (8 gm)[42].

5.5 PRELIMINARY PHYTOCHEMICAL SCREENING

The plant extract of *A. polystachya* were subjected to various test tube reactions to detect the presence of phytoconstituents present in the methanolic extract.

PHYTOCHEMICAL ANALYSIS [64]

5.5.1 Tests for Alkaloids

About 50 mg of the extract was stirred with few ml of dilute hydrochloric acid and filtered. The filtrate was subjected to various alkaloidal reagents. The details of the tests are given here under.

i. **Mayer's test** About 2-3 drops of Mayer's reagent was added to the filtrate slowly along the walls of the test tube. The presence of alkaloids was confirmed by formation of cream coloured precipitate.

ii. **Dragendorff's test** About 2-3 drops of Dragendorff's reagent was added gradually drop wise to the filtrate. A reddish-brown precipitate indicates the presence of alkaloids.

iii. **Wagner's test** About 2-3 drops of Wagner's reagent was gradually added to the filtrate. The presence of alkaloids was confirmed by a reddish-brown precipitate.

iv. **Hager's test** About 2-3 drops of Hager's reagent was added drop wise to the filtrate. The presence of alkaloids was confirmed by a yellow precipitate.

5.5.2 Test for Carbohydrates

i. **Molisch Test** To the extract taken in a test tube, 1 ml of water and 1 ml of 5% (w/v) alcoholic α-naphthol solution were added and mixed well. The mixture was cooled and 1 ml of concentrated sulfuric acid was added along the side of the test tube. The violet color developed at the junction indicates the presence of carbohydrates.

ii. **Benedict's test** To 1 ml of the extract solution, 5ml of Benedict's reagent was added and boiled for 2 minutes and cooled. Formation of a red precipitate confirms the presence of carbohydrates.

iii. **Fehling's Test** To 1 ml of the extract solution, equal quantities of Fehling's solution A and B was added. Upon heating, a brick red precipitate indicates the presence of carbohydrates.

5.5.3 Test for Flavonoids

Shinoda test A small amount of the extract was dissolved in methanol. Magnesium turnings were added to the solution accompanied by a few drops of concentrated hydrochloric acid. A pink colour indicates the presence of flavonoids.

5.5.4 Test for Steroids

i. **Libermann- Buchard Test** Few mg of extract was dissolved in chloroform. To this 1-2 ml of chilled acetic anhydride was added and mixed well. Then 2-3 drops of chilled concentrated sulfuric acid were added along the sides of the walls of the test tube. An array of colours indicates the presence of steroids/tri terpenoids and their glycosides.

ii. **Salkowaski Test** Dissolve the extract in chloroform and add equal volume of concentrated sulfuric acid. Formation of bluish red to cherry red colour in chloroform layer, whereas the acid layer assumes marked green florescence which represents the steroids and sterol components, in the tested extracts.

5.5.5 Test for Phenolic Compounds

i. **Ferric chloride Test** A 5% ferric chloride solution was added to the extract. Appearance of blue-black colour indicates the presence of phenolic compounds.

5.5.6 Test for Tannins

i. **Test with Lead Acetate solution** Lead acetate solution was added to a small quantity of the extract/fraction. A white precipitate confirms the presence of tannins.

ii. **Test with Gelatin solution** Gelatin solution was added to a small quantity of the extract/fraction. Formation of white precipitate indicates the presence of tannins.

5.6 EXTRACTION AND ISOLATION OF COMPONENTS FROM THE ROOTS OF *A. POLYSTACHYA*

5.6.1 Extraction and Isolation of Components from the methanolic extract of the root bark of *A. polystachya*[56]

Roots along with the bark of *A. polystachya* were collected, washed and dried in shade. The dried material was then powdered (500 gm) and exhaustively extracted by maceration with 3 L of methanol for 3 days. After 3 days, the methanolic layer was decanted off. The process was repeated thrice. The solvents from the total extract was distilled off using rotary vacuum evaporator (Roteva) and concentrated to a syrupy consistency and then evaporated to dryness (150 gm).

The methanol soluble fraction (150 gm) was suspended in 1.5L of water and extracted with petroleum ether (60:80) to remove the fatty components completely. The defatted crude extract was further partitioned with chloroform (3x1L) to give a chloroform soluble fraction (90 gm).

90 gm of chloroform fraction was mixed with silica gel (30g, #60-120). The sample was loaded on a column packed with 500g of silica gel (Molychem, #60x120) prepared in petroleum ether (60-80). The column was subjected to elution with different solvent system starting first with 100% petroleum ether followed by petroleum ether: ethyl acetate graded mixtures (95:5, 90:10, 80:20, 70:30, 50:50), 100% ethyl acetate and

finally with graded mixtures of ethyl acetate: methanol (99:1, 98:2, 97:3, 96:4, 95:5). The elutions were monitored by TLC (silica gel G, visualization by UV at 254 nm, 366 nm and vanillin sulphuric acid reagent heated at 110ºC). Each time 10 ml of elute was collected and identical elutes were combined (TLC monitored) and concentrated to 5 ml and kept aside. The elutions carried out with petroleum ether: ethyl acetate (90:10 to 50:50) resulted in 4 fractions containing mixture of compounds and having identical R_f values (7 gm).

The above fraction (7 gm) was mixed with flash grade silica (3 gm, #200-400) using mortar and pestle. This mixture was subjected for rechromatography with column (1ft in length and 2 cm i.d.). The sample was loaded onto a column packed with 150 gm of flash grade silica (Molychem, #60x120).

The mixture was loaded onto the column and elutions were carried out with 100 % petroleum ether, petroleum ether: ethyl acetate graded mixture (90:10, 85:15, 80:20, 75:25, 70:30, 65:35). The elutions were monitored by TLC (silica gel G, visualization by UV at 254 nm, 366 nm and vanillin sulphuric acid reagent heated at 110ºC). Each time 10 ml of the elute was collected and identical elutes were combined (TLC monitored) and concentrated to 5 ml and kept aside.

The elutions carried out with petroleum ether: ethyl acetate (80:20) resulted in a single spot on TLC prepared in petroleum ether (80:20). After removing the solvent, a light-yellow solid was obtained which was designated as RG-APE2 (78 mg). The elutions

carried out with petroleum ether: ethyl acetate (65:35) resulted in a single spot on TLC prepared in petroleum ether: ethyl acetate (65:35). After removing the solvent, a light-yellow solid was obtained which was designated as RG-APE1 (74 mg).

Elutions carried out with 100% ethyl acetate, ethyl acetate: methanol (99:1 and 98:2) resulted in a mixture of compounds having identical R_f values (TLC monitored, ethyl acetate: methanol (98:2). After removing the solvent, a light brown amorphous powder resulted (185 mg).

5.6.2 Purification of compounds using Flash Chromatography[56]

185 mg of the powder was taken and mixed by triturating with flash grade silica (600 mg, #200-400) using mortar and pestle. Pre-packed silica column (Redisep RF, 1 gm) was used. All the parameters were set and monitored using peak track software. The compounds which are UV absorbing i.e. at 254 nm and 366 nm, are only detected by flash chromatography.

The elutions were carried out with ethyl acetate: methanol (98:2) and collected in a test tube. Each time, 8 ml of elutes were collected and identical elutes were combined (TLC monitored, ethyl acetate: methanol 98:2), concentrated and kept aside.

The test tubes from 3-18 resulted in a single spot on TLC (ethyl acetate: methanol, 98:2). After removing the solvent, light brown flakes resulted and the compound was designated as RG-APE3 (68 mg). The test tubes from 22-44 resulted a single spot on TLC (ethyl acetate: methanol, 98:2). After removing the solvent from the test tube, it resulted in a light-yellow powder and the compound was designated as RG-APE4 (77 mg).

Elutions carried out with other solvent systems resulted in a mixture of compound or resinous mass, which were not processed further.

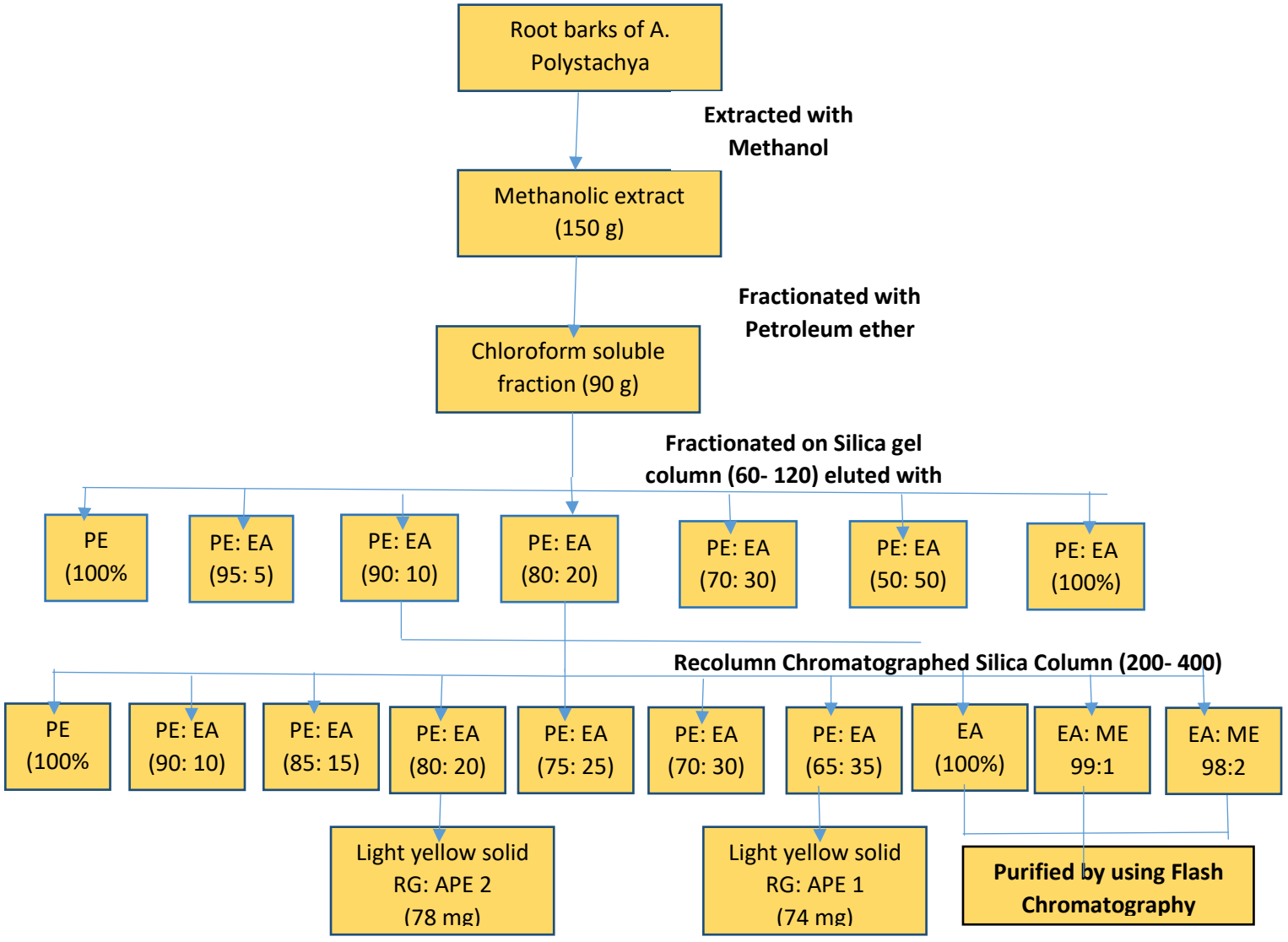

Fig. 7: Extraction and Isolation of Phytoconstituents from the root bark of *A. polystachya*

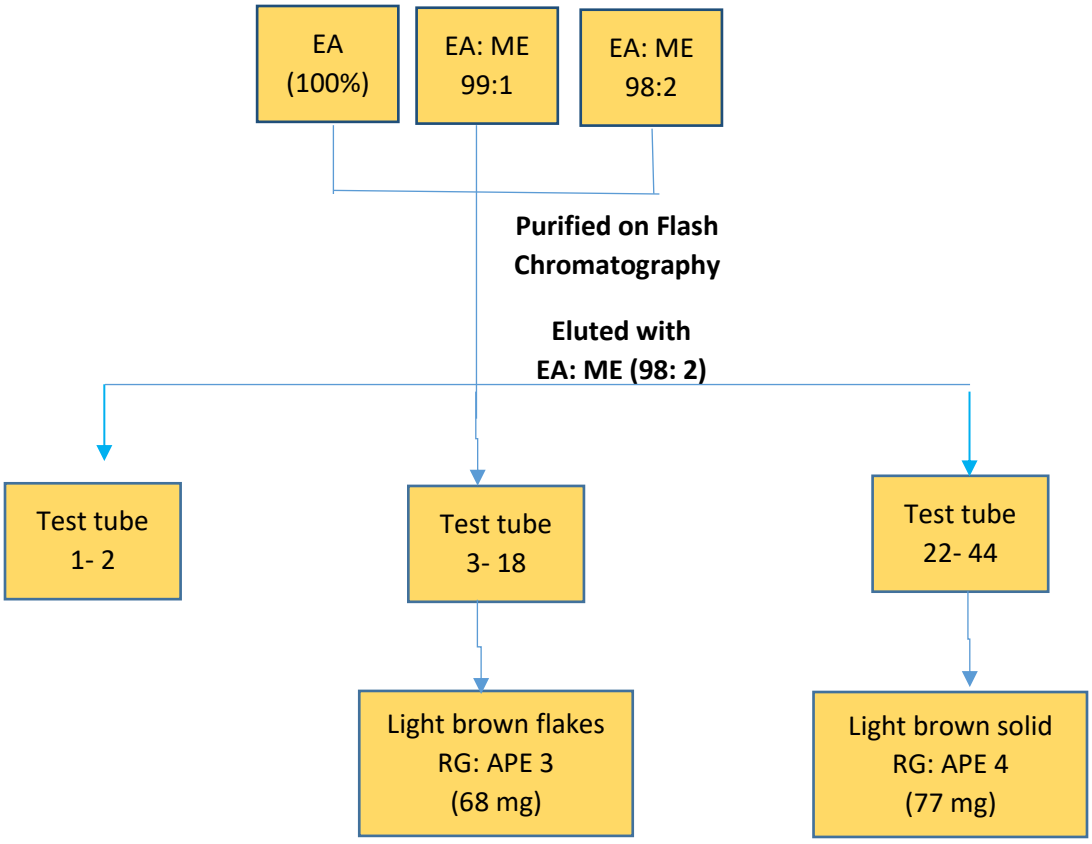

Fig. 8: Purification by using Flash Chromatography

5.6.5 Characterization of Isolated Compounds

5.6.5.1 Compound RG-APE1

Physical state: Light yellow solid

R_f value: 0.60 (solvent system $CHCl_3$: EtOAc 80:20)

Melting point: 123ºC

The compound gave a positive response for Liebermann- Burchard test for triterpenoids.

Spectral Characteristics of Compound

IR (KBr) 3334.92 cm^{-1} (br, OH)

2924.25 cm^{-1} (C-H str. in CH_3)

1724.36 cm^{-1} (C=O str.in ester)

1442.75 cm^{-1} (C-H deformation in CH_3)

1377.17 cm^{-1} (OH, deformation)

1132.21 cm^{-1} (C-O str. in secondary alcohol)

^{1}HNMR ($CDCl_3$) δ 7.5509 (d, 1H, H-1), δ 6.4724 (s, 1H, H-2),

δ 2.1816 (d, 1H, H-5), δ 2.5108 (s,1H, H-6),

δ 3.1835 (s, 1H, H-9), δ 5.1943 (s,1H, H-11),

δ 5.8707 (t,1H, H-12), δ 5.5848 (d,1H, H-13),

δ 2.0304 (t,1H, H-16), δ 3.7364 (t,1H, H-17),

δ 0.9843 (s, 3H, H-18), δ 1.0638 (s,3H, H-19),

δ 7.3975 (d,1H, H-21), δ 6.8561 (s, 1H, H-22),

δ 7.3869 (s, 1H, H-23), δ 1.6665 (s,3H, H-28),

δ 4.8607 (d, 1H, -H29), δ 5.2234 (s, 1H, H-30)

δ 3.4367 (s, 1H, H-2'), δ 1.4091 (s, 1H, H-3'),

δ 1.2339 (d, 1H, H-4'), δ 0.7841 (t, 1H, H-5'),

δ 0.8359 (d, 3H, H-3'-Me),

δ 8.1664 (s, 1H, COOH),

δ 2.0470 (s, 3H, CH_3COO)

^{13}CNMR (CDCl3) δ 153.08 (C-1), δ 122.42 (C-2), δ 169.0 (C-3)

δ 81.93 (C-4), δ 74.06 (C-5), δ 31.25 (C-6)

δ 174.83 (C-7), δ 138.50 (C-8), δ 50.70 (C-9)

δ 39.55 (C-10), δ 74.06 (C-11), δ 80.37 (C-12)

δ 61.20 (C-13), δ 81.90 (C-14), δ 72.30 (C-15)

δ 39.34 (C-16), δ 39.14 (C-17), δ 11.53 (C-18),

δ 28.67 (C-19), δ 123.05 (C-20) δ 110 (C-22),

δ 143.0 (C-23), δ 28.90 (C-28), δ 74.06 (C-29),

δ 119.30 (C-30), δ 174.83 (C-1'), δ 74.06 (C-2′),

δ 39.01.25 (C-3′), δ 22.06 (C-4′), δ 11.39 (C-5′),

δ 15.30 (C-3′-Me), δ 150.08 (C-HCOO),

δ 159.08 (C-CH_3COO), δ 20.7 (C-CH_3COO)

Mass spectra: (ESI-MS)

Molecular Formula: $C_{35}H_{44}O_{13}$

Molecular weight: 672

ESI-MS (m/z): 673.0 (M+H) + The other peaks appeared at 672.27, 643.28, 511.20, 451.18, 433.17, 339.12, 269.12, 165.07, 152.08.

From the melting point, IR, ^{1}HNMR, ^{13}CNMR and Mass spectra, compound RG-APE1 was designated as **Rohituka 7**.

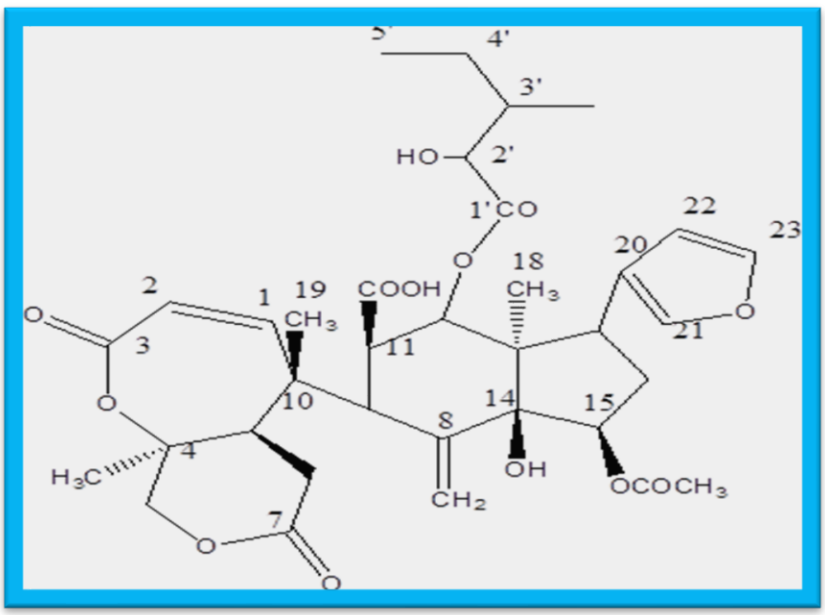

Fig 9: Chemical Structure of RG-APE1 (Rohituka 7)

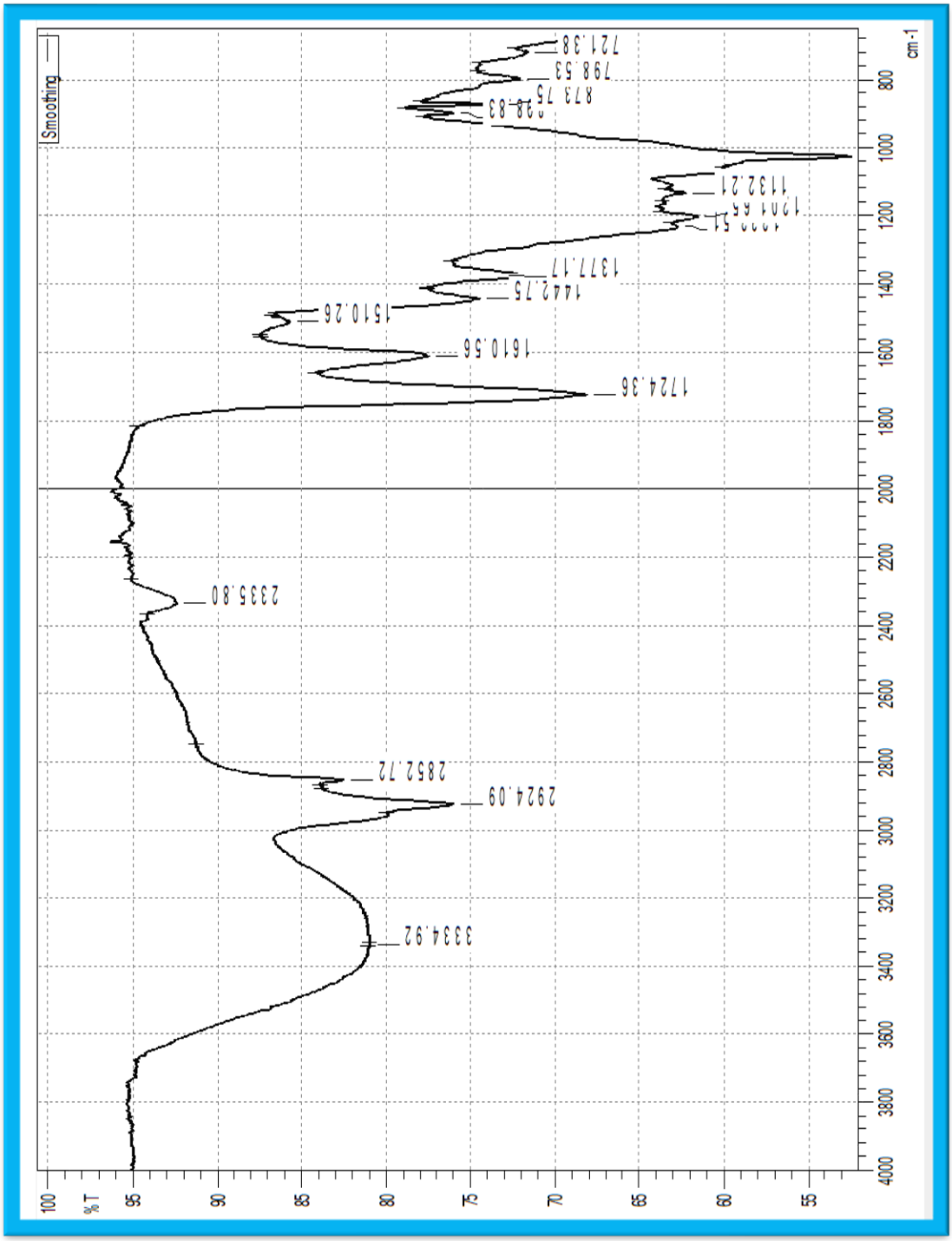

Figure 10: IR Spectrum of Compound RG-APE1 (Rohituka 7)

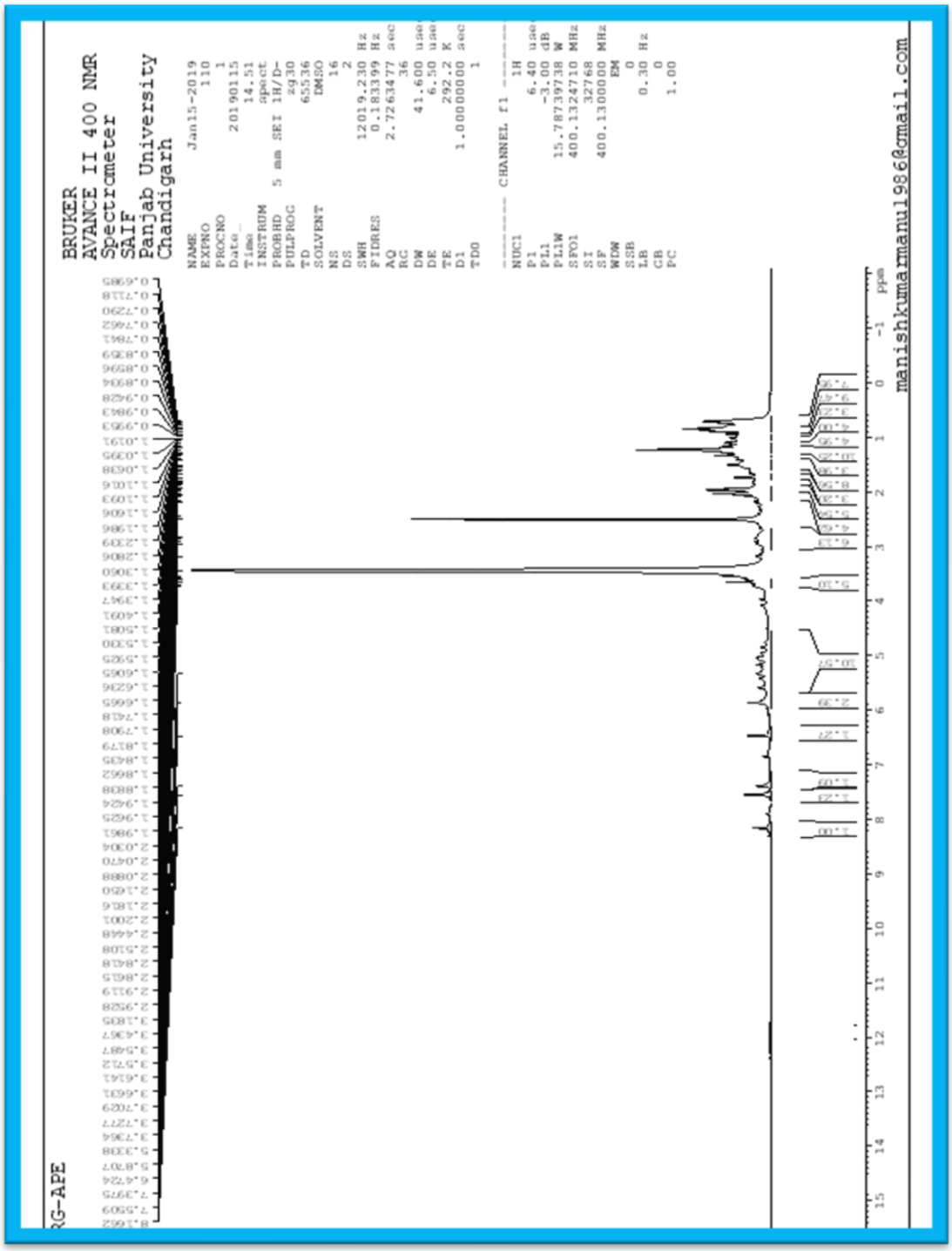

Figure 11: ^{1}H NMR Spectra of Compound RG-APE1 (Rohituka 7)

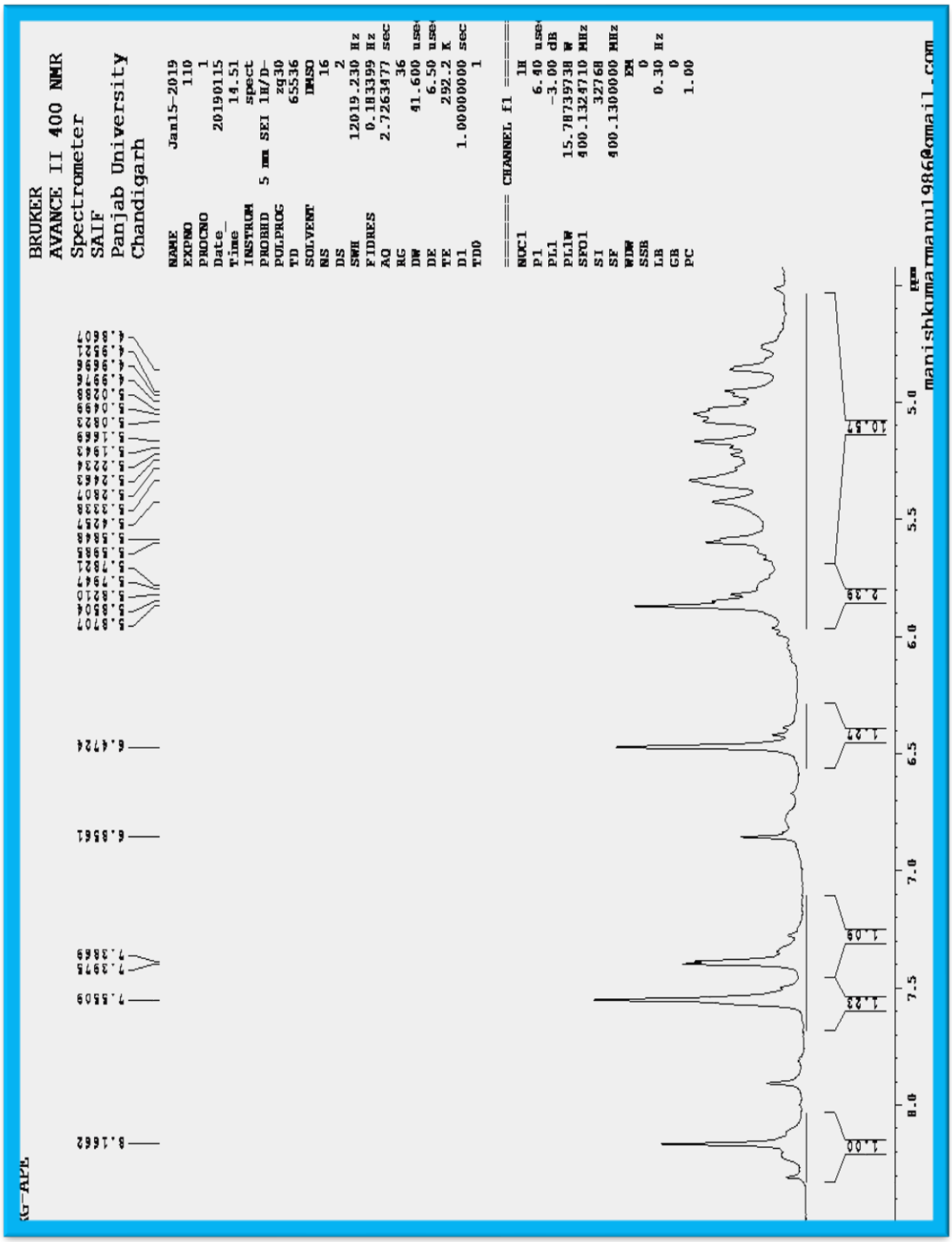

Figure 12: ^{1}H NMR Spectra of Compound RG-APE1 (Rohituka 7)

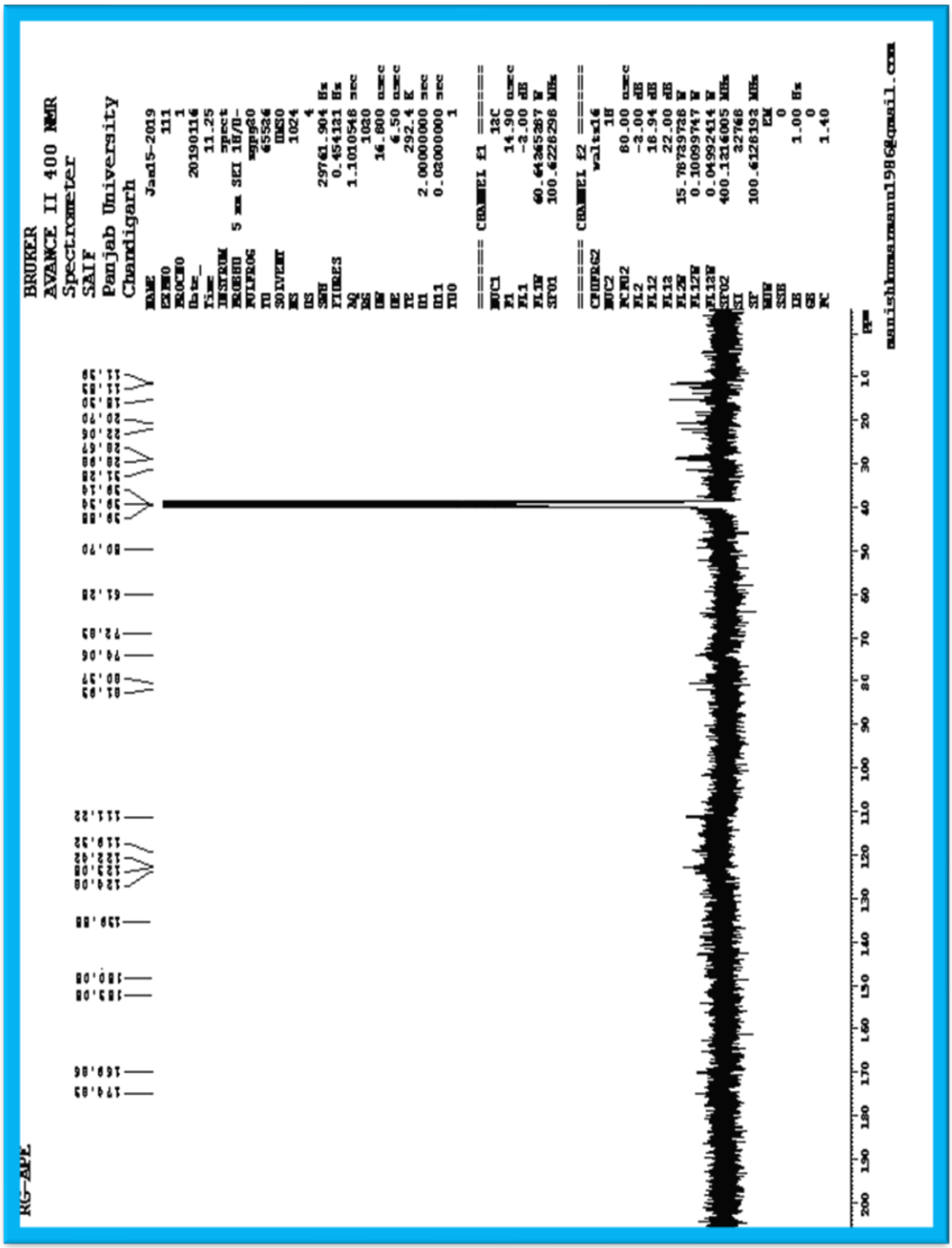

Figure 13: ^{13}C NMR Spectra of Compound RG-APE1 (Rohituka 7)

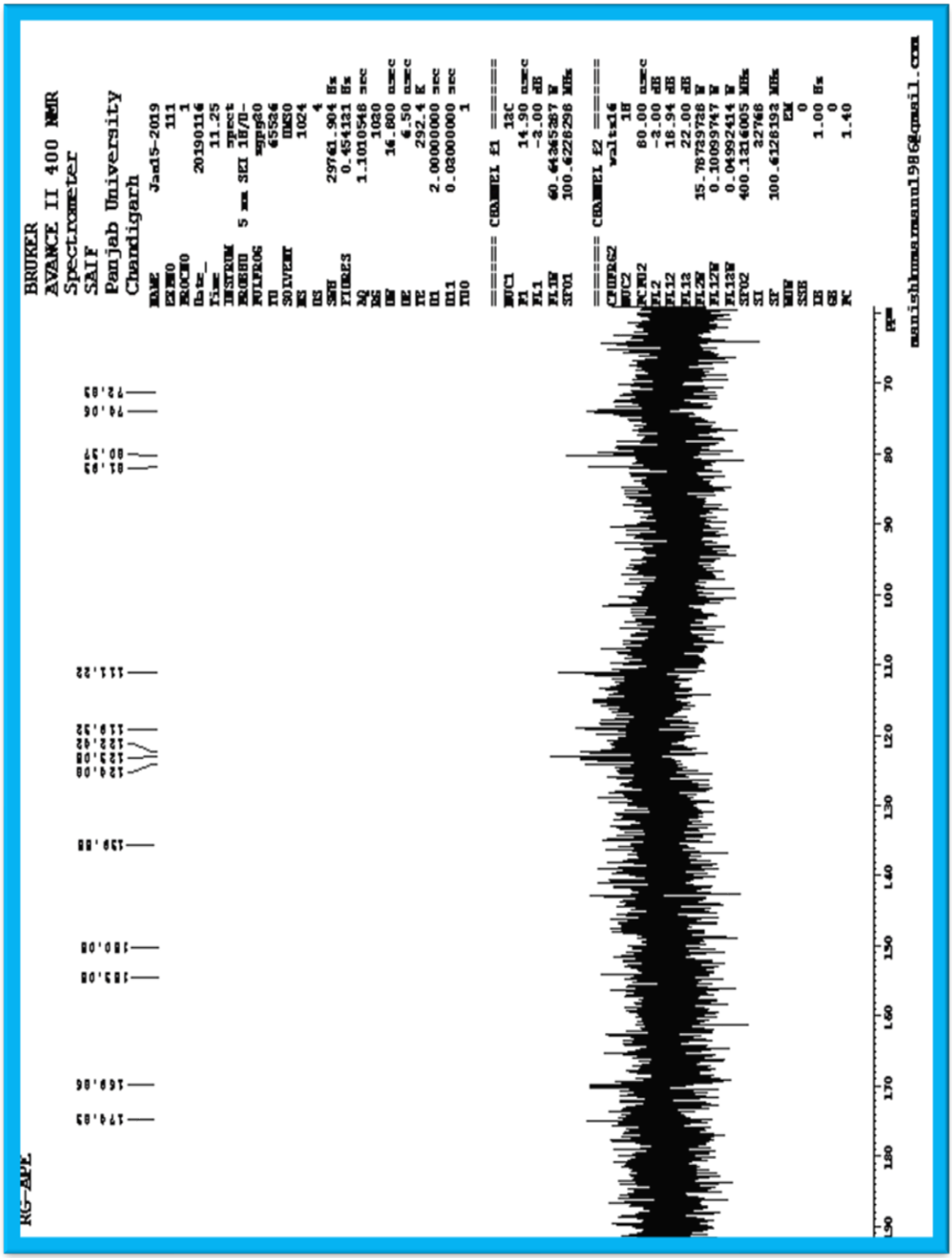

Figure 14: ^{13}C NMR Spectra of Compound RG-APE1 (Rohituka 7)

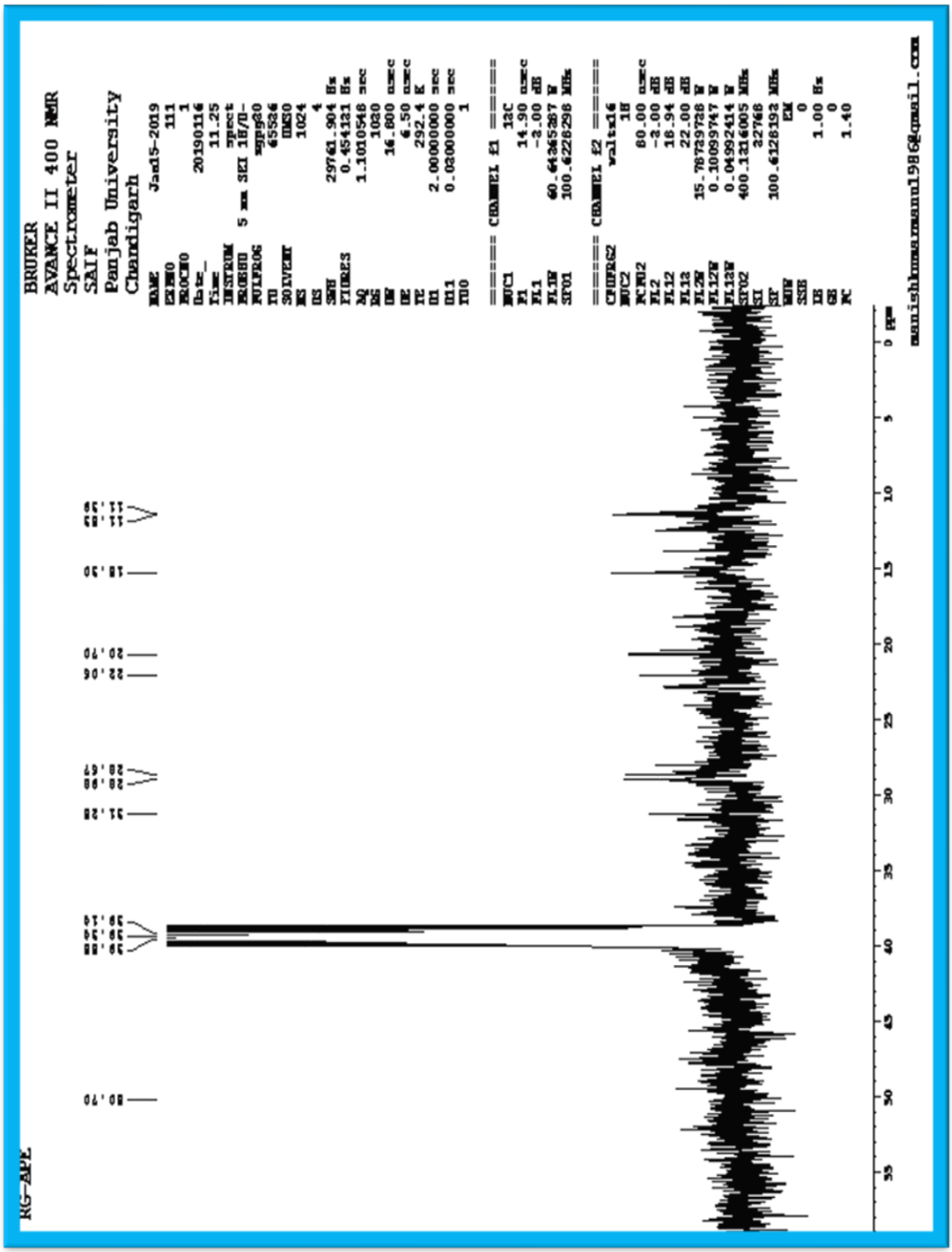

Figure 15: ^{13}C NMR Spectra of Compound RG-APE1 (Rohituka 7)

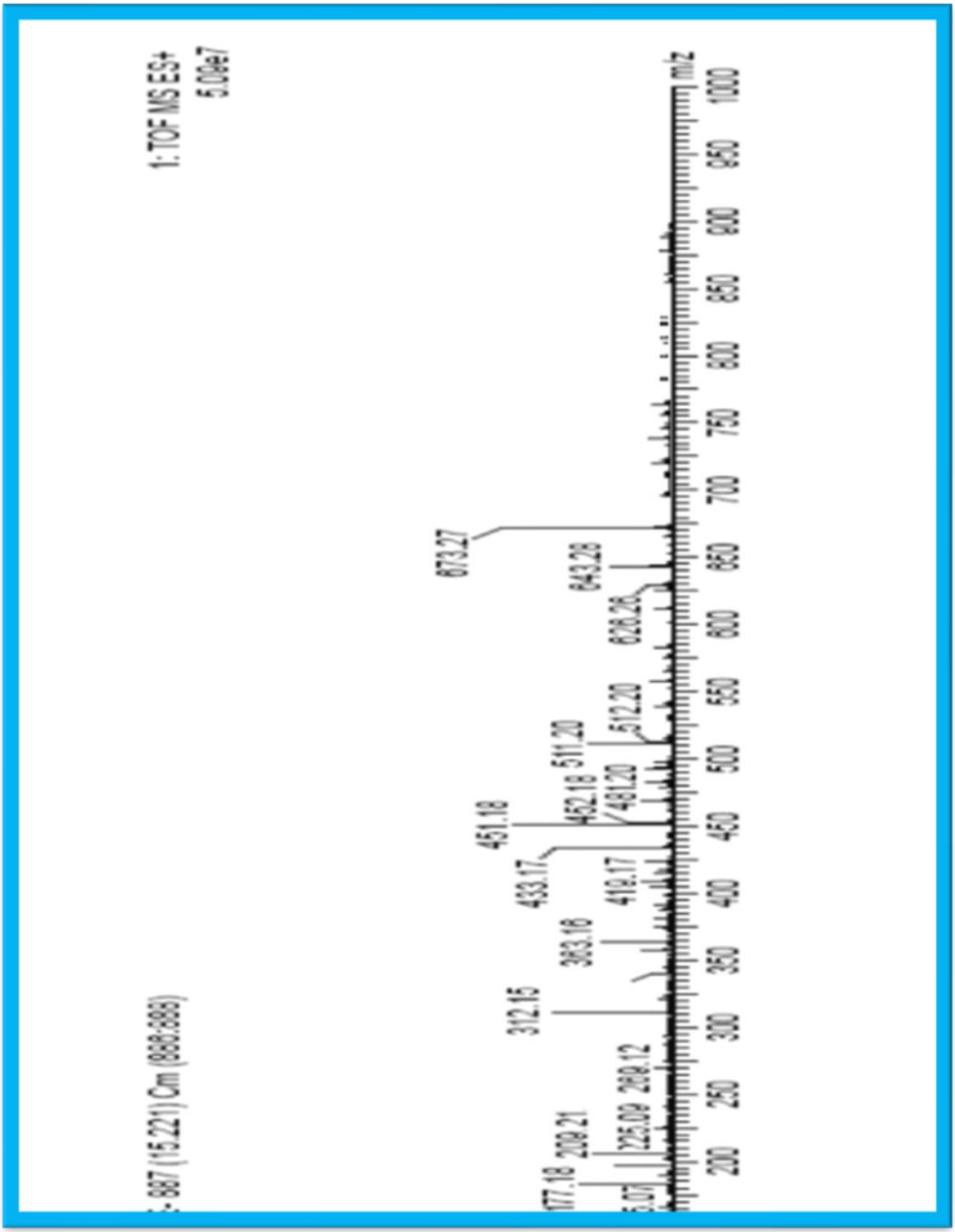

Figure 16: Mass Spectrum of Compound RG-APE1 (Rohituka 7)

5.6.5.2 Compound RG-APE2

Physical state: Light yellow solid

R_f value: 0.65 (solvent system $CHCl_3$: EtOAc 80:20)

Melting point: 122.4ºC

The compound gave a positive response for Liebermann- Burchard test for triterpenoids.

Spectral Characteristics of Compound

IR (KBr) 3389.10 cm^{-1} (br, OH)

2931.25 cm^{-1} (C-H str. in CH_3)

1741.57 cm^{-1} (C=O str.in ester)

1448.90 cm^{-1} (C-H deformation in CH_3)

1379.09 cm^{-1} (OH, deformation)

1031.08 cm^{-1} (C-O str. in secondary alcohol)

^{1}HNMR ($CDCl_3$) δ 3.7364 (t, 1H, H-1), δ 2.9528 (d, 1H, H-2),

δ 2.3029 (d 1H, H-5), δ 2.8218 (m, 1H, H-6),

δ 3.1835 (s, 1H, H-9), δ 4.8607 (s, 1H, H-11),

δ 5.8708(t,1H, H-12), δ 2.841, 2.3360 (t,1H, H-16),

δ 3.7277 (t,1H, H-17), δ 0.8596 (s,1H, H-18),

δ 1.1986 (s, 3H, H-19), δ 7.3975 (d,1H, H-21),

δ 6.4724 (s,1H, H-22), δ 7.5509 (s, 1H, H-23),

δ 1.6665 (s, 1H, H-28), δ 4.9521, 3.7227 (t,1H, H-29),

δ 6.8561(s, 1H, H-30), δ 3.4367 (s, 1H, H-2'),

δ 1.7908 (d, 1H, H-3'), δ 1.1606, 0.9428 (t, 1H, H-4'),

δ 0.6985 (s, 1H, H-5'), δ 0.8934 (t, 3H, H-3'-Me)

^{13}CNMR ($CDCl_3$) δ 78.26 (C-1), δ 28.98 (C-2), δ 167.06 (C-3),

δ 80.37 (C-4), δ 39.34 (C-5), δ 31.25 (C-6),

δ 169.86 (C-7), δ 123.05 (C-8), δ 54.70 (C-9),

δ 50.70 (C-10), δ 74.06 (C-11), δ 78.26 (C-12),

δ 39.55 (C-13), δ 81.93 (C-14), δ 204.08 (C-15),

δ 39.14 (C-16), δ 28.67 (C-17), δ 15.30 (C-19),

δ 119.32 (C-20), δ 139.55 (C-21) δ 111.22 (C-22),

δ 143.20 (C-23), δ 22.06 (C-28), δ 74.06 (C-29),

δ 122.42 (C-30), δ 174.83 (C-1'), δ 74.06 (C-2′),

δ 31.25 (C-3′), δ 20.70 (C-4′), δ 11.39 (C-5′),

δ 11.53 (C-3′-Me)

Mass spectra: (ESI-MS)

Molecular Formula: $C_{32}H_{40}O_{11}$

Molecular weight: 600

ESI-MS (m/z): 601.37 $(M+H)^+$ The other peaks appeared at 599.36, 557.35, 497.33, 479.32, 407.26, 189.07, 152.06.

From the m.p, IR, ^{1}HNMR, ^{13}CNMR and Mass spectra, compound RG-APE2 was designated as **Rohituka 3.**

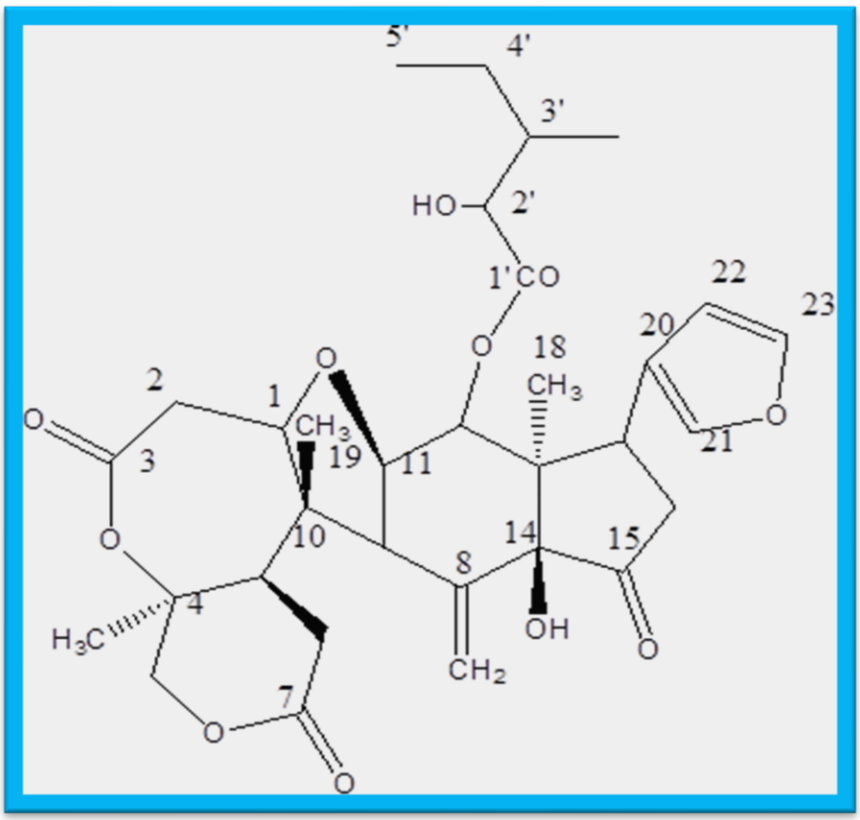

Figure 17: Chemical Structure of Compound RG-APE2 (Rohituka 3)

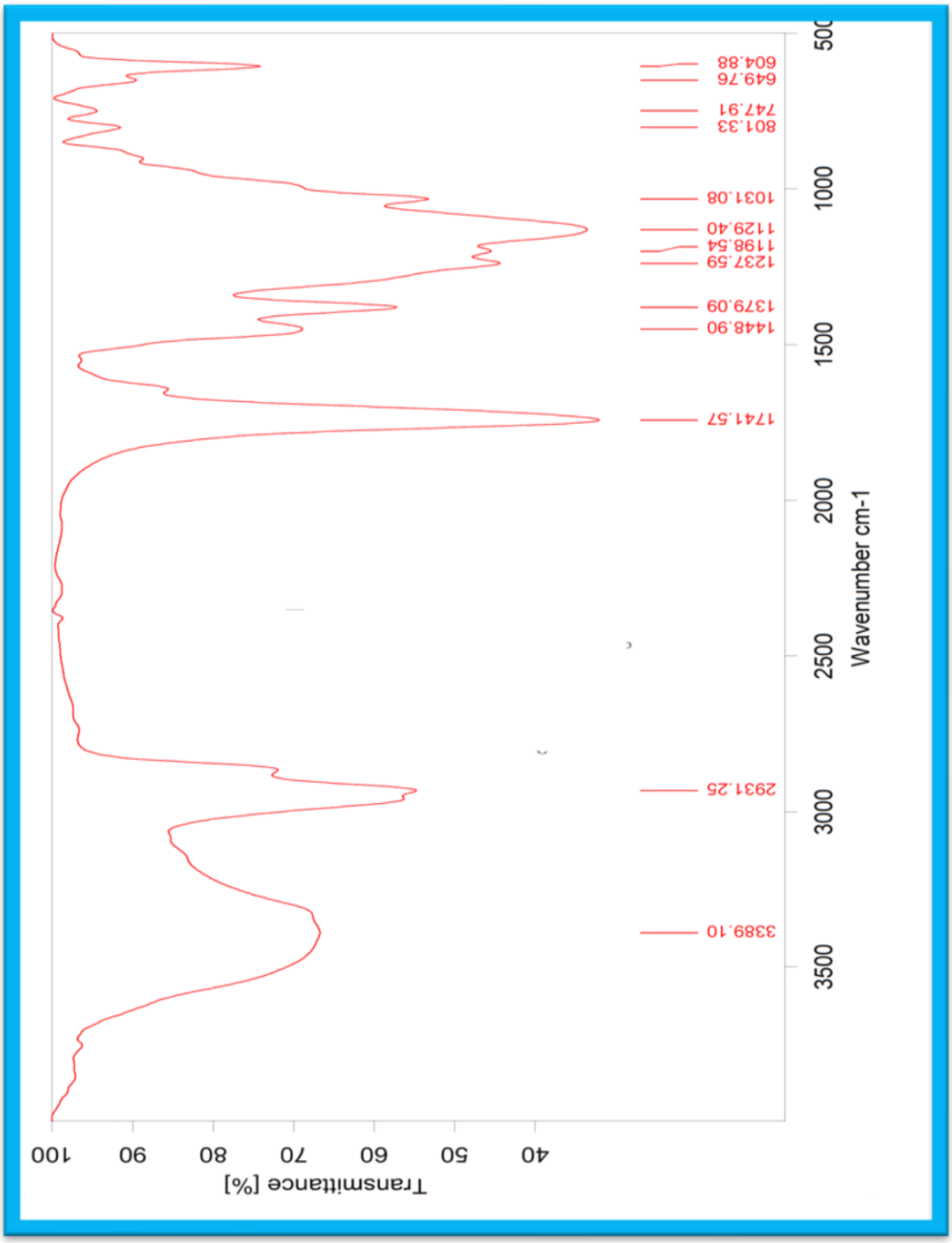

Figure 18: IR Spectrum of Compound RG-APE2 (Rohituka 3)

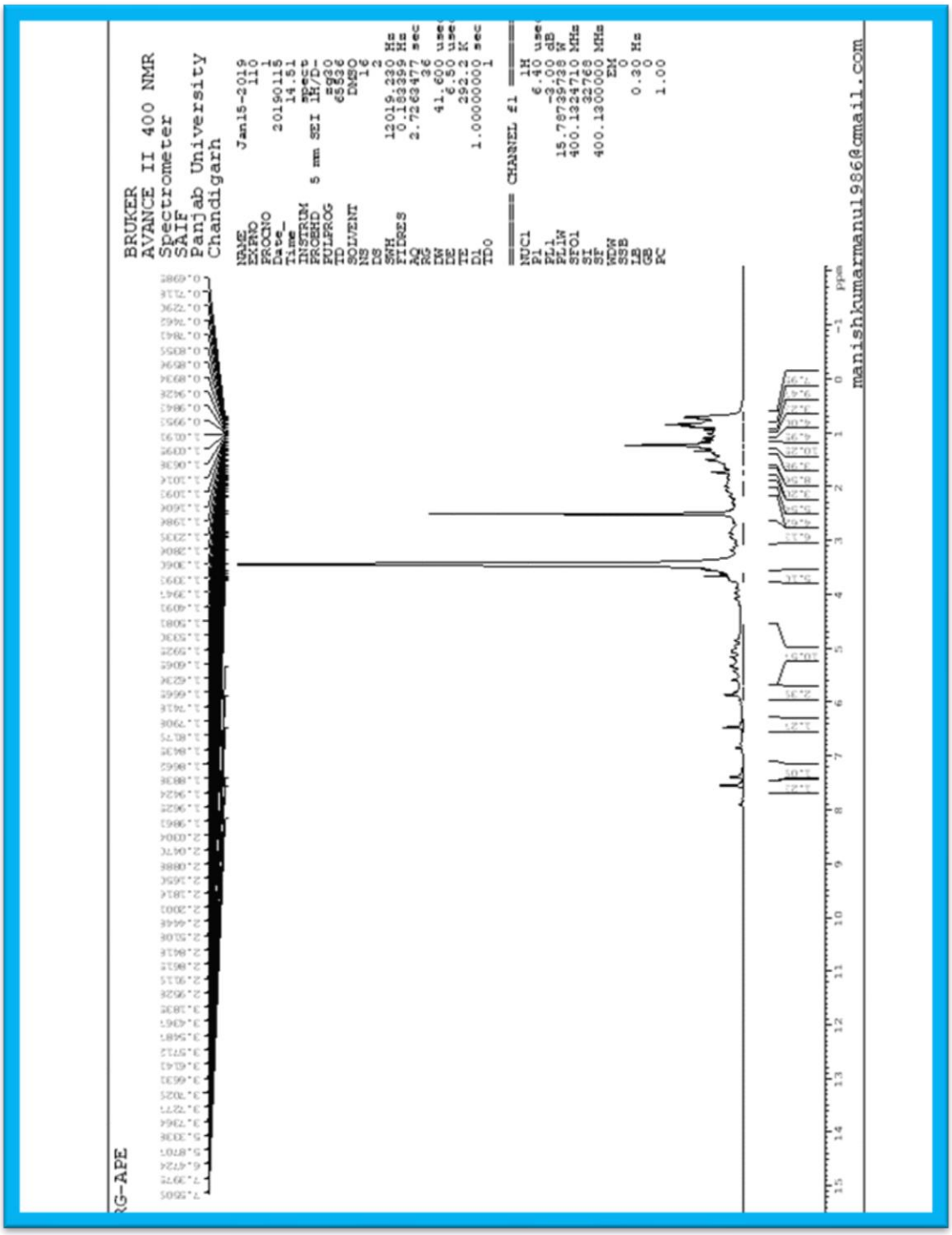

Figure 19: ^{1}H NMR Spectra of Compound RG-APE2 (Rohituka 3)

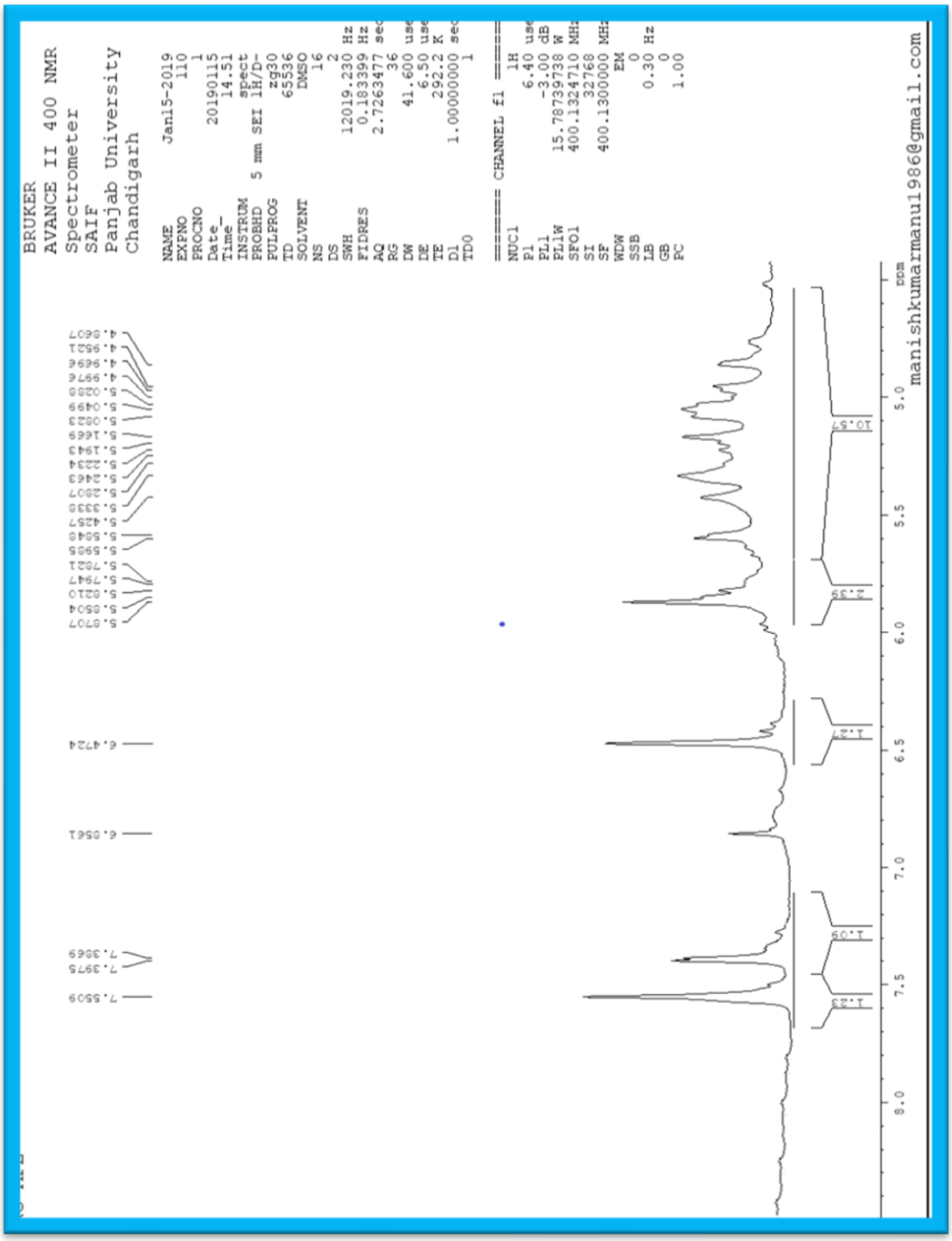

Figure 20: ^{1}H NMR Spectra of Compound RG-APE2 (Rohituka 3)

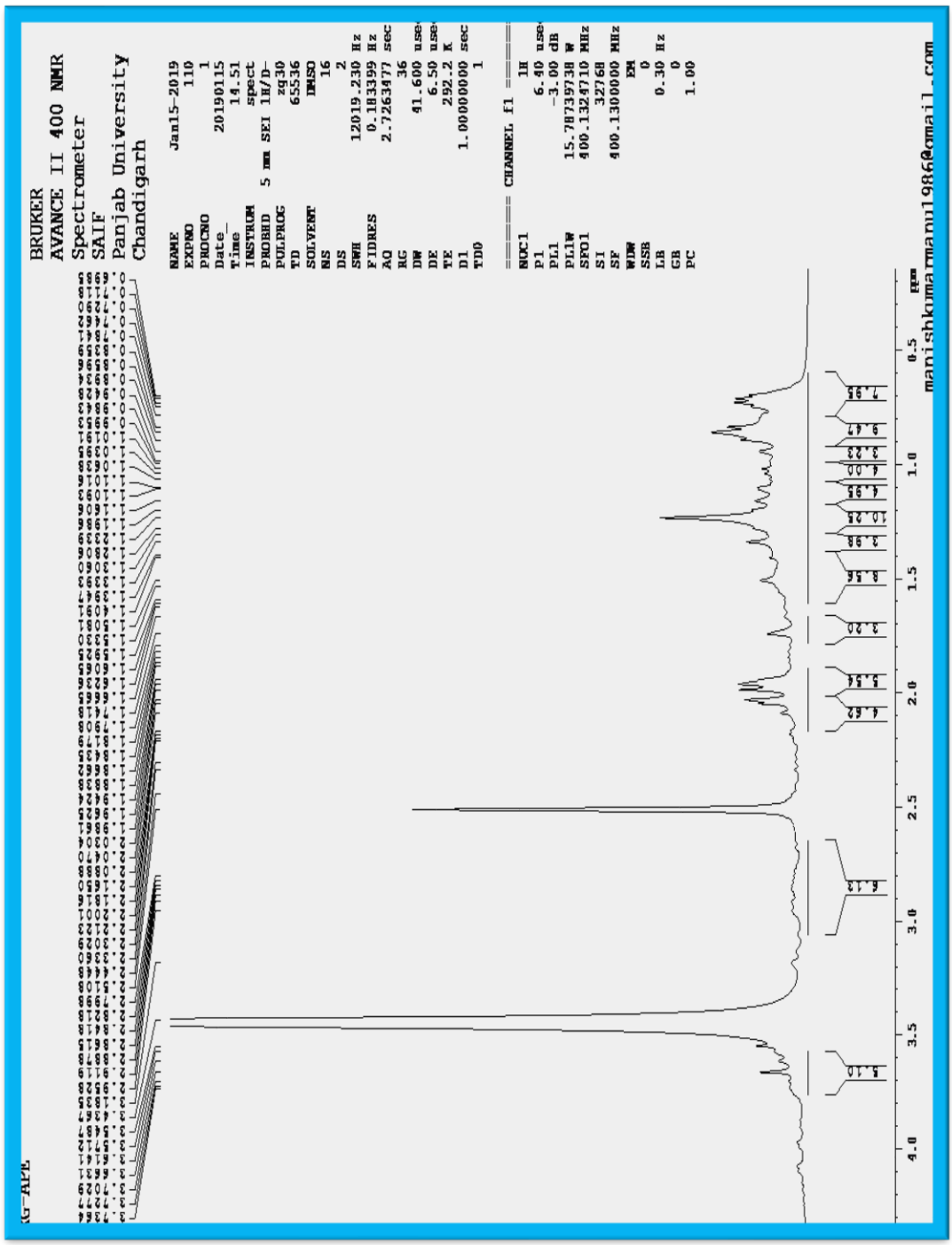

Figure 21: ^{1}H NMR Spectra of Compound RG-APE2 (Rohituka 3)

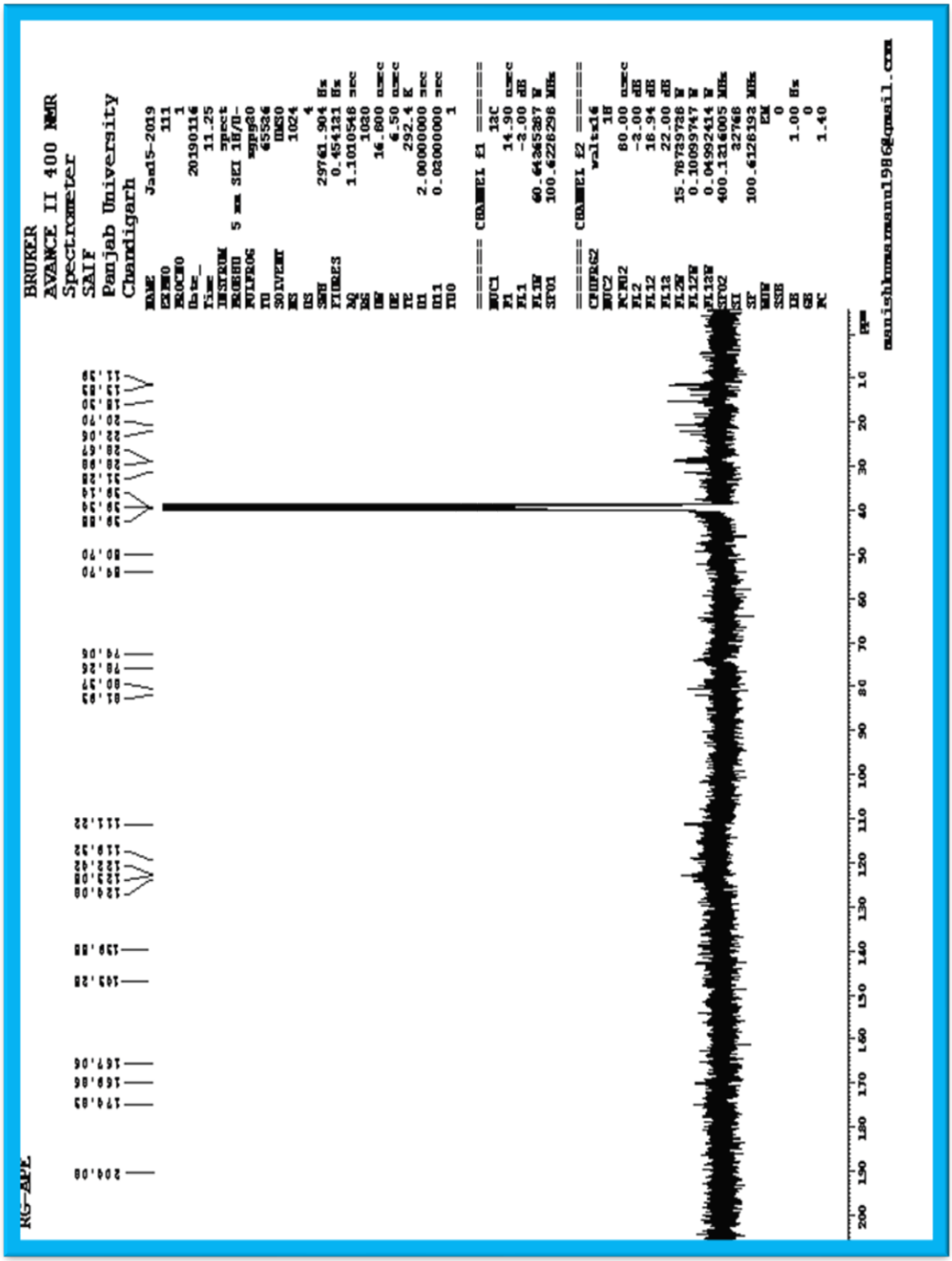

Figure 22: ^{13}C NMR Spectra of Compound RG-APE2 (Rohituka 3)

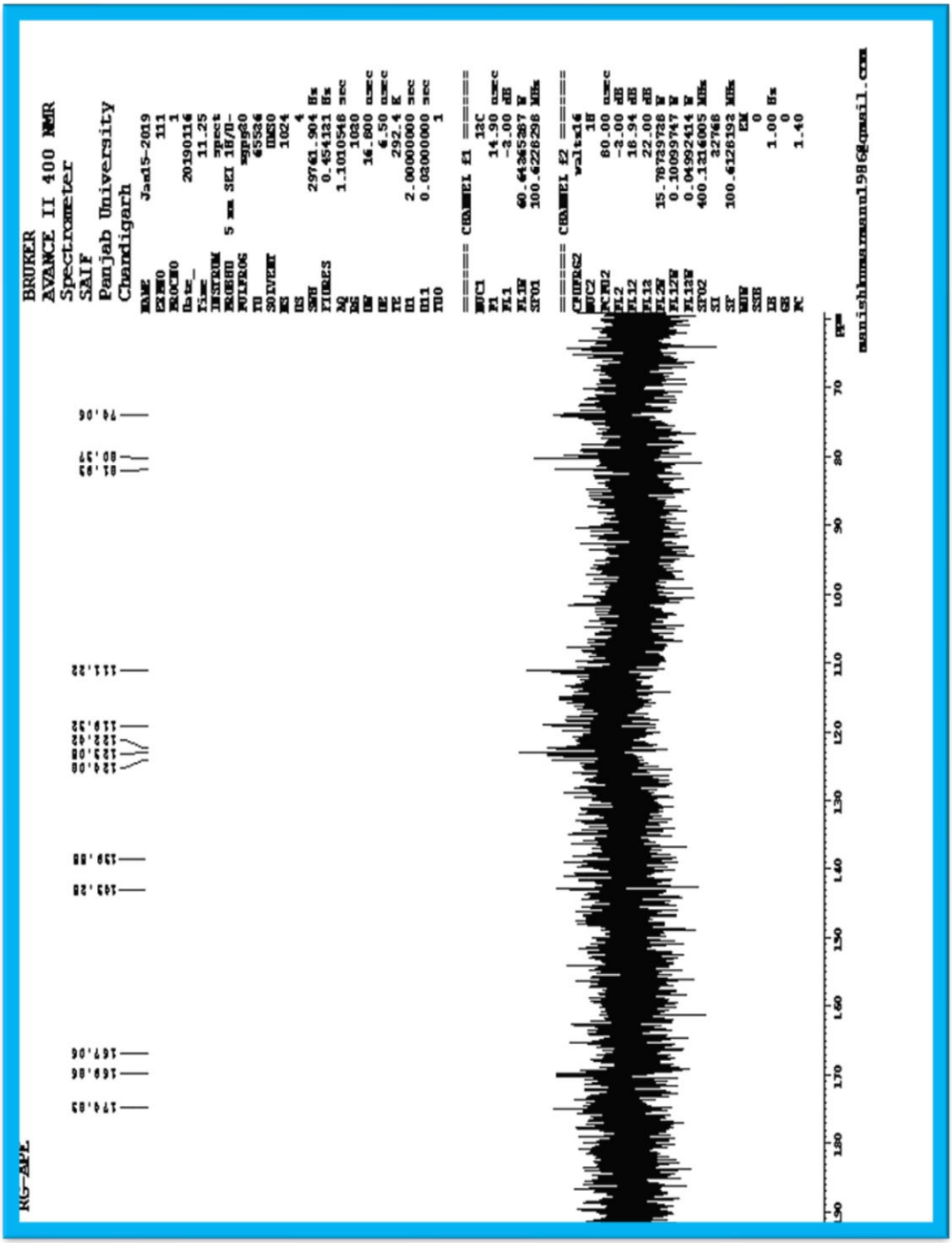

Figure 23: ^{13}C NMR Spectra of Compound RG-APE2 (Rohituka 3)

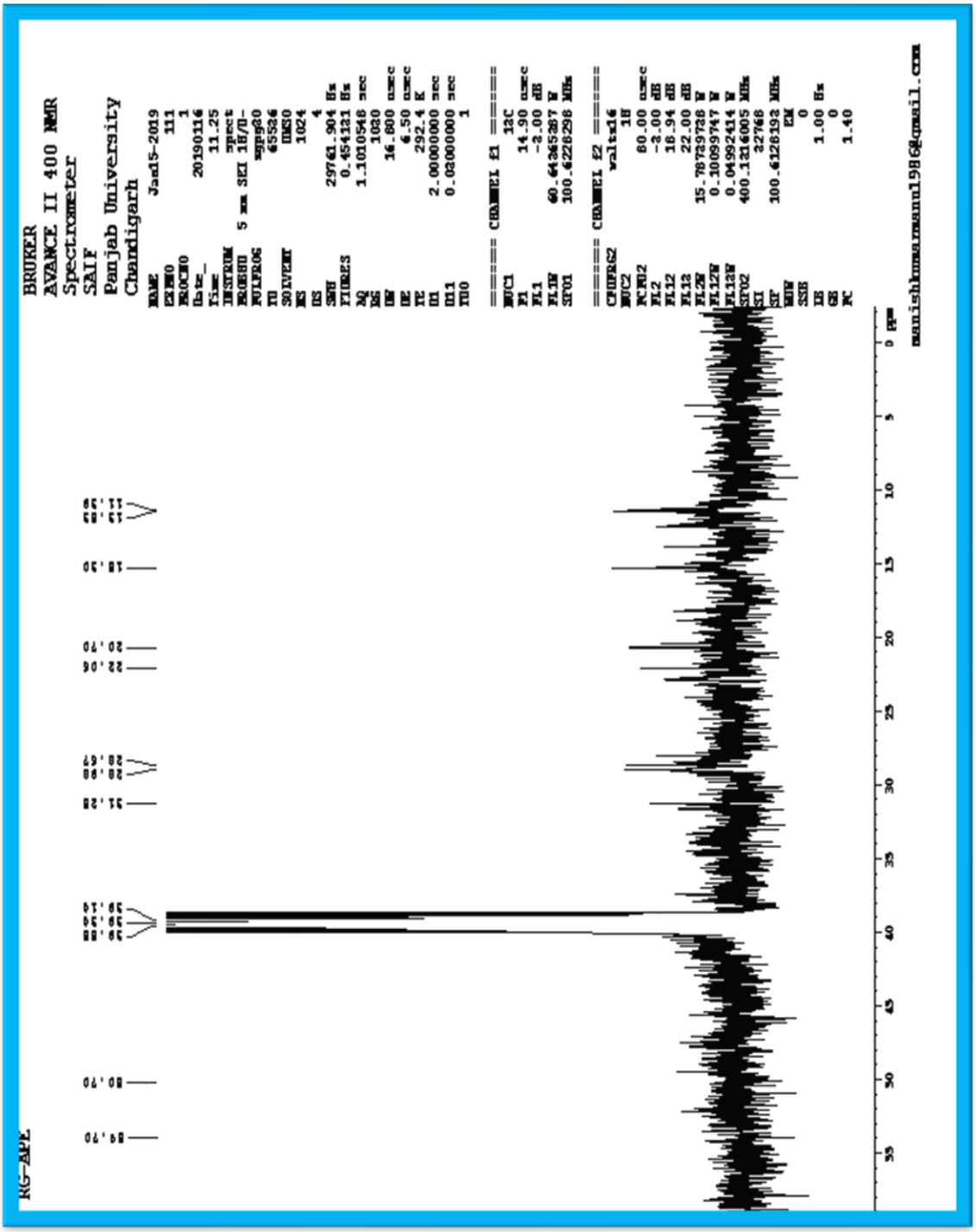

Figure 24: ^{13}C NMR Spectra of Compound RG-APE2 (Rohituka 3)

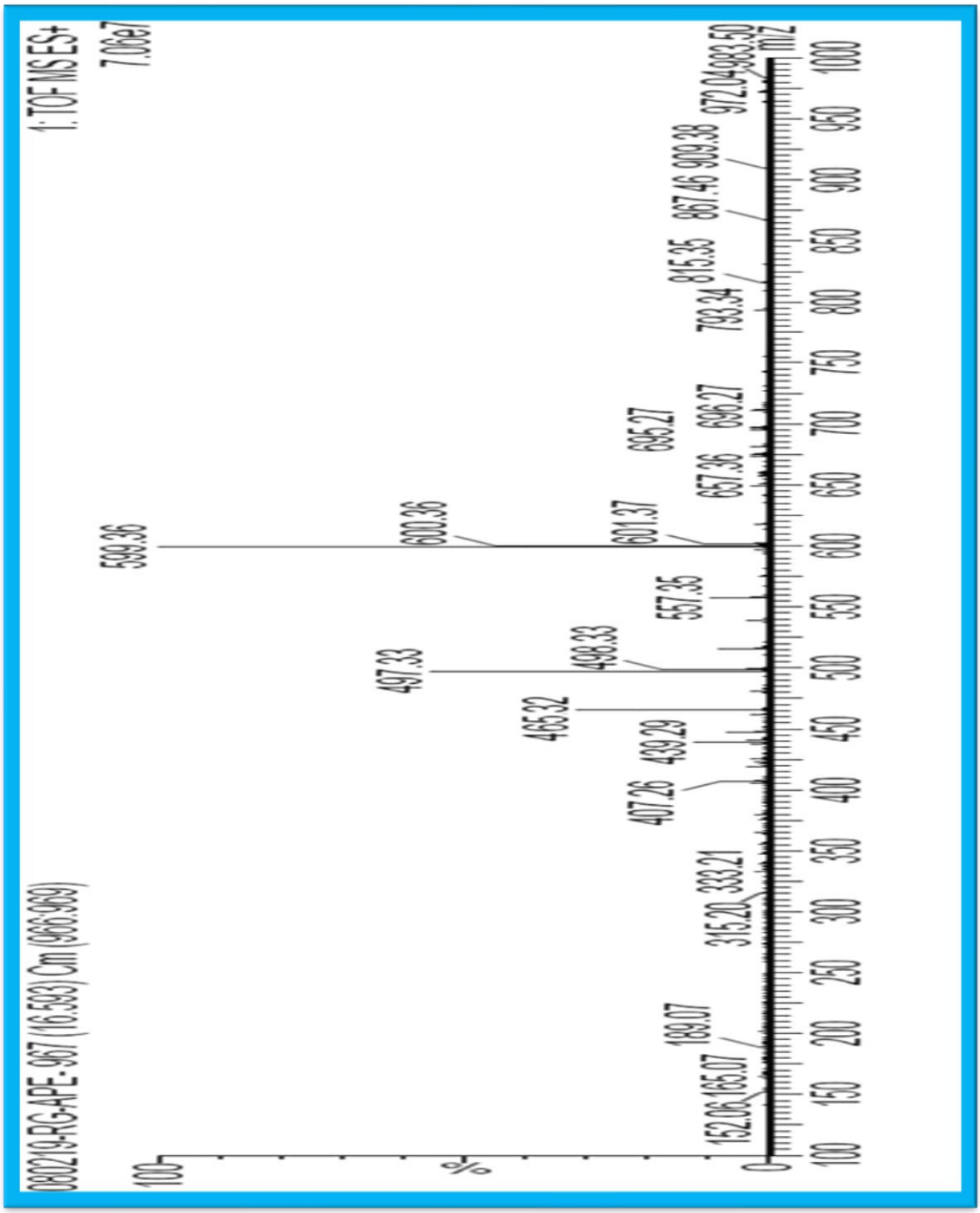

Figure 25: Mass Spectra of Compound RG-APE2 (Rohituka 3)

5.6.5.2 Compound RG-APE3

Physical state Light brown flakes

R_f value 0.371 (solvent system 100% EtOAc)

Melting point 189ºC

The compound gave a positive response for Liebermann- Burchard test for triterpenoids.

Spectral Characteristics of Compound

IR (KBr):	3456.11 cm^{-1} (br, OH)
	1745.0 cm^{-1} (C=O ester)
	1641.22 cm^{-1} & 820.39 cm^{-1}
	(trisubstituted double bond)
	860.37 cm^{-1} (Furan moiety)
	1244.4 cm^{-1} (epoxide ring)
	893.29 cm^{-1} (exocyclic methyl group)
^{1}HNMR (DMSO)	δ 0.96 - δ 1.05 (s, 12H, H-18, H-19,
	H-24, H-25), δ 1.06, 1.33, 1.40,1.17 (s,4H, H-
	11,12), δ 2.26(d,1H, H-5), δ 2.27 (s,2H, H-6),
	δ 2.28 (s,1H, H-9), δ 3.39 (s,1H, H-3),
	δ 3.78 (s,3H, H-27), δ 4.88 (s,1H, H-15),

δ 4.91, δ 5.09 (each s,2H H-26),

δ 5.63 (s,1H, H-17), δ 5.68 (s,1H, H-1),

δ 5.86 (s,1H, H-2,), δ 6.43-δ 7.59 (m,3H, H-21,22,23 of furan), δ 1.27 (s, 3H, H-6″),

δ 3.80- δ 4.49(m, 4H, H-2′,3′,4′5′),

δ 4.52 (s,1H, H-1″),

δ 4.54- δ 4.68(m,4H, H-2″,3″,4″,5″),

δ 4.70-4.87 (m,6H, H-2′,3′,4′,2″,3″,4″-OH),

δ 4.93 (s,2H, H-6′), δ 5.13 (s,1H, H-1′)

^{13}CNMR (DMSO) δ 136.14 (C-1), δ 124.59 (C-2), δ 105.44 (C-3),

δ 37.51 (C-4), δ 39.93 (C-5), δ 39.51 (C-6),

δ 172.93 (C-7), δ 149.50 (C-8), δ 40.14 (C-9),

δ 28.96 (C-10), δ 27.21 (C-11), δ 28.96 (C-12),

δ 39.72 (C-13), δ 78.50 (C-14), δ 59.64 (C-15),

δ 170.14 (C-16), δ 86.50 (C-17), δ 11.41 (C-18),

δ 14.00 (C-19), δ 120.14 (C-20), δ 101.59 (C-21),

δ 140.16 (C-22), δ 142.93 (C-23), δ 20.66 (C-24),

δ 20.41 (C-25), δ 114.14 (C-26), δ 49.85 (C-27),

δ 110.16 (C-1′), δ 90.50 (C-2″), δ 70.14 (C-3′),

δ 79.03 (C-4′), δ 79.16 (C-5′), δ 39.30 (C-6′),

δ 112.12 (C-1″), δ78.83 (C-2′), δ 87.59 (C-3″),

δ 88.03 (C-4″), δ 68.16 (C-5″), δ 15.44 (C-6″)

Mass spectra (ESI-MS)

Molecular Formula: $C_{39}H_{54}O_{16}$

Molecular weight: 778.84

ESI-MS (m/z): 779.0 $(M+H)^+$ the other Peaks appeared at 712.4, 677, 623.3, 560.4, 482, 390.7, 278.8, 144.9

From the m.p, IR, ^{1}HNMR, ^{13}CNMR and Mass spectra, compound RG-APE3 was designated as

Amoorinin-3-O-α-L-Rhamnopyranosyl–(1→6)–β-D-glucopyranoside.

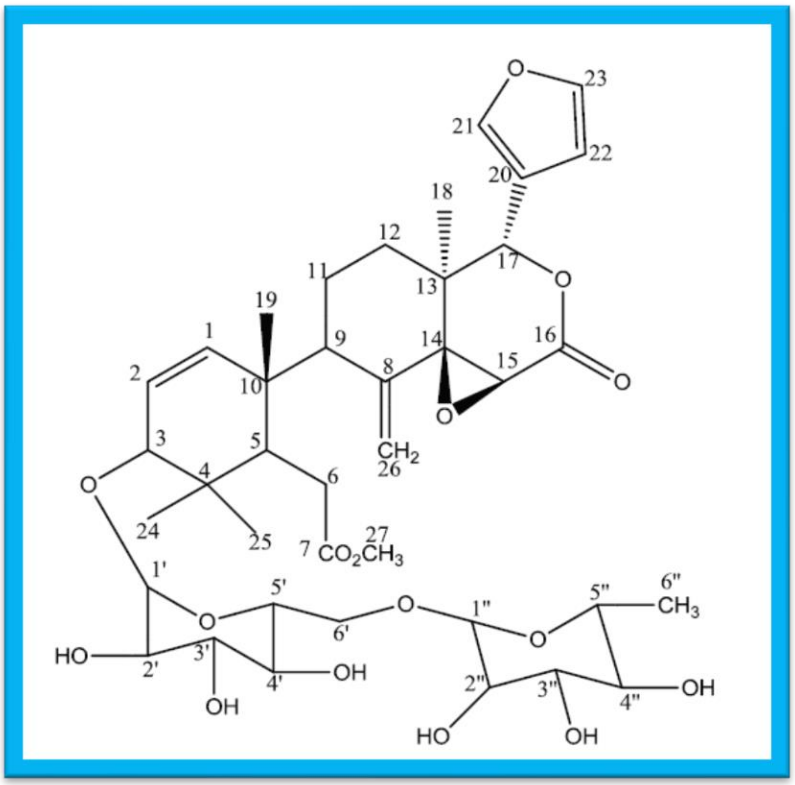

Figure 26: Chemical Structure of Compound RG-APE3

(Amoorinin-3-O-α-L-rhamnopyranosyl– (1→6) –β-D-glucopyranoside)

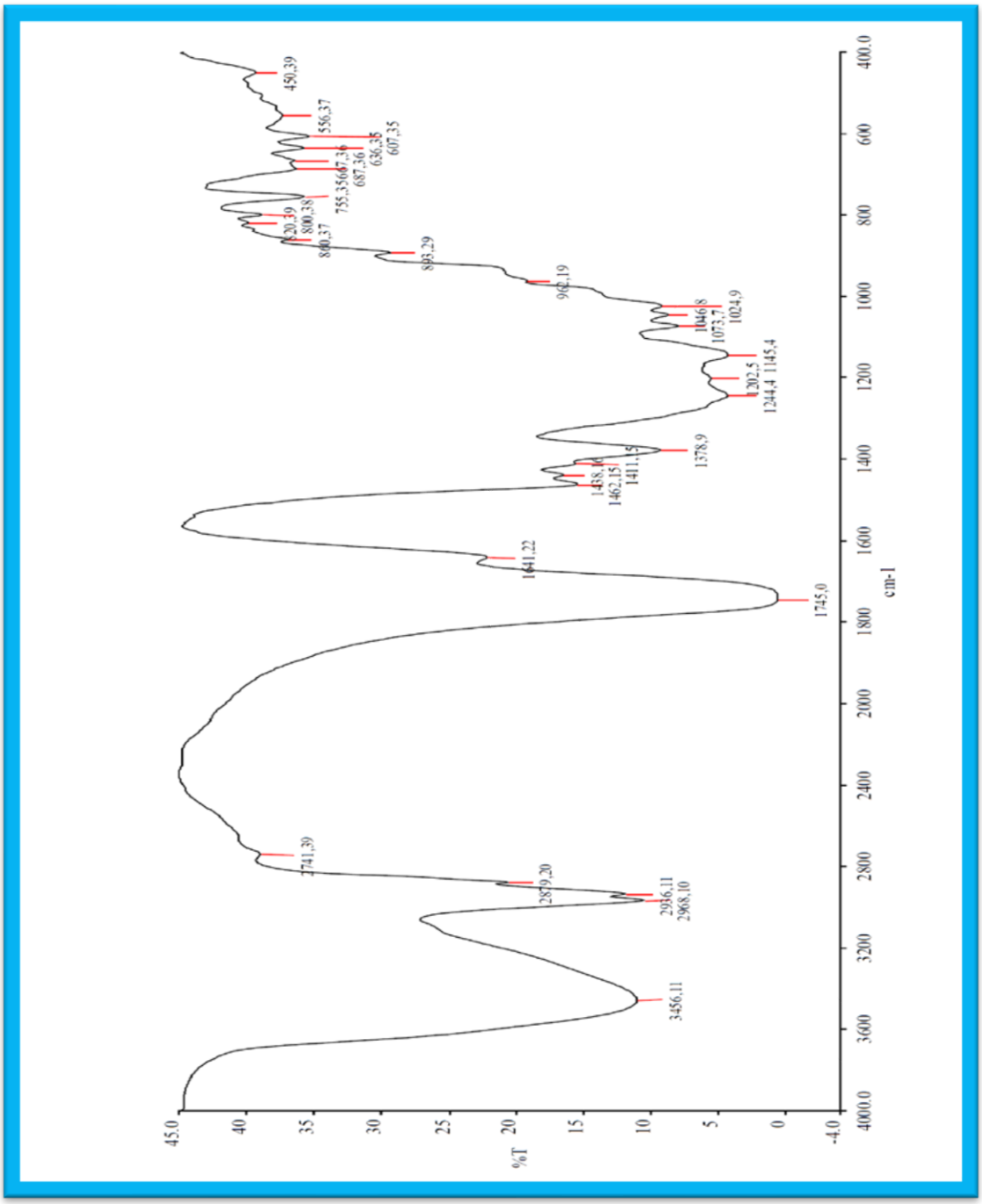

Figure 27: IR Spectrum of Compound RG-APE3

(Amoorinin-3-O-α-L-Rhamnopyranosyl-(1→6) –β-D-Glucopyranoside)

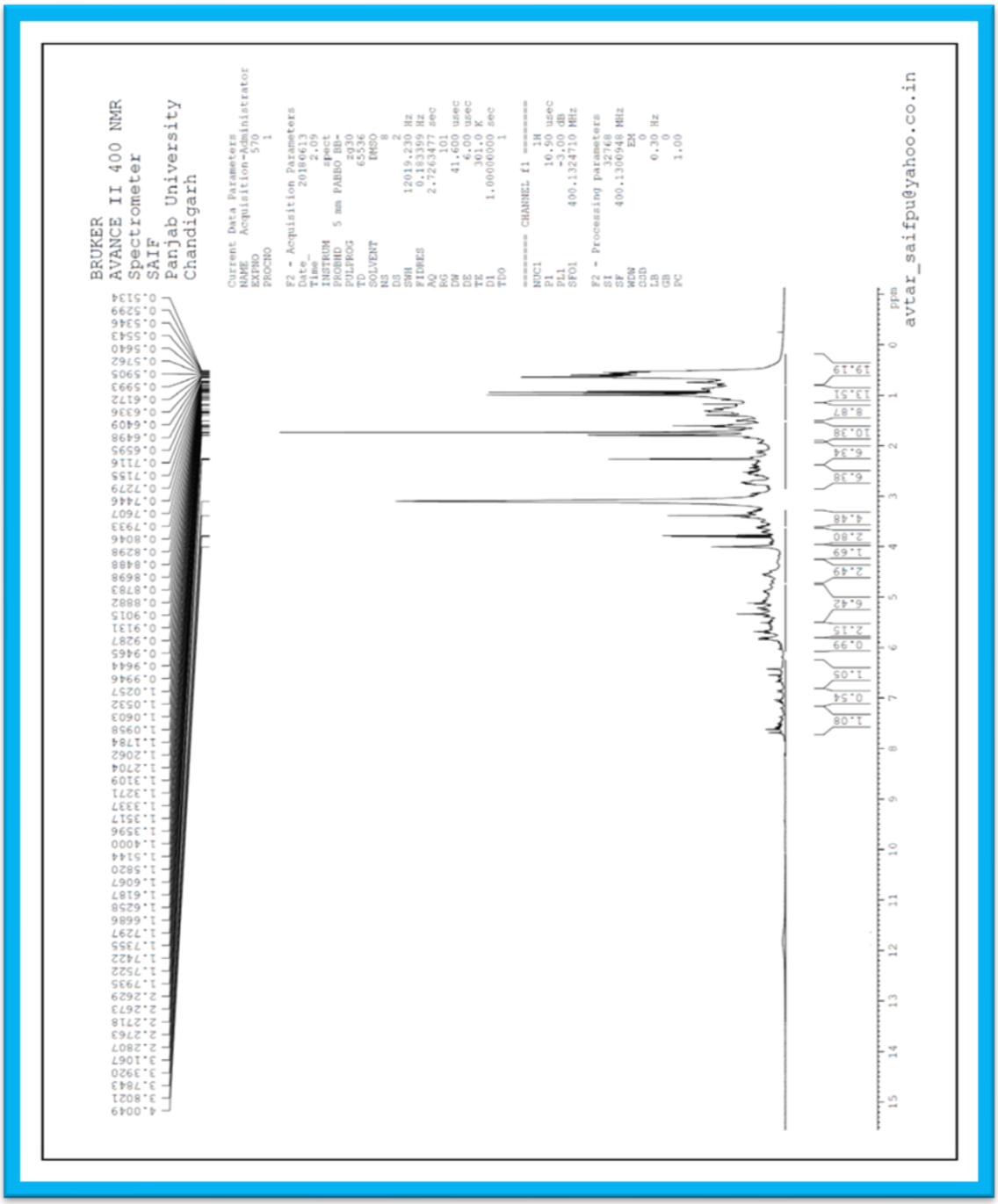

Figure 28: ^{1}H NMR Spectra of Compound RG-APE3

(Amoorinin-3-O-α-L-Rhamnopyranosyl-(1→6) –β- D-Glucopyranoside)

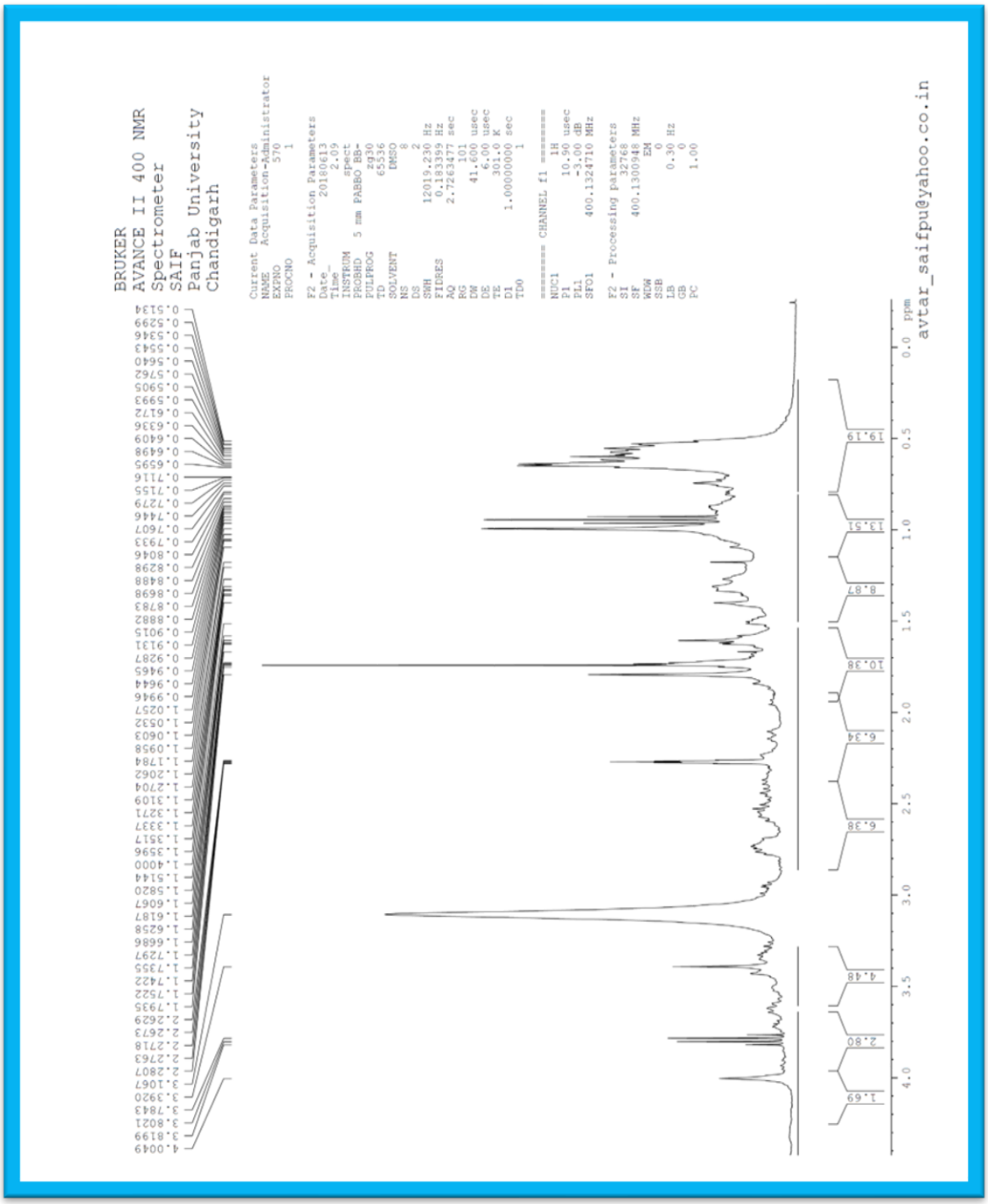

Figure 29: ^{1}H NMR Spectra of Compound RG-APE3

(Amoorinin-3-O-α-L-Rhamnopyranosyl-(1→6) –β-D-Glucopyranoside)

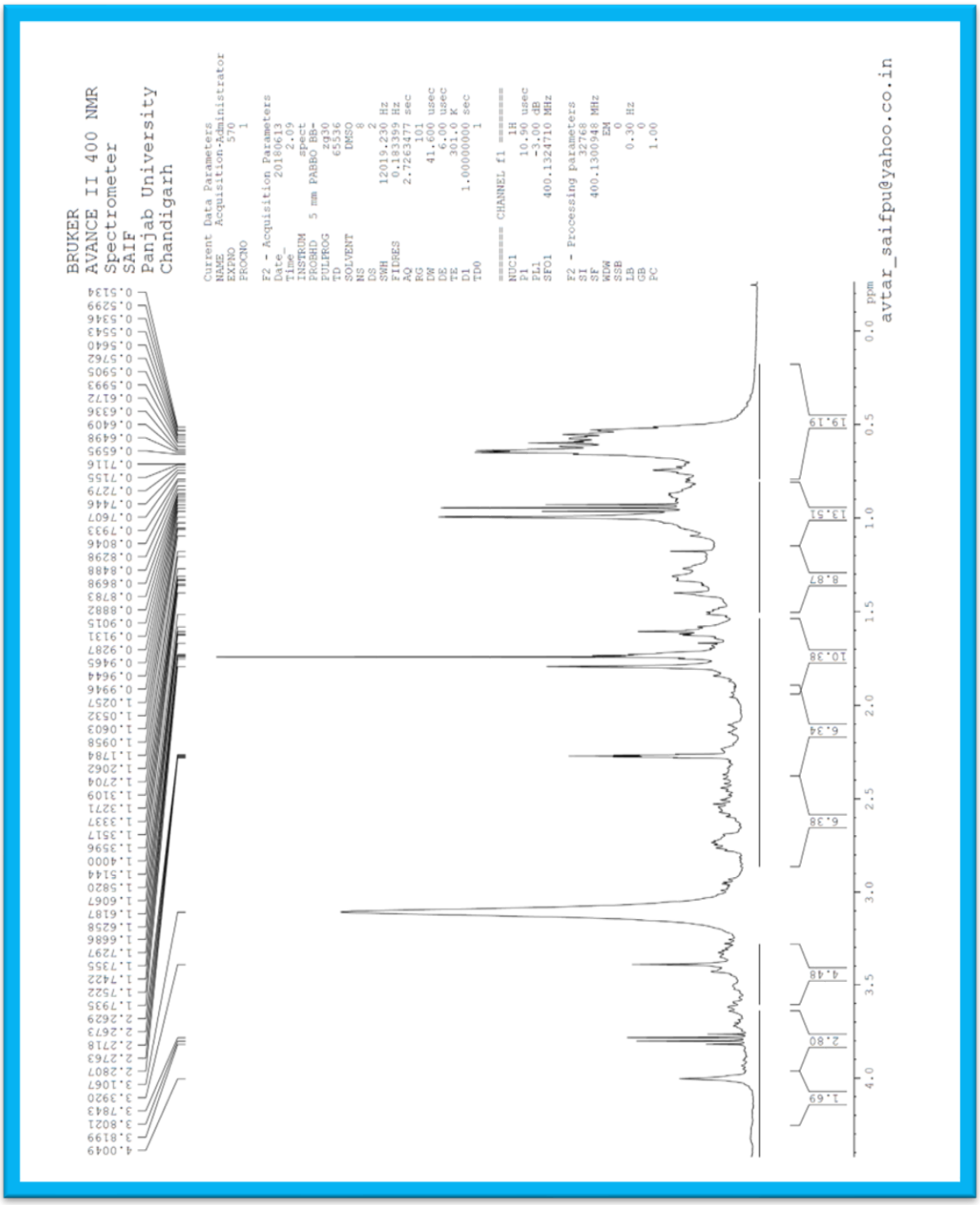

Figure 30: ^{1}H NMR Spectra of Compound RG-APE3

(Amoorinin-3-O-α-L-Rhamnopyranosyl-(1→6) –β-D-Glucopyranoside)

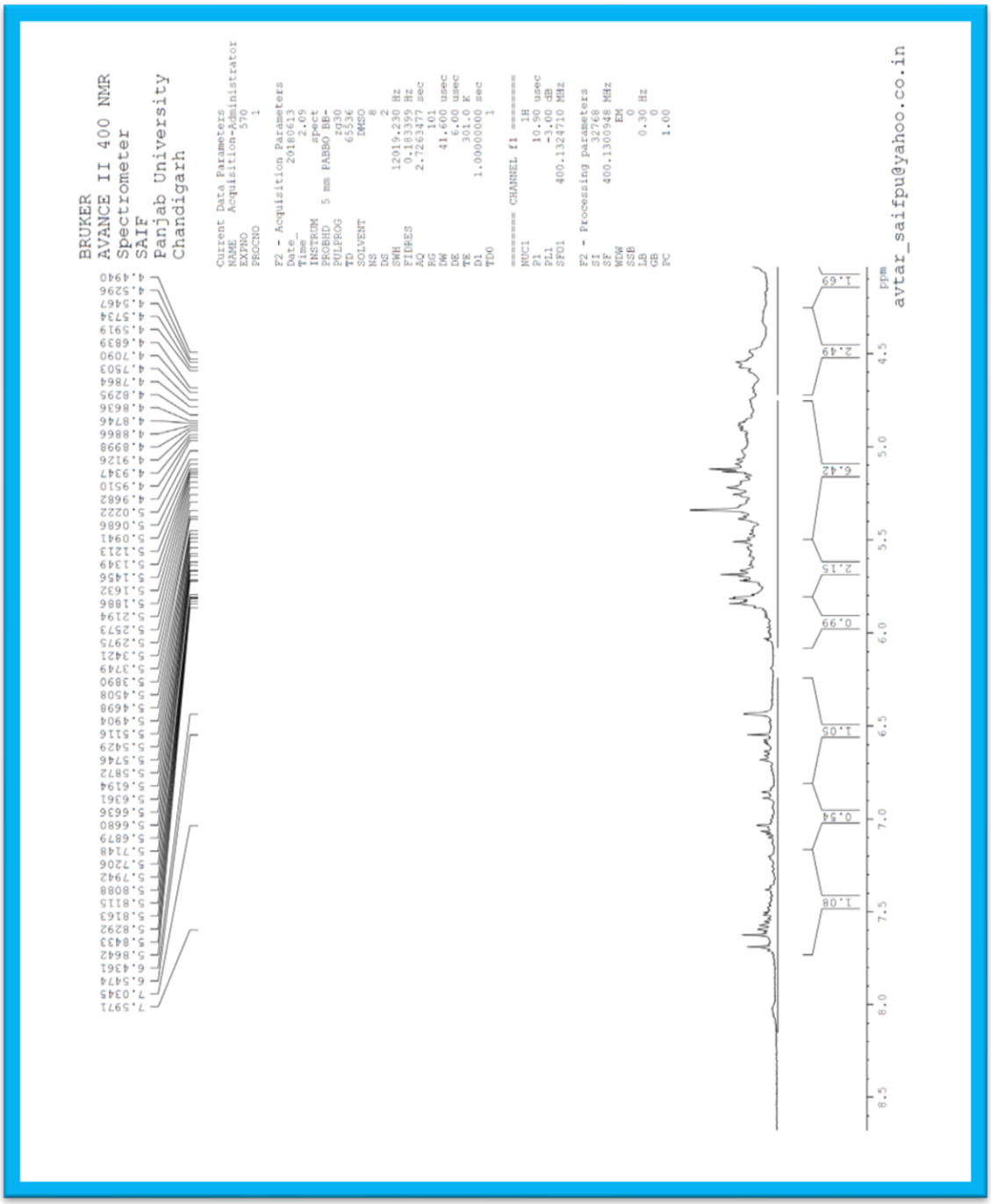

Figure 31: ^{1}H NMR Spectra of Compound RG-APE3

(Amoorinin-3-O-α-L-Rhamnopyranosyl-(1→6) –β- D-Glucopyranoside)

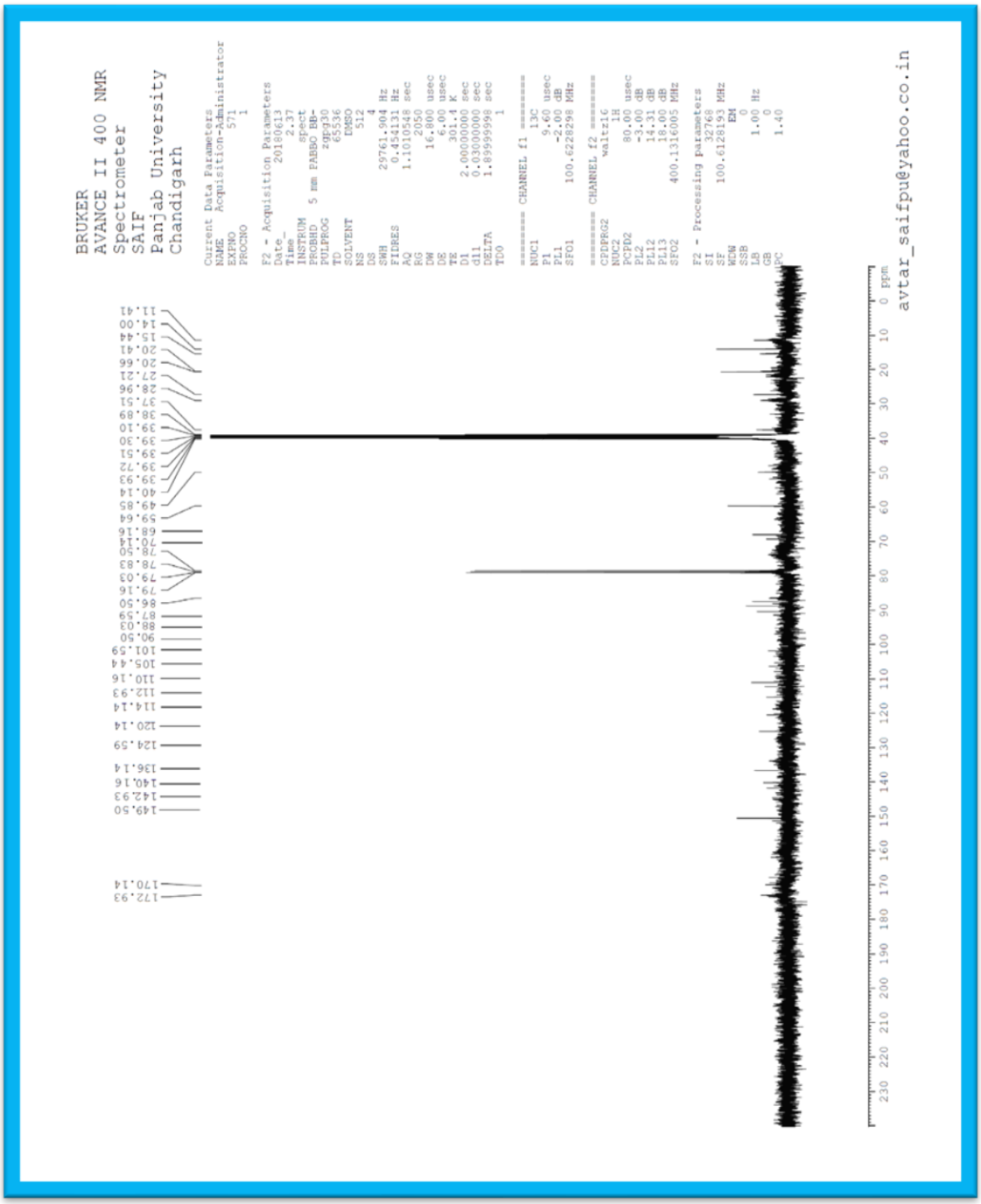

Figure 32: ^{13}C NMR Spectra of Compound RG-APE3

(Amoorinin-3-O-α-L-Rhamnopyranosyl-(1→6) –β- D-Glucopyranoside)

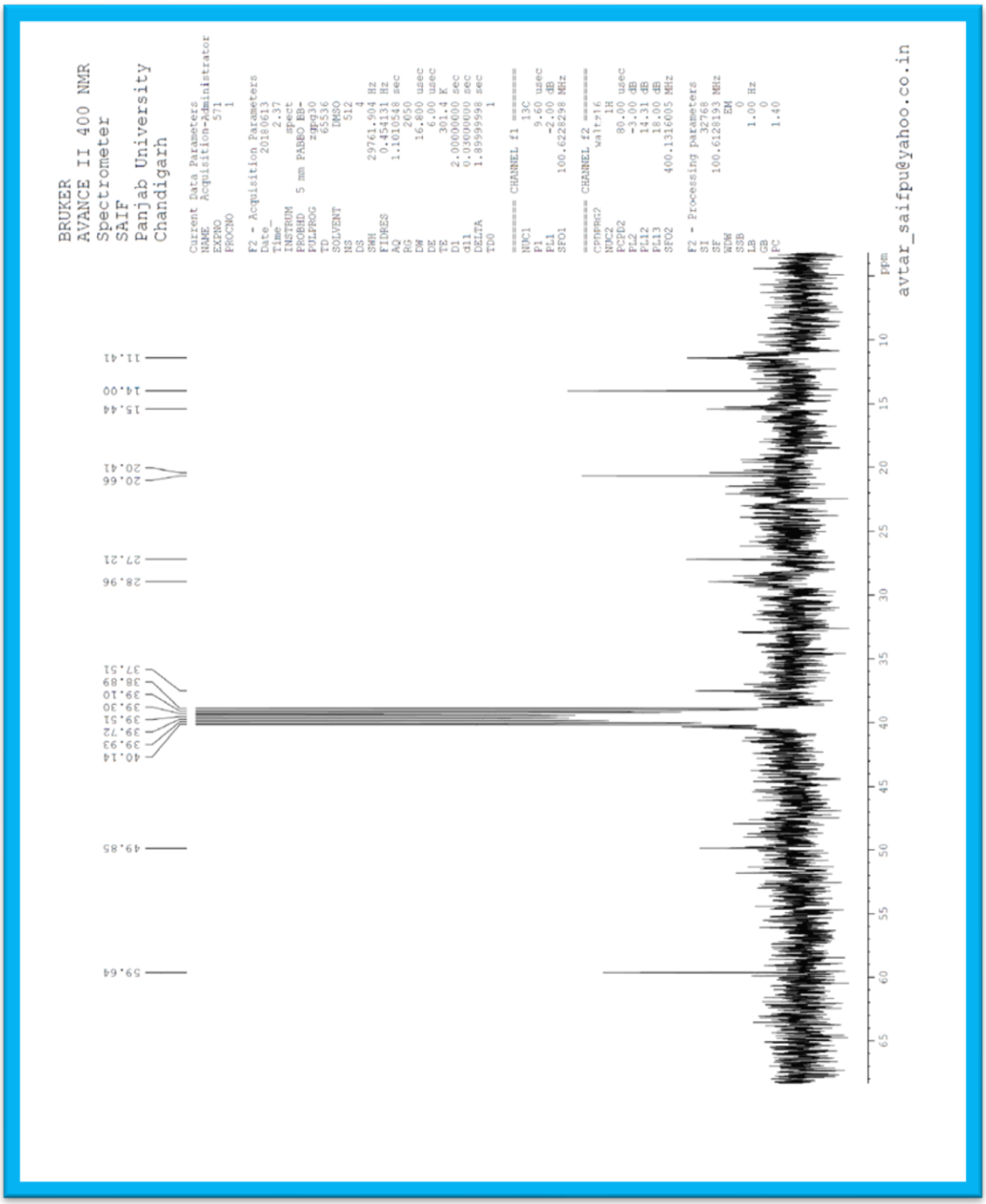

Figure 33: ^{13}C NMR Spectra of Compound RG-APE3

(Amoorinin-3-O-α-L-Rhamnopyranosyl-(1→6) –β-D-Glucopyranoside)

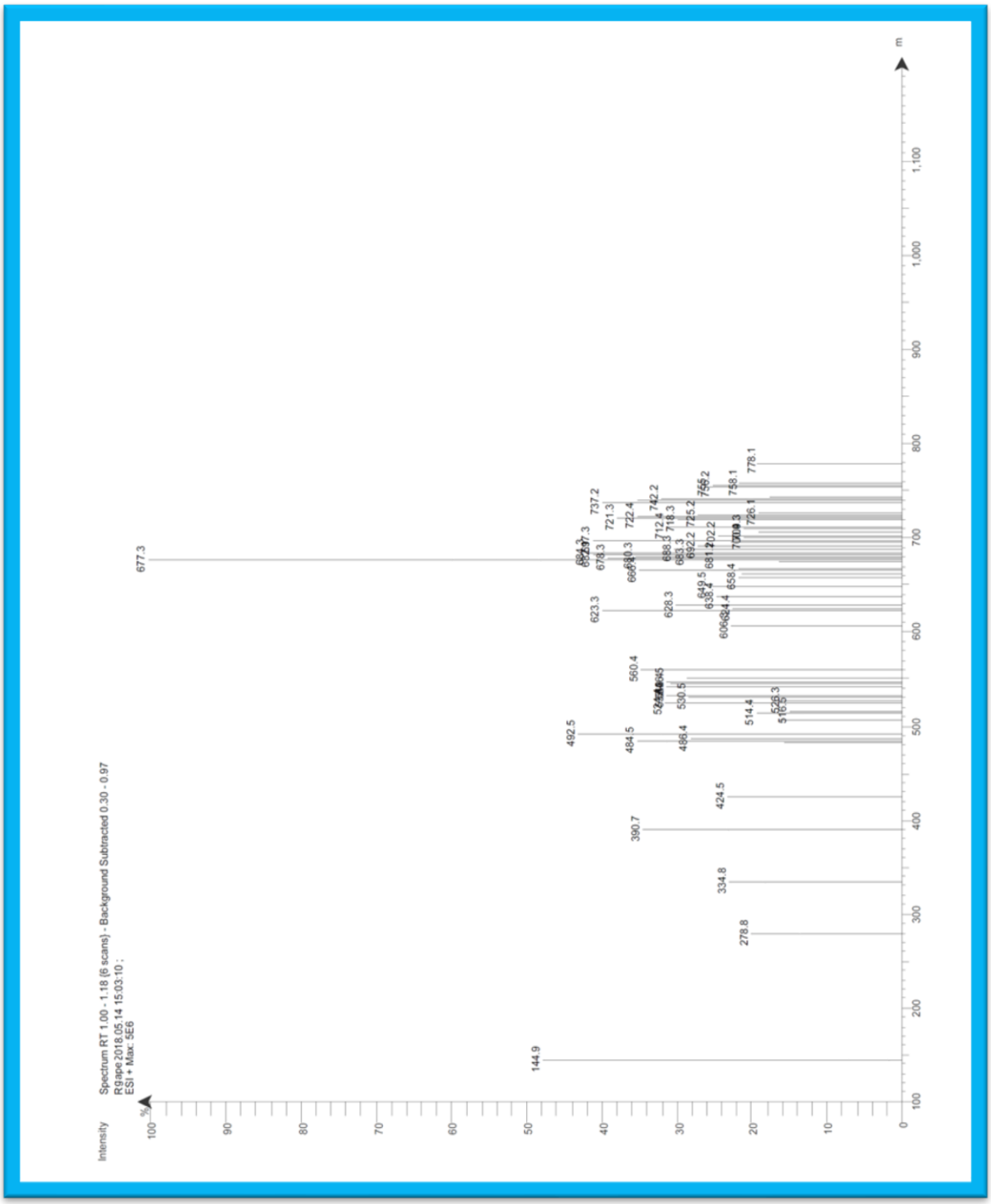

Figure 34: Mass Spectrum of Compound RG-APE3

(Amoorinin-3-O-α-L-Rhamnopyranosyl-(1→6) –β- D-Glucopyranoside)

5.6.5.4 Compound RG-APE4

Physical state Yellow solid

R_f value 0.60 (solvent system $CHCl_3$: EtOAc 60:40)

Melting Point 212^0C

The compound gave positive test for flavanone glycoside.

Spectral Characteristics of Compound

IR (KBr) 3447.18 cm^{-1} (br, OH)

2963.12 cm^{-1} (C-H str.in CH_3)

2877.24 cm^{-1} (C-H str. of OCH_3)

1644.29 cm^{-1} (C=O str flavonone)

1461.18, 1377.10 cm^{-1} (C-H str. in flav)

1234.4, 1147.6, 800.4 cm^{-1}

(C-H str. in flavonone nucleus)

828.41 cm^{-1} (glycoside)

^{1}HNMR (DMSO) δ1.24 (s, 3H, H-6‴- Me), δ 2.13 (s, 3H, H-8 Me),

δ 2.53 (s,1H, H-5″), δ 3.39 (s,1H, H-3″),

δ 3.58 (s,2H, H-6″), δ 3.69 (s,2H, H-6‴),

δ 3.72 (s,1H, H-2‴′), δ 3.77 (s,2H, H-3),

δ 3.82-3.87 (m,9H, H-2″,3″,4″,2‴,3‴,6‴,2‴′,3‴′

4‴′-OH), δ 3.80, 3.93, 4.00 (s, 9H, H-2′, 4′, 7-

3xOMe) δ 6.04 (d, 1H, H-1″),

δ 6.05 (d, 1H, H-1‴), δ 5.07 (d,1H, H-1‴′),

δ 5.38 (m,1H, H-2), δ 6.63 (s,1H, H-6),

δ 6.95 (s,1H, H-3′), δ 7.30 (d,1H, H-5′),

δ 7.32 (d,1H, H-6′), δ 4.02 (s,1H, H-2″),

δ 4.10 (s,1H, H-4″), δ 4.20 (s,1H, H-2‴),

δ 4.54 (s,1H, H-3‴), δ 4.55 (s,1H, H-3‴′),

δ4.56 (s,1H, H-4‴), δ 4.58 (d, 1H, H-4‴′),

δ 5.04 (d, 1H, H-5‴), δ5.07 (m, 1H, H-5‴′),

^{13}CNMR (DMSO) δ 83.03 (C-2), δ 40.15 (C-3), δ 195.15 (C-4),

δ 102.89 (C-4a), δ 164.86 (C-5) δ 130.13 (C-6),

δ 168.37 (C-7), δ 115.37 (C-8) δ 165.67 (C-8a),

δ 11.68 (C-8-Me) δ 129.13 (C-1′),

δ 155.67 (C-2′), δ 114.86(C-3′), δ 159.03 (C-4′),

δ 116.52 (C-5′), δ119.03 (C-6′), δ 55.67, 56.62,

50.15 (C-2′,4′,7- OCH_3 x3), δ 103.03 (C-1″),

δ 78.37 (C-2″), δ 39.52 (C-3″), δ 31.94 (C-4″), δ 81.30 (C-5″), δ 38.89 (C-6″), δ 94.71 (C-1‴), δ 39.94 (C-2‴), δ 79.03 (C-3‴), δ 31.30 (C-4‴), δ 28.71 (C-5‴), δ 25.02 (C-6‴), δ 99.94 (C-1⁗), δ 39.73 (C- 2⁗), δ 39.31 (C-3⁗), δ 29.03 (C-4⁗), δ 28.62 (C-5⁗), δ 18.79 (C-6⁗)

Mass spectra (ESI-MS)

Molecular Formula: $C_{37}H_{50}O_{20}$

Molecular weight: 814.78

ESI-MS (m/z): 816.1 $(M+, 2H)^+$ The other peaks are observed at 751.1, 572.4, 332.7, 159.8, 145.9, 128, 113.9

From the m.p, IR, ^{1}HNMR, ^{13}CNMR and Mass spectra, compound RG-APE4 was designated as

8- Methyl-7, 2′4,′-tri-O-Methylflavonone-5-O-α-L-Rhamnopyranosyl (1→ 4)-β-D- glucopyranosyl-(1→ 6)-β-D-glucopyranoside.

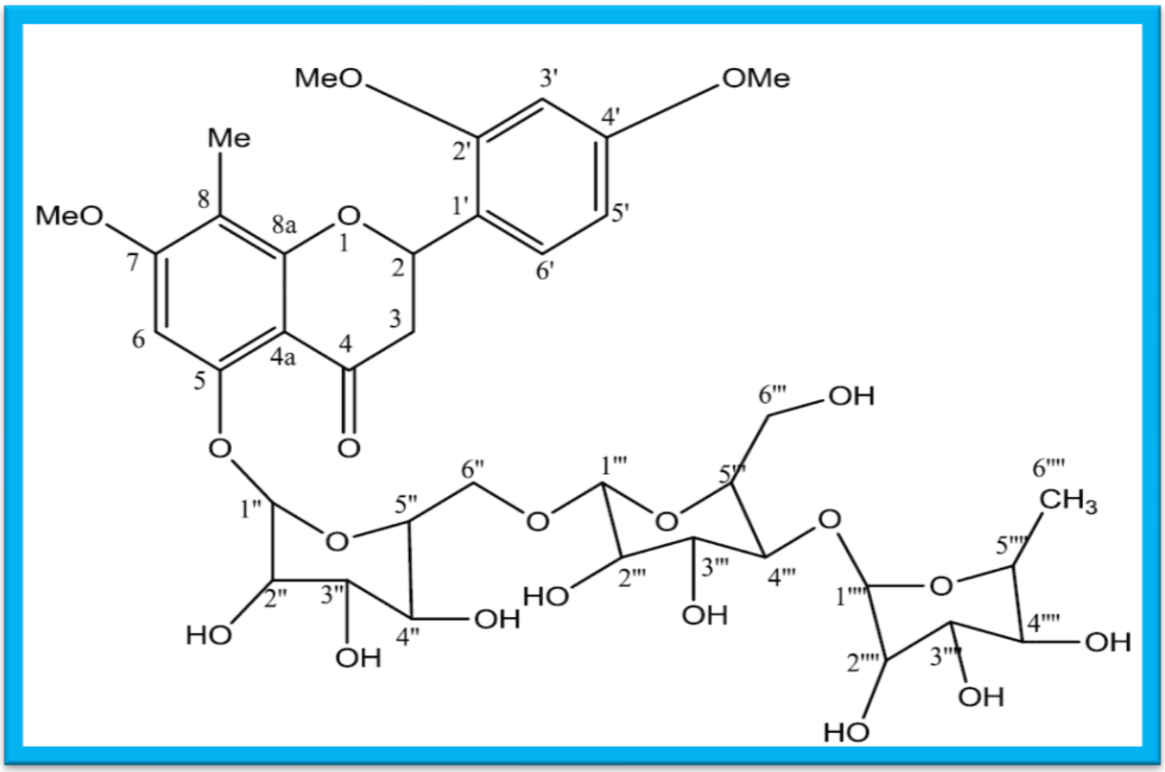

Fig 35: Chemical Structure of Compound RG-APE4

(8- Methyl-7, 2′4,′-tri-O-Methylflavonone-5-O-α-L-Rhamnopyranosyl (1→ 4)-β-D-glucopyranosyl-(1→ 6)-β--glucopyranoside)

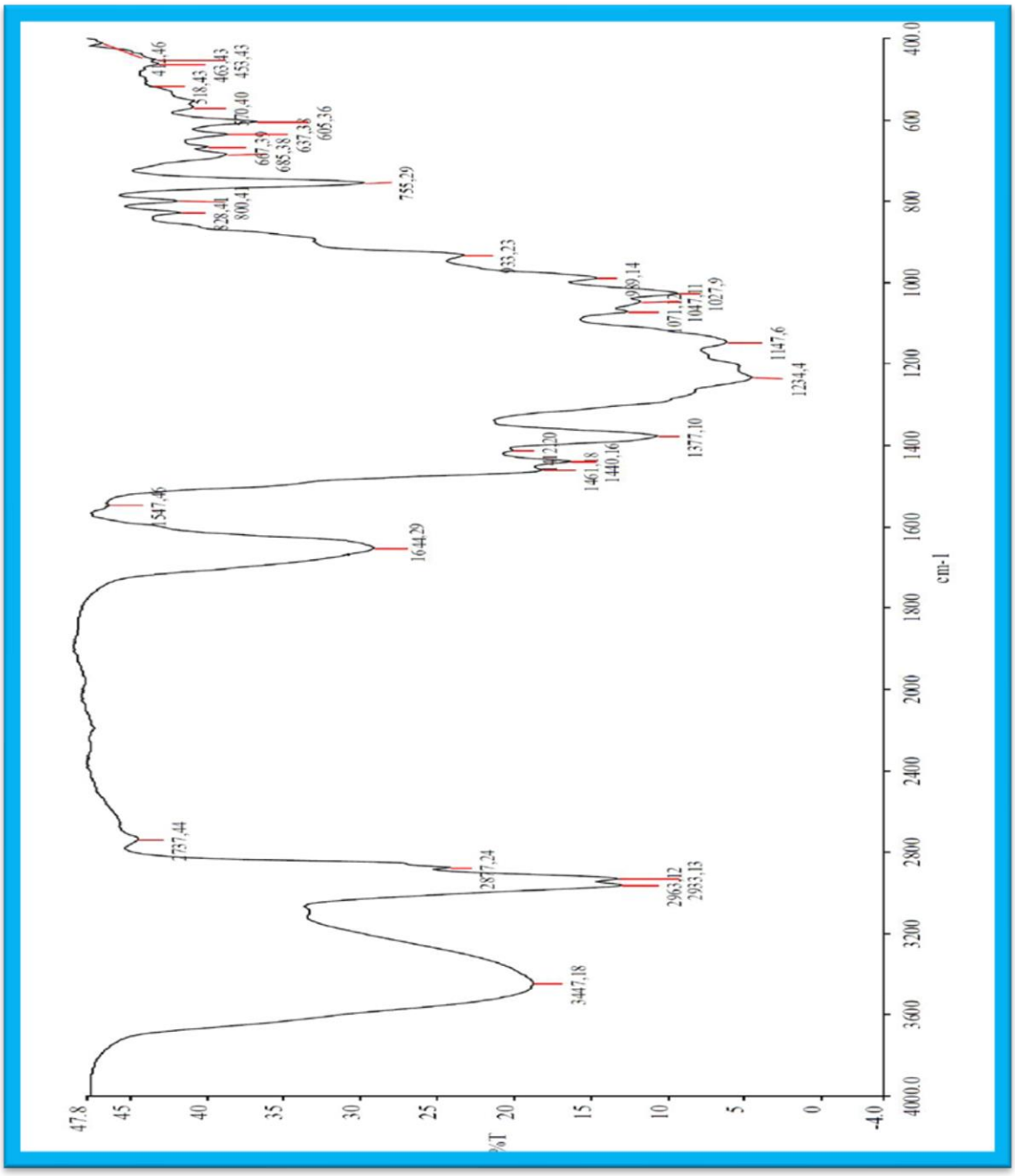

Figure 36: IR Spectrum of Compound RG-APE4

(8- Methyl-7, 2′4,′-tri-O-Methylflavonone-5-O-α-L-Rhamnopyranosyl (1→ 4)-β-D-glucopyranosyl-(1→ 6)-β--glucopyranoside)

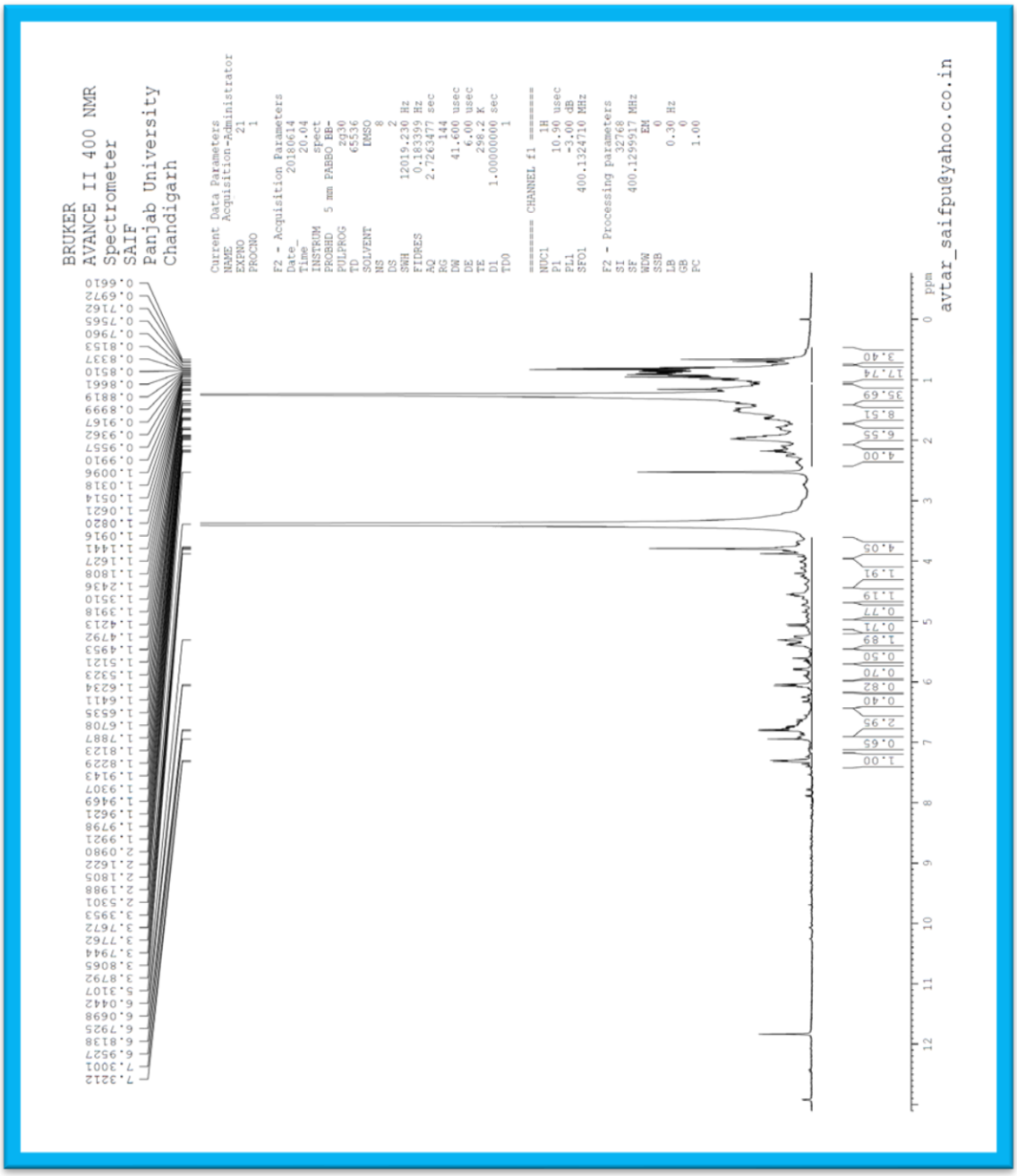

Figure 37: ^{1}H NMR Spectra of Compound RG-APE4

(8- Methyl-7, 2′4,′-tri-O-Methylflavonone-5-O-α-L-Rhamnopyranosyl (1→ 4)-β-D-glucopyranosyl-(1→ 6)-β--glucopyranoside)

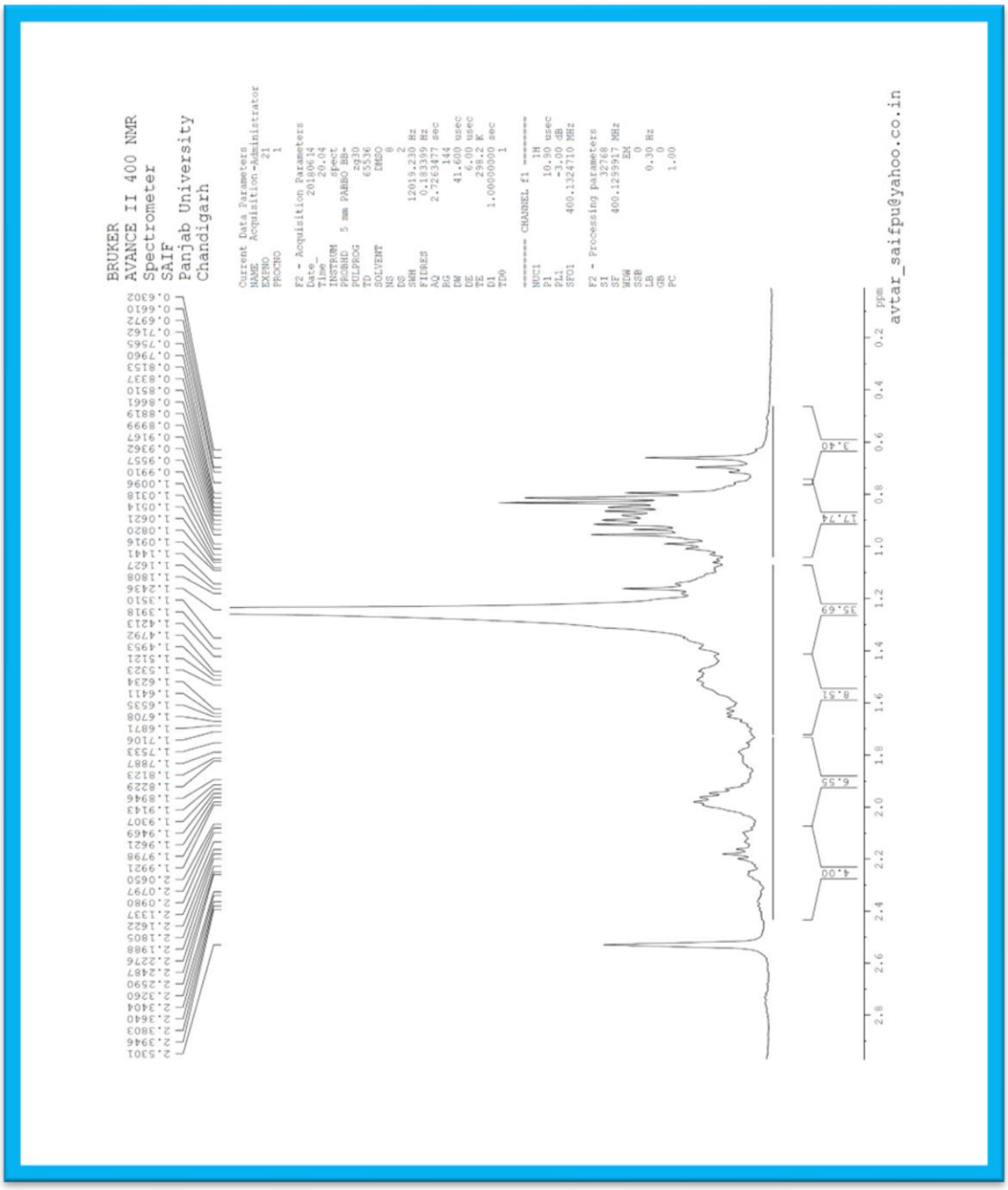

Figure 38: ^{1}H NMR Spectra of Compound RG-APE4

(8- Methyl-7, 2′4,′-tri-O-Methylflavonone-5-O-α-L-Rhamnopyranosyl (1→ 4)-β-D-glucopyranosyl-(1→ 6)-β--glucopyranoside)

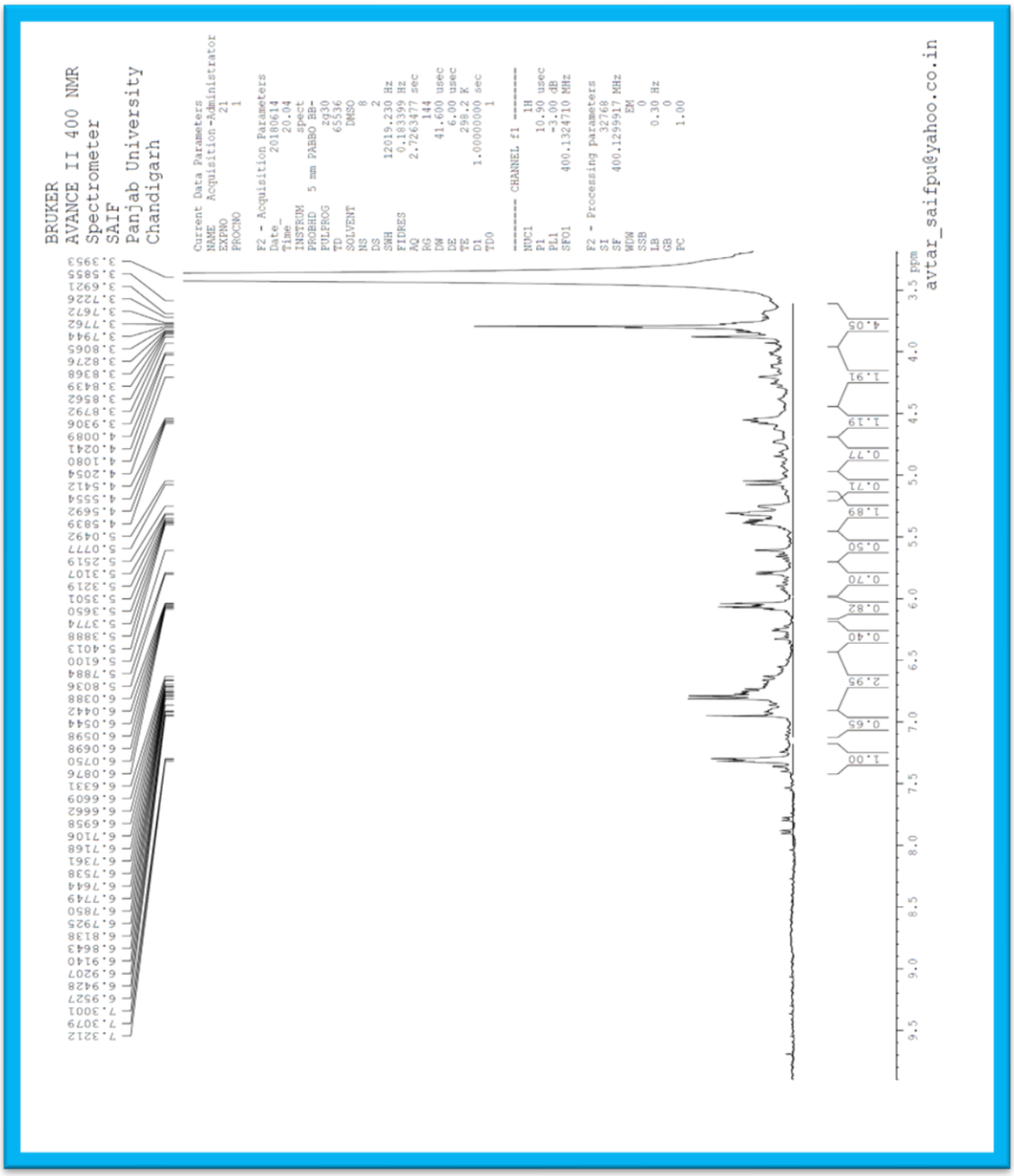

Figure 39: ^{1}H NMR Spectra of Compound RG-APE4

(8- Methyl-7, 2′4,′-tri-O-Methylflavonone-5-O-α-L-Rhamnopyranosyl (1→ 4)-β-D-glucopyranosyl-(1→ 6)-β--glucopyranoside)

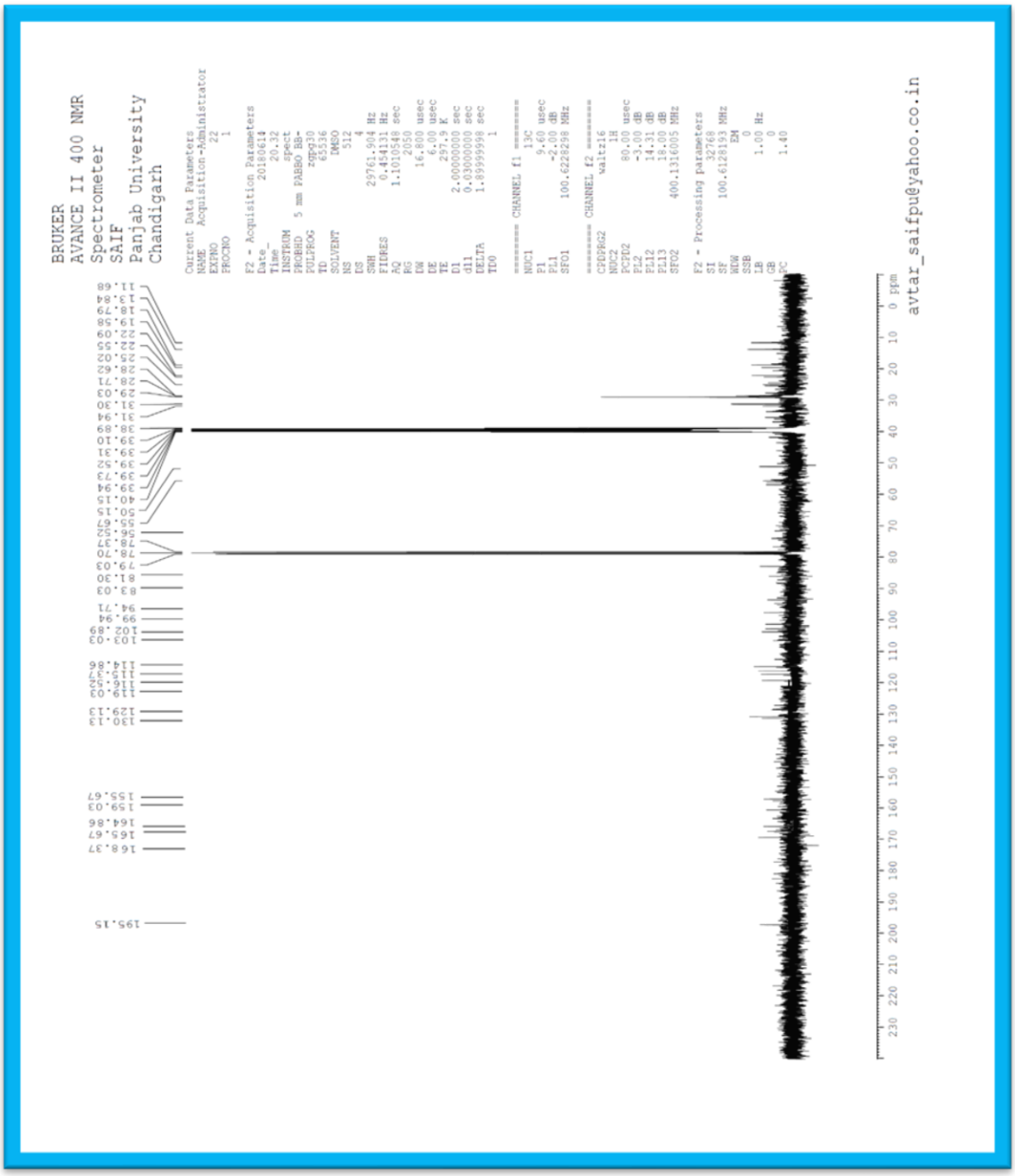

Figure 40: ^{13}C NMR Spectra of Compound RG-APE4

(8- Methyl-7, 2′4,′-tri-O-Methylflavonone-5-O-α-L-Rhamnopyranosyl (1→ 4)-β-D-glucopyranosyl-(1→ 6)-β--glucopyranoside)

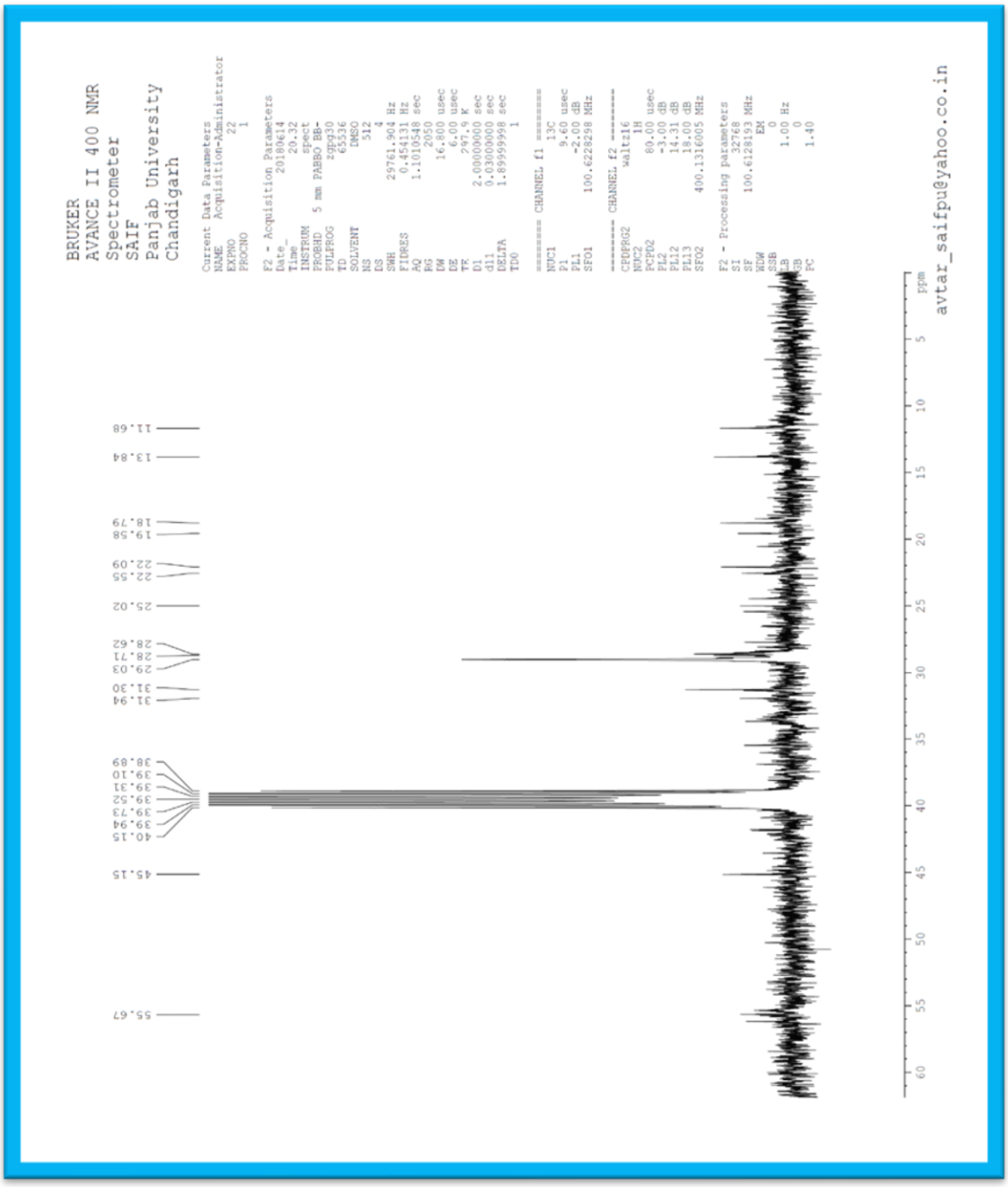

Figure 41: ^{13}C NMR Spectra Compound RG-APE4

(8- Methyl-7, 2′4,′-tri-O-Methylflavonone-5-O-α-L-Rhamnopyranosyl

(1→ 4)-β-D-glucopyranosyl-(1→ 6)-β--glucopyranoside)

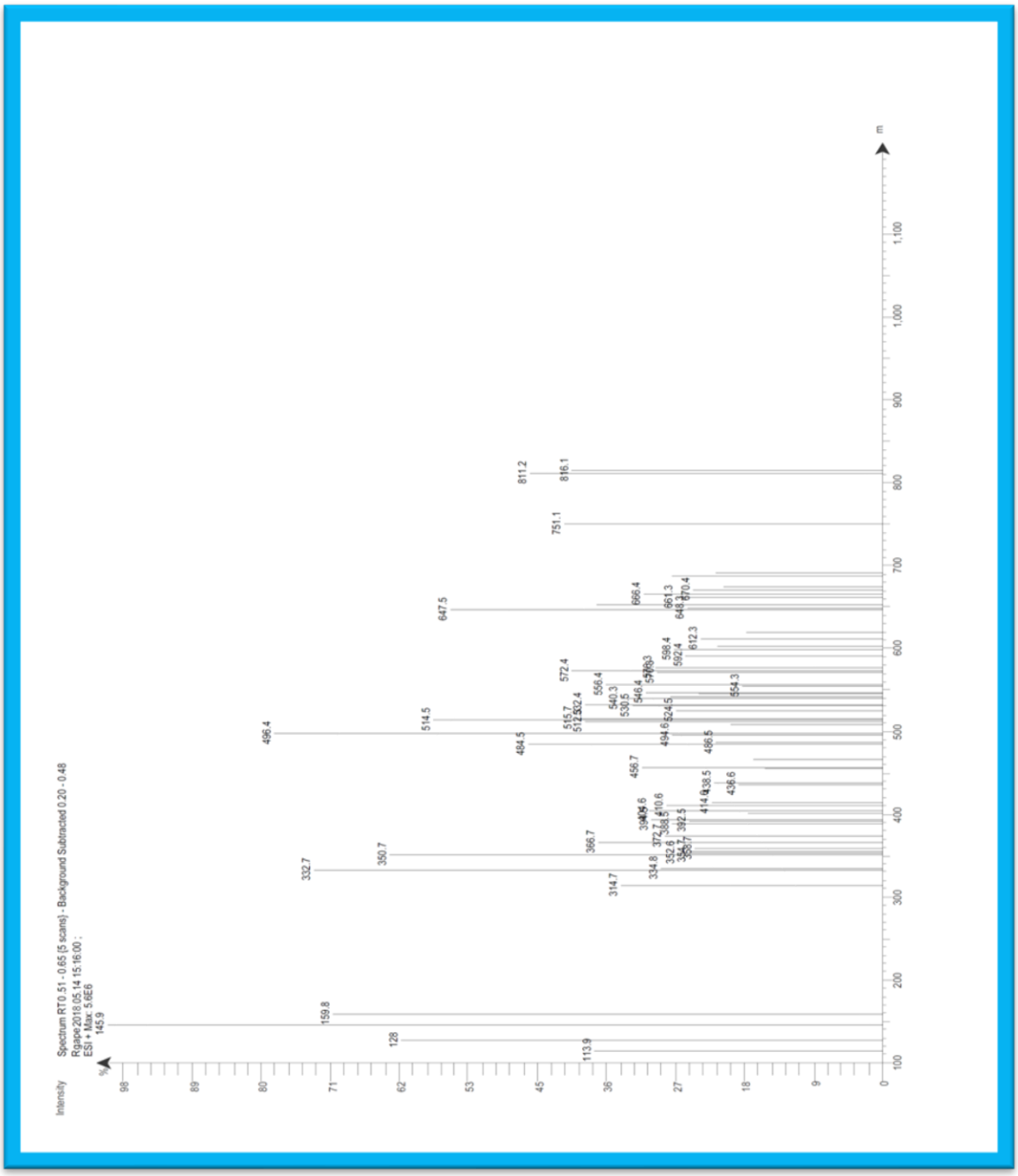

Figure 42: Mass Spectrum of Compound RG-APE4

(8-Methyl-7,2′4,′-tri-O-Methylflavonone-5-O-α-L-Rhamnopyranosyl

(1→4)-β-D-glucopyranosyl-(1→6)-β-D-glucopyranoside)

5.7 *IN VITRO* CYTOTOXIC ACTIVITY OF THE METHANOLIC EXTRACT OF THE ROOT BARK OF *A. POLYSTACHYA* [111,113]

Cytotoxic activity was determined by Sulforhodamine B (SRB) assay. The plant extract of *A. polystachya* was initially solubilized in dimethyl sulfoxide to obtain a stock solution of 100 mg/ml. The sub stock solution was prepared with water and stored in refrigerator prior to use. At the time of drug addition, 1 mg/ml of frozen aliquot was diluted to get 100, 200, 400 and 800 µg/ml. Aliquots of 10 µl of these different dilutions were added to get the final drug concentration to 10, 20, 40 and 80 µg/ml. Two human breast cancer cell lines namely MCF-7 and MDA-MB-231 were seeded at the density of $5x10^3$ cells per well in 96 well plates. The plates were incubated on addition of the extract at 37°C for 48 h. The assay was terminated by the addition of cold trichloro acetic acid. The cells were fixed *in situ* by the gentle addition of 30%w/v TCA (50 µl) and incubated for 60 min at 4°C. The supernatant was discarded, plates were washed with tap water and air dried. SRB solution (50 µl) at 0.4%w/v in 1% acetic acid was added to the wells. The plates were incubated for 20 min at room temperature. The unbound dye was removed by washing with 1 % v/v acetic acid. The plates were air dried and the bound stain was subsequently eluted with 10 millimolar trizma base and absorbance was recorded at 540 nm.

Percentage growth was calculated on a plate by plate basis for test wells relative to control wells. Percentage growth was expressed by using the following formula

$$\frac{\text{Average absorbance of the test well}}{\text{Average absorbance of the control wells}} \times 100$$

5.8 GREEN SYNTHESIS OF *A. POLYSTACHYA* NANOPARTICLES[42]

The 10^{-3} mM silver nitrate solution was freshly prepared by adding 0.16 gm of silver nitrate to 90 ml of millipore water and sonicated for 5 min. 10ml of filtered herbal extract (at a concentration range of 50 mg/ml) was taken in 250 ml conical flask/beakers separately and to this previously prepared 90 ml of silver nitrate solution was added drop wise. The conical flasks were incubated at room temperature overnight for 12 h. A color change from pale yellow to dark brown was checked periodically. The brown color formation indicates that the AgNPs were synthesized from the herbs, and they were centrifuged at 5000 rpm for 15 min in order to obtain the pellets that were used for further study.

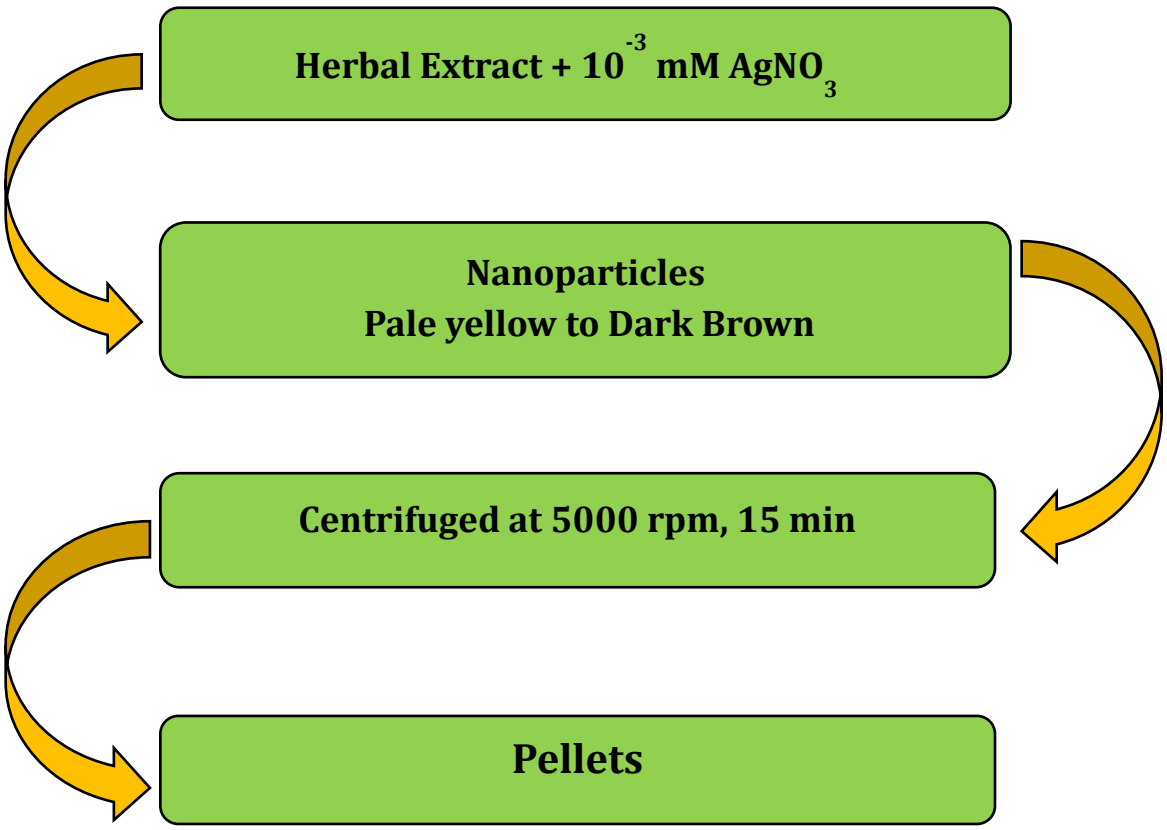

Figure 43: Green Synthesis of AgNPs from the methanolic extract of root bark of *A. polystachya*

5.9 CHARACTERIZATION OF THE SYNTHESIZED NANOPARTICLES OF THE METHANOLIC EXTRACT OF THE ROOT BARK OF *A. POLYSTACHYA* [43,107]

Characterization of AgNPs plays an important role to understand the morphological properties of nanoparticles. The characterisation of the synthesized AgNPs from the methanolic extract of root bark of *A. polystachya* were performed using the following techniques.

5.9.1 UV-Visible Spectroscopy

Green synthesized nanoparticles were confirmed by taking the serial dilutions of sample at regular intervals and the absorption maxima was scanned at 350-800 nm by using UV-2450 (Shimadzu) spectrophotometer.

5.9.2 Fourier Transmission Infra-red Spectroscopy (FTIR)

Bruker FTIR instrument was used to determine the sample functional groups. FTIR measurement was done to identify silver ions and capped plant compounds which could account for the reduction of silver nitrate into AgNPs. The sample was placed on ATR and subjected to FT-IR analysis.

5.9.3 Scanning Electron Microscopy (SEM)

Scanning electron microscopy helps to determine the morphology of nanoparticles. A very small amount of the sample was dropped on a carbon coated copper grid to obtain a thin film. Using a blotting paper, the extra solvent was removed and the film on the SEM grid was then allowed to dry by placing it under a mercury lamp for 5 min.

5.9.4 Energy Dispersive X-Ray Analysis (EDAX)

The sample of AgNPs of *A. polystachya* was taken and subjected to EDAX analysis for Ag and other compounds.

5.9.5 Particle Size Analysis (PSA)

Particle size of *A. polystachya* AgNPs was measured by Particle size analyser (DLS). This instrument gives the average size of nanoparticles. It's a simple technique, where the sample is dissolved in methanol and kept under ultra-sonication for 10 min for proper distribution of nanoparticles in solution and then analysed using DLS.

5.9.6 X-Ray Diffraction (XRD)

The synthesized herbal mediated AgNPs obtained were purified by repeated centrifugation at 5000 rpm for 20 min followed by redispersion of the pellet of AgNPs of *A. polystachya* in 10 ml of deionized water. After drying of the purified AgNPs, the

crystalline structure was analyzed by XRD. The dried mixture of AgNPs was collected for the determination. The instrument was operated at a voltage of 40 kV and at a current of 30 mA with Cu Kα radiation in a configuration of θ- 2 θ.

5.9.7 Transmission Electron Microscopy (TEM)

A small amount of AgNPs of *A. polystachya* were suspended in ethanol (just enough to obtain a slightly turbid solution). The solution was ultrasonicated to disperse the particles. A drop of the solution was then pipetted out and cast on carbon-coated grids of 200 mesh instrument Make Jeol Model JM 2100.

5.9.8 Atomic Force Microscopy (AFM)

A small portion of the synthesized AgNP of *A. polystachya* was weighed. Atomic Absorption Microscope (Bruker) was used for obtaining ultra-high resolution in particle size measurement using the probe – OTESPA-R3 with a scan rate at 0.693 Hz at 256 sample/line and a stiffness k at 25-35 N/m. Atomic Force Microscopy provides an accurate description of size and size distribution.

5.10 CELL CYCLE AND APOPTOTIC ANALYSIS OF SILVER NANOPARTICLES OF *A. POLYSTACHYA* [72,104]

For cytotoxicity assays, the stabilised AgNPs of *A. polystachya* was studied under *in vitro* conditions by using colorimetric MTT assay method. The MCF-7 breast cancer cells were grown in Dulbecco Modified Eagle Medium (DMEM), Fetal Calf Serum (FCS) 10 % in a T25 flask. Cells were seeded in a 6 well microtiter tissue culture plates and serum starved overnight. Cells were treated with FCS and 40 µg/ml of the AgNPs for 24 h. Doxorubicin was used as a positive control. The untreated cells were treated with PBS. After 24 h, the cells were gently trypsinized and washed with Phosphate buffered saline (PBS) twice. Cells were fixed in methanol and stained with 0.1% propidium iodine (SIGMA) and analysed for cell cycle and apoptosis on flow cytometer (BD FACS Cali bur). Events were detected by flow cytometry on the FL2 channel with the detector in logarithmic mode (FL2-H). Doublet discrimination on the FL2 channel is used to identify single cell events.

5.11 ELISA PROTOCOL [87,98,104]

Samples of AgNPs of *A. polystachya* of 100 µl each was added to the 96 well plate/ and kept in incubation for 37^0C overnight. On the following day, the wells were drained and washed with PBS twice. To the sample, 200 µl of freshly prepared blocking buffer comprising of 0.2 % gelatin in 0.05 % Tween 20 (Merck; Germany) in PBS was added and kept aside for 1 h at room temperature. The sample was then washed twice with PBS TWEEN.

To the sample, 100 µl of primary antibody (CASPASE 7 and CASPASE 9) was added and kept aside for 2 h at room temperature. Primary antibody was collected, and was washed twice with PBS TWEEN. Subsequently, 100 µl of secondary antibody (HRP Conjugate,) was added and kept aside for 1 h at room temperature. It was then washed twice with PBS TWEEN. 200 µl of o-Dianisidine dihydrochloride (Sigma Aldrich, USA) was added and set aside for 30 min at room temperature. The reaction was stopped by adding 50 µl of 5N HCl. Optical density was read at 415 nm in an ELISA reader.

The activity of Caspase was calculated using the following formula:

$$\text{Activity of Caspase} = \frac{\text{OD Value}}{\text{Protein Concentration}}$$

5.12 ISOLATION OF TOTAL RNA (TRIZOL METHOD)[117]

Total RNA was isolated using the total RNA isolation kit according to the manufacture instruction (Invitrogen – Product code10296010). Chloroform extraction following centrifugation, exclusively in the aqueous phase whereas proteins are in the interphase and organic phase. On mixing with isopropanol, RNA gets precipitated as a white pellet on the side and the bottom of the tube. 70% confluent cells in 6 well plate (approximately 4 x 105 cells) were treated with the sample and incubated for 24 hours. A set of untreated control was also incubated at 37°C for 24 h in a CO_2 incubator.

After incubation DMEM media was removed aseptically and 200 µL of trizol reagent was added to culture well plate and incubated for 5 min. The contents were then transferred to a fresh sterile eppendorf tube. About 200 µL of chloroform was added and shaken vigorously for 15 sec and incubated for 2-3 min at room temperature, followed by centrifugation at 14000 rpm for 15 min at 40°C. The aqueous layer was collected and 500 µL of 100% isopropanol was added. It was incubated for 10 min at room temperature and then centrifuged at 14000 rpm for 15 min at 40°C. The supernatant was discarded and pellet thus obtained was washed with 200 µL of 75% ethanol (Merck). It was then centrifuged at 14000 rpm for 5 min at 40°C in a cooling centrifuge (Remi CM12). The RNA pellet was dried and suspended in TE buffer.

5.13 GENE EXPRESSION ANALYSIS BY RT-qPCR [70]

Total RNA was extracted using TRI Reagent (Sigma) from liver tissues. The purity and the concentration of total RNA was determined. Template complementary DNA was synthesized using the cDNA preparation kit (Thermoscientific, Product code-AB1453A, Verso cDNA Synthesis kit). Real-Time qRT-PCR analysis was carried out using SYBR Green Master Mix (Applied Biosystem, Life technologies). All reactions were performed in triplicates and data were analysed according to ΔΔCt method.

5.14 PREPARATION OF SILVER NANOSUSPENSION OF *A. POLYSTACHYA*[46]

Silver Nanosuspension (AgNS) of *A. polystachya* was prepared by nano-precipitation method. The prepared *A. polystachya* AgNP (10mg) were added to Sodium Lauryl Sulphate (0.125 %) in 10 ml of deionized water with continuous stirring at 500 rpm for 1h. The solvent was allowed to evaporate to obtain a dry nanosuspension.

5.15 ANTIOXIDANT ACTIVITY[46,120]

Antioxidant activity on the test samples *A. polystachya* extract (APE) and *A. polystachya* Silver Nanosuspension were determined using different assays:

(a) DPPH Scavenging Activity

(b) Nitric Oxide Radical Scavenging Activity

5.15.1 DPPH Scavenging Activity

The antioxidant activity was studied on test samples (APE, AgNS) using DPPH (2,2-diphenyl-2-picrylhydrazyl hydrate) assay.

Preparation of DPPH Reagent

The reaction mixture contained 0.012 mg of DPPH in methanol and various concentrations of the test samples.

Preparation of Standard Ascorbic Acid Solution

50 mg of Ascorbic Acid was dissolved in 50 ml of methanol to obtain stock solution I (1000 µg/ml). 10 ml of stock solution I was diluted to 100 ml with methanol to obtain stock solution II (100 µg/ml). Further dilutions were made by taking stock solution II to obtain 10 -100 µg/ml in methanol.

Sample Preparation

50 mg of methanolic extract was dissolved in 50 ml of methanol to obtain stock solution I (1000 µg/ml). 1 ml of stock solution I was diluted to 10 ml with methanol to obtain 100 µg/ml. Similar dilutions were made to obtain 200-1000 µg/ml.

Procedure

A mixture of 2 ml of standard/sample with 1 ml of DPPH were shaken vigorously and kept in dark for 30 min. Control was prepared using 1ml of DPPH and 2 ml methanol and incubated at room temperature in the dark. The absorbance was measured at 517 nm using a UV-Visible Spectrophotometer against the control.

The antioxidant activity was calculated by determining % inhibition using the following formula:

$$\text{DPPH Scavenging Effect (\%)} = \frac{\text{(Absorbance of control – Absorbance of sample)}}{\text{Absorbance of control}} \times 100$$

5.15.2 Nitric Oxide Scavenging Activity

The antioxidant activity was studied on test samples (APE, AgNS) using sodium nitroprusside and Greiss reagent.

Preparation of 10 mM Sodium Nitroprusside Solution

Sodium Nitroprusside was prepared by weighing 0.26 gm in 100 ml of Phosphate buffered saline (pH 7.4).

Preparation of Griess Reagent

Griess reagent was prepared by mixing the equal volume of 1% sulfanilamide and 0.1% N-1-napthylethylenediamine dihydrochloride.

Preparation of Standard Gallic Acid Solution

50 mg of Gallic Acid was dissolved in 50 ml of methanol to obtain stock solution I (1000 µg/ml). 10 ml of stock solution I was diluted to 100 ml with methanol to obtain stock solution II (100 µg/ml). Further dilutions were made by taking stock solution II to obtain 10 -100 µg/ml in methanol.

Procedure

The test was performed by taking 1ml of standard/sample in a dry test tube and adding 1 ml of 10 mM sodium nitroprusside solution. The mixture was incubated in dark

at room temperature for two and half hours. After incubation, 2 ml of Griess reagent was added and again incubated for 20 min in dark. Absorbance was measured at 540 nm. The control was prepared using 1ml of sodium nitroprusside and 1ml methanol.

The antioxidant activity was calculated by determining % inhibition using the following formula:

Nitric Oxide Scavenging Effect (%)

$$= \frac{\text{(Absorbance of control – Absorbance of sample)}}{\text{Absorbance of control}} \times 100$$

5.16 SULFORHODAMINE B CYTOTOXIC ASSAY IN MCF-7 AND MDA-MB -231 CELL LINE ON *A. POLYSTACHYA* SILVER NANOSUSPENSION [111,113]

The IC50 of the formulation was determined by performing Sulforhodamine B cytotoxic assay. All the experiments were done in triplicates. The assay was performed according to the previously described method with slight modifications. Cells (5000 cells/well) were seeded in sterile 96-well plates. After 24 h, they were treated with concentrations of compounds ranging from (500-7.81 µM). The extracts were dissolved in DMSO (final concentration in solution is less than 1 %). After 48 h, 100 µl of an ice-cold solution of 10 % TCA was added to each well and incubated at 4°C for 1 h. Later, the wells were washed three times with distilled water and dried. 100 µl of SRB (0.057 % w/v in 1 % v/v acetic acid) solution was added to each well and the plates were incubated for 30 min in dark. The plates were rinsed thrice with 1 % v/v acetic acid to remove any unbound dye. After drying the plates at room temperature, the protein bound dye was solubilized by adding 200 µl of 10 mM Tris base to each well. Absorbance was read at 540 nm on a scanning multi-well plate reader (ELx800, BioTek Instruments Inc., Winooski, VT, USA), the percentage cell viability was calculated using excel sheet and IC_{50} values were determined using graph pad prism.

Percentage cell death was calculated by the formula:

$$\% \text{ cell death} = \frac{(\text{OD of control} - \text{OD of test})}{(\text{OD of control})} \times 100$$

5.17 STATISTICAL ANALYSIS

All the tests were performed in triplicates and the average values were reported. The results were expressed as mean ± standard error (SE) followed by ANOVA.

RESULTS & DISCUSSION

"The results you achieve will be in direct proportion to the effort you apply."

6.0 RESULTS AND DISCUSSION

6.1 PRELIMINARY PHYTOCHEMICAL SCREENING

The root barks of *A. polystachya* were subjected for extraction with methanol to yield a methanolic extract. The extract was further subjected to preliminary phytochemical screening to identify the various phytoconstituents present in the extract. The phytochemical screening revealed the presence of alkaloids, carbohydrates, triterpenoids, steroids, tannins and phenolic compounds (Table No. 3) as explained in Materials and Methods (section 5.5).

Table 3: Preliminary phytochemical screening of methanolic extract of the root bark of *A. polystachya*

Sr. No.	Identification Tests	Result
1	Alkaloids	+
2	Carbohydrates	+
3	Triterpenoids & Steroids	+
4	Tannins & Phenolic Compounds	+
5	Proteins	+
6	Glycosides	+
7	Starch	-

6.2 CHARACTERISATION OF ISOLATED COMPONENTS FROM THE METHANOLIC EXTRACT OF THE ROOT BARKS OF *A. POLYSTACHYA*

6.2.1 Isolated Component RG-APE1[112]

The isolated component RG-APE1 have displayed a strong IR absorption at 3334.92 cm^{-1}indicating the presence of the hydroxyl group. The band at 2924.25 cm^{-1} indicated C-H stretching in CH_3. The prominent peak at 1724.36 cm^{-1} shows carbonyl stretching of ester (fig. 10). The ^{1}HNMR exhibited a singlet at δ 5.2234 indicating methyl protons at H-30. The doublet at δ 7.3975 (H-21) and two singlets at δ 6.8561 (H-22) and δ 7.3869 (H-23) indicated the presence of protons in the furan moiety. The peak at δ 8.1664 indicated the presence of carboxylic group. A singlet at δ 2.0470 indicated three methyl protons of CH_3COO. A singlet at δ 3.4367 indicated the presence of a proton at H-2′. The value of δ 1.4091 appeared as a singlet and δ 1.2339 a doublet indicating two protons at H-3′ and H-4′. δ 0.8359 appeared as a doublet indicating three protons at H-3′ -Me (fig. 11,12). The ^{13}CNMR spectrum exhibited values at δ 174.83 (C-7), δ 169.0 (C-3) indicating the presence of two ester groups. δ 150.08 indicated the carbon for COOH. The value of δ 159.08 indicated the presence of carbon for CH_3COO (fig 13-15). The ESI-MS spectrum displayed the molecular ion peak at m/z 673 $(M+H)^+$ corresponding to the molecular formula $C_{35}H_{44}O_{13}$ (fig16). From the above evidences, the compound RG-APE1 was designated as Rohituka 7.

6.2.2 Isolated Component RG-APE2[112]

The isolated component RG-APE2, exhibited strong IR absorption peak at 3389.10 cm^{-1} indicating the presence of the hydroxyl group. The band at 2931.25 cm^{-1} indicated C-H stretching in CH_3. The prominent peak at 1741.57 cm^{-1} shows carbonyl stretching of ester (fig 18). The ^{1}HNMR of this compound exhibited a singlet at δ 6.8561 indicating methyl protons at H-30. The value of doublet δ 7.3975, singlets δ 6.4724 and δ 7.5509 indicated the presence of furan moiety. Here, it is clearly evident that the value of COOH and CH_3COO are absent when compared to Rohituka 7. A singlet at δ 3.4367 and δ 1.7908 indicated the presence of protons at H-2′ and H-3′ and δ 1.1606 at H-4′. The proton at H-5 appeared at 0.6985 as a singlet. A triplet appeared at δ 0.8934 indicating 3 methyl groups at 3′- Me (fig 19-21). The ^{13}CNMR spectrum exhibited a peak at δ 167.06 (C-3), δ 169.0 (C-7) indicating the presence of two ester groups (fig. 22-24). The ESI-MS spectrum displayed the molecular ion peak at m/z 601 $(M+H)^+$ corresponding to the molecular formula $C_{32}H_{40}O_{11}$ (fig. 25). From the above evidences, the compound RG-APE2 was designated as Rohituka 3.

6.2.3 Isolated Component RG-APE3[121]

The isolated compound RG-APE3, displayed IR absorption peak at 3456.11 cm^{-1} indicating the presence of the hydroxyl group. The peak at 1745.0 cm^{-1} corresponds to carbonyl group of esters. The bands at 1641.22 cm^{-1} and 820.39 cm^{-1} indicated trisubstituted double bond. The band at 860.37 cm^{-1} is due to the presence of furan ring. The peak at 1244.4 cm^{-1} corresponds to the epoxide moiety. The peak at 893.29 cm^{-1} is due to the exocyclic methyl group (fig. 27). In the proton NMR spectra, the values at δ 0.96 - δ 1.05 corresponds to 12 hydrogens of 4 methyl groups at H-18,19,24 and 25. The singlet at δ 1.27 corresponds to the methyl protons of the rhamnose at H-6″. The value at δ 5.13 corresponds to 1 hydrogen of H-1′ of glucose molecule. The multiplets at δ 6.43- δ 7.59 is due to three hydrogens of the furan moiety. The singlet at δ 4.91 and δ 5.09 corresponds to methylene protons at H-26 (fig. 28-31). The ^{13}CNMR spectra showed signals at δ 172.93 (C-7), δ 170.14 (C-16) suggesting the presence of two ester groups. The signals at δ 142.93 (C-23), δ 140.16 (C-22), δ 101.59 (C-21) and δ 120.14 (C-20) are characteristics of furan ring (fig. 32,33). The ESI-MS spectrum indicated the molecular ion peak at 779 $(M+H)^+$ corresponding to the molecular formula $C_{39}H_{54}O_{16}$ (fig. 34). From the above evidences the compound RG-APE3 was designated as Amoorinin-3-O-α-L-rhamnopyranosyl–(1→6)–β-D-glucopyranoside.

6.2.4 Isolated Component RG-APE4[121]

The compound RG-APE4, displayed showed IR peak at 3447.18 cm^{-1} indicating the presence of the hydroxyl group. The peak at 2963.12cm^{-1} corresponds to C-H stretching of CH_3. The peak at 2877.24 cm^{-1} corresponds to C-H stretching of CH_3 of methoxy group. The peaks at 1644.29 cm^{-1}, 1461.18 cm^{-1}, 1377.10 cm^{-1}, 1234.4 cm^{-1}, 1147.6 cm^{-1}, 800.4 cm^{-1} is due to C-H stretching in flavonone nucleus. The peak at 828.41 cm^{-1} is due to glycoside (fig. 36). In the proton NMR spectra, the singlet at δ 1.24 is due to methyl protons of the third glucose moiety at H-6′′′. The doublet at δ 5.07 corresponds to the protons of H-1′′′of glucose, the singlet at each δ 3.80, 3.93, 4.00 is due to the protons of the 3 methoxy groups in the structure. The multiplets at δ 3.82-3.87 accounts for hydroxyl protons. The singlet at δ 2.13 accounts for the methyl protons at H-8 (fig. 37-39). The ^{13}CNMR shows signals at δ 55.67, 56.62, 50.15 representing the 3 methoxy groups. The value at δ 195.15 indicates one carbonyl group. δ 11.68 indicates the presence of one methyl group at C-8 (fig. 40, 41). The ESI-MS spectrum indicated the molecular ion peak at 816.1 $(M+2H)^+$ corresponding to the molecular formula $C_{37}H_{50}O_{20}$ (fig. 42). From the above evidences the compound RG-APE4 was designated as 8-methyl-7,2′,4′-tri-O- methylflavonone- 5-O-α-L-rhamnopyranosyl(1→4)-β-D-glucopyranosyl-(1→6)-β-D-glucopyranoside.

6.3 IN-VITRO CYTOTOXIC ACTIVITY OF THE METHANOLIC EXTRACT OF THE ROOT BARK OF *A. POLYSTACHYA* [113,122]

Cytotoxicity screening methods helps to provide important preliminary data to confirm the antineoplastic properties of the selected plant extract for future work. For the cytotoxic study, a number of standards, such as Doxorubicin, Vincristine Sulphate were considered, of which Doxorubicin was selected for the cytotoxic activity of the methanolic extract of the root bark of *A. polystachya.* The methanolic extract of the root bark of *A. polystachya* showed significant cytotoxic activity exhibiting potential biological activity as compared with the standard, Doxorubicin. The cytotoxic effect of methanolic extract of root bark of *A. polystachya* on MCF-7 cells and MDA-MB-231 cells were determined by SRB assay. Growth inhibition was found by a plot of % Control Growth to the Drug concentration (µg/ml). Adriamycin, as a positive control, showed a growth inhibition of <10 µg/ml. The percentage cell growth on MCF-7 cells was found to be 39.8, 21.6, 18.0 and 15.6 at 10, 20, 40 and 80 µg/ml respectively as shown in table 4. In MDA-MB231 cells, the percentage cell growth was found to be 99.2, 80.0, 67.2 and 54.6 at 10, 20, 40 and 80 µg/ml respectively as shown in table 5. Growth inhibition (GI_{50}) of <10 µg and >80 µg was observed in MCF-7 and MDA-MB-231 cell lines depicting that the extract exhibits cytotoxic activity against MCF-7 cell lines than MDA-MB-231 cell lines. Therefore, these results suggested that the methanolic extract of the root bark of *A. polystachya* possesses anti-cancer activity on

MCF-7 cell lines. The findings encouraged us to synthesize AgNPs from the methanolic extract of the root bark of *A. polystachya* and study its effect on cell cycle and apoptosis in human breast cancer cells (MCF-7).

Table 4: Results of % control growth of methanolic extract of the root bark of *A. polystachya* on human breast cancer cell line MCF-7

Compound	Conc. (µg/ml)	% Control Growth				GI_{50} (µg/ml) from graph
		Trial 1	Trial 2	Trial 3	Average	
RG-A	10.0	30.3	49.3	39.6	39.8±9.5007	<10
	20.0	17.8	23.0	24.1	21.6±3.3650	
	40.0	10.9	13.1	0.0	8.0±7.0149	
	80.0	16.8	23.9	6.1	15.6±8.9604	
ADR	10.0	-84.7	-55.0	-66.1	-68.6±15.007	<10
	20.0	-84.5	-56.4	-63.1	-68.0±14.677	
	40.0	-86.6	-64.7	-70.0	-73.8±11.425	
	80.0	-76.8	-49.9	-64.5	-63.7±13.466	

Values are expressed as Mean±Standard Deviation (SD) Values were found out using ANOVA

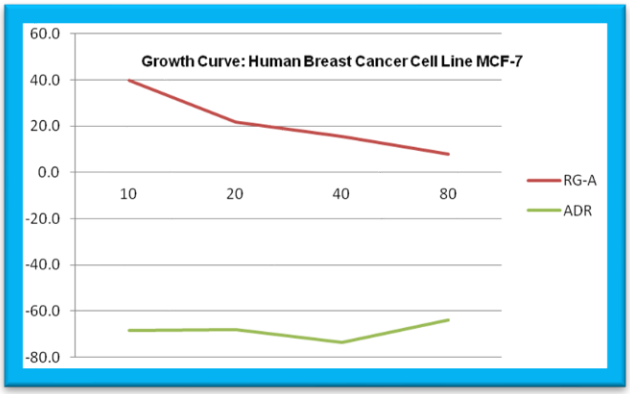

Fig. 44: Growth curve of methanolic extract of the root bark of *A. polystachya* on Human Breast Cancer Cell Line MCF-7

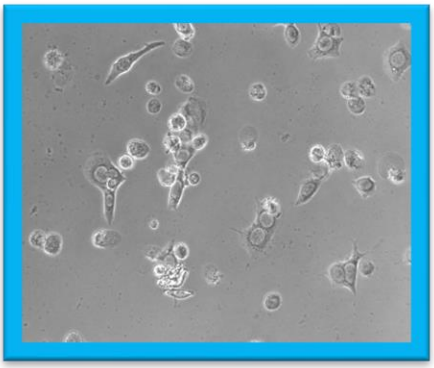

Fig.45: Positive control of Adriamycin

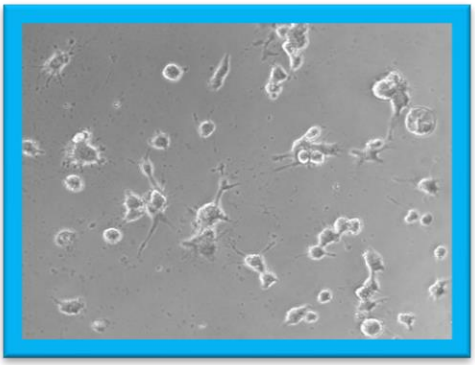

Fig 46: Cytotoxic activity of the Methanolic extract of root bark of *A. polystachya*

Table 5: Results of % control growth of the methanolic extract of root bark of *A. polystachya* on human breast cancer cell lines MDA-MB-231

Sample	Conc. (µg/ml)	% Control Growth Trial 1	Trial 2	Trial 3	Average	GI_{50} (µg/ml) from graph
RG-A	10.0	81.5	84.1	131.9	99.2±28.377	>80
	20.0	53.7	53.7	132.5	80.0±49.495	
	40.0	48.8	46.6	106.1	67.2±33.735	
	80.0	52.8	47.9	63.0	54.6±7.709	
ADR	10.0	-2.6	5.1	-3.9	-0.5±4.864	<10
	20.0	-27.0	1.0	-11.3	-12.4±14.03	
	40.0	-21.3	-4.6	-17.8	-14.6±8.807	
	80.0	2.6	8.7	1.9	4.4±3.740	

Values are expressed as Mean±Standard Deviation (SD) Values were found out using ANOVA

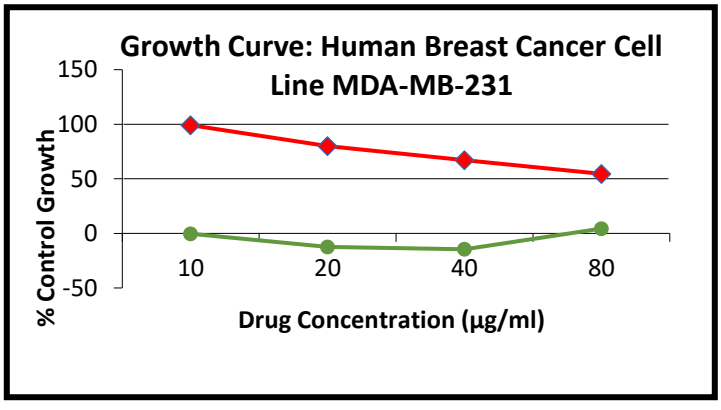

Fig. 47: Growth curve of Human Breast Cancer Cell Line MDA-MB-231

6.4 CHARACTERIZATION OF *A. POLYSTACHYA* SILVER NANOPARTICLES

6.4.1 Visual Observation of synthesized AgNPs[47]

Green synthesis of AgNPs using the methanolic extract of the root bark of *A. polystachya* were carried out. The colour change of the synthesized AgNPs were recorded by visual observation in a conical flask containing silver nitrate solution and the methanolic extract of the root bark of *A. polystachya*. The synthesized AgNPs exhibited a yellowish - brown colour in aqueous solution confirming the formation of AgNPs in the reaction vessel as shown in the fig. 48.

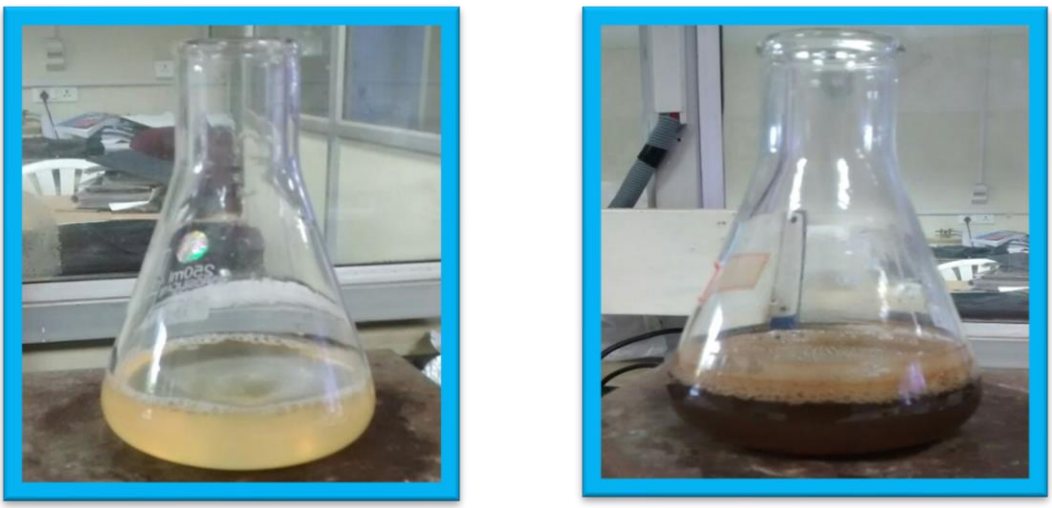

Fig 48: Colour Change from light yellow to yellowish-brown colour confirming the formation of AgNPs of *A. polystachya*

6.4.2 UV-Vis Spectroscopy [47,123]

The UV-Vis absorption spectrum of synthesized AgNPs is shown in Fig. 49. The free electrons present in AgNPs gave surface plasmon resonance band (SPR). The SPR absorption band may be associated to combine variations of electrons of AgNPs in resonance with the light wave. It is obvious that AgNPs in nano range show absorption at the wavelength from 390 – 420 nm due to Mie scattering. Thus, a broad absorption band was observed in the range of 400 – 420 nm which is characteristic of Mie scattering. The absence of other peaks in the spectrum confirms the synthesis of silver nanoparticles.

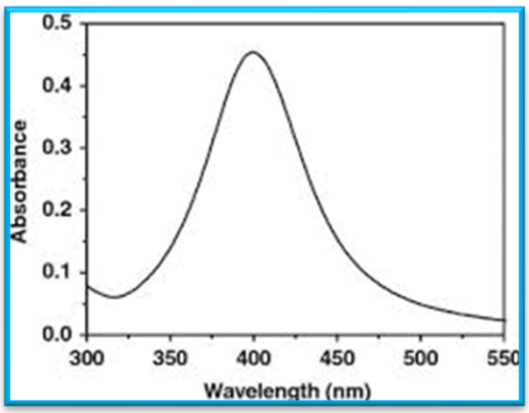

Fig 49: UV- Visible spectra of AgNPs of the methanolic extract of the root bark of *A. polystachya*.

6.4.3 Fourier Transform Infrared Spectroscopy (FTIR)[124]

The IR spectra provides information of the potential biomolecules which are responsible for reducing and capping the bioreduced silver nanoparticles. FTIR technique is widely used to analyze the chemical composition of many compounds. FTIR helps in providing qualitative (identification) and quantitative (amount) analysis of compounds.

FTIR measurements were performed to classify the potential biomolecules responsible for reducing, capping and stabilizing the synthesized metal nanoparticles from the methanolic extract of root bark of *A. polystachya*. FTIR spectrum in fig. 50 depicted that the biosynthesized AgNPs were capped with bimolecular compounds which were responsible for reduction of silver. The bands observed at 3420.4 cm^{-1} and 2923.9 cm^{-1} were assigned to the -OH stretching and -CH stretching vibrations respectively. The presence of C=C str. at 1595.3 cm^{-1} confirmed the presence of broad range of alkene group in the synthesized AgNPs. These results indicated that phytoconstituents such as flavonoids, phenols, alkaloids, etc., are involved in the bioreduction process for the synthesis of AgNPs.

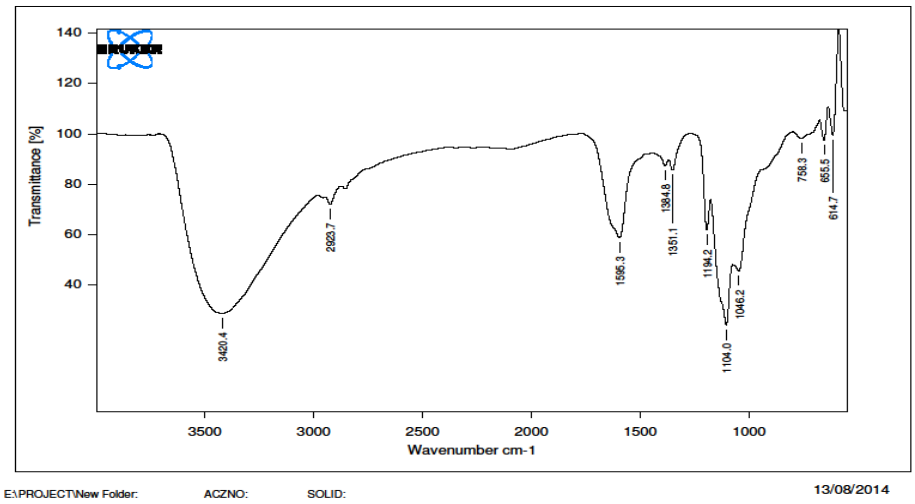

Fig 50: FT-IR spectra of the synthesized AgNPs of the methanolic extract of the root bark of *A. polystachya.*

6.4.4 Scanning Electron Microscopy (SEM)[47,123,124]

Scanning electron microscopy is used to determine the size, shape and morphologies of nanoparticles. SEM provides high resolution images of sample surface and works on a similar principal to that of optical microscope. It helps to measure the scattered electrons from the sample. The measurement can be done at shorter wavelength as the electrons are accelerated by an electric potential. SEM is capable of measuring particle size down to the level of 1 nm and also magnifies images up to 200,000 times.

This technique was employed to evaluate the size, shape and surface morphology of the synthesized AgNPs. It exhibited that almost all the nanoparticles were of spherical shape with no agglomeration. The investigations confirmed that the images of the AgNPs were in nanoscale as shown in fig. 51 (a) and (b).

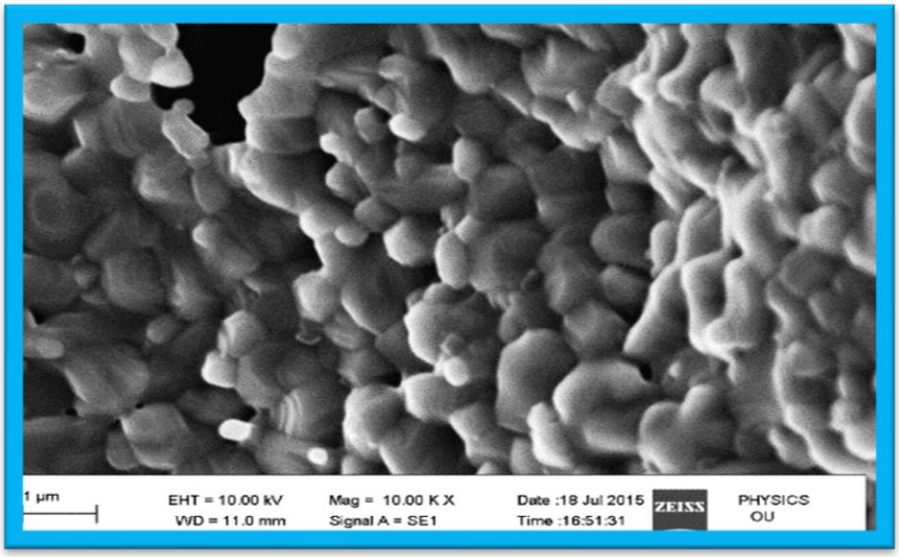

(a)

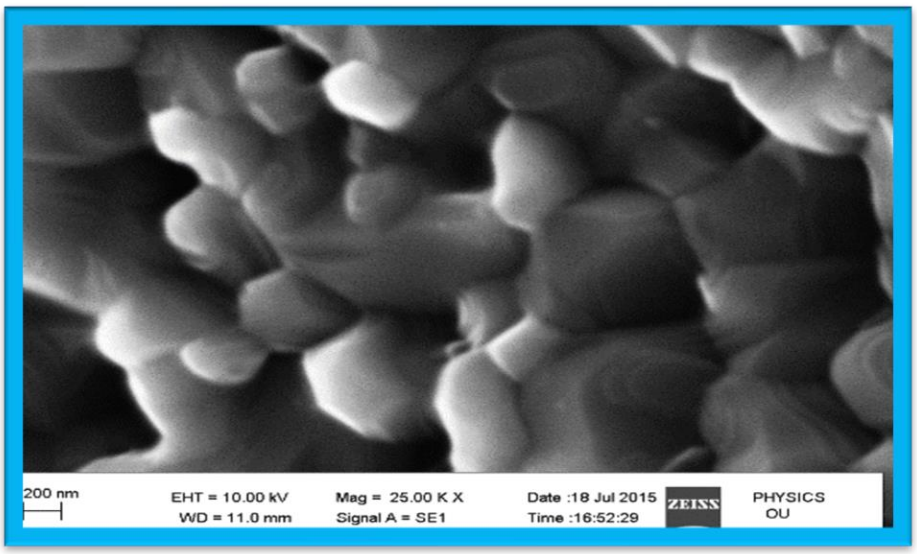

(b)

Fig 51: SEM images of the synthesized AgNPs of the methanolic extract of the root bark of *A. polystachya.*

6.4.5 Energy Dispersive X-Ray Analysis (EDAX)[107,125]

The EDAX technique was studied to identify the synthesis of AgNPs. The EDAX pattern exhibited strong signal energy peaks for silver atom at 3.0, 3.2 and 3.4 keV. The EDAX profile of the sample is shown in fig. 52. The crystalline nature of the synthesized AgNPs which is caused due to the reduction of silver ions. The profile also confirmed the presence of silver and nonappearance of the other peaks indicating the absence of oxides.

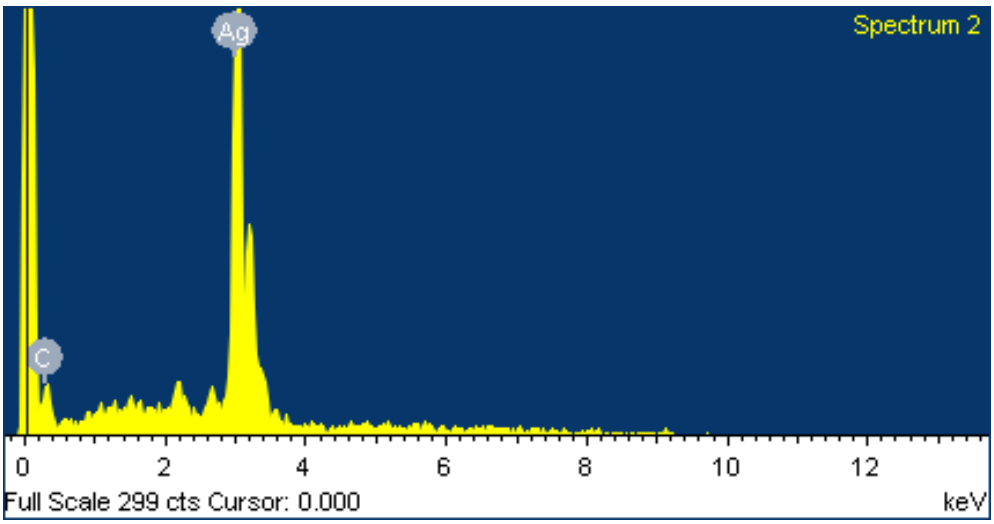

Fig 52: EDAX spectra of synthesized AgNPs of the methanolic extract of the root bark of *A. polystachya.*

6.4.6 X-Ray Diffraction and Particle Size Analysis (XRD and PSA)[126]

X-ray diffraction studies were performed to confirm the crystalline existence of the particles. The XRD pattern exhibited the number of Braggs reflections that can be calculated on the basis of the facial cubic structure of silver. Fig. 53 showed the XRD patterns for AgNPs synthesized from the methanolic extract of the root bark of *A. polystachya*. Three main characteristic diffraction peaks for Ag were observed at 2θ values 38.1°, 44.09° and 64.36°, which corresponded to the 111, 200 and 220, crystallographic planes of the face-centred cubic (fcc) Ag crystals respectively. No other peaks of any crystalline impurity were observed.

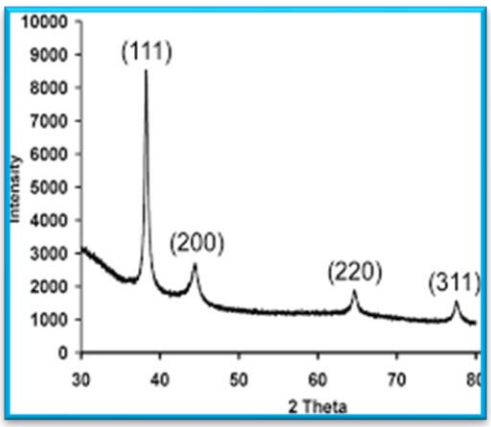

Fig 53: XRD pattern of synthesized AgNPs of the methanolic extract of the root bark of *A. polystachya.*

The particle size analyser was used to measure particle size using intense laser light. Laser diffraction showed aggregated mixture of the particles obtained with the size varying from nanometres to micrometres as shown in fig. 54. The average diameter of particles was found in the range of 10 - 30 nm. The average particle size obtained was 20 nm.

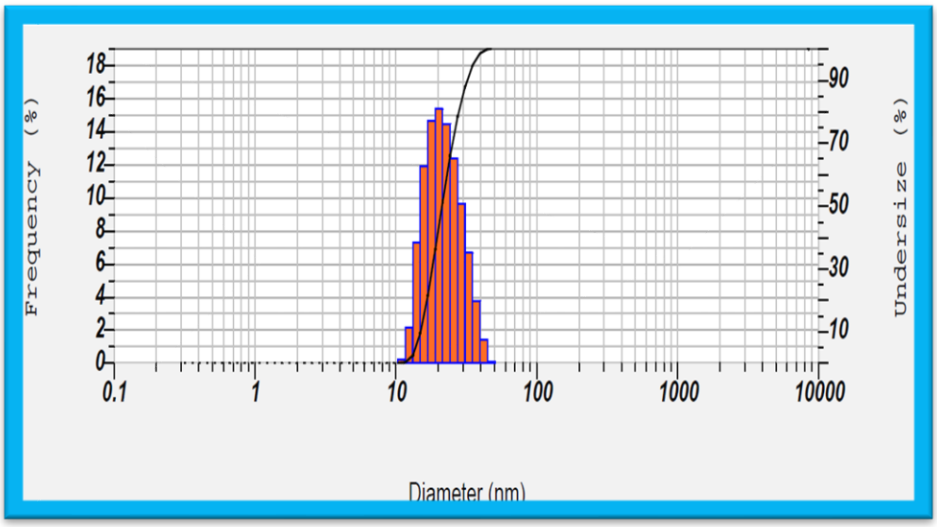

Fig 54: Particle size analysis of AgNPs of the methanolic extract of the root bark of *A. polystachya*

6.4.7 Transmission Electron Microscopy (TEM)[107]

TEM helps to characterize the size, shape and morphology of the synthesized silver nanoparticles. The morphology of synthesized AgNPs were observed at different resolutions i.e., 20 nm and 50 nm as shown in fig. 55. It was evident from the image that the morphology of AgNPs were spherical and in agreement with the shape of a surface plasmon resonance (SPR) band as observed in the UV-vis spectrum. The TEM images of synthesized nanoparticles confirmed that the obtained nanoparticles were at nanoscale. The images revealed also observed that majority of the nanoparticles were spherical in shape while some were agglomerated. The particle size ranged between 7 to 13 nm. The average particle size of these synthesized AgNPs was 8 nm which was in good agreement with the particle size measured by PSA.

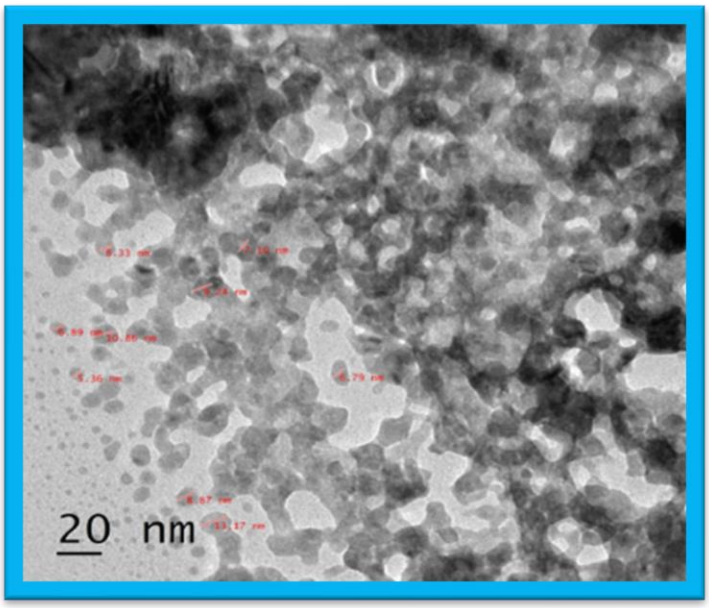

(a)

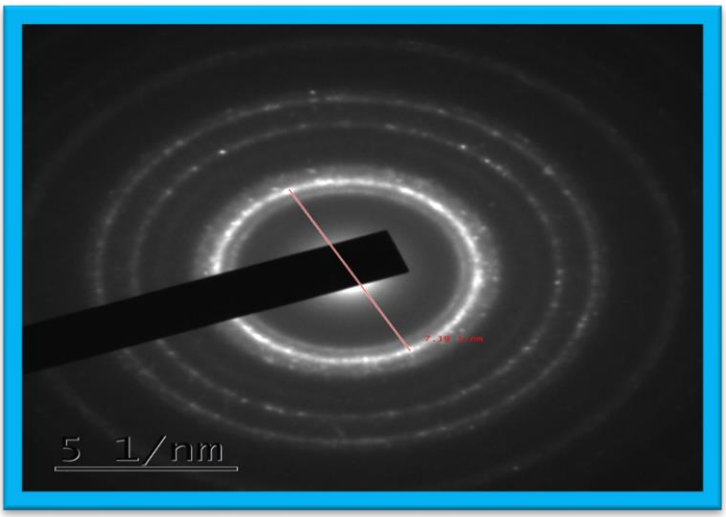

(b)

Fig. 55: TEM images of AgNPs from the methanolic extract of the root bark of *A. polystachya*

6.4.8 Atomic Force Microscopy (AFM)[127]

AFM offers visualization and analysis in three dimensions. This technique is a good analytical tool for structural and morphological characterization of the synthesized AgNPs. Surface images as in fig. 56 showed that the topography of the polymer was fairly regular.

On metallisation, layers of three-dimensional spherical clusters corresponding to AgNPs were developed in the sense of their plasmonic behaviour as shown in fig. 57 and 58. The images depicted an indication of cluster size layers below 5 nm, likely due to the mobility of silver atoms on the polymer surface. The presence of larger clusters was due to the large amount of precursor nanoparticles deposited on the surface.

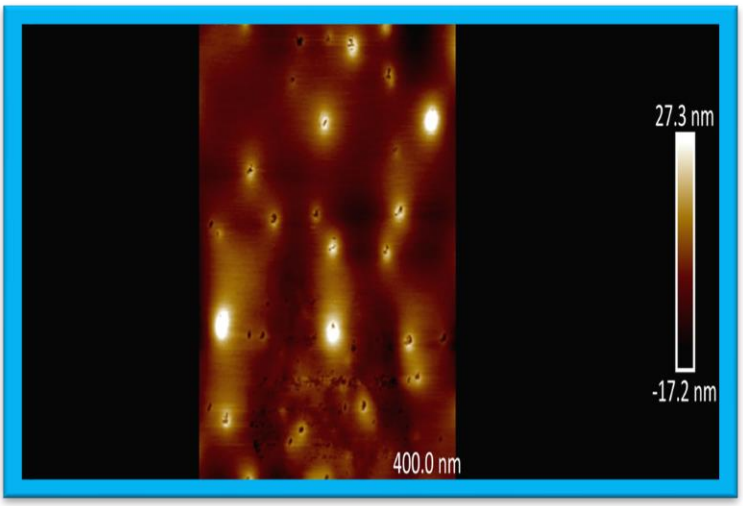

Fig. 56: Morphology of AgNPs of the methanolic extract of the root bark extract of *A. Polystachya*

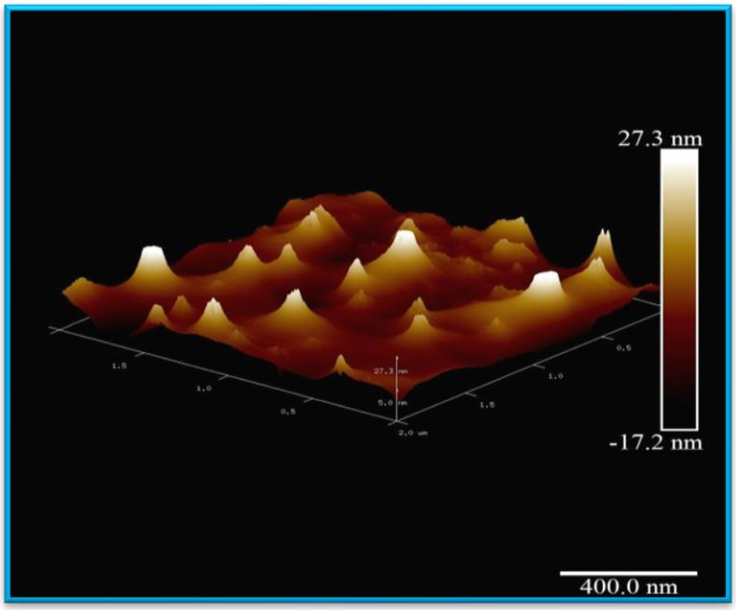

Fig. 57: AFM of the selected 3D image of AgNPs of the methanolic extract of the root bark of *A. polystachya*

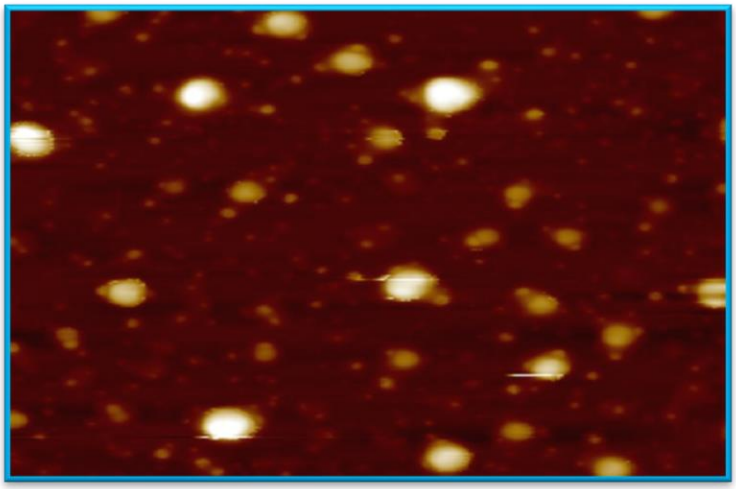

Fig. 58: AFM of the selected 3D image of AgNPs of the methanolic extract of the root bark of *A. polystachya*

6.5 CELL CYCLE AND APOPTOTIC ANALYSIS OF SILVER NANOPARTICLES FROM THE METHANOLIC EXTRACT OF ROOT BARK OF *A. POLYSTACHYA*[128]

Apoptosis is a highly coordinated cycle of cell death characterized by loss of plasma membrane phospholipid asymmetry, enzymatic division of DNA through oligonucleosomal fragmentation and cell segmentation through membranous apoptotic bodies. Most anti-cancer drugs are designed to eliminate rapidly proliferating cancerous cells. They show cytotoxicity and induce apoptosis in cancer cells. Based on the clear indication of cytotoxic potential in the extract of root bark of *A. polystachya*, cell cycle and apoptosis analysis were performed using flow cytometry with the objective to acknowledge whether the cell death mechanism happens through apoptosis induction by the AgNPs of the methanolic extract of root bark of *A. polystachya*.

The cell cycle and apoptosis analysis of AgNPs of *A. polystachya* were shown in fig. 59-63. Treatment of MCF-7 cells with the synthesized AgNPs for 24 h induced apoptosis as investigated using flow cytometry. Doxorubicin was used as a standard and showed apoptosis of 1.5 at 100 mM. The untreated AgNPs (G2) exhibited apoptosis at 18.43. The AgNPs of *A. polystachya* induced apoptosis at 13.62 exhibiting a G2M arrest in MCF cells when treated for 24 h causing mitosis of the cancer cells at a concentration of 40 µg/ml. The G2M arrest induced by AgNPs was higher than the standard doxorubicin. The AgNPs of *A. polystachya* also showed arrest of cancer cell proliferation by a G0/G1 phase arrest.

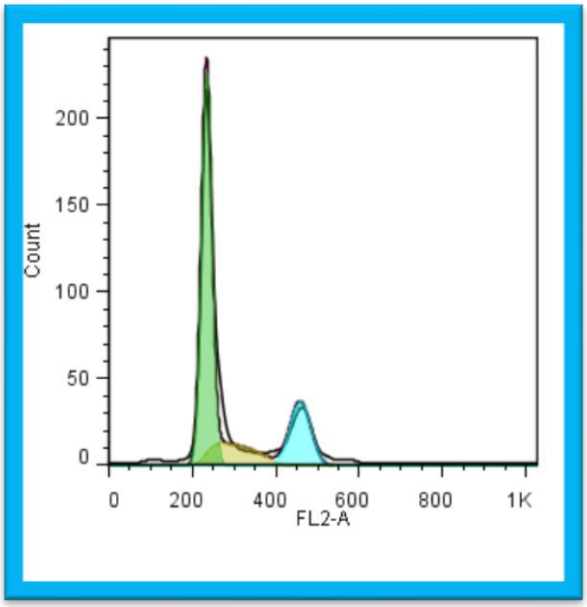

Fig. 59: Cell cycle and apoptosis analysis of the methanolic extract of the root bark of (untreated) of *A. Polystachya*

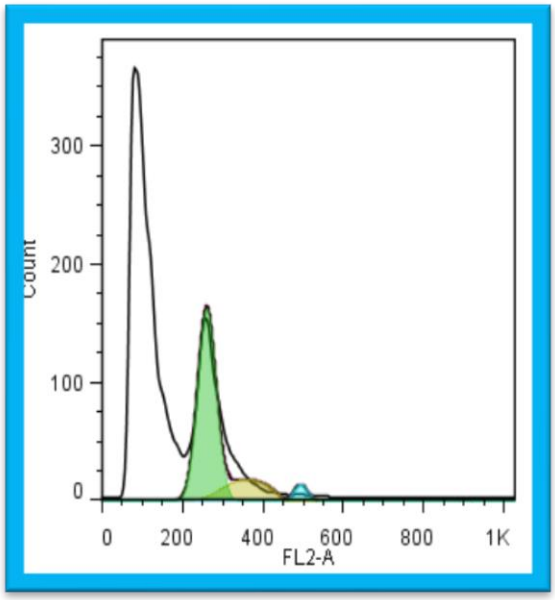

Fig.60: Cell cycle analysis of Doxorubicin Standard

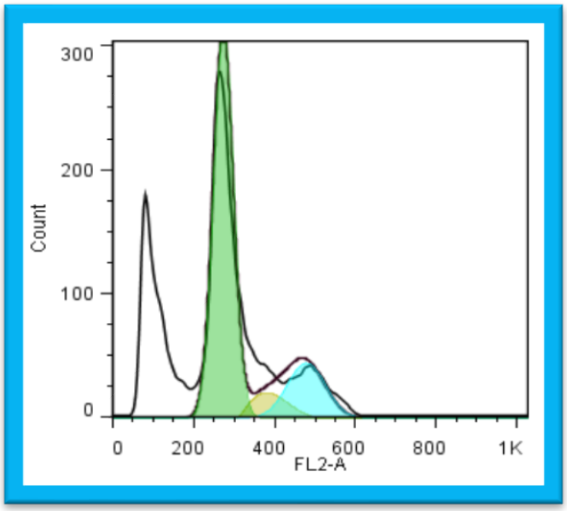

Fig.61: Cell cycle analysis of AgNPs of *A. polystachya*

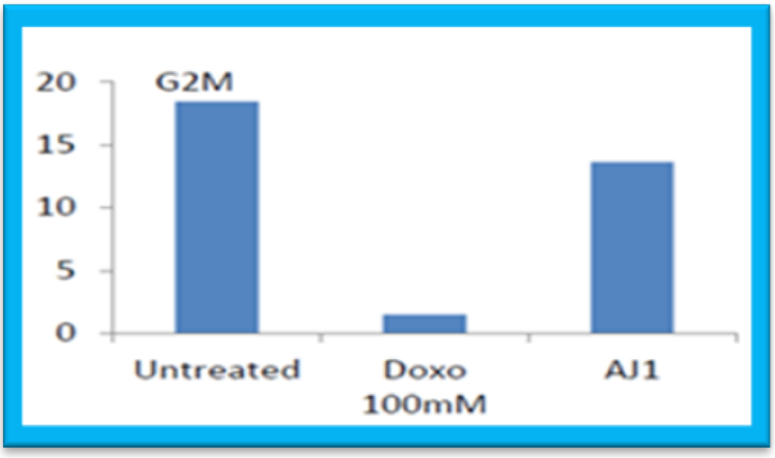

Fig 62: Mitosis (G2M phase arrest) of AgNPs from the methanolic extract of the root bark of *A. polystachya*

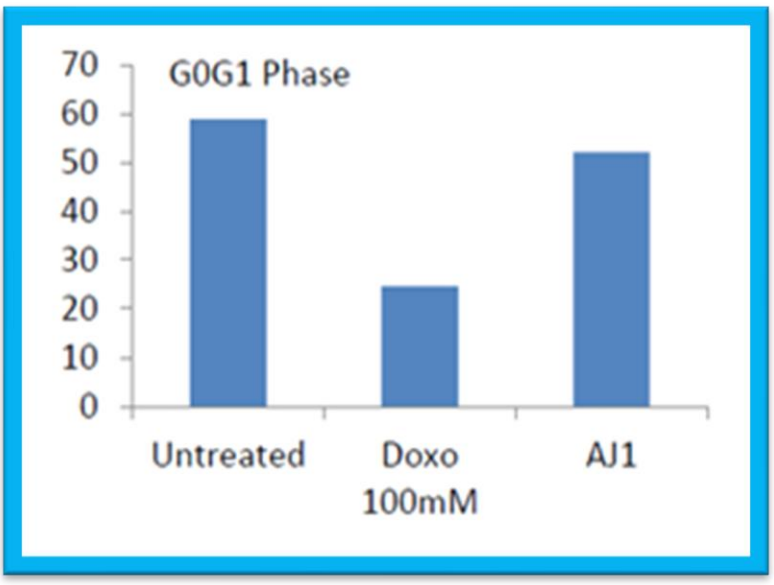

Fig 63: Cancer Cell proliferation (G0G1 phase) of AgNPs of the methanolic extract of the root bark of *A. polystachya*

6.6 ELISA PROTOCOL[129]

Induction of apoptosis in cancer cells is an important analytical tool to treat cancer. Caspases, which are aspartic acid specific cysteine proteases are generally referred as executioners of apoptosis. Caspases are in turn retained in cells as pro caspases and activation of caspases leads to cleavage of cellular substrates leading to morphological changes associated with apoptosis. The mitochondrial membrane bound Caspase 9 is activated by mitochondrial disruption which will lead to the activation of another protease.

In the present study, we measured both, Caspase 9 and Caspase 7 since the former measures the apoptosis initiation and later execution of apoptosis. From the results it can be observed that treatment with *A. polystachya* AgNPs has produced a significant increase of 41.2 % in Caspase 7 levels, when compared with untreated control samples suggesting execution of apoptosis (table 6). In case of Caspase 9, there was a 57.6 % increase in the caspase levels when compared with untreated samples suggesting the initiation of apoptosis (table 7).

Table 6: The activity of Caspase 7 per mg of Protein

Samples	Absorbance	Protein Concentration	Activity Units/mg Protein
Control	0.3640	3.4233370012	0.106329
AgNPs	0.5529	3.1054819142	0.178040

Table 7: The activity of Caspase 9 per mg of Protein

Samples	Absorbance	Protein Concentration	Activity Units/mg Protein
Control	0.3993	3.4233370012	0.116640
AgNPs	0.8099	3.1054819142	0.260797

6.7 ISOLATION OF TOTAL RNA (TRIZOL METHOD)[70]

A wide range of natural substances has been identified as having the potential to induce apoptosis in different tumour cells. Apoptosis is an active type of cell suicide regulated by a gene network, in which the BcL-2 family proteins play a major role in apoptosis control. BcL-2 proteins ensure adequate regulation during development of programmed cell death, and preserve organismal health. BcL-2 protein regarded as anti-apoptotic proteins, when unbalanced, prevents cells from undergoing apoptosis and promote the production of tumors and cancer therapy resistance. BcL-2 protein is found overexpressed in almost all malignant cells. mRNA expression analysis was used to determine the effect of the sample on expression of BcL-2 mRNA (tab 8).

The results revealed that the AgNPs of *A. polystachya*, have produced a significant decrease in BcL-2 expression (approximately 5.7-fold change) when compared with untreated control (tab 10,11). The decrease in BcL-2 can be attributed as the major mechanism of apoptosis contributed by *A. polystachya* AgNPs (fig 64-66).

Signal transducer and activator of transcription 3 (STAT3) is persistently activated in a wide variety of cancer and treatment with the AgNPs produced a considerable decrease in STAT3 suggesting a mechanism contributing to Go/G1 phase arrest.

Table 8: The Forward-Reverse Primer Sequences used for the expression of BcL-2 mRNA

OLIGO NAME	FORWARD		REVERSE	
	SEQUENCE (5' ->3')	Tm	SEQUENCE (5' ->3')	Tm
Human bactin	TCACCCACACTGTGC CCATCTACGA (25)	66.3	CAGCGGAACCGCTC ATTGCCAATGG (25)	67.9
Bcl-2	CCTGTGGATGACTGA GTA	46.2	GAGACAGCCAGGA GAAATCA	49.0
STAT3	GGAGGAGTTGCAGCA AAAAG (20)	57.3	TGTGTTTGTGCCCA GAATGT (20)	55.3

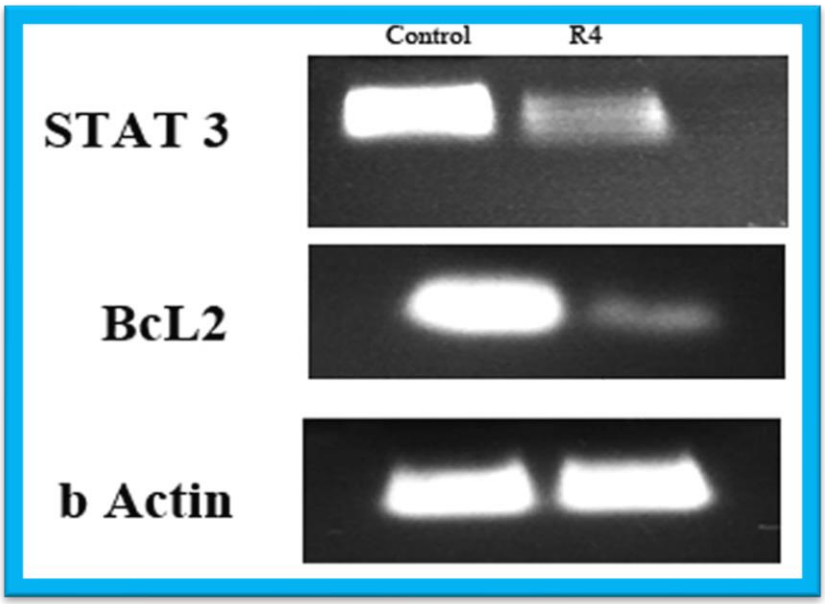

Fig 64: Expression Analysis of genes; STAT 3, BcL2 and b Actin using Real Time PCR for control and AgNPs of *A. polystachya*

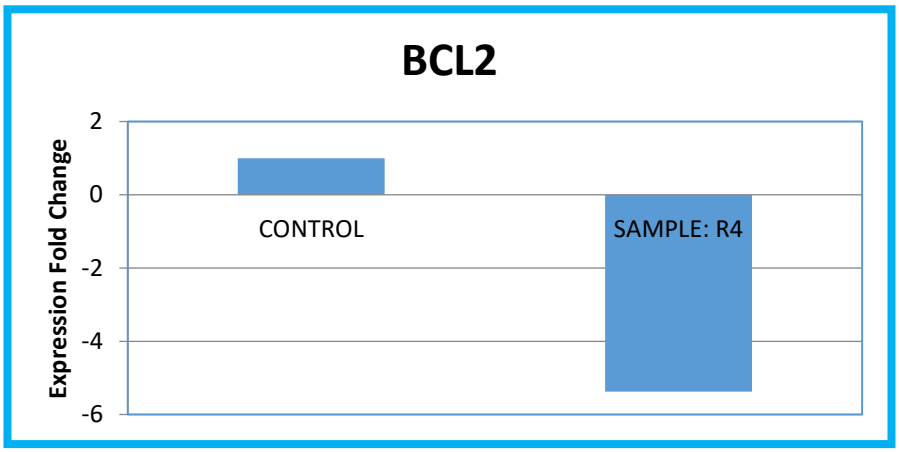

Fig 65: Graphical Representation of Expression Analysis of gene BcL-2 using qRT-PCR for control and AgNPs of *A. polystachya*

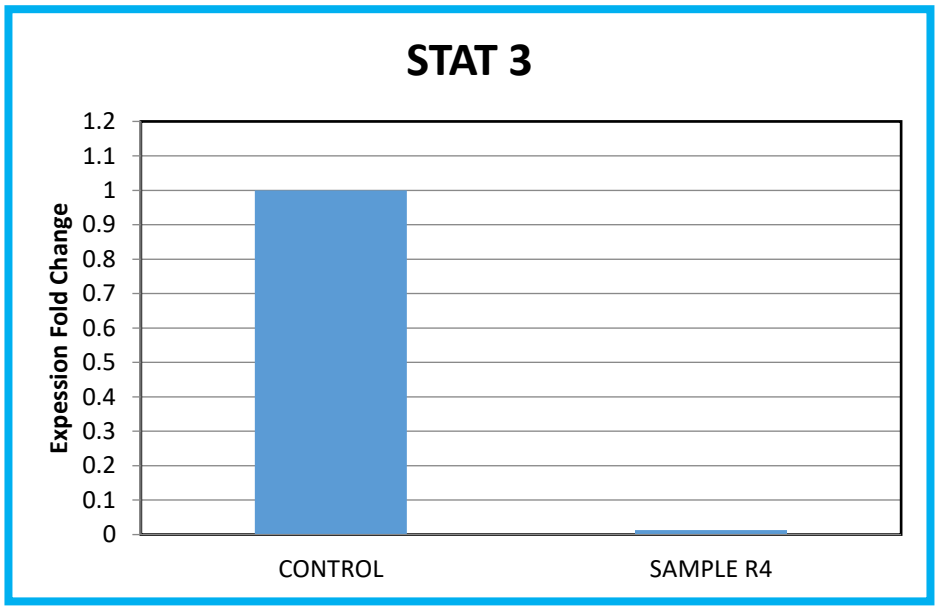

Fig 66: Graphical Representation of Expression Analysis of gene STAT3 using qRT-PCR for control and AgNPs of *A. polystachya*

Table 9: Expression Analysis of gene STAT 3 using qRT-PCR

	STAT
CONTROL	1
SAMPLE-R4	-5.376497598

Table 10: Expression Fold Change for Caspase - 7

Average Experimental Ct Value	Average Control Ct Value	Average Control Ct Value	ΔCt Value (Experimental)	ΔCt Value (Control)	Delta Delta Ct Value	Expression Fold Change
HE	TC	HC	ΔCTE	ΔCTC	ΔΔCt	2^-ΔΔCt
19.75	-	23.85	6.54	8.97	-2.43	5.376497598
-	32.81	-				

Table 11: Expression Fold Change for Caspase - 9

Average Experimental Ct Value	Average Control Ct Value	Average Control Ct Value	ΔCt Value (Experimental)	ΔCt Value (Control)	Delta Delta Ct Value	Expression Fold Change
HE	TC	HC	ΔCTE	ΔCTC	ΔΔCt	2^-ΔΔCt
22.93	-	23.85	15.27	8.97	6.30	0.012662154
-	32.81	-				

6.8 ANTIOXIDANT ACTIVITY [46]

Nanosuspension of the methanolic extract of the root bark of *A. polystachya* was prepared by the nanoprecipitation method. The methanolic extract and AgNS were subjected to free scavenging activity against DPPH and Nitric Oxide radicals. DPPH scavenging activity is a well-known method which helps to determine the antioxidant potential of medicinal plants in a short time period. The DPPH scavenging ability of the extract and AgNS were given in table 13 and 14. The AgNS has shown significant IC_{50} value of 8.36 µg/ml and 300.24 µg/ml was reported for the extract. The standard ascorbic acid has shown IC_{50} value of 12.06 µg/ml.

The scavenging ability of nitric oxide on the root bark extract of *A. polystachya* and its formulated nanosuspension were determined by the *in vitro* development of radical nitric oxide using sodium nitroprusside. The free radicals combine with oxygen to create nitrite ions. Nitric oxide scavengers interact with oxygen and thereby reduces to nitrite ion formation. The results of Nitric Oxide scavenging activity are given in table 16 and 17. The standard gallic acid has shown IC_{50} value of 64.63µg/ml. AgNS has shown promising activity with IC_{50} value of 4.04 µg/ml while the extract has shown 605.81 µg/ml (table 18).

6.8.1 DPPH Radical Scavenging Activity

Table 12: DPPH Radical Scavenging Activity of Standard Ascorbic Acid

Test tube	Conc. µg/ml	Absorbance at 517nm				% Scavenging activity*
		Trial 1	Trial 2	Trial 3	Average	
A.	2	0.899	0.894	0.892	0.895 ± 0.004	4.61 ± 0.09
B.	4	0.800	0.798	0.795	0.797 ± 0.003	14.99 ± 0.09
C.	6	0.709	0.710	0.702	0.707 ± 0.004	24.65 ± 0.24
D.	8	0.585	0.586	0.585	0.585 ± 0.006	37.61 ± 0.11
E.	10	0.55	0.549	0.544	0.547 ± 0.003	41.74 ± 0.15
F.	12	0.448	0.447	0.442	0.446 ± 0.003	52.61 ± 0.16
G.	14	0.386	0.385	0.382	0.384 ± 0.002	59.14 ± 0.09
H.	16	0.307	0.307	0.302	0.305 ± 0.002	67.56 ± 0.15
I.	18	0.242	0.242	0.24	0.241 ± 0.001	74.38 ± 0.06
J.	20	0.205	0.201	0.198	0.201 ± 0.004	78.65 ± 0.18
K.	control	0.941	0.937	0.937	0.398 ± 0.002	IC_{50} = 12.06 ± 0.031

* n=3. The results are expressed as mean ±SEM.

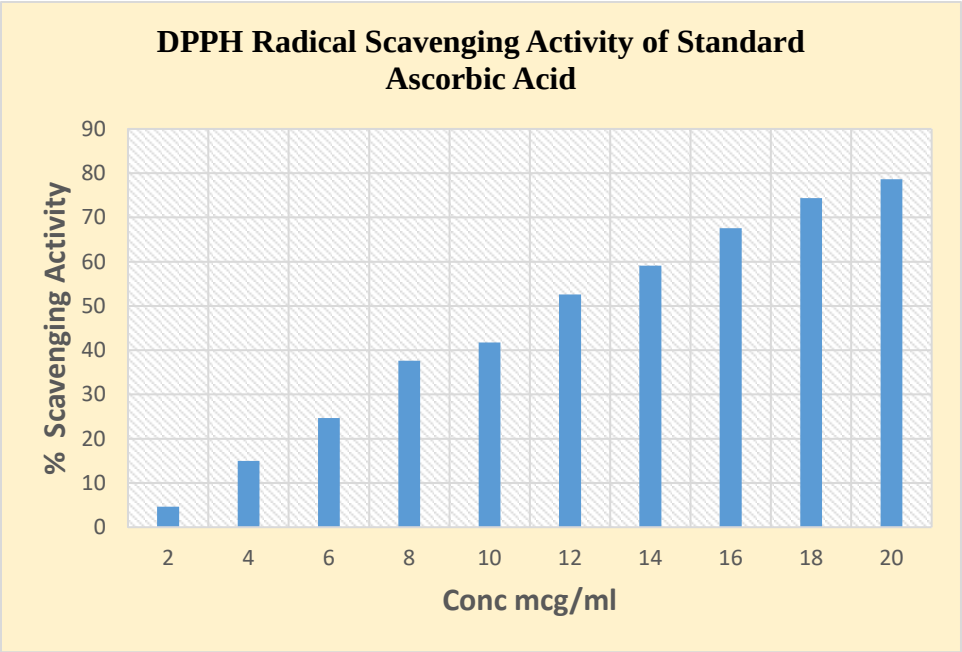

Fig 67: DPPH Radical Scavenging Activity of Standard Ascorbic Acid

Table 13: DPPH Scavenging Activity on the methanolic extract of the root bark of *A. polystachya*

Conc. µg/ml	Absorbance at 517nm				% Scavenging Activity*
	Trial 1	Trial 2	Trial 3	Average	
100	0.614	0.613	0.614	0.614 ± 0.00057	26.54 ± 0.139
200	0.567	0.568	0.567	0.567 ± 0.00057	32.08 ± 0.023
300	0.418	0.419	0.417	0.418 ± 0.001	49.96 ± 0.086
400	0.309	0.308	0.309	0.308 ± 0.00057	63.13 ± 0.123
500	0.251	0.250	0.251	0.251 ± 0.00057	69.99 ± 0.087
600	0.178	0.179	0.177	0.178 ± 0.001	78.69 ± 0.105
700	0.148	0.148	0.149	0.148 ± 0.00057	82.25 ± 0.076
800	0.133	0.135	0.133	0.134 ± 0.00115	83.99 ± 0.127
900	0.093	0.095	0.093	0.0936 ± 0.0012	88.79 ± 0.127
1000	0.091	0.093	0.093	0.0916 ± 0.0012	88.95 ± 0.133
Blank	0.835	0.836	0.835	--	--

* n=3. The results are expressed as mean ±SEM.

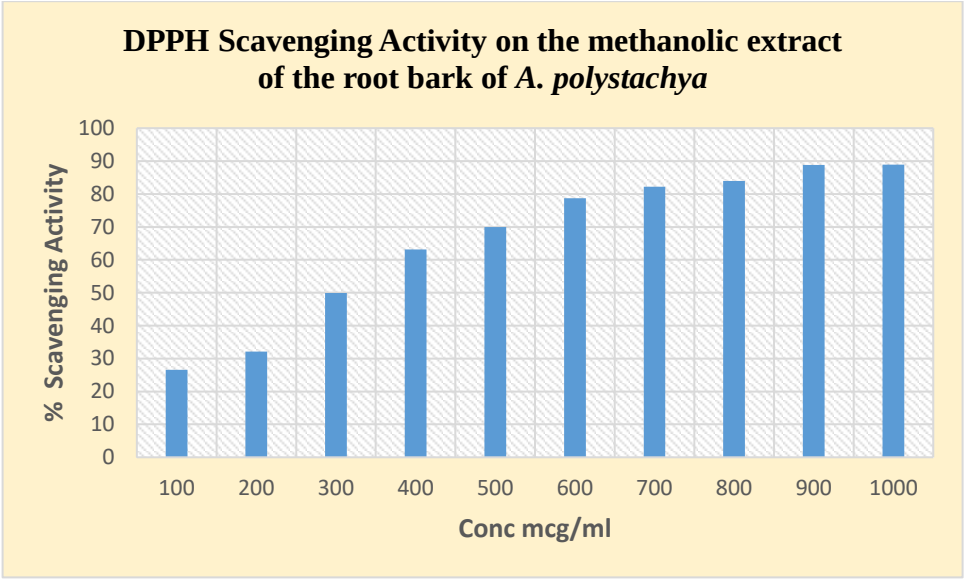

Fig 68: DPPH Scavenging Activity on the methanolic extract of the root bark of *A. polystachya*

Table 14: DPPH Scavenging Activity on *A. polystachya* Silver Nanosuspension

Conc. µg/ml	Absorbance at 517nm				% Scavenging Activity*
	Trial 1	Trial 2	Trial 3	Average	
1	1.277	0.802	0.830	0.969 ± 0.267	10.19 ± 6.110
2	1.162	0.743	0.710	0.872 ± 0.252	19.27 ± 8.415
3	1.042	0.683	0.676	0.800 ± 0.209	25.67 ± 5.769
4	0.993	0.623	0.633	0.750 ± 0.211	30.59 ± 5.435
5	0.927	0.555	0.568	0.683 ± 0.211	36.98 ± 6.057
6	0.895	0.550	0.555	0.667 ± 0.198	38.40 ± 5.588
7	0.827	0.512	0.521	0.620 ± 0.178	42.83 ± 5.038
8	0.760	0.468	0.516	0.581 ± 0.157	46.16 ± 2.493
9	0.683	0.344	0.461	0.496 ± 0.172	54.61 ± 5.857
10	0.654	0.265	0.322	0.413 ± 0.210	62.97 ± 10.12
Blank	1.344	0.878	0.999	1.074 ± 0.242	--

* n=3. The results are expressed as mean ±SEM.

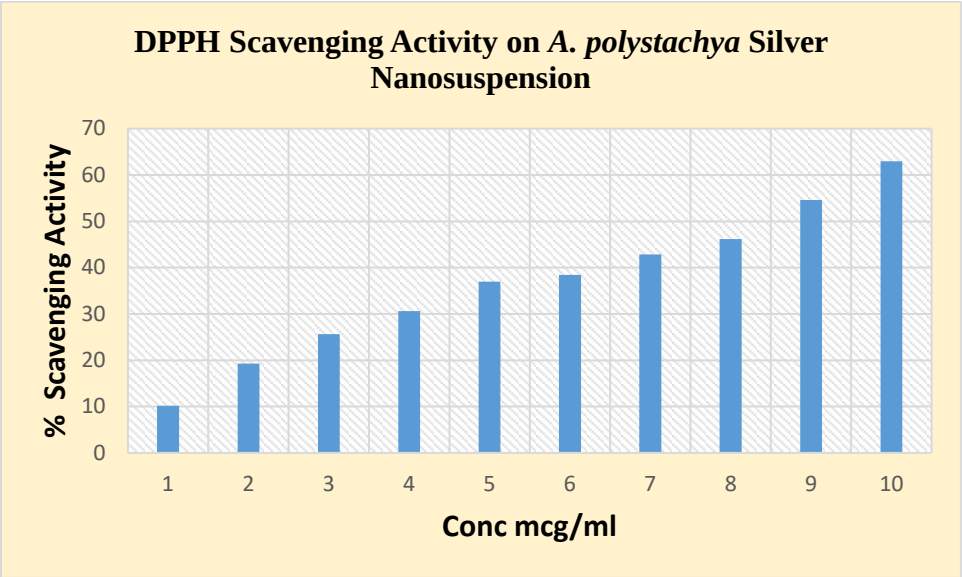

Fig 69: DPPH Scavenging Activity on *A. polystachya* Nanosuspension

Table 15: Nitric Oxide Radical Scavenging Activity of Standard Gallic acid

Test tube	Conc. µg/ml	Absorbance			Average	% Scavenging Activity*
		Trial 1	Trial 2	Trial 3		
A.	10	0.76	0.763	0.765	0.763 ± 0.003	33.81 ± 0.19
B.	20	0.729	0.725	0.723	0.726 ± 0.003	37.02 ± 0.16
C.	30	0.692	0.698	0.695	0.695 ± 0.003	39.68 ± 0.12
D.	40	0.659	0.658	0.661	0.659 ± 0.002	42.86 ± 0.17
E.	50	0.629	0.622	0.627	0.626 ± 0.004	45.76 ± 0.25
F.	60	0.592	0.593	0.597	0.594 ± 0.003	48.53 ± 0.20
G.	70	0.561	0.565	0.568	0.565 ± 0.004	51.17 ± 0.22
H.	80	0.524	0.528	0.522	0.525 ± 0.004	54.64 ± 0.07
I.	90	0.489	0.492	0.493	0.491 ± 0.002	57.53 ± 0.13
J.	100	0.454	0.457	0.459	0.456 ± 0.003	60.54 ± 0.16
K.	control	1.152	1.156	1.149	1.152 ± 0.004	IC_{50} = 64.63

* n=3. The results are expressed as mean ±SEM.

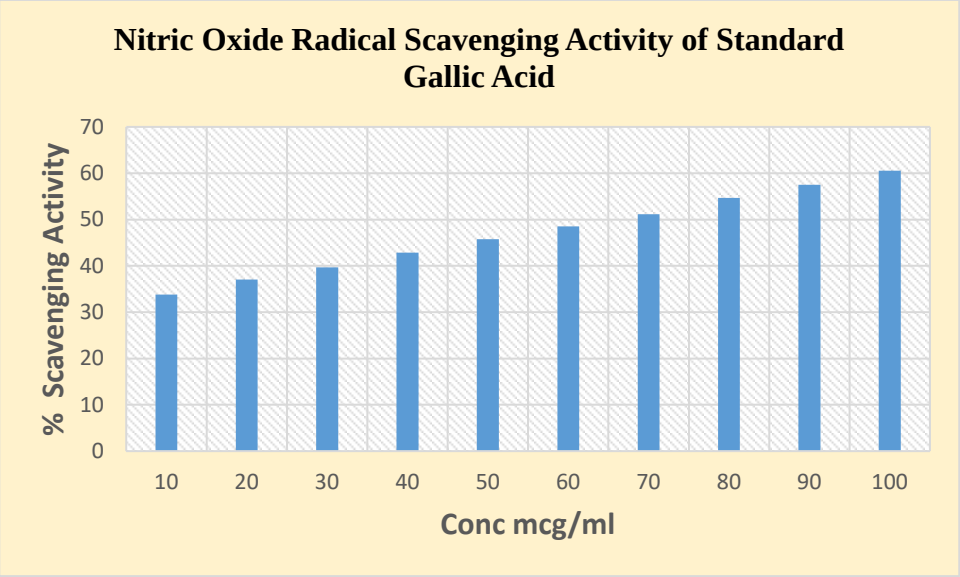

Fig 70: Nitric Oxide Radical Scavenging Activity of Standard Gallic Acid

Table 16: Nitric Oxide Scavenging Activity on the methanolic extract of the root bark of *A. polystachya*

Conc. µg/ml	Absorbance at 510nm				% Scavenging Activity*
	Trial 1	Trial 2	Trial 3	Average	
100	0.377	0.387	0.365	0.376 ± 0.011	40.76±2.774
200	0.362	0.369	0.352	0.361 ± 0.008	45.21±3.299
300	0.352	0.354	0.333	0.346 ± 0.012	45.48±2.925
400	0.339	0.341	0.362	0.347 ± 0.013	45.36±0.865
500	0.324	0.352	0.360	0.345 ± 0.019	45.69±2.071
600	0.311	0.312	0.340	0.321 ± 0.016	49.52±1.534
700	0.293	0.301	0.296	0.296 ± 0.004	53.31±1.106
800	0.286	0.278	0.263	0.275 ± 0.012	56.59±2.765
900	0.262	0.281	0.266	0.269 ± 0.010	57.56±1.847
1000	0.246	0.251	0.273	0.256 ± 0.014	59.63±1.373
Blank	0.624	0.632	0.651	0.636 ± 0.014	--

* n=3. The results are expressed as mean ±SEM.

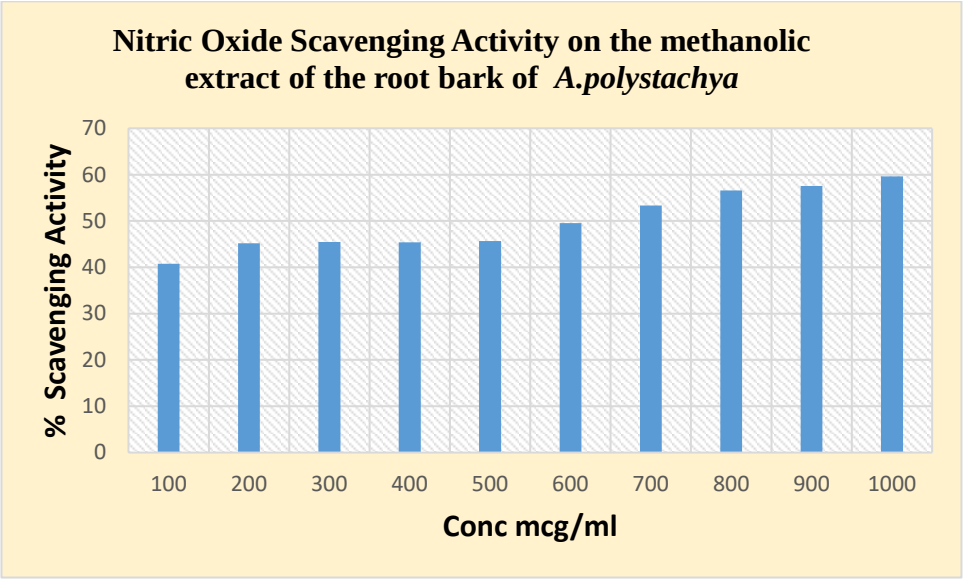

Fig. 71: Nitric Oxide Scavenging Activity on the methanolic extract of the root bark of *A. polystachya*

Table 17: Nitric Oxide Scavenging Activity on *A. polystachya* Silver Nanosuspension

Conc. µg/ml	Absorbance at 517nm				% Scavenging Activity*
	Trial 1	Trial 2	Trial 3	Average	
1	0.119	0.123	0.105	0.116 ± 0.009	10.56 ± 7.007
2	0.115	0.113	0.179	0.136 ± 0.037	18.46 ± 7.198
3	0.103	0.192	0.189	0.095 ± 0.007	30.40 ± 9.558
4	0.050	0.073	0.072	0.065 ± 0.013	49.49 ± 12.965
5	0.049	0.068	0.065	0.060 ± 0.009	55.81 ± 5.831
6	0.046	0.059	0.043	0.049 ± 0.008	62.18 ± 1.880
7	0.040	0.053	0.049	0.047 ± 0.006	63.24 ± 6.724
8	0.039	0.051	0.034	0.041 ± 0.008	68.60 ± 2.061
9	0.033	0.048	0.026	0.035 ± 0.011	72.92 ± 4.163
10	0.033	0.041	0.022	0.032 ± 0.009	79.12 ± 9.532
Blank	0.129	0.151	0.222	0.167±0.048	--

* n=3. The results are expressed as mean ±SEM.

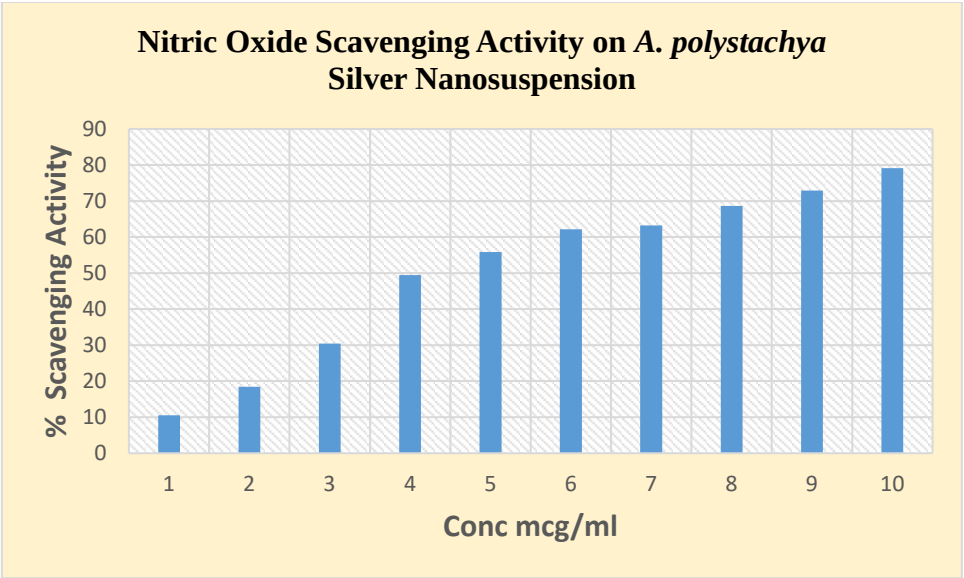

Fig. 72: Nitric Oxide Scavenging Activity on *A. polystachya* Silver Nanosuspension

Table 18: IC_{50} Values of the Methanolic Extract of the root bark of *A. polystachya* and *A. polystachya* Silver Nanosuspension

Sample	IC_{50} Value (µg/ml)	
	DPPH Scavenging Activity	Nitric Oxide Scavenging Activity
A.polystachya Extract	300.24 ± 0.414	605.81 ± 31.30
A. polystachya Nanosuspension	8.36 ± 0.921	4.04 ± 0.510

Values are expressed as Mean±Standard Deviation (SD) Values were found out using ANOVA

6.9 SULFORHODAMINE B CYTOTOXIC ASSAY IN MCF-7 CELL LINE AND MDA-MB-231 CELL LINE ON *A. POLYSTACHYA* SILVER NANOSUSPENSION [113,122]

The methanolic extract of the root bark of *A. polystachya* and synthesized silver nanoparticles were found to have potential cytotoxic activity. This encouraged us to formulate and evaluate the AgNS for cytotoxic activity using the Sulforhodamine B Cytotoxic Assay on MCF-7 and MDA-MB cell lines. The AgNS was tested at concentration ranges between 500-7.81 µM. The results were obtained in triplicates as shown in table 19 and 20. *A. polystachya* AgNS showed IC_{50} value of 0.58 µM in MCF-7 cell lines, and more than 1000 µM in MDA-MB-231 cell lines. The AgNS showed significant cytotoxic activity when compared with the methanolic extract and the AgNPs of *A. polystachya*.

Table 19: SRB Assay Results of AgNS of *A. polystachya* on MCF-7 Cell line

Sample	Conc.	Absorbance (nm) Trial 1	Trial 2	Trial 3	Average Abs	% Cell Death*z	IC_{50}
AgNS	500.00	0.341	0.336	0.323	0.333 ± 0.00929	73.25 ± 2.0435	0.58
	250.00	0.417	0.350	0.379	0.382 ± 0.03360	69.34 ± 0.6534	
	125.00	0.328	0.492	0.393	0.404 ± 0.08258	67.55 ± 13.807	
	62.50	0.422	0.459	0.446	0.442 ± 0.01877	64.50 ± 2.7390	
	31.25	0.453	0.450	0.438	0.447 ± 0.00793	64.13 ± 1.1376	
	15.63	0.494	0.448	0.472	0.471 ± 0.02300	62.17 ± 3.0359	
	7.81	0.534	0.514	0.492	0.513 ± 0.02100	58.80 ± 2.4070	
Control		0.797	0.876	0.869	1.246		
		1.637	2.109	1.188			

Values are expressed as Mean±Standard Deviation (SD) Values were found out using ANOVA

Table 20: SRB Assay Results of AgNS of *A. polystachya* on MDA-MB231 Cell line

Sample	Conc.	Absorbance (nm) Trial 1	Trial 2	Trial 3	Average	% Cell Death*	IC_{50}
AgNS	500.00	0.315	0.321	0.294	0.310 ± 0.01412	5.78 ± 0.2642	>1000
	250.00	0.314	0.315	0.279	0.303 ± 0.02050	8.00 ± 0.5412	
	125.00	0.314	0.294	0.286	0.298 ± 0.01442	9.42 ± 0.4558	
	62.50	0.371	0.296	0.294	0.320 ± 0.04389	2.63 ± 0.3607	
	31.25	0.363	0.300	0.298	0.320 ± 0.03696	2.63 ± 0.3037	
	15.63	0.348	0.310	0.262	0.307 ± 0.04301	6.79 ± 0.7908	
	7.81	0.330	0.343	0.265	0.313 ± 0.04179	4.96 ± 0.6622	
Control		0.316	0.321	0.323	0.329		
		0.328	0.342	0.344			

Values are expressed as Mean±Standard Deviation (SD) Values were found out using ANOVA

CONCLUSION

"It always seems impossible until its done."

7.0 CONCLUSIONS

Keeping in perspective the objectives of this investigation, the experimental work along with a comprehensive assessment/analyses of the resulting data, the following conclusions are drawn:

1. Overall, the methanolic extract from the root bark of *A. polystachya* exhibited cytotoxic activity on MCF-7 cells – an essential target in the treatment of breast cancer.
2. The methanolic extract of the root bark of *A. polystachya* resulted in the isolation of four phytochemical constituents viz., Rohituka 7, Rohituka 3, Amoorinin-3-O-α-L-rhamnopyranosyl–(1→6)–β-D-glucopyranoside and 8-methyl-7,2,ʿ4ʹ-tri-O-methylflavonone-5-O-α-L-rhamnopyranosyl(1→4)-β-D-glucopyranosyl-(1→6)-β-D-glucopyranoside, which are known to exhibit anti-cancer activity.
3. The methanolic extract of the root bark of *A. polystachya* was effectively synthesized into AgNPs by a simple and efficient Green Synthesis method.
4. Characterisation of the synthesized AgNPs revealed that the methanolic extract is a good source for the formation of nanoparticles and subsequently to formulate AgNS to target breast cancer.
5. Specific effects of AgNPs of *A. polystachya* against human breast cancer cells employing flow cytometry, revealed that the AgNPs of *A. polystachya* caused a significant arrest of cells at G_2M phase higher than that of Doxorubicin, possibly,

suggesting that AgNPs from the methanolic extract of the root bark of *A. polystachya* acts by intervening in cell cycle specific mechanism that induces mitotic arrest and apoptosis in breast cancer cells.

6. The formulated AgNS of *A. polystachya* showed better free radical scavenging activity than its crude extract.

7. Additionally, AgNS of *A. polystachya* exhibited better scavenging activity using Nitric Oxide assay when compared to that of DPPH assay.

8. The antioxidant activity of the methanolic extract and nanosuspension of *A. polystachya* is due to the presence of polyphenolic compounds such as flavonoids, limonoids and tannins. The activity may be attributable to the hydrogen or the electron donating ability of the groups present in the structure – a postulation to be confirmed.

9. In general, the cytotoxic effects of the methanolic extract and the AgNS of the root bark of *A. polystachya* may be attributed to the presence of isolated components, individually or in combination, viz., Rohituka 7, Rohituka 3, Amooranin and Methyl flavanone. The isolated components can be considered as the essential evaluation minimally required to ascertain that the extract or the AgNS has a potential cytotoxic activity against carcinoma.

In addition to the Results and Discussion afforded in Chp. 6, the following information is provided to further support the above conclusions.

Anti-cancer drugs show cytotoxicity and induce apoptosis in cancer cells as they are designed to eliminate the rapidly proliferating cancerous cells. Apoptosis is a highly coordinated cycle of cell death characterized by loss of plasma membrane phospholipid asymmetry, enzymatic division of DNA through oligonucleosomal fragmentation and cell segmentation through membranous apoptotic bodies. Several anti-cancer drugs act by blocking cell cycle. Cancer cell cycle specific drugs have drawn considerable attention as they act on specific cancer cell cycle check points (G_0/G_1 phase and G_2M phase) and inhibit cancer cell proliferation (G_0/G_1 phase arrest) or mitosis (G_2M phase arrest).

Adriamycin also known as Doxorubicin, is an anthracycline derivative that kills cancerous cells by damaging their genes and interfering with their reproduction. It binds directly to DNA by intercalation between base pairs on the DNA helix and inhibition of macromolecular biosynthesis. Doxorubicin slows or stops the growth of cancer cells by inhibiting the progression of topoisomerase II, an enzyme which relaxes supercoils in DNA for transcription. This leads to the blockage of DNA and RNA synthesis and fragmentation of DNA. Doxorubicin being a powerful iron-chelator, can complex with iron and bind DNA and cell membranes to create free radicals that instantly cleave the membranes of DNA and the cells. Considering Doxorubicin, used as a reference standard, it can be postulated that the synthesized AgNPs exhibit the cytotoxic

activity as demonstrated in this investigation. However, reconfirmation and validation of this presumed mechanism of action of AgNPs needs to be further investigated.

The anticancer activity of AgNPs of *A. polystachya* was higher on MCF-7 breast cancer cell than MD-MBA23 cell lines. As a result, the AgNPs synthesized from the methanolic extract of the root bark of *A. polystachya* may have potential utility as an anticancer agent for treatment of human breast cancer. This observation has to be reconfirmed as well.

The B-cell lymphoma-2 (BcL-2) family consists of approximately 15 proteins with pro-and anti-apoptotic subgroups. Such a clear differentiation needs to be evaluated to pin down which specific protein(s) could be potentially responsible for the present observations. It is well known that while pro-apoptotic members contribute to the programmed death of apoptotic cells, anti-apoptotic agents mainly stabilize the mitochondrial membrane potential and prevent the release of apoptosis-inducing factors. Hence, the key is to ascertain the status of mitochondria in the control as well as silver nanoparticles. This would be complementary experimentation necessary to reach closer to deciding the potential 'true' mechanism and/or the activity potential of the synthesized AgNPs. The interpretation is a little bit over-reaching attributing the decrease in BcL-2 solely to the presence of the synthesized AgNPs when compared to untreated control. A positive control, i.e., a known BcL-2 inhibiting (decreasing) compound at the same quantitative level as that of the load of the synthesized AgNPs, along with the control – ensuring a 3-way comparison – could determine, prima facie, the potential of the test

compound in the treatment of malignant cells. The expression of Bcl-2 varies with different types of carcinoma, i.e., leukemia, brain sarcoma, colorectal malignancy, head and neck carcinoma, etc. While decrease in the expression of BcL-2 in any of the malignancy situations/conditions is welcome, the significance of such a decrease, e.g., “approximately 5.7 fold change” as interpreted from the data, although collectively and not specifically in conjunction with some specified target malignancy (brain, blood, colorectal, etc.) could be reported with appropriate relevant perspective.

Green synthesis of AgNPs from plant extracts within the domain of nano-biotechnology can provide a potential platform to explore the formulation of AgNS that can possibly be eco-friendly (devoid of residual organic solvents) compositions.

7.1 Scope of Future Work

The present work was successfully attempted to determine the *in vitro* cytotoxic activity of the AgNS, from the methanolic extract of the root bark of *A. polystachya* by targeting the cancerous breast cells. While this investigation provides the necessary rationale and possible preliminary proof of the cytotoxic potential of AgNS prepared from the methanolic extract of *A. polystachya*, these results have to be validated on a larger scale combined with optimizing the focus of the investigation to quantify such cytotoxicity relative to the components (individual and/or collective) along with their respective percentage strengths in the extract. Additionally, a preliminary assessment of cytotoxic potential of specific percentage strengths of the "active component(s)" in an appropriate carcinoma induced animal model is in order. Furthermore, the various postulates stated in the aforementioned conclusions need to be investigated. Subsequent to comprehensive analysis of the resulting data, steps to be taken to pursue this methanolic extract based AgNS of *A. polystachya* for its viability as a potential product for the treatment of breast cancer will emerge.

BIBLIOGRAPHY

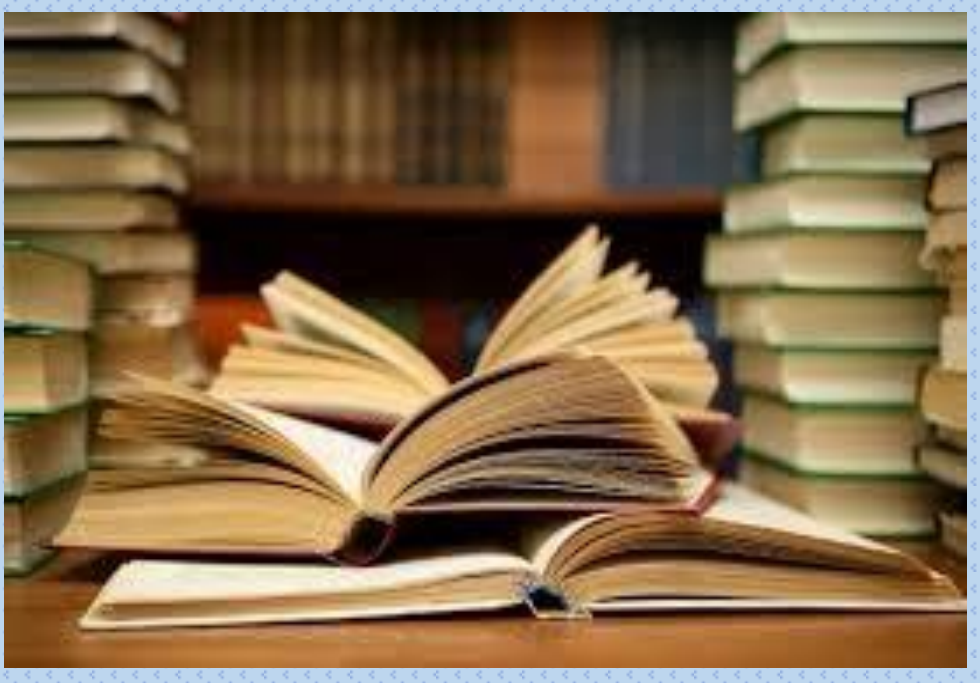

"The road to knowledge begins with the turn of the page."

8.0 BIBLIOGRAPHY

1. Harvey A. Natural products in drug discovery. Drug Dis Today. 2008;13(19-20):894–901.
2. Elham S, Siamak SS, Behzad B. Herbal Medicine as Inducers of Apoptosis in Cancer Treatment. Adv Pharm Bull. 2014;4(1):421-7.
3. Patil SD, Chaudhari MA, Sapkale PV, Chaudhari RB. A recent review on anticancer herbal drugs. J Drug Dis Ther. 2013;1(6):77-84.
4. Jena J. A Study on Natural Anticancer Plants. Int J Pharmaceut Chem Sci. 2012;1(1):365-8.
5. Obaya AJ, Sedivy JM. Regulation of cyclin-Cdk activity in mammalian cells. Cell Mol Life Sci. 2002;59:126-42.
6. Assoian RK, Zhu X. Cell anchorage and the cytoskeleton as partners in growth factor dependent cell cycle progression. Curr Opin Cell Biol. 1997;9:93-8.
7. Niculescu AB, Chen X, Smeets M, Hengst L, Prives C, Reed SI. Effects of p21(Cip1/Waf1) at both the G1/S and the G2/M cell cycle transitions: pRb is a critical determinant in blocking DNA replication and in preventing endoreduplication. Mol Cell Biol. 1998;18:629-43.
8. Bunz F, Dutriaux A, Lengauer C, Waldman T, Zhou S, Brown JP. Requirement for p53 and p21 to sustain G2 arrest after DNA damage. Science. 1998;282:1497-1501.

9. Guoyan Y, Xun Li, Xiaoli Li, Lu Wang, Jia Li, Xue Song, et al. Traditional Chinese medicine in cancer care: a review of case series published in the Chinese literature. Evid Based Complement Alternat Med. 2012;751046:1-8.
10. Pfeffer CM, Singh AT. Apoptosis: a target for anticancer therapy. Int. J. Mol. Sci. 2018;19(2):448.
11. Wang Z, Wang N, Chen J, Shen, J. Emerging Glycolysis Targeting and Drug Discovery from Chinese Medicine in Cancer Therapy. Evid. -Based Complementary Altern. Med. 2012;1–13.
12. Azadmehr A, Hajiaghaee R, Afshari A, Amirghofran Z, Refieian-Kopaei M, yousofi Darani H, et al. Evaluation of *in vivo* immune response activity and *in vitro* anti-cancer effect by *Scrophularia megalantha*. J Med Plants Res. 2011;5(11):2365-8.
13. Koehn FE, Carter GT. The evolving role of natural products in drug discovery. Nat Rev Drug Discov. 2005;4(3):206-20.
14. Adams JM. The Bcl-2 Protein Family: Arbiters of Cell Survival. Science. 1998; 281(5381):1322–6.
15. Hemaiswarya S, Doble M. Potential synergism of natural products in the treatment of cancer. Phytother Res. 2006;20(4):239-49.
16. De Araujo JRF, De Souza TP, Pires JG, Soares LA, De Araujo AA, Petrovick PR, et al. A dry extract of *Phyllanthus niruri* protects normal cells and induces

apoptosis in human liver carcinoma cells. Exp Biol Med. (Maywood) 2012;237(11):1281-8.

17. Qi F, Li A, Inagaki Y, Gao J, Li J, Kokudo N, et al. Chinese herbal medicines as adjuvant treatment during chemo or radio-therapy for cancer. Biosci Trends. 2010;4(6):297-307.
18. Wheat J, Currie G. Herbal medicine for cancer patients: An evidence-based review. Int J Altern Med. 2008;5(2):1-11.
19. Ramachandran C, Rodriguez S, Ramachandran R, Raveendran Nair PK, Fonseca H, Khatib Z, et al. Expression profiles of apoptotic genes induced by curcumin in human breast cancer and mammary epithelial cell lines. Anticancer Res. 2005;25(5):3293-302.
20. Taraphdar AK, Roy M, Bhattacharya RK. Natural products as inducers of apoptosis: Implication for cancer therapy and prevention. Curr Sci. 2001;80(11):1387-96.
21. Clement MV, Hirpara JL, Chawdhury SH, Pervaiz S. Chemopreventive agent resveratrol, a natural product derived from grapes, triggers CD95 signalling-dependent apoptosis in human tumor cells. Blood. 1998;92(3):996-1002.
22. Cheah YH, Nordin FJ, Tee TT, Azimahtol HL, Abdullah NR, Ismail Z. Antiproliferative property and apoptotic effect of xanthorrhizol on MDA-MB-231 breast cancer cells. Anticancer Res. 2008;28(6A):3677-89.

23. Smith-Hall C, Larsen HO, Pouliot M. People, plants and health: a conceptual framework for assessing changes in medicinal plant consumption. J Ethnobiol Ethnomed. 2012; 8(43):1-11.
24. Yang HL, Chen CS, Chang WH, Lu FJ, Lai YC, Chen CC, et al. Growth inhibition and induction of apoptosis in MCF-7 breast cancer cells by *Antrodia camphorata*. Cancer Lett. 2006;231(2):215-27.
25. Pal SK, Shukla Y. Herbal medicine: current status and the future. Asian Pac J Cancer Prev. 2003;4(4):281-8.
26. Yang S, Zhao Q, Xiang H, Liu M, Zhang Q, Xue W, et al. Antiproliferative activity and apoptosis-inducing mechanism of constituents from *Toona sinensis* on human cancer cells. Cancer Cell Int. 2013;13(1):12.
27. Abdullaev FI. Cancer Chemopreventive and tumoricidal properties of saffron (*Crocus sativus* L.). Exp Biol Med. (Maywood) 2002;227(1):20-5.
28. Plummer SM, Holloway KA, Manson MM, Munks RJ, Kaptein A, Farrow S, et al. Curcumin suppresses colon cancer cell invasion via AMPK-induced inhibition of NF-κB, uPA activator and MMP9. Oncogene. 1999;18(44):6013-20.
29. Ireson CR, Jones DJ, Orr S, Coughtrie MW, Boocock DJ, Williams ML, et al. Metabolism of the cancer Chemopreventive agent curcumin in human and rat intestine. Cancer Epidemiol Biomarkers Prev. 2002;11(1):105-11.

30. Duflos A, Kruczynski A, Barret JM. Novel aspects of natural and modified vinca alkaloids. Curr Med Chem Anticancer Agents. 2002;2(1):55-70.
31. Nobili S, Lippi D, Witort E, Donnini M, Bausi L, Mini E, et al. Natural compounds for cancer treatment and prevention. Pharmacol Res. 2009;59(6):365-78.
32. Fauzee NJ. Taxanes: Promising anti-cancer drugs. Asian Pac J Cancer Prev. 2011;12(4):837-51.
33. Shoeb M. Anticancer agents from medicinal plants. Bangladesh J Pharmacol. 2006;1:35-41.
34. Yang HL, Chen CS, Chang WH, Lu FJ, Lai YC, Chen CC, *et al.* Growth inhibition and induction of apoptosis in MCF-7 breast cancer cells by *Antrodia camphorata.* Cancer Letters. 2006;231(2):215–27.
35. https://www.cancer.net/cancer-types/breast-cancer/introduction. [cited March 2020].
36. Key TJ, Verkasalo PK, Banks E. Epidemiology of breast cancer. Lancet Oncol. 2001;2(3):133–40.
37. https://www.nationalbreastcancer.org/breast-anatomy. [cited March 2020]
38. https://www.medicalnewstoday.com/articles/316977#breast-anatomy.[cited March 2020]

39. Shanker K, Mohan GK, Sandhya RM, Pravallika PL. Herbal Drugs and Herbal Mediated Silver Nano Particles as Anti Diabetics: A New Horizon. Int J Pharm Sci Rev Res. 2015;31(2):142-8.
40. Rajasekhar R, Antony BM, Nagendra NG. Green Synthesis, Characterization and *in vitro* Antibacterial Studies of Gold Nanoparticles by using *Senna siamea* Plant Seed Aqueous Extract at Ambient Conditions. Asian J Chem. 2013;25(15):8541-44.
41. Sharma G, Nam JS, Sharma A, Lee SS. Antimicrobial Potential of Silver Nanoparticles Synthesized Using Medicinal Herb *Coptidis rhizome*. Molecules. 2018;23(2268):1-12.
42. Shanker K, Mohan GK, Hussain MA, Jayarambabu N, Pravallika PL. Green Biosynthesis, Characterization, *in vitro* Antidiabetic Activity, and Investigational Acute Toxicity Studies of Some Herbal-mediated Silver Nanoparticles on Animal Models. Pharmacogn Mag. 2017;13(49):188–92.
43. Gaddala B, Nataru S. Synthesis, characterization and evaluation of silver nanoparticles through leaves of *Abrus precatorius* L.: an important medicinal plant. Applied Nanoscience. 2014;5(1):99-104.
44. Panyam J, Williams D, Dash A, Leslie-Pelecky D, Labhasetwar V. Solid-state Solubility Influences Encapsulation and Release of Hydrophobic Drugs from PLGA/PLA Nanoparticles. J Pharm Sc. 2004;93(7):1804-14.

45. Gomes A, Ghosh S, Sengupta J, Datta P, Gomes A. Herbonanoceuticals: A New Step Towards Herbal Therapeutics. Med Aromat Plants. 2014;3(3):1-9.
46. Nazish J, Saba A, Khalil ur Rahmanb, Tuba F, Fareeha A, Rubab S. Formulation and characterization of nanosuspension of herbal extracts for enhanced antiradical potential. J Exp Nanosci. 2015;11(1):72-80.
47. Geethalakshmi R, Sarada DVL. Gold and silver nanoparticles from *Trianthema decandra*: synthesis, characterization and antimicrobial properties. Int J Nanomedicine. 2012;7:5375-84.
48. Hussain JI, Kumar S, Hashmi AA, Khan Z. Silver nanoparticles: preparation, characterization, and kinetics. Adv Mater Lett. 2011;2(3):188-94.
49. Morones JR, Elechiguerra JL, Camacho A, Holt K, Kouri JB, Ramírez JT, et al. The bactericidal effect of silver nanoparticles. Nanotechnology. 2005;16(10):2346–53.
50. Raihan Khan T, Karmakar P, Das A, Banik R. Evaluation of Cytotoxic and Anthelmintic activities of bark extracts of *Aphanamixis Polystachya* (Wall,). Int Res J Pharm. 2013;4(4):126-9.
51. Chan LL, George S, Ahmad I, Gosangari SL, Abbasi A, Cunningham BT, et al. Cytotoxicity effects of *Amoora rohituka* and *chittagonga* on breast and pancreatic cancer cells. Evid Based Complementary Altern Med. 2011;860605:1-8.
52. Hegde K, Moitra G. Evaluation of Anticancer Activity of Extract of *Aphanamixis polystachya* (Wall.) Parker Leaves. Int J Pharm Res Sch. 2014;3(2):876-81.

53. Geetanjali B, Dev JK, Goswami AK, Dibya JB, Nabajit D. Free Radical Scavenging Potential and Antibacterial activity of leaves of *Aphanamixis polystachya* (wall.) R.N. Parker. Eu J Bio Pharm Sci. 2016; 3(8):309-13.
54. Gole MK, Dasgupta S, Sur K, Ghosal J. Hepatoprotective effect of *Amoora Rohituka*. Int J Pharmacog. 1997;35(5):318-22.
55. Agarwal SK, Verma S, Singh SS, Kumar S. A new limonoid from *Aphanamixis polystachya*. Ind J Chem. 2001;40B:536-8.
56. Zhang Y, Wang JS, Wang XB, Cheng Gu Y, Wei DD, Gua C, et al. Limonoids from the Fruits of *Aphanamixis polystachya* (Meliaceae) and their Biological Activities. J Agric Food Chem. 2013;61:2171−82.
57. Kirtikar KR, Basu BD, Indian Medicinal Plants. Vol 1. 2nd ed. Dehradun: International Book Distributor; 2005.
58. Sir Hooker JD. The Flora of British India. Vol 1. Delhi: Periodical Experts; 1872.
59. Shetty BV, Kaveriappa KM, Bhat GK. Plant Resources of Western Ghats and Lowlands of Dakshina Kannada and Udupi Districts. Karnataka. Pilkula Nisarga Dharma Society; 2002.
60. www.the plantlist.org [cited March 2015].
61. www.en.wikipedia.org/wiki/Meliaeceae [cited 2015].
62. Nadkarni AK. Indian Materia Medica. Vol 1. Bombay: Bombay Popular Prakashan; 2009.
63. Bhat GK. Flora of Udupi. Karnataka: Indian Naturalist (Regd); 2003.

64. Shweta SS, Rani WC, Tapadiya GG, Khadabadi SS. *Aphanamixis polystachya* (wall.) Parker - An Important Ethnomedicinal Plant. Int J Pharm Sci Rev Res. 2014; 24(1):25-8.
65. Chowdhury R, Rashid RB. Effect of the crude extracts of Amoora rohituka stem bark on gastrointestinal transit in mice. Ind J Pharmacol. 2003;35(5):304-7.
66. Khare CP. Indian Medicinal Plants. An illustrated Dictionary, Berlin: Springer; 2007.
67. Jagetia GC, Venkatesha VA. Determination of Antineoplastic Activity of Rohituka, *Aphanamixis polystachya* (Wall) RN Parker in Hela Cells: Correlation with Clonogenicity and DNA Damage. Int J Complement Alt Med. 2016;3(4):1-11.
68. Valan MF. Isolation and characterization of the active principle from the bark of *Aphanamixis polystachya.* Asian J Pharm Res. 2014;4(1):19-23.
69. Alluri KV, Rao CV, Rao TV, Reddy KN, Trimurtulu G. *In vitro* and *in vivo* antioxidant activity of *Aphanamixis polystachya* bark. J Infect.Dis. 2009;5(2):60-7.
70. Liza Meutia S, Gus Permana S, Elza Ibrahim A. Areca nut extract demonstrated apoptosis-inducing mechanism by increased caspase-3 activities on oral squamous cell carcinoma. F1000Research. 2018;7(723):1-33.
71. Zhou C, Ma J, Su M, Shao D, Zhao J, Zhao T, et al. Down-regulation of STAT3 induces the apoptosis and G1 cell cycle arrest in esophageal carcinoma ECA109 cells. Cancer Cell Int. 2018;18(53):1-12.

72. Banerjee PP, Bandyopadhyay A, Harsha SN, Policegoudra RS, Bhattacharya S, Karak N, et al. *Mentha arvensis* (Linn.)-mediated green silver nanoparticles trigger caspase 9-dependent cell death in MCF7 and MDA-MB-231 cells. Breast Cancer: Targets and Therapy. 2017; 9:265-78.
73. Mohanta YK, Panda SK, Jayabalan R, Sharma N, Bastia AK, Mohanta TK. Antimicrobial, antioxidant and cytotoxic activity of silver nanoparticles synthesized by leaf extract of *Erythrina suberosa* (Roxb.). Front Mol Biosci. 2017;4(14):1-9.
74. Patil SP, Kumbhar ST. Antioxidant, antibacterial and cytotoxic potential of silver nanoparticles synthesized using terpenes rich extract of *Lantana camara* L. leaves. Biochem Biophy. 2017;10:76-81.
75. Mitiku AA, Yilma B. Antibacterial and antioxidant activity of silver nanoparticles synthesized using aqueous extract of *Moringa stenopetala* leaves. Afr J Biotechnol. 2017;16(32):1705-16.
76. Otunola GA, Afolayan AJ, Ajayi EO, Odeyemi SW. Characterization, antibacterial and antioxidant properties of silver nanoparticles synthesized from aqueous extracts of *Allium sativum*, *Zingiber officinale*, and *Capsicum frutescens*. Phcog Mag. 2017;13(50):201-8.
77. Ahmed S, Saifullah AM, Swami BL, Ikram S. Green synthesis of silver nanoparticles using *Azadirachta indica* aqueous leaf extract. J Radiat Res Appl Sc. 2016;9(1):1-7.

78. Orangi M, Pasdaran A, Shanehbandi D, Kazemi T, Yousefi B, Hosseini BA, Baradaran B. Cytotoxic and apoptotic activities of methanolic subfractions of *Scrophularia oxysepala* against human breast cancer cell line. Evid Based Complementary Altern Med. 2016;8540640:1-10.
79. Thilagavathi T, Kathiravan G, Srinavasan K. Antioxidant activity and synthesis of silver Nanoparticles using the leaf extract of *Limonia acidissima*. Int J Pharm Bio Sci. 2016;7(4):201-5.
80. Mahendran G, Kumari BR. Biological activities of silver nanoparticles from *Nothapodytes nimmoniana* (Graham) Mabb. fruit extracts. Food Science and Human Wellness. 2016;5(4):207-18.
81. Upendra N, Gulati N, Chauhan S. Antioxidant and Antibacterial Potential of Silver Nanoparticles: Biogenic Synthesis Utilizing Apple Extract. Int J Pharm. 2016; 7141523:1-9.
82. Phull AR, Abbas Q, Ali A, Raza H, Zia M, Haq IU. Antioxidant, cytotoxic and antimicrobial activities of green synthesized silver nanoparticles from crude extract of *Bergenia ciliata*. Future J Pharm Sci. 2016;2(1):31-6.
83. Saminathan K. Herbal Synthesis of Silver Nanoparticles using *Eclipta alba* and its antimicrobial activity. Int J Curr Microbiol App Sci. 2015;4(3):1092-7.
84. Mollick MR, Rana D, Dash SK, Chattopadhyay S, Bhowmick B, Maity D, et al. Studies on green synthesized silver nanoparticles using *Abelmoschus esculentus*

(L.) pulp extract having anticancer (*in vitro*) and antimicrobial applications. Arab J Chem. 2015;12(8):2572-84.

85. Firdhouse MJ., Lalitha P. Biosynthesis of silver nanoparticles using the extract of *Alternanthera sessilis*- antiproliferative effect against prostate cancer cells. Cancer Nanotechnology. 2013;4(6):137-43.
86. Krishnamurthy PT, Vardarajalu A, Wadhwani A, Patel V. Identification and characterization of a potent anticancer fraction from the leaf extracts of *Moringa oleifera L*. Ind J of Exp Biology. 2015;53:98-103.
87. Bhatia D., Mandal A., Nevo E., Bishayee, A. Apoptosis-inducing effects of extracts from desert plants in HepG2 human hepatocarcinoma cells. Asian Pacific J Trop Biomed. 2015;5(2):87–92.
88. Yin Sim T, Latifah SY, Jhi Biau F, Agustono W, Norsharina I, Yoke KC, et al. Induction of Apoptosis in MCF-7 Cells via Oxidative Stress Generation, Mitochondria Dependent and Caspase-Independent Pathway by Ethyl Acetate Extract of *Dillenia suffruticosa* and Its Chemical Profile. PLOSONE. 2015;10(6): 1-25.
89. Vinmathi V, Jacob JPS. Synthesis, characterization, antibacterial and cytotoxic studies of silver nanoparticles using aqueous extracts of *Crataeva nurvala* leaves – a Green nano-biotechnological approach. World J Pharm Res. 2014; 4(1):953-62.

90. Sriram T, Pandidurai V. Synthesis of silver nanoparticles from leaf extract of *Psidium guajava* and its antibacterial activity against pathogens. Int J Curr Microbiol App Sci. 2014; 3(3):146-52.
91. Vega-Baudrit J, Alvarado-Meza R, Solera-Jiménez F. Synthesis of silver nanoparticles using chitosan as a coating agent by sonochemical method. Avances en Química. 2014;9(3):125-9.
92. Revathi S, Saraswathi U, Jayanthi V. *In-vitro* evaluation of anti-hepatocarcinogenic activity of a herbal formulation (*chathurmuka chooranam*) against HepG2 cells. Int J Pharm Sci. 2014;6:254-6.
93. Sung-Hwan K, Je-Won K, Suk-Kyu K, In-Chul L, Jung-Mo S, Chang jong M, et al. Silver nanoparticles induce apoptotic cell death in cultured cerebral cortical neurons. Mol Cell Toxicol. 2014;10(2):173-9.
94. Abdel-Aziz MS, Shaheen MS, El-Nekeety AA, Abdel-Wahhab MA. Antioxidant and antibacterial activity of silver nanoparticles biosynthesized using Chenopodium murale leaf extract. J Saudi Chem Soc. 2014;18(4):356-63.
95. Ragasa CY, Aguilar ML, Bugayong ML, Jacinto SD, Li WT, Shen CC. Terpenoids and sterol from *Aphanamixis polystachya*. J Chem Pharm Res. 2014;6(6):65-8.
96. Lalitha P, Firdhouse J. Green synthesis of silver nanoparticles using the aqueous extract of *Portulaca oleracea* (L.). Asian J Pharm Clin Res. 2013;6:92-94.

97. Lalitha A, Subbaiya R, Ponmurugan P. Green synthesis of silver nanoparticles from leaf extract *Azhadirachta indica* and to study its anti-bacterial and antioxidant property. Int J Curr Microbiol App Sci. 2013;2(6):228-35.

98. Maliyakkal N, Udupa N, Pai KSR, Rangarajan A. Cytotoxic and apoptotic activities of extracts of *Withania somnifera* and *Tinospora cordifolia* in human breast cancer cells. Int J App Res Nat Prod. 2013;6(4):1-10.

99. Sarkar AS, Pathan AH, Md. Jamaluddin AT, Ferdous Ara, Shakhawat HB, Md. Rakibul I. Phytochemical Analysis and Bioactivities of *Aphanamixis polystachya* (Wall.) R. Parker Leaves from Bangladesh. J Biol Sci. 2013;13(5):393-9.

100. Ansari Q, Ahmed SA, Waheed MA, Juned S. Extraction and determination of antioxidant activity of *Withania somnifera* Dunal. Eur J Exp Biol. 2013;3(5):502-7.

101. Yuet YL, Buong WC, Mitsuaki N, Son R. Synthesis of silver nanoparticles by using tea leaf extract from *Camellia sinensis*. Int J Nanomedicine. 2012;7:4263-7.

102. Sasikala A, Savithramma N. Biological synthesis of silver nanoparticles from *Cochlospermum religiosum* and their antibacterial efficacy. J Pharm Sci Res. 2012;4(6):1836.

103. Firdhouse MJ, Lalitha P, Sripathi SK. Novel synthesis of silver nanoparticles using leaf ethanol extract of *Pisonia grandis* (R. Br). Der Pharma Chemica. 2012;4(6):2320-6.

104. Vanmathi K, Selvi TS. Isolation and characterization of silver nanoparticles from *Fusarium oxysporum*. Int J Curr Microbiol App Sci. 2012; 1(1):56-62.

105. Shameli K, Ahmad MB, Ali Z, Parvanh S, Parvaneh S, Yadollah A. Green biosynthesis of silver nanoparticles using *Curcuma longa* tuber powder. Int J Nanomed. 2012;.7:5603-10.

106. Boucher D, Blais V, Denault JB. Caspase-7 uses an exosite to promote poly (ADP ribose) polymerase 1 proteolysis. Proc Natl Acad Sci. 2012;109(15):5669-74.

107. Tamizhamudu E, Arunachalam KD. Memecylon edule leaf extract mediated green synthesis of silver and gold nanoparticles. Int J Nanomedicine. 2011;6:1265-78.

108. Veerasamy R, Xin TZ, Gunasagaran S, Xiang TF, Yang EF, Jeyakumar N, Dhanaraj SA. Biosynthesis of silver nanoparticles using mangosteen leaf extract and evaluation of their antimicrobial activities. J Saudi Chem Soc. 2011;15(2):113-20.

109. Saklani S, Mishra AP, Rawat A, Chandra S. Free Radical Scavenging (DPPH) and Ferric Reducing Ability (FRAP) of *Aphanamixis polystachya* (Wall) Parker. Int J Drug Dev Res. 2011;3(4):271-4.

110. Saumya SM, Mahaboob BP. *In vitro* evaluation of free radical scavenging activities of *Panax ginseng* and lagerstroemia speciosa: a comparative analysis. Int J Pharm Pharm Sci. 2011;3(1):165-9.

111. Lamkanfi M, Kanneganti TD, Van Damme P, Berghe TV, Vanoverberghe I, Vandekerckhove J, et al. Targeted peptidecentric proteomics reveals caspase-7 as a substrate of the caspase-1 inflammasomes. Mol Cell Proteomics. 2008;7(12):2350-63.

112. Zhang H, Chen F, Wang X, Wu D, Chen Q. Complete assignments of ^{1}H and ^{13}CNMR data for rings A, B-seco limonoids from the seed of *Aphanamixis polystachya*. Magn Reson Chem. 2007;45:189–92.

113. Houghton P, Fang R, Techatanawat I, Steventon G, Hylands P, Lee CC. The sulphorhodamine (SRB) assay and other approaches to testing plant extracts and derived compounds for activities related to reputed anticancer activity. Methods. 2007; 42(4):377–87.

114. Zhang HP, Wu SH, Luo XD, Ma YB, Wu DG. A new limonoid from the seed of *Aphanamixis polystachya*. Chinese Chem Let. 2002;13(4):341-2.

115. Chowdhury R, Hasan CM, Rashid MA. Guaiane Sesquiterpenes from *Amoora rohituka*. Phytochemistry. 2003;62:1213-6.

116. Rabi T, Karunagaran D, Krishnan Nair M, Bhattathiri VN. Cytotoxic activity of amooranin and its derivatives. Phytothe Res. 2002;16(S1):84-6.

117. Kang-Beom K, Eun-Kyung K, Byung-Cheul S, Eun-A S, Jeong-Yeh Y, Do-Gon Ryu. *Herba houttuyniae* extract induces apoptotic death of human promyelocytic leukaemia cells via caspase activation accompanied by dissipation of

mitochondrial membrane potential and cytochrome c release. Exp Mol Med. 2003;35(2):91-97.

118. Zhou G, Stevens Jr. Multiple parameters for the comprehensive evaluation of the susceptibility of *Escherichia coli* to the silver ion metals. Bio Metals. 1998;11(1), 27–32.
119. Chatterjee A, Kundu AB. Isolation, structure and stereochemistry of aphanamixin - A new triterpene from wall and parker. Tetrahedron Lett. 1967;8(16):1471-6.
120. Krishnaraju AV, Rao CV, Rao TV, Reddy KN, Trimurtulu G. *In vitro* and *in vivo* antioxidant activity of *Aphanamixis polystachya* bark. Am J Infect Dis. 2009;5(2):60-7.
121. Srivastav SK, Srivastav SD, Srivastav S. New Biologically active Limonoids and Flavonoids from *Aphanamixis polystachya*. Ind J Chem. 2003;42B:3155-8.
122. Vichai V, Kirtikara K. Sulforhodamine B colorimetric assay for cytotoxicity screening. Nat Protoc. 2006;1(3):1112–6.
123. Singh R, Wagh P, Wadhwani S, Gaidhani S, Kumbhar A, Bellare J, et al. Synthesis, optimization, and characterization of silver nanoparticles from *Acinetobacter calcoaceticus* and their enhanced antibacterial activity when combined with antibiotics. Int J Nano. 2013;8:4277–90.

124. Devaraj P., Kumari P., Aarti C., Renganathan A. Synthesis and Characterization of Silver Nanoparticles using Cannonball Leaves and their Cytotoxic Activity against MCF-7 Cell Line. J Nanotechnol. 2013;598328:1-5.

125. Vijayakumar M, Priya K, Nancy FT, Noorlidah A, Ahmed ABA. Biosynthesis, Characterization and anti-bacterial effect of plant-mediated silver nanoparticles using *Artemisia nilagirica*. Ind Crops Prod. 2013;41:235–240.

126. Awwad AM, Salem NM. Green Synthesis of Silver Nanoparticles by Mulberry Leaves Extract. J Nanosci Nanotechnol. 2012;2(4):125-8.

127. Ajitha B, Reddy AKY, Reddy SP. Green synthesis and characterization of silver nanoparticles using *Lantana camara* leaf extract. Mat Sci Eng. 2015;49:373–81.

128. Chang HY, Yang X. Proteases for Cell Suicide: Functions and Regulation of Caspases. Microbiol Mol Biol R. 2000;64(4):821–46.

DECLARATION

This is to certify that Ms. Rajashree Ramachandra Jirage is pursuing her Ph.D. on the topic entitled, *"Green Synthesis, Characterization and Biological Evaluation of some Anti-Cancerous Nanoparticles from Herbs"*, at Goa College of Pharmacy under the guidance of Dr. Arun B. Joshi has chosen the plant *Aphanamixis polystachya* for her study.

The selected plant, *Aphanamixis polystachya (Wall) R.N. Parker* has already been authenticated by Dr. K. Gopalkrishna Bhatt, Udupi and Mr. Dinesh Naik, Mangalore, in the year 2013. The specimen was deposited in the herbarium of Department of Pharmacognosy, Goa College of Pharmacy, Panaji-Goa bearing the number: GCP.Pharmacog.05/2013.

Date: 12/03/2015
Place: Panaji-Goa

Dr. Arun B. Joshi
Professor & Head
Department of Pharmacognosy
Goa College of Pharmacy
Panaji-Goa

PUBLICATIONS

Published

1. Gude R, Joshi A, Bhandarkar A, Shirodker A, Bhangle S. Synthesis and Characterization of silver nanoparticles from the roots of *Aphanamixis polystachya*. World J Pharm Res. 2016;5805:1399-1408.
2. R. Gude, Joshi A, Bhandarkar A. Anti-oxidant, cytotoxic and apoptotic studies of root bark assisted silver nanoparticles from *A. polystachya*. Int J Res Pharm Sci. 2019;10(2):943-50.
3. R. Gude, A. Joshi, A. Bhandarkar. Isolation and Cytotoxic Potential of Silver Nanosuspension of the roots of Aphanamixis polystachya. Int. J. Pharm. Sci. 2020;11(11): 1000-09.

WORLD JOURNAL OF PHARMACEUTICAL RESEARCH
SJIF Impact Factor 6.805
Volume 5, Issue 7, 1399-1408. Research Article ISSN 2277– 7105

SYNTHESIS AND CHARACTERISATION OF SILVER NANOPARTICLES FROM THE ROOTS OF APHANAMIXIS POLYSTACHYA

Rajashree Gude*, Arun B. Joshi, Anant Bhandarkar, Akshata Shirodker, Shraddha Bhangle

Goa College of Pharmacy, Panaji- Goa 403 001.

Article Received on
12 May 2016,

Revised on 01 June 2016,
Accepted on 22 June 2016

DOI: 10.20959/wjpr20167-6604

***Corresponding Author**
Rajashree Gude
Goa College of Pharmacy,
Panaji- Goa 403 001.

ABSTRACT

Nanoscience and Nanotechnology are having a wide range of applications such as green chemistry, biology, medicinal chemistry, physics, materials science and engineering. Over the past few decades, nanoparticles of noble metals such as silver (bio synthesized) exhibited significantly distinct physical, chemical and biological properties. To overcome the problem of bioavailability, an effort was made to synthesize silver nanoparticles (SNP) using various concentrations of methanolic extract from the roots of *Aphanamixis Polystachya* by ultrasonification and were characterized by using various techniques like XRD, SEM, PSA, UV, FT-IR and EDX. Morphology and metal composition of synthesized nano particles were determined by SEM and EDAX respectively. Size of SNP were analyzed by using PSA. Further the SNP were also characterized by UV spectroscopy. A sharp peak was observed between 400nm- 420nm indicating the formation of SNP. FTIR analysis showed that the biosynthesized SNP were capped with bimolecular compounds which were responsible for reduction of silver. The bands at 3420.8 cm-1 and 2923.9 cm-1 have shown the formation of secondary amines. X-ray diffraction confirmed the predominantly spherical shape and poly dispersed SNP. It may be concluded that the methanolic extract of *Aphanamixis Polystchya* can be a good source for the synthesis of SNP.

KEYWORDS: *Aphanamixis Polystchya*, Herbal mediated Silver Nanoparticles (SNP), Bioavailability, Nanoscience and Nanotechnology, Nano medicine.

INTRODUCTION

Cancer is a major health problem globally affecting 15% population. It is an uncontrolled growth and quick division of the abnormal cells in the body. It is projected that by 2020, the incidence of cancer levels will increase to 15 million cases causing deaths.[1]

In the treatment of cancer many synthetic and chemotherapeutic agents have been developed, that show various side effects. Many of the plants traditionally have reported to possess antitumor activity.[1]

The medicinal plant chosen for the work is *Aphanamixis polystachya* which is a highly valued species for mankind and has been thoroughly investigated for its highly potential medicinal value.[2]

Design and development of herbal nanoparticles has become a frontier research in the field of nanotechnology. Development of this novel drug delivery system will help in overcoming various constraints like bioavailability, solubility and stability of the herbal drug.[3]

The present study is to formulate the extract of the root bark of the plant *Aphanamixis polystachya* into silver nano particles.

MATERIALS AND METHODS

DESCRIPTION OF THE PLANT

Aphanamixis polystachya belonging to the family Meliaceae, is an evergreen medium sized tree with a dense spreading crown and a straight cylindrical bole up to 15m in height and 1.5-1.8m in width. In Sanskrit, it is known as anavallabha, ksharayogya, lakshmi, lakshmivana, lohita.[2]

1. General Experimental Procedure

The root barks of the plant *Aphanamixis polystachya* were collected, washed and dried. The dried root barks were powdered and sieved. 500gm of the powdered drug was taken and exhaustively macerated with methanol. After three days, the methanolic layer was decanted off. The process was repeated three times. The solvent from the total extract was distilled off using a rotary evaporator. The concentrate was evaporated to a thick syrupy consistency and then evaporated to dryness.

2. Preliminary Phytochemical Screening (Qualitative Analysis)

The preliminary phytochemical studies were performed to confirm the availability of different phytoconstituents present in the methanolic extract. (Table No.1).

3. Synthesis of Herbal mediated Silver Nano Particles

The 10^{-3} mM Silver nitrate solution was prepared. 10ml of herbal extract was taken in 250 ml conical flask/beakers separately and to this 90 ml of $AgNO_3$ solution was added. The conical flasks were incubated at room temperature. A color change of the leaf extracts from pale yellow to dark brown was checked periodically. The brown colour formation indicates that the silver nanoparticles were synthesized from the herbal extract, and they were centrifuged at 5000 rpm for 15 minutes in order to obtain the pellet that is used for further study. The supernatant was used for characterisation.

4. Characterization Of Synthesized Silver Nano Particles

a) UV-Vis spectral analysis

The colour change in reaction mixture (metal ion solution + extract) was recorded through visual observation. The bio reduction of silver ions in aqueous solution was monitored by periodic sampling of aliquots (0.5 ml) and subsequently measuring UV-Vis spectra of the solution. UV-Vis spectra of these aliquots were monitored as a function of time of reaction on UV-Vis spectrophotometer UV-2450 (Shimadzu).

b) XRD analysis and PSA

The synthesized herbal mediated SNPs obtained were purified by repeated centrifugation at 5000 rpm for 20 min followed by redispersion of the pellet of SNPs in 10 ml of deionized water. After drying of purified SNPs, the crystalline structure was analyzed by XRD. The dried mixture of SNPs was collected for the determination of the formation of SNPs. The instrument operated at a voltage of 40 kV and a current of 30 mA with Cu Kα radiation in a θ- 2 θ configuration. The crystallite domain size was calculated from the width of XRD peaks, assuming that they are free from non-uniform strains, using the Scherrer's formula: D= 0.94 λ / β Cos θ 1) where D is the average crystallite domain size perpendicular to the reflecting planes, λ is the X-ray wavelength, β is the full width at half maximum (FWHM), and θ is the diffraction angle.

Particle size measurement was determined by using Particle size analyzer. SNPs samples were taken in 10 ml of ethanol and water test tubes, both test tubes were ultra sonicated (15

minutes) for proper distribution of nanoparticles in solution. The average particle sizes of SNPs were between 20-60 nm.

c) SEM and EDAX analysis

FESEM analysis was done using thin films of the sample were prepared on a carbon coated copper grid by just dropping a very small amount of the sample on the grid, extra solution was removed using a blotting paper and then the film on the SEM grid were allowed to dry by placing it under a mercury lamp for 5 min.

Further the sample of SNPs was taken and subjected to EDAX instrument for Ag and other compound analyses.

d) FTIR

Buker FTIR instrument was used to determine the sample functional groups. FTIR measurement was done to identify silver ions and capped plant compounds which could account for the reduction of silver nitrate into silver nanoparticles. The sample was mixed with KBr. Thin sample pellet was prepared by pressing with the Hydraulic Pellet Press and subjected to FT-IR analysis.

RESULTS AND DISCUSSION

UV-visible Spectroscopy

The formation of silver nanoparticles was followed by measuring absorbance at a wavelength range from 400–800 nm. The characteristic bands were detected around 400–450 nm. These absorption bands were assumed to correspond to the silver nanoparticles.

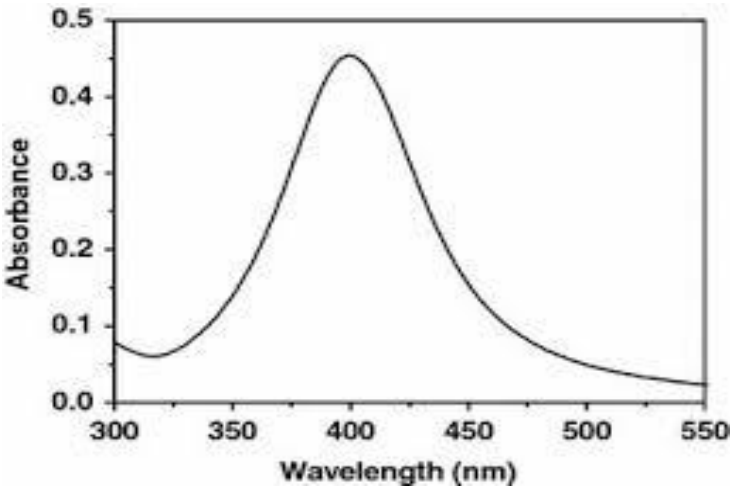

Fig 1: UV visible spectra of synthesized SNPs.

Fig 2: Brown colour formation confirming

Fig3: Tree of *Aphanamixis polystachya* formation of SNPs.

XRD and PSA

Figure 4 shows the XRD pattern of powder silver nanoparticles. The presence of peaks at 2θ values 38.1°, 44.09°, 64.36°, corresponds to (111), (200), (220), planes of silver, respectively. Thus, the XRD spectrum confirmed the crystalline structure of silver nanoparticles. No peaks of other impurity crystalline phases have been detected.

The particle size was analyzed using particle size analyzer. The particle size was analyzed under the category of intensity of laser light on the sample particle. Laser diffraction revealed that the particles obtained are aggregated mixture with size ranging between nanometers and micrometers as shown in the Figure 5. The average particle diameter was found to be 20 nm.

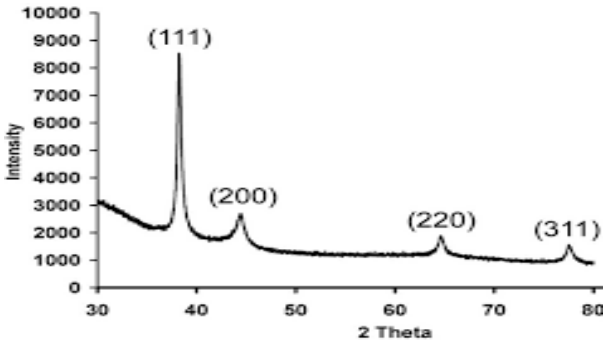

Fig 4: XRD pattern of synthesized SNPs.

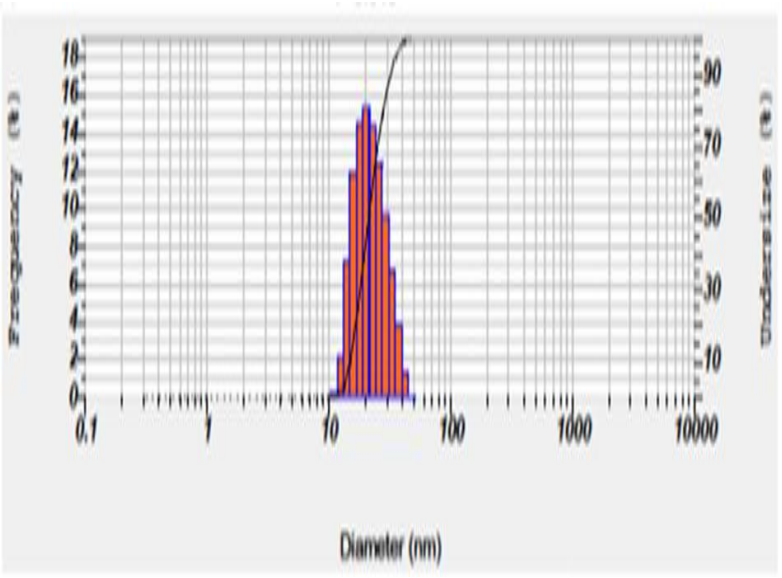

Fig 5: Particle size analysis of SNPs.

SEM and EDAX

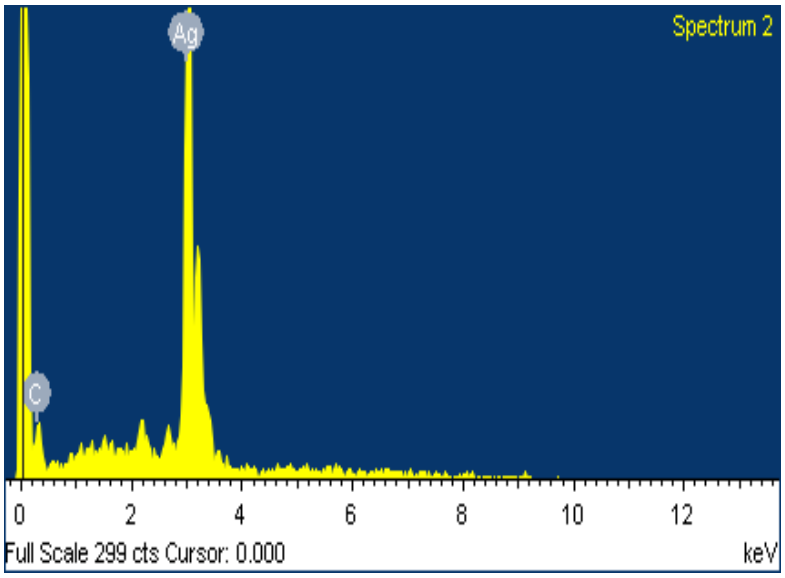

Figure 6 (a) and (b) show the SEM images of silver nanoparticles. It exhibits that almost all the nanoparticles were of spherical shape with no agglomeration.

The peaks observed index graph at 3.0, 3.2 and 3.4 keV correspond to silver. Therefore, the EDX profile of sample indicates that the silver nanoparticles sample contain pure silver, with no oxide.

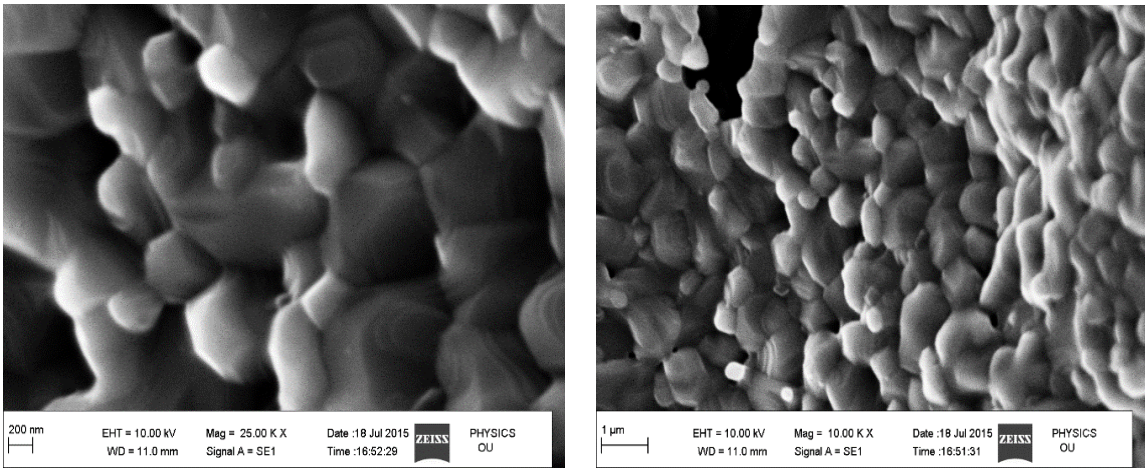

Fig 6 (a) & (b) shows SEM images of the synthesized SNPs.

Figure

Fig 7 shows the EDAX spectra of synthesized SNPs.

FTIR

FTIR measurement was carried out to identify the biomolecules for capping and stabilization of the metal nanoparticles synthesized from Aphanamixis polystachya. FT-IR analysis as seen in fig 8 showed that the biosynthesized silver nanoparticles were capped with bimolecular compounds which were responsible for reduction of silver, the bands seen at 3420.4 cm-1 and 2923.9 cm-1 were assigned to the stretching and bending vibrations of secondary amines respectively.

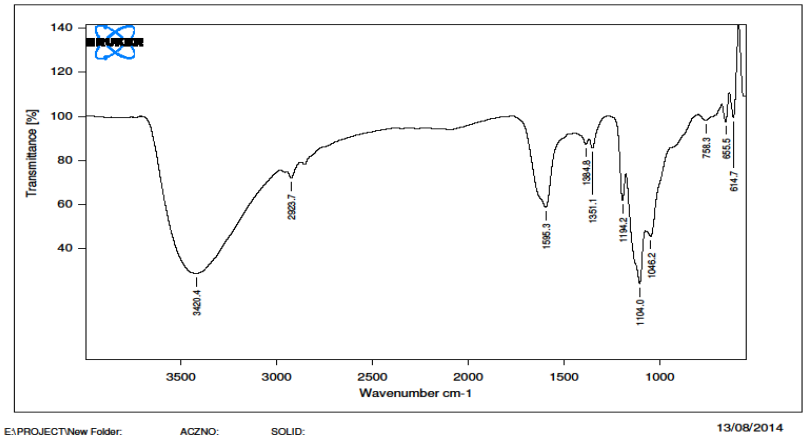

Fig 8 shows the FT-IR spectra of the synthesized SNPs.

Table No.:1 showing the preliminary characterisation done to confirm phytoconstituents.

Sr. No.	Identification Tests	Result
1	Alkaloids	+
2	Carbohydrates	+
3	Triterpeniods & Steroids	+
4	Tannins & Phenolic Compounds	+
5	Proteins	+
6	Glycosides	+
7	Starch	-

CONCLUSION

Green Synthesis is an easy method to synthesize silver nanoparticles from the root barks of *Aphanamixis polystachya*. The synthesized nanoparticles were characterized and found that the methanolic extract was a good source of formation of nanoparticles.

REFERENCES

1. http://www.who.int/mediacentre/news/releases/2003/pr27/en/.
2. Shweta SS, Rani WC, Tapadiya GG, Khadabadi SS. Aphanamixis polystachya (wall.) Parker - An Important Ethnomedicinal Plant. Int. J. Pharm. Sci. Rev. Res., Jan – Feb 2014; 24(1): 25-28.
3. Thirumurugan G, et.al; Nanotechnology: an effective tool for enhancing bioavailability and bioactivity of phytomedicine, Asian Pac J Trop Biomed., 2014 May; 4(Suppl 1): S1–S7.
4. Valan MF, Isolation and characterisation of the active principle from the bark of Aphanamixis polystachya; Asian Journal of Pharmaceutical Research, 2014; 4(1): 19-23.
5. Mishra AP, Sarla Saklani, Subhash Chandra, Abhishek Mathur, Luigi Milella, Priyanka Tiwari., Aphanamixis polystachya (wall.) Parker, Phytochemistry, Pharmacological properties and medicinal uses: An overview; World Journal of Pharmacy and Pharmaceutical Sciences, 2014; 3(6): 2242-2252.
6. Sarker AA, Chowdhury FA, Farjana Khatun., Phytochemical Screening and In vitro Evaluation of Pharmacological Activities of Aphanamixis polystachya (Wall) Parker Fruit Extracts; Tropical Journal of Pharmaceutical Research, 2013; 12(1): 111-116.
7. Rani WC, Shweta S, Tapadiya GG, Khadabadi SS; Evaluation of Phytochemical and Anticancer Potential of Aphanamixis polystachya (Wall.) Parker Stem Bark using in-vitro

Models; International Journal of Pharmaceutical Sciences Review & Research, 2014; 28(1): 138.

8. Karunakar Hegde, Gargi Moitra; Evaluation of Anticancer Activity of Extract of Aphanamixis polystachya (Wall.) Parker Leaves; International Journal for Pharmaceutical Research Scholars, 2014; (2): 876-881.
9. Tanveer RK, Karmarkar Palash, Das Abhijit, Banik Rana, Sattar MM. Evaluation of cytotoxic and anthelmintic activities of bark extract of Aphanimixis polystachya (Wall). International Research Journal of Pharmacy, 2013; 4(4).
10. Md. AAS, Md. RK, Md. AK, Sudhir Karna and Mohammad AR. In vitro Membrane Stabilizing Activity, Total Phenolic Content, Free Radical Scavenging and Cytotoxic Properties of Aphanamixis polystachya (Wall.); Bangladesh Pharmaceutical Journal, July 2010; 13: No. 2.
11. Sarker AA, Pathan AH, Phytochemical Analysis and Bioactivities of Aphanamixis polystachya (Wall) R. Parker Leaves from Bangladesh; Journal of Biological Sciences, 2013; 13(5): 393-399.
12. Enamala Narmadha, Hemashenpagam N, Vimal SS, Vasantha RS, Characterization of coriander sativum mediated silver nanoparticles and evaluation of its antimicrobial and wound healing activity; Indo American Journal of Pharmaceutical Research, 2013; 3(7): 5404-5409.
13. Konwar Ranjit, Baquee AA, Nanoparticle: An overview of preparation, characterisation and application; International Research Journal of Pharmacy, 2013; 4(4): 47-57.
14. Sarla Saklani, Mishra AP, Pharmacognostic, Phytochemical and Antimicrobial Screening of Aphanamixis polystachya, An Endangered Medicinal Tree; International Journal of Pharmacy and Pharmaceutical Sciences, 2012; 4(3): 235-240.
15. Hussain JI, Sunil Kumar, Hashmi AA, Zaheer Khan, Silver nanoparticles: preparation, characterization, and kinetics; Advanced Materials Letters, 2011; 2(3): 188-194.
16. Pandey Govind, Some important anti cancer herbs- A review; International Journal of Pharmacy, 2011; 2(7): 45-52.
17. Giriraj T Kulkarni, Herbal drug delivery systems: An emerging area in Herbal drug research; Journal of Chronotherapy and Drug Delivery, 2011; 2(3): 113-119.
18. Ajazuddin, S. Saraf, Applications of novel drug delivery system for herbal formulations; Fitoterepia, 2010; 81: 680-689.

19. Krishnaraju AV, Rao CA, Rao TVN, Reddy KN and Golakoti Trimurtulu. In vitro and In vivo Antioxidant Activity of Aphanamixis polystachya Bark; American Journal of Infectious Diseases, 2009; 5(2): 60-67.
20. Di-Cai Li et al, Application of targeted drug delivery system in Chinese medicine; Journal of Controlled Release, 2009; 138: 103–112.

ORIGINAL ARTICLE

INTERNATIONAL JOURNAL OF RESEARCH IN PHARMACEUTICAL SCIENCES

Published by Pharmascope Publications Journal Home Page: www.pharmascope.org/ijrps

Anti-oxidant, Cytotoxic and Apoptotic studies of root bark assisted Silver Nanoparticles from *Aphanamixis polystachya*

Rajashree Gude*[1], Arun B. Joshi[2], Anant Bhandarkar[2]

[1]Department of Pharmaceutics, Goa College of Pharmacy, 18th June Road, Panaji Goa, India
[2]Department of Pharmacognosy, Goa College of Pharmacy, 18th June Road, Panaji Goa, India

Article History:

Received on: 26.12.2018
Revised on: 22.03.2019
Accepted on: 25.03.2019

Keywords:

Apoptosis,
Silver nanosuspension,
DPPH,
Nitric Oxide

ABSTRACT

The aim of the present investigations was to fabricate and prepare silver nanoparticles from the root bark of *Aphanamixis polystachya* available in Western Ghats of India and also to assess their antioxidant, cytotoxic and apoptotic activity. The root bark extract of the plant, *A. polystachya* was used for the green synthesis of silver nanoparticles (AgNP). The AgNP were characterized with the help of UV-Vis Spectrophotometry, Fourier-transform infrared spectroscopy (FTIR), Energy Dispersive X-Ray Analysis (EDAX), Scanning Electron Microscopy (SEM), Transmission Electron Microscopy (TEM), X-ray Diffraction (XRD)and Thermogravimetric analysis. The cytotoxic and apoptotic effects were studied using methanolic extract and AgNP of *A. polystachya* on human breast cancer cells (MCF-7 and MDA-MB-231). Silver nanosuspension was formulated, and *in vitro*, antioxidant activity by DPPH assay and Nitric Oxide assay were assessed on a methanolic extract of the root bark and silver nanosuspension of *A. polystachya.* The percentage cell growth on MCF-7 cells was found to be 39.8, 21.6, 18.0 and 15.6 at 10, 20, 40 and 80µg/ml respectively. In the case of MDA-MB231 cells, the percentage of cell growth was found to be 99.2, 80.0, 67.2 and 54.6 at 10, 20, 40 and 80 µg/ml. Growth inhibition (GI50) of <10µg and >80µg was observed in MCF-7 and MDA-MB231 cell lines. *A. polystachya* silver nanosuspension significantly enhanced the antiradical potential against nitric oxide scavenging assay (IC50 4.7µg/ml) as compared with methanolic extract of *A. polystachya*. The formulation of silver nanosuspension of *A. polystachya* significantly enhanced the antiradical potential as compared with the methanolic extract of root bark of *A. polystachya.*

* Corresponding Author

Name: Rajashree Gude
Phone: +91-9923035727
Email: rajigude@yahoo.com

ISSN: 0975-7538

DOI: https://doi.org/10.26452/ijrps.v10i2.365

Production and Hosted by

Pharmascope.org

INTRODUCTION

Cancer is a major health problem globally affecting 15% population. It is uncontrolled growth and quick division of the abnormal cells in the body. It is projected that by 2020, the incidence of cancer levels will increase to 15 million cases causing deaths (Gude R. *et al.,* 2016). In the treatment of cancer, many synthetic and chemotherapeutic agents have been developed, that show various side effects. Many of the plants traditionally have reported possessing antitumor activity.

Design and development of herbal nanoparticles have become frontier research in the field of nanotechnology. Development of this novel drug delivery system will help in overcoming various constraints like bioavailability, solubility and stability of the herbal drug (Thirumurugan G. *et al.,* 2014). There are many techniques of synthesising silver nanoparticles. Most of them are expensive or

involve the use of hazardous chemicals. Formulation of nanoparticles has achieved attention as it is efficient, inexpensive and environmentally safe.

The medicinal plant chosen for the work was *A. polystachya* which is a highly valued species for humankind and has been thoroughly investigated for its high potential therapeutic value. The bark of *A. polystachya*has been reported to exhibit a wide range of properties like antioxidant, antitumor, ant hepatic and radioprotective (Shweta SS. *et al.,* 2014).

The root bark of the plant *A. polystachya* is rich in diterpenes, limonoids, lignans, flavonoid, glycosides, chromone, triterpenes, sesquiterpenes and alkaloids which contribute to the antioxidant properties of the plant (Phull AR. *et al.,* 2016).

Extensive work has been done on different parts of the tree, but it was observed that the root bark of the plant had not been explored much (Zang H. *et al.,* 2007). Hence, the present study has been designed to evaluate the anticancer and antioxidant activities of the methanolic extract of the root bark of the plant *A. polystachya* and formulate the extract into silver nanosuspension (Agnihotri VK. *et al.,* 2016; Jain A. *et al.,* 2016).

MATERIALS AND METHODS

Silver nitrate was purchased from Loba Chemie. The root bark of *A. polystachya* was obtained from Mangalore, Dakshina Karnataka, India. The i*n vitro* cytotoxic activity and apoptosis studies were carried out at Deshpande Labs., Bhopal. DPPH (2,2-diphenyl-2-picrylhydrazyl hydrate) was purchased from Molychem, sodium nitroprusside from Loba Chemie. Greiss reagent was prepared using sulphanilamide from Thomas Baker and naphthyethylene diamine from DFCL Labs.

Collection of Plant material and Extract

The root barks of the plant *A. polystachya* were collected, washed and dried. The dried root barks were powdered and sieved. 500g of the powdered drug was taken and exhaustively macerated with methanol. After three days, the methanolic layer was decanted off. The process was repeated three times. The solvent from the total extract was distilled off using a rotary evaporator. The concentrate was evaporated to a thick syrupy consistency and then evaporated to dryness (Gude R. *et al.,* 2016).

Preliminary Phytochemical Investigation: The preliminary phytochemical studies were performed to confirm the availability of different phytoconstituents present in the methanolic extract (Gude R. *et al.,* 2016).

Synthesis of Herbal Mediated Silver Nanoparticles: The 10^{-3} mM Silver nitrate solution was prepared. 10ml of herbal extract was taken in a conical flask separately and to this 90 ml of $AgNO_3$ solution was added. The conical flasks were incubated at room temperature. A colour change of the leaf extracts from pale yellow to dark brown was checked periodically. The brown colour formation indicates that the silver nanoparticles were synthesized from the herbal extract, and they were centrifuged at 5000 rpm for 15 mins to obtain pellets that are used for further study. The supernatant was used for characterisation.

Characterisation of Synthesized Silver Nanoparticles

The silver nanoparticles were characterised with the help of UV-Vis Spectrophotometry, FTIR, EDAX, SEM, TEM, XRD and Thermogravimetric analysis. UV-Vis Spectrophotometry, FTIR, EDAX, SEM studies have been reported in the previously published paper (Gude R. *et al.,* 2016).

In-vitro Cytotoxic Activity

Cytotoxic activity of plant extract was determined by Sulforhodamine B (SRB) assay. The plant extract was initially solubilised in dimethyl sulfoxide to obtain a stock solution of 100mg/ml. The sub-stock solution was prepared with water and stored in the refrigerator before use. At the time of drug addition, 1mg/ml of the frozen aliquot was diluted to get 100, 200, 400 and 800 µg/ml. Aliquots of 10 µl of these different dilutions were added to get the final drug concentration to 10, 20, 40 and 80 µg/ml.

Two human breast cancer cell lines namely MCF-7and MDA-MB-231were seeded at the density of $5x10^3$ cells per well in 96 well plates. After the addition of the extract, the plates were incubated at 37°C for 48 h. The assay was terminated by the addition of cold trichloroacetic acid. The cells were fixed in situ by the gentle addition of 30%w/v TCA (50ul) and incubated for 60min at 4°C. The supernatant was discarded, plates were washed with tap water and air dried. SRB solution (50µl) at 0.4%w/v in 1% acetic acid was added to each well and plates were incubated for 20min at room temperature. The unbound dye was removed by washing with 1% v/v acetic acid. The plates were air dried, and the bound stain was subsequently eluted with 10millimolar trizma base, and absorbance was recorded at 540nm.

Percentage growth was calculated on a plate by plate basis for test wells relative to control wells. Percentage growth was expressed by using the following formula:

$$\frac{Average\ absorbance\ of\ the\ test\ well}{Average\ absorbance\ of\ the\ control\ wells} x\ 100$$

Cell Cycle and Apoptosis Analysis of AgNP

For cytotoxicity assays, the stabilised AgNP was studied under *in vitro* conditions by using colourimetric MTT assay method. The MCF-7 breast cancer cells were grown in Dulbecco Modified Eagle Medium (DMEM), Fetal Calf Serum (FCS) 10% in a T25 flask. Cells were seeded in a 6 well microtiter tissue culture plates and serum starved overnight. Cells were treated with FCS and 40µg/ml of the AgNP for 24 hours. Doxorubicin was used as a positive control. The untreated cells were treated with PBS. After 24hours, the cells were gently trypsinized and washed with Phosphate buffered saline (PBS) twice. Cells were fixed in methanol and stained with 0.1% propidium iodine (SIGMA) and analysed for cell cycle and apoptosis on a flow cytometer (BD FACS Cali bur). Events were detected by flow cytometry on the FL2 channel with the detector in logarithmic mode (FL2-H). Doublet discrimination on the FL2 channel is used to identify single cell events.

Preparation of *Aphanamixis Polystachya* Silver Nanosuspension

Silver Nanosuspension of *A. polystachya* was prepared by the nanoprecipitation method. The prepared *A. polystachya* silver nanoparticles (10mg) were added to sodium lauryl sulphate (0.125%) in 10ml of deionised water with continuous stirring at 500 rpm for 1h. The solvent was allowed to evaporate to obtain a dry nanosuspension (Jahana N. *et al.,* 2015).

Antioxidant Activity: Antioxidant activity on the test samples [methanolic extract of root bark of *A. polystachya* and *A. polystachya* Silver Nanosuspension (AgNS)] were determined using different assays like DPPH Scavenging Activity and Nitric Oxide Radical Scavenging Activity.

DPPH Scavenging Activity: The antioxidant activity was studied on a methanolic extract of root bark of *A. polystachya* and *A. polystachya* Silver Nanosuspension using DPPH (2,2-diphenyl-2-picrylhydrazyl hydrate) assay. The reaction mixture contained 0.012mg of DPPH in methanol and various concentrations of the test samples. The samples were shaken vigorously and kept in the dark for 30 min. Control was prepared using 1ml of DPPH and 2ml methanol and incubated at room temperature in the dark.

The absorbance was measured at 517nm using a UV-Visible Spectrophotometer against the control. The antioxidant activity was calculated by determining % inhibition using the following formula:

$$DPPH\ Scavenging\ Effect\ (\%) = \frac{(Absorbance\ of\ control - Absorbance\ of\ sample}{Absorbance\ of\ control} x\ 100$$

Nitric Oxide Scavenging Activity

The antioxidant activity was studied on a methanolic extract of root bark of *A. Polystachya* and *A. polystachya* Silver Nanosuspension using sodium nitroprusside and Greiss reagent. The test was performed by taking 1ml of the test sample in a dry test tube and adding 1ml of 10mM sodium nitroprusside solution. The mixture was incubated in the dark at room temperature for two hours.

Griess reagent was prepared by mixing the equal volume of 1% sulfanilamide and 0.1% N-1-naphthyl ethylenediamine dihydrochloride. After incubation, 2ml of Griess reagent was added and again incubated for 20 min in the dark. Absorbance was measured at 540nm. The control was prepared using 1ml of nitroprusside and 1ml of methanol.

RESULTS

Phytochemical screening

Preliminary phytochemical screening was done to confirm the presence of phytoconstituents (Gude R. *et al.,* 2016).

Synthesis and characterisation of Nanoparticles of Aphanamixis *Polystachya*

Nanoparticles of *A.polystachya* was synthesised by green synthesis. The same was confirmed by characterisation with UV-Vis Spectrophotometry, FTIR, EDAX, SEM, TEM, XRD and TGA studies and reported in the research paper (Gude R. *et al.,* 2016).

UV-Visible Spectroscopy

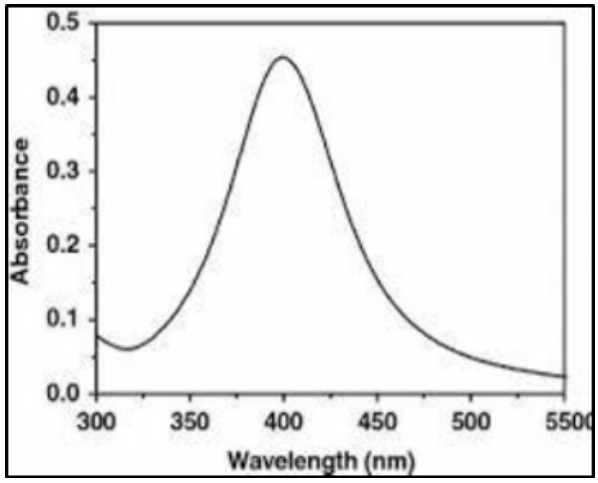

Figure 1: UV-Visible spectra of Synthesized AgNP

The formation of silver nanoparticles was followed by measuring absorbance at a wavelength range from 400–800 nm. The characteristic bands were detected around 400–450 nm. These absorption bands were assumed to correspond to the silver nanoparticles as shown in fig.1 (Gude R. *et al.,* 2016).

Particle Size Analysis

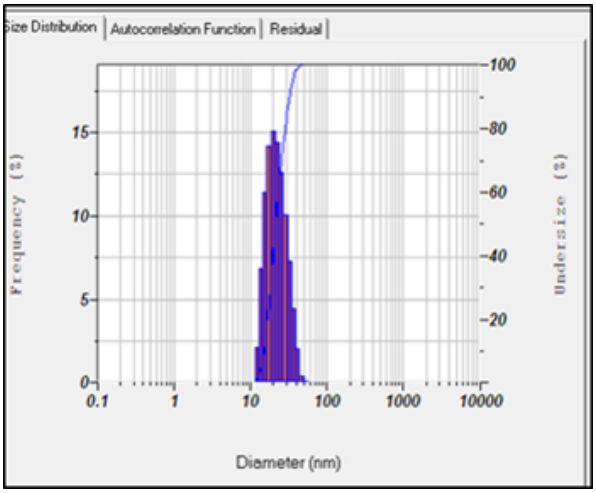

Figure 2: Particle size analysis of AP AgNP

The particle size was analysed using particle size analyser. The particle size was analysed under the category of the intensity of laser light on the sample particle. Laser diffraction revealed that the particles obtained are aggregated mixture with size ranging between nanometres and micrometres as shown in Figure 2. The average particle diameter was found to be 20 nm (Gude R. *et al.,* 2016).

XRD Analysis

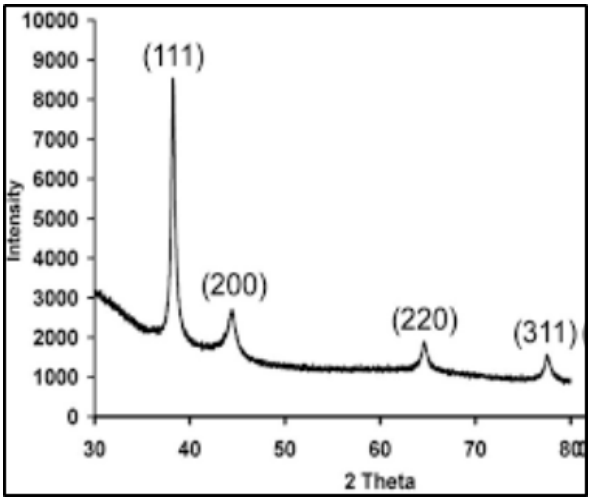

Figure 3: X-ray diffraction pattern for AP AgNP

Figure 3 shows the XRD pattern of powder silver nanoparticles. The presence of peaks at 2θ values 38.1°, 44.09°, 64.36°, corresponds to (111), (200), (220), planes of silver, respectively. Thus, the crystalline structure of silver nanoparticles is evident from the spectrum. No peaks of other impurity crystalline phases have been detected (Gude R. *et al.,* 2016).

FTIR Analysis

FTIR measurement was carried out to identify the biomolecules for capping and stabilisation of the metal nanoparticles synthesized from *A. polystachya*. FT-IR analysis as seen in fig 4 showed that the biosynthesized silver nanoparticles were capped with bimolecular compounds which were responsible for the reduction of silver, the bands were seen at3420.4 cm^{-1}, and 2923.9 cm^{-1} were assigned to the stretching and bending vibrations of secondary amines respectively (Gude R. *et al.,* 2016).

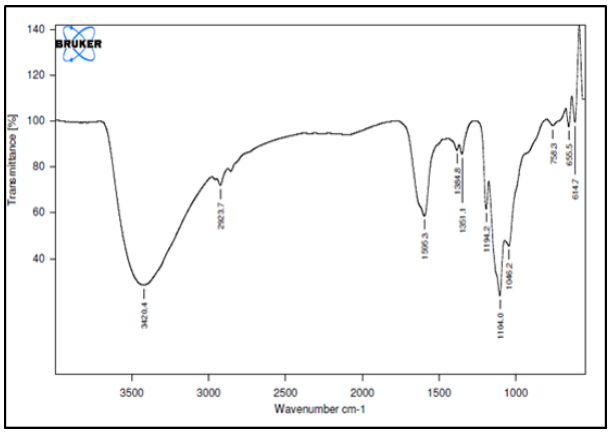

Figure 4: FTIR spectra of the synthesised AgNP

SEM and EDAX Analysis

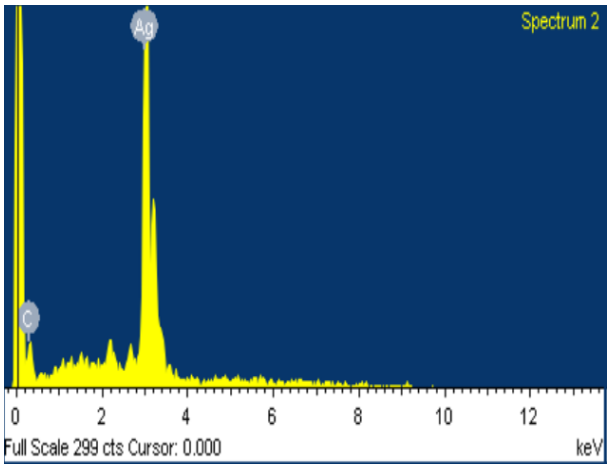

Figure 5: EDAX spectra of synthesised AgNP of A. polystachya

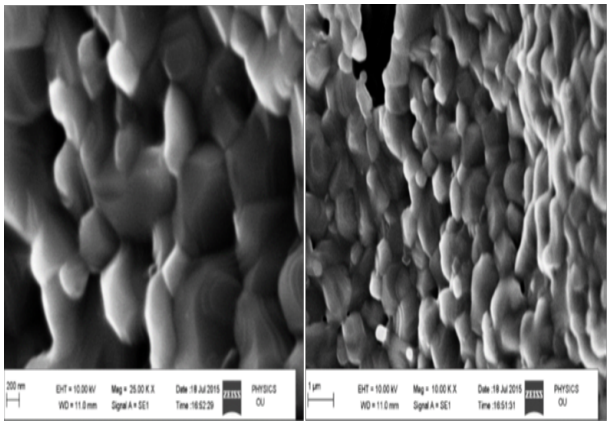

Figure 6: SEM images of AgNP of A. polystachya

The peaks observed index graph at 3.0, 3.2 and 3.4 keV correspond to silver. Therefore, the EDX profile of the sample indicates that the silver

nanoparticles sample contain pure silver, with no oxide (fig.5). Figure 6 shows the SEM images of silver nanoparticles. It exhibits that almost all the nanoparticles were spherical with no agglomeration (Gude R. *et al.,* 2016).

Transmission Electron Microscopy (TEM)

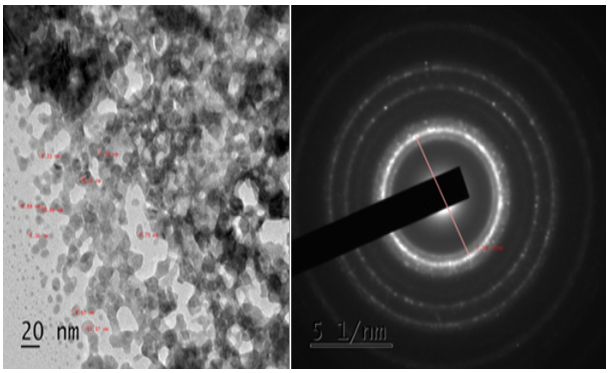

Figure 7: TEM images of AgNP of A. polystachya

The morphology of synthesised AgNP was observed at different resolutions, i.e., 20 nm and 50 nm in TEM (Fig. 7). The TEM images of synthesized nanoparticles confirm that the obtained nanoparticles were at nano-scale. From the images, it is observed that most of the nanoparticles are spherical, and a few agglomerated nanoparticles were also observed. Images also depict that there is a variation in particle size and distribution of size. It may be noted that the average particle size estimated was between 8 nm, and particle size ranges from 7 to 13 nm. The size of these silver nanoparticles conforms with the size of earlier reported biosynthesised nanoparticles.

Atomic Force Microscopy

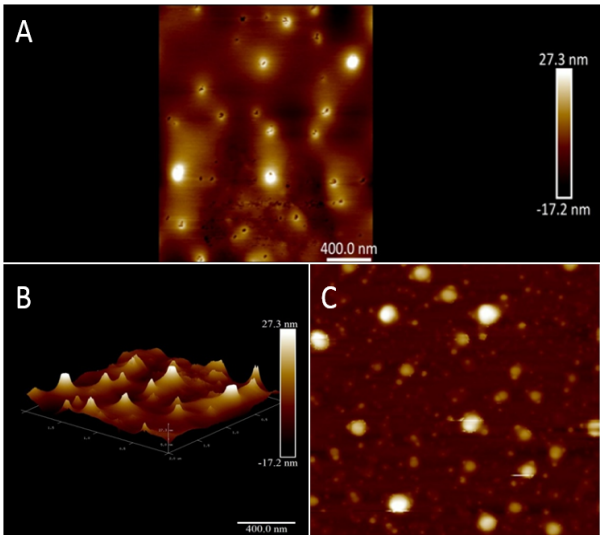

Figure 8: A) Topography of the polymer; B) and C) The formation of layers of three-dimensional spherical clusters

It can be seen in the surface images [Fig: 8(A)] that the topography of the polymer is fairly regular. Figure 8(B) and 8(C) shows the formation of layers of three-dimensional spherical clusters, after metallization, corresponding to silver nanoparticles in the sense of their plasmonic behaviour. The images depict little definition of cluster size for layers less than 5 nm, possibly due to the mobility of silver atoms on the surface of the polymer, the presence of larger clusters is shown and better defined due to a large amount of precursor nanoparticles deposited.

***In-vitro* Cytotoxic Activity**

The cytotoxic effect of methanolic extract of root bark of *A. polystachya* on MCF-7 cells was determined by SRB assay. The percentage of cell growth was found to be 39.8, 21.6, 18.0 and 15.6 at 10, 20, 40 and 80µg/ml. In MDA-MB231 cells, the percentage cell growth was found to be 99.2, 80.0, 67.2 and 54.6 at 10, 20, 40 and 80 µg/ml respectively. Growth inhibition (GI50) of<10µg and>80µg was observed in MCF-7 and MDA-MB231 cell lines respectively. The results obtained in MCF-7 cell lines encouraged us to synthesise AgNP of methanolic extract of root bark of *A. polystachya* and study its effect on cell cycle and apoptosis in human breast cancer cells (MCF-7).

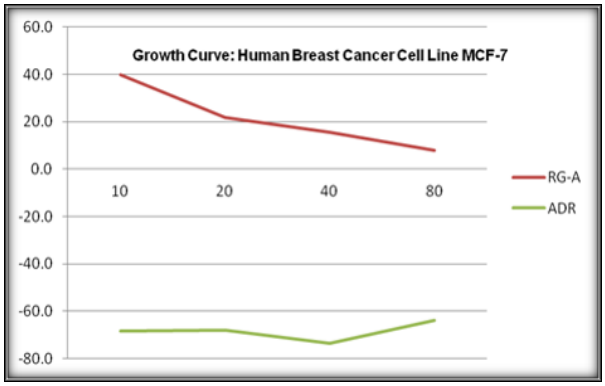

Figure 9: Growth curve on human breast cancer cell line MCF-7

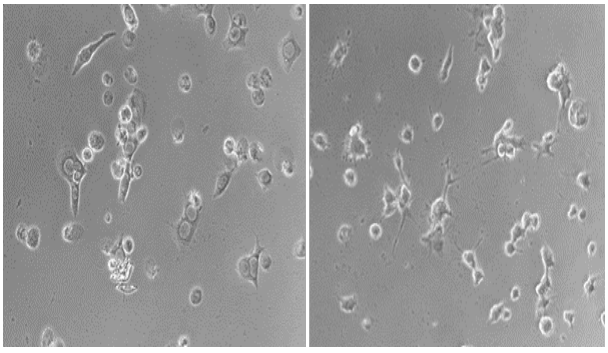

Figure 10: Positive control (Adriamycin) Methanolic extract of root bark of A.polystachya

Cell Cycle and Apoptosis Analysis of AgNP of *A. polystachya*

The cell cycle and apoptosis analysis of AgNP of *A. polystachya* was found to be as shown in graphs (fig. 9, 10,11). Untreated sample G2 was 18.43,

Table 1: Results of % Control growth on human breast cancer cell line MDA-MB-231

Drug Concentrations (µg/ml)	Experiment 1				Experiment 2			
	10	20	40	80	10	20	40	80
RG-A	81.5	53.7	48.8	52.8	84.1	53.7	46.6	47.9
ADR	-2.6	-27.0	-21.3	2.6	5.1	1.0	-4.6	8.7

n= 3 (3 experiments performed)

Table 1: Results of % Control growth on human breast cancer cell line MDA-MB-231 (Contd...)

Drug Concentrations (µg/ml)	Experiment 1				Experiment 2			
	10	20	40	80	10	20	40	80
RG-A	131.9	132.5	106.1	63.0	99.2	80.0	67.2	54.6
ADR	-3.9	-11.3	-17.8	1.9	-0.5	-12.4	-14.6	4.4

n= 3 (3 experiments performed)

doxorubicin was 1.5, and the test sample was 13.62 which indicated that the apoptosis in the test sample G2M cells is higher than doxorubicin.

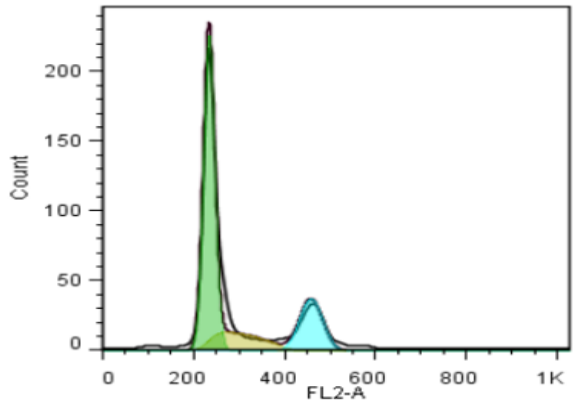

Figure 11: Untreated Sample

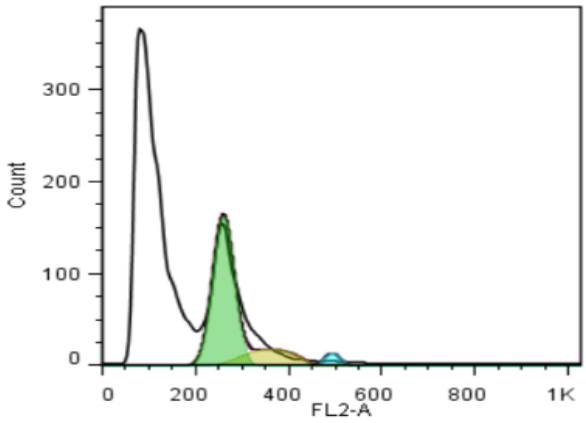

Figure 12: Doxorubicin Standard

Scavenging Activity

Two antioxidant assays were used to determine the antioxidant activity of the extract of root bark of A. *polystachya* and formulated silver nanosuspension.

Results of two assays (DPPH, Nitric oxide) were reported. Table 2 shows the IC_{50} value that indicates the concentration of antioxidant required to neutralise 50% of free radicals. The lower value of IC_{50} indicates high inhibitory effect. DPPH scavenging activity is a well-known method which helps to determine the antioxidant potential of medicinal plants in a short period. On determining the scavenging activities on the methanolic extract of root bark of A. *polystachya* and the formulated nanosuspension, it was observed that the nanosuspension of *A. polystachya* exhibited the minimum IC_{50} value compared to that of the extract.

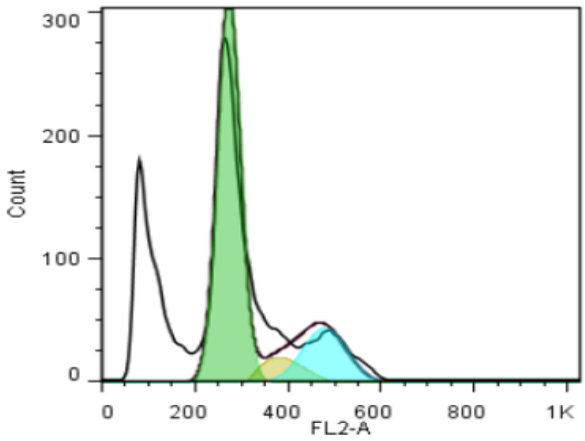

Figure 13: Test Sample

Nitric oxide radical scavenging potential to extract the root bark of A. *polystachya* and its formulated nanosuspension was determined by the generation of nitric oxides radical *in vitro* by sodium nitroprusside. The free radicals lead to the production of nitrite ions by reacting with oxygen. Nitric oxide scavengers compete with oxygen and thereby diminish the formation of nitrites ions.

Table 2: IC50 Values of Aphanamixis Polystachya extract and formulation

Sample	IC_{50} Value (µg/ml)	
	DPPH Scavenging Activity	Nitric Oxide Scavenging Activity
AP Extract	300.36	598.01
AP Nano suspension	8.36	4.71

DISCUSSION

Green Synthesis is an easy method to synthesize silver nanoparticles from the root barks of *Aphanamixis Polystachya*. The synthesized nanoparticles were characterised and found that the methanolic extract was a good source for the formation of nanoparticles. Nanoparticles are a promising drug delivery system for increasing the bioavailability of poorly soluble herbal drugs. The extract of root bark of *Aphanamixis Polystachya* was used to synthesize silver nanoparticles and subsequently formulated into silver nanosuspension.

Anti-cancer drugs show cytotoxicity and induce apoptosis in cancer cells as they are designed to eliminate rapidly proliferating cancerous cells. Apoptosis is a highly organised cell death process characterised by loss of plasma membrane phospholipid asymmetry, enzymatic cleavage of the DNA into oligonucleosomal fragmentation and segmentation of the cells into membrane-bound apoptotic bodies. The current study investigated the induction of apoptosis in breast cancer cells upon treatment with silver nitrate particles of the methanolic extract of *A. polystachya*. A number of anti-cancer drugs are known to act by blocking cell cycle. Cancer cell cycle specific drugs has drawn considerable attention as they act on specific cancer cell cycle checkpoints (G_0/G_1 phase and G_2M phase) and inhibit cancer cell proliferation (G_0/G_1 phase arrest) or mitosis (G_2M phase arrest). We have investigated the cell cycle pharmacological specific effects of AgNP of *A. polystachya* against human breast cancer cells by using flow cytometry. The data revealed that the methanolic AgNP of *A. polystachya* caused a significant arrest of cells at G_2M phase higher than Doxorubicin. These data suggest that methanolic extract of AgNP of *A. polystachya* act by cell cycle specific mechanism inducing mitotic arrest and apoptosis in breast cancer cells.

Silver nanosuspension of *Aphanamixis polystachya* showed freer radical scavenging activity than its crude extract. Also, it was observed that silver nanosuspension of *Aphanamixis polystachya* exhibited better scavenging activity using nitric oxide assay than DPPH assay.

The antioxidant activity of the extract and nanosuspension of *A. polystachya* is due to the presence of polyphenolic compounds such as flavonoids and tannins. This may be attributable to the hydrogen or electron donating ability of the groups present in the structure.

CONCLUSION

The results indicated anticancer activities of AgNP of *A. Polystachya* was higher on MCF-7 breast cancer cell line. Therefore, the extract of root bark of A. *Polystachya* containing silver nanoparticles might be a potential alternative agent for human breast cancer therapy.

The potential zeta studies indicated that the biosynthesized AgNPs possess long-term stability. It can be concluded that silver nanosuspension of *Aphanamixis Polystachya* significantly enhanced the antiradical potential as compared with its crude extract. Biological synthesis of silver nanoparticles has increased its importance in an eco-friendly, cost-effective and stable manner.

Acknowledgement

The authors wish to thank Goa College of Pharmacy, Govt. of Goa for the facility provided to carry out the work. The authors also wish to thank Deshpande Labs, Bhopal, Madhya Pradesh for conducting cytotoxic and apoptotic studies on the root bark extract and silver nanoparticles of *A. polystachya* and ACTREC, Tata Memorial Centre, Navi Mumbai' for their anti-cancer drug screening facility (ACDSF).

Author Contribution

Mrs Rajashree Gude carried out the actual research work as mentioned in the manuscript. Dr Arun B. Joshi and Dr Anant Bhandarkar guided and assisted Mrs Rajashree Gude in carrying out the research activities.

REFERENCES

Abdul Qaiyum Ansari et al.; European Jour of Exp Biology, 2013, 3:502-7.

Abdul-Rehman Phull et al.; Future Jour of Pharm Sciences, 2016; 2:31-6.

Agnihotri VK, Srivastava SD, Srivastava SK. A new limonoid, amoorinin, from the stem bark of *Amoora rohituka*. Planta Med, 1987;53:298–9.

Ajaz, Ajazuddin & Saraf, Shailendra; Fitoterapia,2010; 81:680-9.

Chatterjee A, Kundu AB, Chakrabortty T, Chandrasekharan S. Extractives of A*phanamixis polystachya* wall (Parker). Tetrahedron, 1970;26:1859–67.

G. Mahendran et al.; Food Sci and Human Wellness, 2016;5:207–18.

G. Rajasekhar Reddy et al.; Asian Jour of Chemistry,2013;25:9249-54.

Gloria Aderonke Otunola et al; Pharmacogn Mag ,2017; 13(Suppl 2): 201–8.

http://www.who.int/mediacentre/news/releases/2003/pr27/en/.

Jain A, Srivastav SK. 8-C-Methyl-Quercetin-3-0-P-D-Xylopyranoside, A new flavone glycoside from the roots of *Amoora rohituka*. J Nat Prod, 1985;48: 299–301.

Jay Vyas, Shafkat Rana, Antioxidant Activity and Biogenic Synthesis of Selenium Nanoparticles using the leaf extract of *aloe vera*, Int Jour of Current Pharma Research; 2017;9: 147-52.

M. Pandya et al; Dhaval. Der Pharmacia Lettre; 2011; 3:129-40.

Md. Masud RM et al.; Arabian Jour of Chem; 2015.

Md. Nur Alam et al; Saudi Pharm Jour, 2013; 21: 143–52.

Mishra AP, Sarla Saklani, Subhash Chandra, Abhishek Mathur, Luigi Milella, Priyanka Tiwari., *Aphanamixis polystachya* (wall.) Parker, Phytochemistry, Pharmacological properties and medicinal uses: An overview; World Jour of Pharmacy and Pharm Sciences, 2014;3: 2242-52.

Mitiku AA and Belete Yilma; African Jour of Biotech, 2017;16:1705-16.

Mohamed S. Abdel-Aziz et al.; Jour of Saudi Chem Society,2014;18:356–63.

Nazish Jahana et al; Jour of Experimental Nanoscience, 2015.

Patil SP and Kumbhar ST; Biochem and Biophysics Reports, 2017; 10:76–81.

R Gude; AB Joshi; A Bhandarkar; A Shirodker; S Bhangle, Synthesis and characterisation of silver nanoparticles from the roots of *aphanamixis polystachya*, World Jour of Pharm Research, 2016;5:1399-1408.

Saklani Sarla et al; Int J Drug Dev & Research,2011; 3:271-4.

Sarker AA, Chowdhury FA, Farjana Khatun., Phytochemical Screening and In vitro Evaluation of Pharmacological Activities of *Aphanamixis polystachya* (Wall) Parker Fruit Extracts; Tropical Jour of Pharm Research, 2013;12:111-6.

Saumya SM & Mahaboob Basha P; Int Jour of Pharmacy and Pharm Sciences, 2011; 3:165-9.

Shweta SS, Rani WC, Tapadiya GG, Khadabadi SS. *Aphanamixis polystachya* (wall.) Parker - An Important Ethnomedicinal Plant. Int J Pharm Sci Rev Res,2014; 24: 25-8.

Soumya Menon, Happy Agarwal, S. Rajesh Kumar, S. Venkat Kumar. Green synthesis of silver nanoparticles using medicinal plant *Acalypha indica* leaf extracts and its application as an antioxidant and antimicrobial agent against foodborne pathogens, Int Jour of Applied Pharma,2017; 9: 42-50.

Thilagavathi. T et al., Int J Pharm Bio Sci, 2016; 7:201 –5.

Thirumurugan G, et al.; Nanotechnology: an effective tool for enhancing bioavailability and bioactivity of phytomedicine, Asian Pac J Trop Biomed,2014;4 Suppl 1: 1–7.

Upendra Nagaich et al., Jour of Pharmaceutics, 2016:1-8.

Valan MF, Isolation and characterisation of the active principle from the bark of *Aphanamixis polystachya*; Asian Jour of Pharm Research, 2014;4:19-23.

Yugal K. Mohanta et al; Frontiers in Molecular Biosciences, 2017;4:1-9.

Zhang H, Chen F, Wang X, Wu D, Chen Q. Complete assignments of 1H and 13C NMR data for rings A, B-seco limonoids from the seed of *Aphanamixis polystachya*. Magn Reson Chem, 2007;45:189–92.

IJPSR (2020), Volume 11, Issue 11 (Research Article)

INTERNATIONAL JOURNAL OF PHARMACEUTICAL SCIENCES AND RESEARCH

Received on 18 October 2019; received in revised form, 04 February 2020; accepted, 04 March 2020; published 01 November 2020

ISOLATION AND CYTOTOXIC POTENTIAL OF SILVER NANOSUSPENSION OF THE ROOTS OF *APHANAMIXIS POLYSTACHYA*

R. Gude *, A. Joshi, A. Bhandarkar and D. Mayenkar

Goa College of Pharmacy, 18th June Road, Panaji - 403001, Goa, India.

Keywords:

Aphanamixis Polystachya, Isolation, Herbal mediated Silver Nanosuspension, SRB Assay, cytotoxic activity

Correspondence to Author:
R. Gude

Associate Professor,
Goa College of Pharmacy, 18th June Road, Panaji - 403001, Goa, India.

E-mail: rajigude@yahoo.com

ABSTRACT: Objective: The study was aimed to isolate the components from the methanolic extract of the root bark of *Aphanamixis polystachya* and to confirm their potential cytotoxicity of the methanolic extract, silver nanoparticles and silver nanosuspension of the root bark of *A. polystachya*. **Method:** Isolation from the methanolic extract of root barks of *A. polystachya* were performed using column chromatography technique. Cytotoxic activity on MCF-7 and MDA-MB cell lines by SRB Assay was conducted on silver nanosuspension of *A. polystachya*. **Results:** The components isolated from methanolic extract of root bark of *A. Polystachya* by column chromatography were confirmed as Rohituka 7, Rohituka 3, Amoorinin-3-o-α-l-Rhamnopyranosyl-(1→6)–β-D-Glucopyra-noside and 8-Methyl-7, 2′,4′-tri-O-Methylflavonone-5-O-α-L-Rhamnopyranosyl (1→4)-β-D- glucopyranosyl-(1→6)-β-D-glucopyranoside on the basis of IR, ^{1}HNMR, ^{13}C NMR and MS. The prepared silver nanosuspension, tested in concentrations ranging between 500-7.81 µM showed IC_{50} value at 0.58 µM in MCF-7 cell line, and IC_{50} in MDA-MB cell line being greater than 1000µM. **Conclusion:** Column chromatography of the methanolic extract of root barks of *A. polystachya* led to the isolation of Rohituka 7, Rohituka 3, Amoorinin-3-O-α-L-Rhamnopyranosyl-(1→6)–β-D Glucopyranoside and (methyl-7,2′,4′-tri-O-methyl flavonone-5-O-α-L-rhamnopyranosyl(1→4)-β-D-glucopyranosyl-(1→6)-β-D-glucopyranoside. SRB Assay confirmed that silver nanosuspension of *A. polystachya* to be potentially cytotoxic. The isolated components have already proven to possess cytotoxic activity. Hence, the study suggests that silver nanosuspension exhibited better cytotoxic activity.

INTRODUCTION: Cancer is a major health problem globally, affecting 15% of the population. It is an uncontrolled growth and quick division of the abnormal cells in the body. It is projected that by 2020, the incidence of cancer levels will increase to 15 million cases, causing deaths [1].

QUICK RESPONSE CODE

DOI: 10.13040/IJPSR.0975-8232.11(11).5766-74

This article can be accessed online on www.ijpsr.com

DOI link: http://dx.doi.org/10.13040/IJPSR.0975-8232.11(11).5766-74

In the treatment of cancer, many synthetic and chemotherapeutic agents have been developed, having various side effects. Many of the plants traditionally have reported possessing antitumor activity [1].

The medicinal plant chosen for the work is *A. polystachya*, which is a highly valued species for mankind and has been thoroughly investigated for its high potential medicinal value [2]. The design and development of herbal nanoparticles have become frontier research in the field of nanotechnology. Development of this novel drug delivery system will help in overcoming various constraints like

bioavailability, solubility and stability of the herbal drug [3]. The present study is to isolate the components from the methanolic extract of the root bark of the plant *A. polystachya* having potential cytotoxic activity. The extract was formulated into silver nanoparticles and subsequently into silver nanosuspension and assessed for cytotoxic activity by SRB method.

MATERIALS AND METHODS:

Authentication of the Plant: The root bark of *A. polystachya* were identified and obtained from Mangalore, Dakshina Karnataka, India. The plant part was identified and authenticated by Dr. Gopal Krishna Bhatt, Poorna Prajnya College Udupi-Karnataka, India, and Dr. Dinesh Nayak, Mangalore-Karnataka, India bearing number: GCP.Pharmacog.05/2013. The herbarium was deposited in the Department of Pharmacognosy, Goa College of Pharmacy.

Description of the Plant: *A. polystachya* is an evergreen medium-sized tree with a dense spreading crown and a straight cylindrical bole up to 15m in height and 1.5-1.8 m in width belonging to the family Meliaceae. In Sanskrit, it is known as Anavallabha, Ksharayogya, Lakshmi, Lakshmivana, Lohita [4].

Kingdom	:	Plantae
Phylum	:	Magnoliophyta
Class	:	Magnoliospida
Order	:	Sapindales
Family	:	Meliaceae
Genus	:	Aphanamixis
Species	:	*Aphanamixis polystachya*
Botanical Name	:	*Aphanamixis polystachya* (Wall) R.N. Parker
Synonyms	:	*Algaia polystachya* Wall & *Amoora rohituka* (Roxb.) Wt. & Arn.

Distribution: *A. polystachya* is native to temperate Asia, tropical China, Indian subcontinent-Peninsula, Northeast India, Bhutan, Sri Lanka, Myanmar, Thailand, Malaysia, Indonesia, Papua, New Guinea, and the Philippines. In India, it is found distributed in the Sub-Himalayan tract from the Rapti river eastwards, Sikkim up to 6000 ft., Assam, Burma, Chota Nagpur, Konkan, W. Ghats, and adjoining hill ranges from the Poona district southwards to Tinnevelly up to 3500 ft [5].

General Experimental Procedure: Roots, along with the bark, were collected, washed, and dried in the shade. The dried material was then powdered (500 g) and exhaustively extracted by maceration with 3 liters of methanol for 3 days. After 3 days, the methanolic layer was decanted off. The process was repeated thrice. The solvents from the total extract were distilled off using a rotary vacuum evaporator (Roteva) and concentrated to a syrupy consistency and then evaporated to dryness (150g).

Preliminary Phytochemical Screening (Qualitative Analysis): The preliminary phytochemical studies were performed to confirm the availability of different phytoconstituents present in the methanolic extract [2, 6].

Synthesis of Herbal mediated Silver Nanoparticles of *A. polystachya*: The 10^{-3} mM Silver nitrate solution was prepared. 10 ml of herbal extract was taken in 250 ml conical flask/ beakers separately, and to this 90 ml of $AgNO_3$ solution was added. The conical flasks were incubated at room temperature. A color change of the leaf extracts from pale yellow to dark brown was checked periodically. The brown color formation indicates that the silver nanoparticles were synthesized from the herbal extract, and they were centrifuged at 5000 rpm for 15 min in order to obtain the pellet that is used for further study. The supernatant was used for characterization [6].

Extraction and Isolation of Components from the Methanolic extract of the Roots of *A. polystachya*: The methanol soluble fraction (150g) was suspended in 1.5 L of water and extracted with petroleum ether (60:80) to remove the fatty components completely. The defatted crude extract was further partitioned with chloroform (3 × 1L) to give a chloroform soluble fraction (90g). 90g of chloroform fraction was mixed with silica gel (30g, #60-120). The sample was loaded on a column packed with 500g of silica gel (Molychem, #60 × 120) prepared in petroleum ether (60-80). The column was subjected to elution with different solvent system starting first with 100% petroleum ether followed by petroleum ether: ethyl acetate graded mixtures (95:5, 90:10, 80:20, 70:30, 50:50), 100% ethyl acetate and finally with graded mixtures of ethyl acetate: methanol (99:1, 98:2, 97:3, 96:4, 95:5).

The elutions were monitored by TLC (silica gel G, visualization by UV at 254nm, 366nm and vanillin sulphuric acid reagent heated at 110 °C). Each time 10ml of elutes were collected and identical elutes were combined (TLC monitored) and concentrated to 5ml and kept aside. The elutions carried out with petroleum ether: ethyl acetate (90:10 to 50:50) resulted in 4 fractions containing mixture of compounds and having identical R_f values (7g).

7g was mixed with flash grade silica (3g, #200-400) using mortar and pestle. This mixture was subjected for rechromatography with column (1ft in length and 2cm i.d.). The sample was loaded onto a column packed with 150g of flash grade silica (Molychem, #60 × 120). The mixture was loaded onto this column and the elutions were carried out with 100% petroleum ether, petroleum ether: ethyl acetate graded mixture (90:10, 85:50, 80:20, 75:25, 70:30, and 65:35). The elutions were monitored by TLC (silica gel G, visualization by UV at 254nm, 366nm and vanillin sulphuric acid reagent heated at 110 °C). Each time 10ml of the elutes were collected and identical elutes were combined (TLC monitored) and concentrated to 5ml and kept aside. The elutions carried out with petroleum ether: ethyl acetate (80:20) resulted in a single spot on TLC prepared in petroleum ether (80:20).

After removing the solvent, a light yellow solid was obtained which was designated as RG-APE2 (78mg). The elutions carried out with petroleum ether: ethyl acetate (65:35) resulted in a single spot on TLC prepared in petroleum ether: ethyl acetate (65:35). After removing the solvent, a light-yellow solid was obtained which was designated as RG-APE1 (74 mg). Elutions carried out with 100% ethyl acetate, ethyl acetate: methanol (99:1 and 98:2) resulted in a mixture of compounds having identical R_f values [TLC monitored, ethyl acetate: methanol (98:2)]. After removing the solvent, a light brown amorphous powder resulted (185 mg).

Purification of Compounds using Flash Chromatography (Combi Flash Chromatograph): 185 mg of the powder was taken and mixed by triturating with flash grade silica (600 mg, #200-400) using mortar and pestle. Pre-packed silica column (Redisep RF, 1 gm) was used. All the parameters were set and monitored using peak track software.

The compounds which are UV absorbing *i.e.* at 254 nm and 366 nm, are only detected by flash chromatography. The elutions were carried out with ethyl acetate: methanol (98:2) and collected in a test tube. Each time, 8ml of elutes were collected and identical elutes were combined (TLC monitored, ethyl acetate: methanol 98:2), concentrated and kept aside. The test tubes from 3-18 resulted in a single spot on TLC (ethyl acetate: methanol, 98:2).

After removing the solvent, light brown flakes resulted and the compound was designated as RG-APE3 (68 mg). The test tubes from 22-44 resulted a single spot on TLC (ethyl acetate: methanol, 98:2). After removing the solvent, it resulted in a light yellow powder and the compound was designated as RG-APE4 (77 mg). The elutions carried out with other solvent systems resulted a mixture of compounds or resinous mass, which were not processed further.

Preparation of Silver Nanosuspension of *A. polystachya*: Silver Nanosuspension of *A. polystachya* (AgNS) was prepared by nano-precipitation method. The prepared *A. polystachya* silver nanoparticles (10 mg) were added to sodium lauryl sulphate (0.125%) in 10 ml of deionised water with continuous stirring at 500 rpm for 1 h. The solvent was allowed to evaporate to a dry nanosuspension [7].

Cytotoxic Assay of Nanosuspension of *A. polystachya*: The IC_{50} of AgNS was determined by performing the Sulforhodamine B (SRB) Assay for cytotoxicity. The SRB assay was performed according to the described method [7, 8, 10] with slight modifications using concentrations of compounds ranging from 500-7.81 µM.

Absorbance was read at 540 nm on a scanning multi-well plate reader (EL × 800, BioTek Instruments Inc., Winooski, VT, USA), the percentage cell viability was calculated using excel sheet and IC_{50} values were determined using graph pad prism. All the experiments were conducted in triplicates. The percentage cell death was calculated using the formula:

% Cell death = [(OD of control − OD of test) / (OD of control)] × 100

Characterization of Isolated Compounds:
Spectral Data:

RG-APE 1: Light yellow solid; R_f = 0.060 (solvent system $CHCl_3$: EtOAc 80:20); m.p.: 123 °C;

IR (KBr): 3334.92 cm^{-1}, 2924.25 cm^{-1}, 1724.36 cm^{-1}, 1442.75 cm^{-1}, 1377.17 cm^{-1}, 1132.21 cm^{-1}.

^{1}HNMR ($CDCl_3$): δ 7.5509 (d, 1H, H-1), δ 6.4724 (s, 1H, H-2), δ 2.1816 (d, 1H, H-5), δ 2.5108 (s,1H, H-6),δ 3.1835 (s, 1H, H-9), δ 5.1943 (s,1H, H-11),δ 5.8707 (t,1H, H-12), δ 5.5848 (d,1H, H-13), δ 2.0304 (t,1H, H-16), δ 3.7364 (t,1H, H-17), δ 0.9843 (s, 3H, H-18), δ 1.0638 (s,3H, H-19), δ 7.3975 (d,1H, H-21), δ 6.8561 (s, 1H, H-22),δ 7.3869 (s, 1H, H-23), δ 1.6665 (s,3H, H-28),δ 4.8607 (d, 1H, -H29), δ 5.2234 (s, 1H, H-30), δ 3.4367 (s, 1H, H-2'), δ 1.4091 (s, 1H, H-3'), δ 1.2339 (d, 1H, H-4'), δ 0.7841 (t, 1H, H-5'), δ 0.8359 (d, 3H, H-3'-Me),δ 8.1664 (s, 1H, COOH), δ 2.0470 (s, 3H, CH_3COO).

^{13}CNMR ($CDCl_3$): δ 153.08 (C-1), δ 122.42 (C-2), δ 169.0 (C-3), δ 81.93 (C-4), δ 74.06 (C-5), δ 31.25 (C-6), δ 174.83 (C-7), δ 138.50 (C-8), δ 50.70 (C-9), δ 39.55 (C-10), δ 74.06 (C-11), δ 80.37 (C-12), δ 61.20 (C-13), δ 81.90 (C-14),δ 72.30 (C-15), δ 39.34 (C-16), δ 39.14 (C-17), δ 11.53 (C-18), δ 28.67 (C-19), δ 123.05 (C-20) δ 110 (C-22), δ 143.0 (C-23), δ 28.90 (C-28), δ 74.06 (C-29), δ 119.30 (C-30), δ 174.83 (C-1'), δ 74.06 (C-2′), δ 39.01.25 (C-3′), δ 22.06 (C-4′), δ 11.39 (C-5′), δ 15.30 (C-3′-Me), δ 150.08 (C-HCOO), δ 159.08 (C-CH_3COO), δ 20.7 (C-CH_3COO).

Mass Spectra: (LC-MS): $C_{35}H_{44}O_{13,}$ mol. wt: 672; LC-MS (m/z): 672.16 $(M+)^+$. The other peaks appeared at 672.27, 643.28, 511.20, 451.18, 433.17, 339.12, 269.12, 165.07, 152.08. From the m.p, IR, ^{1}HNMR, ^{13}CNMR, and MS, compound RG-APE1 was designated as Rohituka 7.

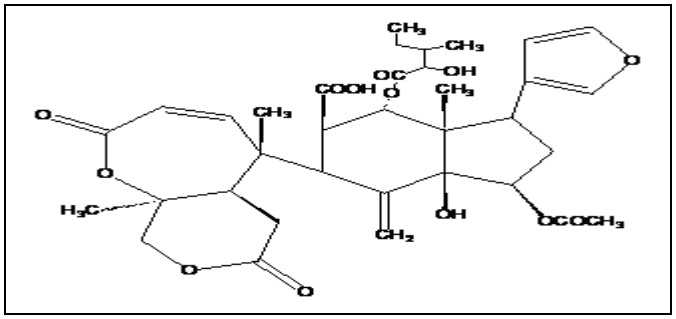

FIG. 1: CHEMICAL STRUCTURE OF RG-APE1 (ROHITUKA 7)

RG-APE2: Light yellow solid; R_f value: 0.065 (solvent system $CHCl_3$: EtOAc 80:20); m.p.: 122.4 °C; positive response for Liebermann- Burchard test for triterpenoids.

IR (KBr): 3389.10 cm^{-1}, 2931.25 cm^{-1}, 1741.57 cm^{-1}, 1448.90 cm^{-1}, 1379.09 cm^{-1}, 1031.08 cm^{-1}.

^{1}HNMR ($CDCl_3$): δ 3.7364 (t, 1H, H-1), δ 2.9528 (d, 1H, H-2), δ 2.3029 (d 1H, H-5), δ 2.8218 (m, 1H, H-6), δ 3.1835 (s, 1H, H-9), δ 4.8607 (s, 1H, H-11), δ 5.8708(t,1H, H-12), δ 2.841, 2.3360 (t,1H, H-16), δ 3.7277 (t,1H, H-17), δ 0.8596 (s,1H, H-18), δ 1.1986 (s, 3H, H-19), δ 7.3975 (d,1H, H-21), δ 6.4724 (s,1H, H-22), δ 7.5509 (s, 1H, H-23),δ 1.6665 (s, 1H, H-28), δ 4.9521, 3.7227 (t,1H, H-29),δ 6.8561(s, 1H, H-30), δ 3.4367 (s, 1H, H-2'), δ 1.7908 (d, 1H, H-3'), δ 1.1606, 0.9428 (t, 1H, H-4'), δ 0.6985 (s, 1H, H-5'), δ 0.8934 (t, 3H, H-3'-Me).

^{13}CNMR ($CDCl_3$): δ 78.26 (C-1), δ 28.98 (C-2), δ 167.06 (C-3), δ 80.37 (C-4), δ 39.34 (C-5), δ 31.25 (C-6), δ 169.86 (C-7), δ 123.05 (C-8), δ 54.70 (C-9), δ 50.70 (C-10), δ 74.06 (C-11),δ 78.26 (C-12), δ 39.55 (C-13), δ 81.93 (C-14),δ 204.08 (C-15), δ 39.14 (C-16), δ 28.67 (C-17), δ 15.30 (C-19), δ 119.32 (C-20), δ 139.55 (C-21) δ 111.22 (C-22), δ 143.20 (C-23), δ 22.06 (C-28), δ 74.06 (C-29), δ 122.42 (C-30), δ 174.83 (C-1'), δ 74.06 (C-2′), δ 31.25 (C-3′), δ 20.70 (C-4′), δ 11.39 (C-5′), δ 11.53 (C-3′-Me).

Mass Spectra (LC-MS): $C_{32}H_{40}O_{11}$, Mol. wt: 600, $(M+)^+$. The other peaks appeared at 599.36, 557.35, 497.33, 479.32, 407.26, 189.07, 152.06. From the m.p, IR, ^{1}HNMR, ^{13}CNMR and Mass spectra, compound RG-APE2 was designated as Rohituka 3.

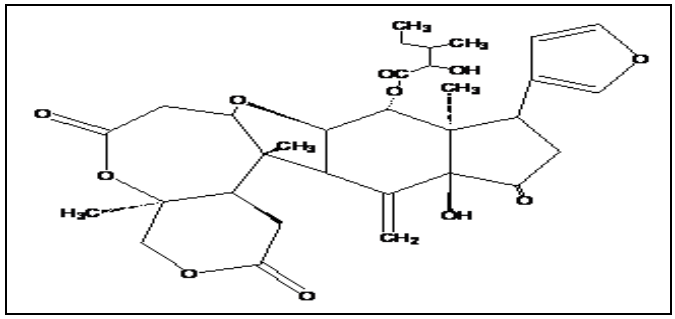

FIG. 2: CHEMICAL STRUCTURE OF RG-APE2 (ROHITUKA 3)

RG-APE3: Light brown flakes; R_f value: 0.371 (solvent system 100% EtOAc); m.p.: 189 °C;

positive response for Molisch's test for carbohydrates and belongs to the limonoid class.

IR (KBr): 3456.11 cm^{-1}, 1745.0 cm^{-1}, 1641.22 cm^{-1}, 820.39 cm^{-1}, 860.37 cm^{-1}, 1244.4 cm^{-1}, 893.29 cm^{-1}, 820.39 cm^{-1}

^{1}HNMR (DMSO): δ 0.96 - δ 1.05 (s, 12H, H-18, H-19,H-24, H-25), δ 1.06, 1.33, 1.40,1.17 (s,4H, H-11,12), δ 2.26(d,1H, H-5), δ 2.27 (s,2H, H-6),δ 2.28 (s,1H, H-9), δ 3.39 (s,1H, H-3),δ 3.78 (s,3H, H-27), δ 4.88 (s,1H, H-15),δ 4.91, δ 5.09 (each s,2H H-26), δ 5.63 (s,1H, H-17), δ 5.68 (s,1H, H-1),δ 5.86 (s,1H, H-2,), δ 6.43-δ 7.59 (m,3H, H-21,22,23 of furan), δ 1.27 (s, 3H, H-6″), δ 3.80- δ 4.49(m, 4H, H-2′,3′,4′5′), δ 4.52 (s,1H, H-1″), δ 4.54- δ 4.68(m,4H, H-2″,3″,4″,5″),δ 4.70-4.87 (m,6H, H-2′,3′,4′,2″,3″,4″-OH), δ 4.93 (s,2H, H-6′), δ 5.13 (s,1H, H-1′).

^{13}CNMR (DMSO): δ 136.14 (C-1), δ 124.59 (C-2), δ 105.44 (C-3), δ 37.51 (C-4), δ 39.93 (C-5), δ 39.51 (C-6), δ 172.93 (C-7), δ 149.50 (C-8), δ 40.14 (C-9), δ 28.96 (C-10),δ 27.21 (C-11), δ 28.96 (C-12), δ 39.72 (C-13),δ 78.50 (C-14),δ 59.64 (C-15), δ 170.14 (C-16), δ 86.50 (C-17), δ 11.41 (C-18), δ 14.00 (C-19), δ 120.14 (C-20) δ 101.59 (C-21), δ 140.16 (C-22) δ 142.93 (C-23), δ 20.66 (C-24), δ 20.41 (C-25), δ 114.14 (C-26) δ 49.85 (C-27), δ 110.16 (C-1′), δ 90.50 (C-2″), δ 70.14 (C-3′), δ 79.03 (C-4′), δ 79.16 (C-5′) δ 39.30 (C-6′), δ 112.12 (C-1″) ,δ78.83 (C-2′) δ 87.59 (C-3″), δ 88.03 (C-4″) δ 68.16 (C-5″), δ 15.44 (C-6″).

Mass Spectra (ESI-MS): $C_{39}H_{54}O_{16}$, mol.wt.: 778.84, 778.1 $(M+)^{+}$. The other peaks appeared at 712.4, 677, 623.3, 560.4, 482, 390.7, 278.8, 144.9.

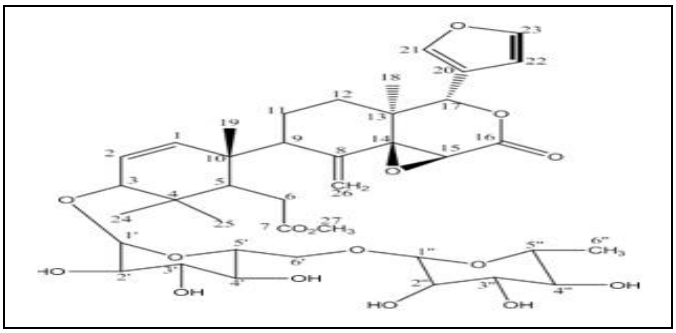

FIG. 3: CHEMICAL STRUCTURE OF COMPOUND RG-APE3(Amoorinin-3-O-α-L-Rhamnopyranosyl-(1,6) –β-D- Glucopyranoside)

From the m.p., IR, ^{1}HNMR, ^{13}CNMR, and MS, compound RG-APE3 was designated as Amoorinin-3-O-α-L-Rhamnopyranosyl–(1→6) –β-D-Glucopyranoside.

RG-APE4: Yellow Solid; R_f value: 0.06 (solvent system $CHCl_3$: EtOAc 60:40); m.p.: 212 °C; positive test for flavanone glycoside.

IR (KBr): 3447.18 cm^{-1}, 2963.12 cm^{-1}, 2877.24 cm^{-1}, 1644.29 cm^{-1}, 1461.18 cm^{-1}, 1377.10 cm^{-1}, 1234.4 cm^{-1}, 1147.6 cm^{-1}, 800.4 cm^{-1}, 828.41 cm^{-1}.

^{1}HNMR (DMSO): δ1.24 (s, 3H, H-6‴- Me), δ 2.13 (s, 3H, H-8 Me), δ 2.53 (s,1H, H-5″), δ 3.39 (s,1H, H-3″), δ 3.58 (s,2H, H-6″), δ 3.69 (s,2H, H-6‴), δ 3.72 (s,1H, H-2⁗), δ 3.77 (s,2H, H-3), δ 3.82-3.87 (m,9H, H-2″,3″,4″,2‴,3‴,6‴,2⁗,3⁗4⁗-OH), δ 3.80, 3.93, 4.00 (s, 9H, H-2′, 4′, 7-3xOMe) δ 6.04 (d, 1H, H-1″), δ 6.05 (d, 1H, H-1‴), δ 5.07 (d,1H, H-1⁗), δ 5.38 (m,1H, H-2), δ 6.63 (s,1H, H-6), δ 6.95 (s,1H, H-3′), δ 7.30 (d,1H, H-5′), δ 7.32 (d,1H, H-6′), δ 4.02 (s,1H, H-2″), δ 4.10 (s,1H, H-4″), δ 4.20 (s,1H, H-2‴), δ 4.54 (s,1H, H-3‴), δ 4.55 (s,1H, H-3⁗), δ4.56 (s,1H, H-4‴), δ 4.58 (d, 1H, H-4⁗), δ 5.04 (d, 1H, H-5‴), δ5.07 (m, 1H, H-5⁗).

^{13}CNMR (DMSO): δ 83.03 (C-2), δ 40.15 (C-3), δ 195.15 (C-4), δ 102.89 (C-4a), δ 164.86 (C-5) δ 130.13 (C-6), δ 168.37 (C-7), δ 115.37 (C-8) δ 165.67 (C-8a), δ 11.68 (C-8-Me) δ 129.13 (C-1′),δ 155.67 (C-2′), δ 114.86(C-3′),δ 159.03 (C-4′) δ 116.52 (C-5′), δ119.03 (C-6′), δ 55.67, 56.62, 50.15 (C-2′,4′,7-OCH_3 x3), δ 103.03 (C-1″), δ 78.37 (C-2″), δ 39.52 (C-3″), δ 31.94 (C-4″), δ 81.30 (C-5″), δ 38.89 (C-6″), δ 94.71 (C-1‴), δ 39.94 (C-2‴), δ 79.03 (C-3‴), δ 31.30 (C-4‴), δ 28.71 (C-5‴), δ 25.02 (C-6″), δ 99.94 (C-1⁗), δ 39.73 (C-2⁗), δ 39.31 (C-3⁗), δ 29.03 (C-4⁗), δ 28.62 (C-5⁗), δ 18.79 (C-6⁗).

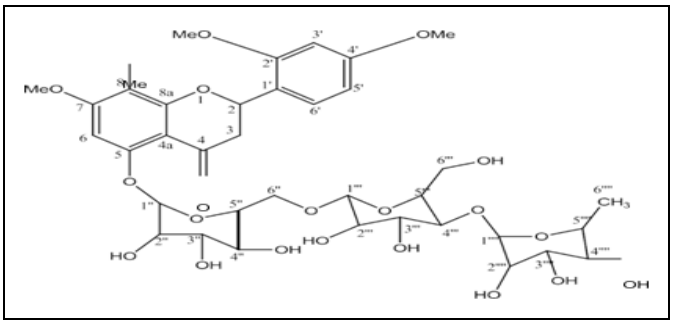

FIG. 4: CHEMICAL STRUCTURE OF COMPOUND RG-APE4 – (methyl-7,2′,4′-tri-O-methyl flavonone-5-O-α-L-rhamnopyranosyl (1→4)-β-D-glucopyranosyl-(1→ 6)-β-D-glucopyranoside)

M**ass Spectra (ESI-MS):** $C_{37}H_{50}O_{20}$, mol. wt.: 814.78, 816.1 (M+, 2H) $^{+}$. The other peaks are observed at 751.1, 572.4, 332.7, 159.8, 145.9, 128, 113.9. From the m.p., IR, ^{1}HNMR, ^{13}CNMR and MS, compound RG-APE4 was designated as 8-methyl- 7, 2′, 4′- tri- O- methylflavonone-5-O-α-L-rhamno-pyranosyl (1 4)-β-D-glucopyranosyl-(1 6)-β-D-glucopyranoside.

RESULTS: Extensive column chromatography isolated four compounds, Rohitika 7 **Fig. 1**, Rohituka 3 **Fig. 2**, Amoorinin-3-O-α-L-Rhamno-pyranosyl-(1→6) –β-D- Glucopyranoside **Fig. 3** and Methyl-7,2′,4′-tri-O-methyl flavonone-5-O-α-L-rhamnopyranosyl (1→4)- β- D-glucopyranosyl-(1→6)-β-D-glucopyranoside **Fig. 4**. The structures of the isolated compounds were established by interpretation of their spectroscopic data, by IR, ^{1}HNMR, ^{13}CNMR and MS with those published in the reference papers.

The formulated *A. polystachya* nanosuspension was tested in concentration ranges between 500-7.81 µM on MCF-7 and MDA-MB cell lines. It was found that the IC_{50} value obtained was 0.58 µM in MCF-7 cell line, and the IC_{50} in MDA-MB is greater than 1000.

DISCUSSION: In this study, an attempt was made to isolate the components from the methanolic extract of the root bark extract of *A. polystachya.*

The compound RG-APE1 showed an m.p. at 123.0 °C and positive response for Liebermann- Burchard test for triterpenoids. The IR spectrum showed a strong absorption at 3334.92 $cm^{-1,}$ indicating the presence of the hydroxyl group. The band at 2924.25 cm^{-1} indicated C-H stretching in CH_3. The prominent peak at 1724.36 cm^{-1} shows carbonyl stretching of ester. The ^{1}HNMR displayed exhibited a singlet at δ 5.2234, indicating methyl protons at C-30. The doublet at δ 7.3975 (C-21) and two singlets at δ 6.8561 (C-22) and δ 7.3869 (C-23) indicated the presence of protons in the furan moiety. The peak at δ 8.1664 indicated the presence of the carboxylic group. A singlet at δ 2.0470 indicated three methyl protons of CH_3COO. A singlet at δ 3.4367 indicated the presence of proton at C-2'. The value at δ 1.4091 appeared as a singlet and δ 1.2339 a doublet indicating two protons at c-3,' and C-4'.δ0.8359 appeared as a doublet indicating three protons at C-3'-Me. The ^{13}CNMR spectrum exhibited values at δ 174.83 (C-7), δ 169.0 (C-3), indicating the presence of two ester groups. δ 150.08 indicated the carbon for COOH. The value at δ 159.08 indicated the presence of carbon for CH_3COO.

The LC-MS spectrum displayed the molecular ion peak at m/z 672 correspondings to the molecular formula $C_{35}H_{44}O_{13}$. From the above evidence, the compound RG-APE1was designated as Rohituka 7.

The compound **RG-APE2** showed a m. p. at 122.4 °C. It showed a positive response for Liebermann-Burchard test for triterpenoids. The IR spectrum showed a strong absorption at 3389.10 $cm^{-1,}$ indicating the presence of the hydroxyl group. The band at 2931.25 cm^{-1} indicated C-H stretching in CH_3. The prominent peak at 1741.57 cm^{-1} shows carbonyl stretching of ester. The ^{1}HNMR of this compound exhibited a singlet at δ 6.8561indicating methyl protons at C-30. The value at doublet δ 7.3975, singlets δ6.4724 and δ 7.5509 indicated the presence of furan moiety. Here it is clearly noted that the value of COOH and CH_3COO are absent when compared to Rohituka 7. A singlet at δ 3.4367 and δ 1.7908 indicated the presence of protons at C-2' and C-3' and d 1.1606 at C-4'. The proton at C-5 appeared at 0.6985 as a single. A triplet appeared at δ 0.8934, indicating 3 methyl groups at 3'- Me. The ^{13}CNMR spectrum exhibited a peak at δ 167.06 (C-3), δ 169.0 (C-7), indicating the presence of two ester groups. The LC-MS spectrum displayed the molecular ion peak at m/z 600 correspondings to the molecular formula $C_{32}H_{40}O_{11}$. From the above evidence, the compound RG-APE2was designated as Rohituka 3.

The compound RG-APE3 showed a m. p. at 189 °C and a positive response to Molisch's test for carbohydrates and belong to the limonoid class. The IR spectra showed a peak at 3456.11 $cm^{-1,}$ indicating the presence of the hydroxyl group. The peak at 1745.0 cm^{-1} corresponds to the carbonyl group of the ester. The peaks at 1641.22 cm^{-1} and 820.39 cm^{-1} indicated a trisubstituted double bond. The peak at 860.37 cm^{-1} is due to the presence of furan ring. The peak at 1244.4 cm^{-1} corresponds to the epoxide moiety. The peak at 820.29 cm^{-1} is due to the glycoside moiety.

In the proton NMR spectra, the singlets at δ 0.96, δ 0.99,δ 1.09,δ 1.05 corresponds to 12 hydrogens of 4 methyl groups at C-18, 19, 24, 25. The singlet at δ 1.27 corresponds to the methyl protons of the rhamnose at C-6″. The value at δ 5.13 corresponds to 1 hydrogen of C-1′ of a glucose molecule. The multiplets at δ 6.43- δ 7.59 is due to three hydrogens of the furan moiety. The singlet at δ 4.91, δ 5.09, corresponds to methylene protons at C-26.

The ^{13}CNMR spectra showed signals at δ 172.93 (C-7), δ 170.14 (C-16) suggesting the presence of two ester groups. The signals at δ 142.93 (C-23), δ 140.16 (C-22), δ 101.59 (C-21), δ 120.14 (C-20) are characteristic of furan ring. The LC-MS spectrum indicated the molecular ion peak at 778.1 [M+] corresponding to the molecular formula $C_{39}H_{54}O_{16}$.

From the above evidences the compound RG-APE3 was designated as Amoorinin-3-O-α-L-rhamno-pyranosyl – (1→6) –β-D-glucopyranoside.

The compound RG-APE4 showed m.p. at 212 °C and a positive test for flavanone glycoside. The IR spectra showed peaks at 3447.18 $cm^{-1,}$ indicating the presence of hydroxyl group. The peak at 2963.12 cm^{-1} corresponds to C-H stretching of CH_3. The peak at 2877.24 cm^{-1} corresponds to the C-H stretching of in CH_3 of methoxy group. The peaks at 1644.29 cm^{-1}, 1461.18 cm^{-1}, 1377.10 cm^{-1}, 1234.4 cm^{-1}, 1147.6 cm^{-1}, 800.4 cm^{-1} is due to C-H stretching in flavonone nucleus. The peak at 828.40 cm^{-1} is due to a glycoside. In the proton NMR spectra, the singlet at δ 1.24 is due to methyl protons of the third glucose moiety at C-6′′′′. The doublet at δ 5.07 corresponds to the protons of C-1′′′′of glucose, the singlet at each δ 3.80, 3.93, and 4.00 is due to the protons of the 3 methoxy group in the structure. The multiplets at δ 3.82-3.87 account for hydroxyl protons. The singlet at δ 2.13 accounts for the methyl protons at C-8.

The ^{13}CNMR shows signals at δ 55.67, 56.62, and 50.15 representing the 3 methoxy groups. The value at δ 195.15 indicates one carbonyl group. The value at δ 11.68 was indicative of one methyl group at C-8. The LC-MS spectrum indicated the molecular ion peak at 816.11 [M+] corresponding to the molecular formula $C_{37}H_{50}O_{20}$. From the above evidences the compound RG-APE4was designated as 8- methyl-7, 2′, 4′-tri-O-methyl-flavonone-5-O-α-L- rhamnopyranosyl (1→4)-β-D-glucopyranosyl- (1→6) -β- D-glucopyranoside.

The isolated compounds from the methanolic extract of root bark of *A. polystachya* have been reported to have potential anti-cancer activity on MCF-7 and MDA-MB cell lines [8]. The cytotoxic studies were performed on Silver Nanosuspension of *A. polystachya*. It was seen that the formulation showed potent cytotoxic activity. This activity can be attributed to the isolated components which have been already reported to possess potential cytotoxic effects against human cell lines [9]. It can thus be concluded that the silver nanosuspension of *A. polystachya* can be suggested for breast cancer activity, which is eco-friendly, cost-effective, and stable.

CONCLUSION: The investigation justifies that the isolated components from the methanolic extract of the root bark of *A. polystachya*, RG-APE1, RG-APE2, RG-APE3, and RG-APE4 have been proven to have cytotoxic activity [8]. Based on these preliminary investigations, we formulated the root bark extract of *A. polystachya* into silver nano-particles and subsequently into silver nanosuspension which exhibited better cytotoxic activity than the root bark extract of the plant. The use of AgNP has emerged as a novel approach in cancer therapy. These studies suggest that formulating into AgNS can be further used in drug targeting the anti-cancer cells and create an impact on the human health

ACKNOWLEDGEMENT: The authors wish to thank authorities of the Directorate of Technical Education, Govt. of Goa and Principal, Goa College of Pharmacy for the facilities provided to carry out the research work. The authors also wish to thank Panjab University, Chandigarh-India, for carrying out the NMR and Mass Spectrometry studies on the methanolic extract of root bark of *A. polystachya* and Manipal College of Pharmaceutical Sciences, Manipal- India for carrying out the cytotoxic study on the nanosuspension of *A. polystachya*.

CONFLICTS OF INTEREST: The authors confirm that this article content has no conflict of interest.

REFERENCES:

1. http://www.who.int/mediacentre/news/releases/2003/pr27/en/.
2. Shweta SS, Rani WC, Tapadiya GG and Khadabadi SS: *Aphanamixis polystachya* (wall.) Parker - an important ethnomedicinal plant. Int J Pharm Sci Rev Res 2014; 24(1): 25-28.
3. Thirumurugan G: Nanotechnology: an effective tool for enhancing bioavailability and bioactivity of phytomedicine. Asian Pac J Trop Biomed 2014; 4(1): S1-S7.
4. http://biofuelpark.com/aphanamixis-polystachya-wall-r-parker/.
5. Kirtikar KR, Basu BD, Indian Medicinal Plants. Vol I. 2nd ed. Dehradun: International Book Distributor 2005: 551-53.
6. Gude R, Joshi AB, Bhandarkar A, Shirodker A and Bhangle S: Synthesis and characterisation of silver nanoparticles from the roots of *Aphanamixis polystachya*. World Jour of Pharm Research 2016; 2(5): 1399-408.
7. Jahan N, Aslam S, Rahman KU, Fazal T, Anwar F and Saher R: Formulation and characterisation of nanosuspension of herbal extracts for enhanced antiradical potential. Journal of Experimental Nanoscience 2016; 11(1): 72-80.
8. Houghton P, Fang R, Techatanawat I, Steventon G, Hylands PJ and Lee CC: The sulphorhodamine (SRB) assay and other approaches to testing plant extracts and derived compounds for activities related to reputed anticancer activity. Methods 2007; 42(4): 377-87.
9. Zhang Y, Wang JS, Wang XB, Gu YC and Kong LY: Polystanins A–D, four new protolimonoids from the fruits of *Aphanamixis polystachya*. Chem Pharm Bull 2013; 61(1): 75-81.
10. Vichai V and Kirtikara K: Sulforhodamine B colorimetric assay for cytotoxicity screening. Nature Protocols 2006; 1(3): 1112-16.
11. Shanker K, Mohan GK, Hussain MA, Jayarambabu N and Pravallika PL: Green biosynthesis, characterization, in vitro antidiabetic activity, and investigational acute toxicity studies of some herbal-mediated silver nanoparticles on animal models. Pharmacogn Mag 2017; 13(49): 188-92.
12. Mohanta YK, Panda SK, Jayabalan R, Sharma N, Bastia AK and Mohanta TK: Antimicrobial, antioxidant and cytotoxic activity of silver nanoparticles synthesized by leaf extract of *Erythrina suberosa* (Roxb.). Frontiers in Molecular Biosciences 2017; 4(14): 1-9.
13. Sultana N, Rahman MO, Tahia F, Hassan MA and Rashid MA: Antioxidant, cytotoxicity and antimicrobial activities of *Aphanamixis polystachya* (wall.) R. N. Parker. Bangladesh J Bot 2017; 46(4): 1381-87.
14. Wang GW, Jin HZ and Zhang WD: Constituents from Aphanamixis species and their biological activities. Phytochemistry Reviews 2013; 12(4): 915-42.
15. Zhang HP, Wu SH, Luo XD, Ma YB and Wu DG: A new limonoid from the seed of *Aphanamixis polystachya*. Chinese Chemical Letters 2002; 13(4): 341-42.
16. Brown DA and Taylor DA: Limonoid extractives from *Aphanamixis polystachya*. Phytochemistry 1978; 17(11): 1995-9.
17. Agarwal SK, Verma S, Singh SS and Kumar S: A new limonoid from *Aphanamixis polystachya*. Indian J Chem 2001; 40B: 536-38.
18. Srivastava SK, Srivastava SD and Srivastava S: New biologically active limonoids and flavonoids from *Aphanamixis polystachya*. Indian J Chem 2003; 42B; 3155-58.
19. Agnihotri VK, Srivastava SD and Srivastava SK: A new limonoid, amoorinin, from the stem bark of Amoorarohituka. Plantamedica 1987; 53(03): 298-9.
20. Samir KS, Panadda P, Choudhuri SC, Takashi OM and Ishibashi M: A new lignan from *Aphanamixis polystachya*. J Nat Med 2006; 60: 258-60.
21. Ragasa CY, Aguilar ML, Ng VA, Bugayong ML, Jacinto SD, Li WT and Shen CC: Terpenoids and sterol from *Aphanamixis polystachya*. J Chem Pharm Res 2014; 6(6): 65-8.
22. Lin CJ, Lo IW, Lin YC, Chen SY, Chien CT, Kuo YH, Hwang TL, Liou SS and Shen YC: Tetranortriterpenes and Limonoids from the roots of *Aphanamixis polystachya*. Molecules 2016; 21(9): 1167.
23. Wang GW, Jin HZ and Zhang WD: Constituents from Aphanamixis species and their biological activities. Phytochemistry reviews 2013; 12(4): 915-42.
24. Zhang H, Chen F, Wang X, Wu D and Chen Q: Complete assignments of 1H and 13C NMR data for rings A, B-seco limonoids from the seed of *Aphanamixis polystachya*. Magn Reson Chem 2007; 45(2): 189-92.
25. Zhang Y, Wang JS, Wang XB, Gu YC, Wei DD, Guo C, Yang MH and Kong LY: Limonoids from the fruits of *Aphanamixis polystachya* (Meliaceae) and their biological activities. J Agric Food Chem 2013; 61(9): 2171-82.
26. Lakshmi V, Pandey K, Kapil A, Singh N, Samant M, Dube A: *In-vitro and in-vivo* leishmanicidal activity of *Dysoxylum binectariferum* and its fractions against Leishmania donovani. Phytomedicine2007; 14(1):36-42.
27. Valan MF: Isolation and characterisation of the active principle from the bark of *Aphanamixis polystachya*. Asian Journal of Pharmaceutical Research 2014; 4(1): 19-23.
28. Mishra AP, Saklani S, Chandra S, Mathur A, Milella L and Tiwari P: *Aphanamixis polystachya* (wall.) Parker, Phytochemistry, Pharmacological properties and medicinal uses: An overview. World Journal of Pharmacy and Pharmaceutical Sciences 2014; 3(6): 2242-52.
29. Sarker AA, Chowdhury FA and Farjana Khatun: Phytochemical screening and *in-vitro* evaluation of pharmacological activities of *Aphanamixis polystachya* (Wall) Parker fruit extracts. Tropical Journal of Pharmaceutical Research 2013; 12(1): 111-16.
30. Rani WC, Shweta S, Tapadiya GG and Khadabadi SS: Evaluation of Phytochemical and Anticancer Potential of *Aphanamixis polystachya* (Wall.) Parker Stem Bark using *in-vitro* models. International Journal of Pharmaceutical Sciences Review & Research 2014; 28(1): 138-42.
31. Hegde K and Moitra G: Evaluation of anticancer activity of extract of *Aphanamixis polystachya* (Wall.) Parker leaves. International Journal for Pharmaceutical Research Scholars 2014; 3(2): 876-81.
32. Khan TR, Karmarkar P, Das A, Banik R and Sattar MM: Evaluation of cytotoxic and anthelmintic activities of bark extract of *Aphanimixis poystachya* (Wall). International Research Journal of Pharmacy 2013; 4(4): 126-29.
33. Md AAS, Md RK, Md AK, Sudhir K, and Mohammad AR: *In-vitro* membrane stabilizing activity, total phenolic content, free radical scavenging and cytotoxic properties of *Aphanamixis polystachya* (Wall.). Bangladesh Pharmaceutical Journal 2010; 13(2): 55-9.
34. Sarker AA and Pathan AH: Phytochemical Analysis and Bioactivities of *Aphanamixis polystachya* (Wall) R. Parker Leaves from Bangladesh. Journal of Biological Sciences 2013; 13(5): 393-99.

35. Enamala N, Hemashenpagam N, Vimal SS and Vasantha RS: Characterization of *Coriander sativum* mediated silver nanoparticles and evaluation of its antimicrobial and wound healing activity. Indo American Journal of Pharmaceutical Research 2013 3(7): 5404-09.
36. Konwar R and Baquee AA: Nanoparticle: An overview of preparation, characterisation and application. International Research Journal of Pharmacy 2013; 4(4): 47-57.
37. Saklani S and Mishra AP: Pharmacognostic, phytochemical and antimicrobial screening of *A. polystachya*, an endangered medicinal tree. International J of Pharmacy and Pharmaceutical Sci 2012; 4(3): 235-40.
38. Gude R, Joshi A and Bhandarkar A: Anti-oxidant, cytotoxic and apoptotic studies of root bark assisted silver nanoparticles from *Aphanamixis polystachya*. Int J Res Pharm Sci 2019; 10(2): 943-50.

How to cite this article:
Gude R, Joshi A, Bhandarkar A and Mayenkar D: Isolation and cytotoxic potential of silver nanosuspension of the roots of *Aphanamixis polystachya*. Int J Pharm Sci & Res 2020; 11(11): 5766-74. doi: 10.13040/IJPSR.0975-8232.11(11).5766-74.